

**The Mount Isa Deep Copper Orebodies**  
**Characteristics and Structural Controls on**  
**Mineralisation**

by  
Steve R. Law, BSc (Hons)

Submitted in fulfillment of the requirements for the degree of  
Master of Exploration Geoscience  
University of Tasmania (April, 1999)

This Thesis contains no material which has been accepted for a degree or diploma by the University or any other institution, except by way of background information and duly acknowledged in the Thesis. To the best of my knowledge and belief no material previously published or written by another person except where due acknowledgement is made is contained in the text of this Thesis.

A handwritten signature in cursive script, appearing to read "S. Law", positioned above a horizontal dashed line.

Steve R. Law

This thesis may be made available for loan. Copying of any part of this thesis is prohibited for two years from the date this statement was signed; after that time limited copying is permitted in accordance with the *Copyright Act 1968* .

SLaw.

Steve R. Law

30,4,99

## ***Acknowledgements***

I wish to thank Mount Isa Mines Limited for their support during the preparation of this thesis. Thanks also to my supervisors Ron Berry and Peter McGoldrick for their much needed advice, and to Peter Jones for helpful discussions on ideas about the structural nature of the 3500 Orebody. I am grateful for the encouragement from my work colleagues Anita Pendreigh, Matt Ridgway and Jillian Lee and to Steve de Kruijff for reading the original draft of the thesis.



## ***Abstract***

The 3000 and 3500 orebodies form part of the world class copper deposit at Mount Isa. The Deep Copper Mine (now renamed Enterprise Mine) came into production in 1993 and provided the opportunity to study the characteristics of these orebodies and the structural controls on copper and cobalt mineralisation.

In the Enterprise Mine orebodies, chalcopyrite and silica rich breccia cores are surrounded by a halo of recrystallised dolomitic shales and siliceous shales with lesser dolomite breccias. A distinctive talc+pyrrhotite alteration zone occurs on the footwall of the 3500 Orebody adjacent to a band of sub-economic Ag-Pb-Zn mineralisation, which has associated phyllosilicate alteration. The Ag-Pb-Zn mineralisation is unrelated to the chalcopyrite and silica-dolomite alteration.

The two orebodies are situated on the west dipping limb of the Mount Isa Fold, which formed during the third period of regional deformation ( $D_3$ ). There are two main structural controls that localised the copper bearing hydrothermal fluids:

(1) The basement contact fault is a large scale regional fault that has been affected by all three regional deformation periods. It separates the Urquhart Shale (orebody host sequence) from the older Eastern Creek Volcanics. The position of  $D_3$  related flexures in the basement contact fault are a major control on the localisation of copper mineralisation and possibly of cobalt mineralisation.

(2) Bedding parallel shear zones and associated splay shear zones form an anastomosing network within the orebodies. The orientation of bedding and faults, and indicators that bedding plane slip was an important process, suggest that the shear zones formed towards the latter stages of development of the Mount Isa Fold and that the shear zone geometry strongly influenced the position of the orebodies. The bedding parallel shear zones were pathways for the hydrothermal fluids, especially in the up-dip direction. They have a strong influence on local variations in copper distribution. The shear zones flatten in dip towards the basement contact fault and propagate from  $D_3$  flexures. The shear zone networks are most extensively developed in the more laminated sections of the original stratigraphy, and occur as contacts between different layers variously affected by the carbonate and silica bearing hydrothermal fluids.

<b>Introduction</b>	<b>1</b>
<b>1.1 Introduction</b>	<b>1</b>
<b>1.2 Scope</b>	<b>1</b>
<b>1.3 Methodology</b>	<b>2</b>
1.3.1 Structural Study	2
1.3.2 Grade Distribution Study	2
<b>1.4 History</b>	<b>3</b>
<b>1.5 Regional Geology</b>	<b>4</b>
<b>1.7 Mine Sedimentology</b>	<b>7</b>
1.7.1 Urquhart Shale	7
1.7.2 Native Bee Siltstone	7
1.7.3 Depositional Model	8
<b>1.8 Regional Structure</b>	<b>8</b>
<b>1.9 Mine Structure</b>	<b>10</b>
1.9.1 Early Structural Ideas	10
1.9.1.1 1942	10
1.9.1.2 1961	11
1.9.1.3 1972	12
1.9.2 Contemporary Ideas	12
<b>Alteration</b>	<b>17</b>
<b>2.1 Introduction</b>	<b>17</b>
<b>2.2 ‘Rock Type’ Descriptions</b>	<b>17</b>
2.2.1 Shale and Pyritic shale	18
2.2.2 Fractured siliceous shale	18
2.2.3 Siliceous shale	18
2.2.4 Irregularly brecciated dolomitic shale	19
2.2.5 Recrystallised shale	19
2.2.6 Summary	19
<b>2.3 Rock type Distribution and Formation</b>	<b>20</b>
2.3.1 Distribution	20
2.3.1.1 Deep Copper orebodies	20
2.3.1.2 Comparison with 1100 orebody	22

2.3.2 'Rock Type' Formation	25
2.3.2.1 <i>Silicification and Dolomitisation Alteration Processes</i>	25
<b>2.4 3500 Orebody Footwall Alteration</b>	<b>29</b>
2.4.1 Footwall Pyrite Band	29
2.4.2 Talc Alteration	29
2.4.3 Pb - Zn Mineralised Zone and Phyllosilicate Alteration	29
2.4.4 Interpretation	30
2.4.4.1 <i>Talc Alteration</i>	30
2.4.4.2 <i>Phyllosilicate Alteration and Pb-Zn Mineralisation</i>	31
<b>2.5 Copper Grade Relationship with Silicification</b>	<b>32</b>
2.5.1 Observations	32
2.5.2 Interpretation	35
<b>2.6 Conclusions</b>	<b>35</b>
<b>Basement Contact Fault</b>	<b>37</b>
<b>3.1 Contact Zone and Basement Rock Types</b>	<b>37</b>
3.1.1 Carbonaceous Mylonite	38
3.1.2 Buck Quartz	38
3.1.3 Character of the basement contact fault	38
3.1.4 Slaty Shale	42
3.1.5 Quartzite	42
3.1.6 Greenstone	42
3.1.7 Siliceous Greenstone	42
<b>3.2 Geometry of Basement Rocks</b>	<b>43</b>
<b>3.3 Significance of geometry of Eastern Creek Volcanics</b>	<b>47</b>
<b>3.4 Basement Contact Fault Geometry</b>	<b>47</b>
3.4.1 3000 Orebody	48
3.4.2 3500 Orebody	48
<b>3.5 Slaty Shale Distribution</b>	<b>56</b>
<b>3.6 Copper Distribution</b>	<b>56</b>
<b>3.7 Discussion</b>	<b>59</b>
<b>3.8 Conclusions</b>	<b>62</b>
<b>Orebody Structure</b>	<b>63</b>

<b>4.1 Introduction</b>	<b>63</b>
4.1.1 Terminology	63
<b>4.2 Physical Character</b>	<b>64</b>
4.2.1 3000 Orebody	64
4.2.2 3000 Orebody Hangingwall Contact	70
4.2.3 3500 Orebody	78
<b>4.3 Local Copper Grade Variations</b>	<b>81</b>
4.3.1 Detail of 3500 Orebody - 6390 mN section	81
<b>4.4 Shear Zone Geometry and Distribution Patterns</b>	<b>84</b>
4.4.1 3000 Orebody shear zones	84
4.4.2 3500 Orebody shear zones	84
4.4.3 Urquhart Shear	95
4.4.4 Mount Isa Fold Zone	96
<b>4.5 Fault Movement</b>	<b>98</b>
<b>4.6 Orientation Data</b>	<b>101</b>
<b>4.7 Discussion</b>	<b>105</b>
4.7.1 Orebody Formation	105
4.7.2 Ductility contrasts	106
4.7.3 Fracture Networks	108
4.7.4 Geometrical Considerations	111
4.7.5 Reactivation of Pre-existing Structures	113
<b>Copper and Cobalt Mineralisation</b>	<b>114</b>
<b>5.1 Introduction</b>	<b>114</b>
<b>5.2 Copper - Relationship to 'Rock type'</b>	<b>114</b>
<b>5.3 Copper Distribution</b>	<b>115</b>
5.3.1 3000 Orebody	116
5.3.2 3500 Orebody	116
<b>5.4 Copper – Relationship to Structure</b>	<b>138</b>
<b>5.5 Cobalt - Relationship to 'Rock type'</b>	<b>141</b>
<b>5.6 Cobalt Distribution</b>	<b>142</b>
5.6.1 3000 Orebody	142
5.6.2 3500 Orebody	143

<b>5.7 Cobalt - Relationship to Copper and Structure</b>	<b>143</b>
<b>5.8 Discussion</b>	<b>147</b>
<b>Synopsis</b>	<b>148</b>
<b><i>References</i></b>	<b>151</b>

## List of Figures

Fig 1.1:	Locality Map (Adapted from Blake, 1986).	6
Fig 1.2:	Leichhardt River Fault Trough (Adapted from Blake, 1987).	6
Fig 1.3:	1972 Interpretation of the Deep Copper orebodies (After Stoker, 1972).	14
Fig 1.4:	Surface plan of the Mount Isa Fold Zone. (From MIM internal exploration review, 1992).	15
Fig 1.5:	Cross section 6085 mN (From MIM internal exploration review, 1992).	16
Fig 2.1:	Generalised distribution of alteration 'rock types' around the Deep Copper orebodies.	21
Fig 2.2:	Alteration 'rock type' distribution in the 1100 Orebody at 4200 mN (Adapted from Waring, 1990).	24
Fig 2.3:	Cross sections at 6175 mN, 6330 mN and 6480 mN showing the distribution of the footwall pyrite band, talc+pyrrhotite zone and Pb-Zn mineralised zone.	28
Fig 2.4:	Section 6205 mN - Silicification and economic mineralisation.	33
Fig 2.5:	Plan 25A (2150 mRL) - Silicification and economic mineralisation.	34
Fig 3.1a:	740 Xcut 29E. Basement contact fault. Layered buck quartz and carbonaceous mylonite. Clay gouge on sharp lower contact with greenstone.	40
Fig 3.1b:	740 Xcut 29E. Interpretation of figure 3.1a.	41
Fig 3.2:	Equal area stereogram of poles to bedding in quartzites.	43
Fig 3.3:	Detailed mapping of the Eastern Creek Volcanics beneath the basement contact fault on 28D.	45
Fig 3.4a & b:	Photograph and interpretative sketch of a quartzite/greenstone contact. T62 Decline 30A sublevel. Fault is dipping east and bedding in quartzite is dipping west (Width of view 1.5m, looking south).	46
Fig 3.5a:	Contour map of the upper surface of the basement contact fault (contours at 10m intervals). The marked locations are those where the fault zone orientation was measured and where the detailed information for Figs 3.6, 3.7, 3.8 and 3.9 was collected.	50

Fig 3.5b:	Equalarea stereograms of poles to fault planes, from the six localities shown in Fig 3.5a.	51
Fig 3.6:	Detailed mapping of the basement contact fault on 26L below the 3000 Orebody.	52
Fig 3.7:	Detailed mapping of the basement contact fault on 26B below the 3000 Orebody.	53
Fig 3.8:	Detailed mapping of the basement contact fault on 26D below the 3000 Orebody.	54
Fig 3.9:	Detailed mapping of the basement contact fault on 29E adjacent to the 3500 Orebody.	55
Fig 3.10:	5% and 8% copper contours of the 3000 and 3500 orebodies overlain on the contour map of the upper surface of the basement contact fault. The copper contours are representative of copper grade distribution immediately adjacent to the fault surface.	58
Fig 3.11:	Section 4500 mN and section 5719 mN showing flat sections of basement contact fault below the 1100 Orebody and the 1900 Orebody (Adapted from Bell <i>et.al.</i> 1988).	61
Fig 4.1:	Locations of faults and shear zones described in Table 4.1.	67
Fig 4.2:	3000 Orebody R618 CO 26B. Close up of a shear zone with a sharp boundary fault showing a marked transition to very high grade copper mineralisation. Well developed internal foliation within the black carbonaceous body of the shear zone. The shear zone is weakly mineralised. Dipping 35° to the NW, this shear zone would intersect the basement contact fault ~20 metres down dip in the plane of the shear zone (looking east) (length of hammer 32 cm).	69
Fig 4.3:	3000 Orebody 85 Xcut 23A. One metre wide fault zone adjacent to a small lens of fractured siliceous shale (looking south) (distance between the two rockbolts is 0.9m).	69
Fig 4.4:	3000 Orebody Hangingwall Contact Zone. 390 Xcut 25A - mapping detail and locations of figs 4.5a(i) & (ii), 4.5b(i) & (ii) and 4.5c(i) & (ii).	71
Fig 4.5a(i):	3000 Orebody Hangingwall Contact Zone 390 Xcut 25A looking northwest (White paint lines are two metres apart).	72

Fig 4.5a(ii):	3000 Orebody Hangingwall Contact Zone 390 Xcut 25A looking northwest. Drawing of main structural features and copper mineralisation.	73
Fig 4.5b(i):	3000 Orebody Hangingwall Contact Zone 390 Xcut 25A looking northwest. (White paint lines are two metres apart).	74
Fig 4.5b(ii):	3000 Orebody Hangingwall Contact Zone 390 Xcut 25A looking northwest. Drawing of main structural features and copper mineralisation.	75
Fig 4.5c(i):	3000 Orebody Hangingwall Contact Zone 390 Xcut 25A looking northwest. (White paint lines are two metres apart).	76
Fig 4.5c(ii):	3000 Orebody Hangingwall Contact Zone 390 Xcut 25A looking northwest. Drawing of main structural features and copper mineralisation.	77
Fig 4.6:	3500 Orebody U61 NDR 26B. The 1 metre thick layered chalcopyrite, pyrrhotite and pyrite ore is bounded by graphitic shear zones 0.3 and 0.5 metres thick. Note that the shear zones are also mineralised. The layering of the pyrrhotite is parallel to the shear zone foliation which in turn is parallel to the local bedding orientation (looking up - 1m paint lines).	80
Fig 4.7:	3500 Orebody 515 Xcut 26B. Boundary between massive fractured siliceous shale breccia and sheared siliceous shale zone. The sheared siliceous shale shows the characteristic appearance of the shear zones within the 3500 Orebody. The contact with the breccia is a sharp fault plane (looking south - 10cm markers on pole).	80
Fig 4.8:	Cross section 6390 mN - assay data from diamond drillholes with interpreted shear zones. Highlighted assays show position of samples for mineralogical analysis.	83
Fig 4.9a:	Alteration and shear zones - 23A sublevel.	85
Fig 4.9b:	Alteration and shear zones - 24A sublevel.	86
Fig 4.9c:	Alteration and shear zones - 25A sublevel.	87
Fig 4.9d:	Alteration and shear zones - 26B sublevel.	88
Fig 4.10a:	Alteration and shear zones - 6025 mN cross section.	89
Fig 4.10b:	Alteration and shear zones - 6115 mN cross section.	90
Fig 4.10c:	Alteration and shear zones - 6205 mN cross section.	91
Fig 4.10d:	Alteration and shear zones - 6300 mN cross section.	92
Fig 4.10e:	Alteration and shear zones - 6390 mN cross section.	93
Fig 4.10f:	Alteration and shear zones - 6480 mN cross section.	94



Fig 4.11:	Poles to fault surfaces (large dots) and bedding (small dots) from within the Urquhart Shear zone (measurements taken from location shown in Fig 4.12).	95
Fig 4.12:	Interpretation of underground exposure of the Urquhart Shear. 160 Xcut 25A (looking north - Field of view 9 metres).	96
Fig 4.13:	Schematic diagram of possible relationship between the shear zones in the 3000 and 3500 orebodies and the Urquhart Shear and the Mount Isa Fold Zone.	97
Fig 4.14:	Plunge and trends of slickenlines on 3500 Orebody fault surfaces.	98
Fig 4.15a:	3500 Orebody corner 435 Xcut and V60 FWDR 25A. Slickenlines on graphitic fault surface in shales on the footwall of the 3500 Orebody (looking southwest Pencil 14cm).	100
Fig 4.15b:	3500 Orebody U61 NDR off 395 Xcut 28D. Slickenlines on fault surface within the 3500 Orebody (looking east. Pencil 17cm).	100
Fig 4.16:	Orientation data for all bedding and faults 3000 Orebody.	101
Fig 4.17a:	Comparison of poles to bedding data for each sublevel in the 3000 Orebody.	102
Fig 4.17b:	Comparison of poles to fault plane data (within shear zones) for each sublevel in the 3000 Orebody.	103
Fig 4.18:	Detailed mapping of deformed bedding adjacent to the basement contact fault 25A.	104
Fig 4.19:	Fault network on 24A and 25A sublevels - 3000 Orebody.	110
Fig 4.20:	Model for the generation of fractures at thrust bends by low angle Riedel shearing in steep shear zones (From Wibberley, 1997).	112
Fig 5.1a:	Copper mineralisation & shear zones - 23A sublevel.	118
Fig 5.1b:	Cobalt mineralisation & shear zones - 23A sublevel.	119
Fig 5.2a:	Copper mineralisation & shear zones - 24A sublevel.	120
Fig 5.2b:	Cobalt mineralisation & shear zones - 24A sublevel.	121
Fig 5.3a:	Copper mineralisation & shear zones - 25A sublevel.	122
Fig 5.3b:	Cobalt mineralisation & shear zones - 25A sublevel.	123
Fig 5.4a:	Copper mineralisation & shear zones - 26B sublevel.	124
Fig 5.4b:	Cobalt mineralisation & shear zones - 26B sublevel.	125
Fig 5.5a:	Copper mineralisation and shear zones - 6025 mN cross section.	126
Fig 5.5b:	Cobalt mineralisation and shear zones - 6025 mN cross section.	127
Fig 5.6a:	Copper mineralisation and shear zones - 6115 mN cross section.	128
Fig 5.6b;	Cobalt mineralisation and shear zones - 6115 mN cross section.	129

Fig 5.7a:	Copper mineralisation and shear zones - 6205 mN cross section.	130
Fig 5.7b:	Cobalt mineralisation and shear zones - 6205 mN cross section.	131
Fig 5.8a:	Copper mineralisation and shear zones - 6300 mN cross section.	132
Fig 5.8b:	Cobalt mineralisation and shear zones - 6300 mN cross section.	133
Fig 5.9a:	Copper mineralisation and shear zones - 6390 mN cross section.	134
Fig 5.9b:	Cobalt mineralisation and shear zones - 6390 mN cross section.	135
Fig 5.10a:	Copper mineralisation and shear zones - 6480 mN cross section.	136
Fig 5.10b:	Cobalt mineralisation and shear zones - 6480 mN cross section.	137
Fig 5.11:	Copper mineralisation - Longsections at 1900 mE, 2000 mE and 2050 mE.	140
Fig 5.12a:	Cobalt vs copper values 3000 Orebody.	145
Fig 5.12b:	Cobalt vs copper values 3500 Orebody.	146

### **List of Tables**

Table 4.1:	Physical characteristics of faults and shear zones on 24A sublevel.	65
Table 4.2:	Results of quantitative bulk mineral XRD analysis of 3500 Orebody samples.	82

# **Introduction**

## **1.1 Introduction**

World class copper, silver, lead and zinc orebodies have been the focus of mining activity at Mount Isa in Northwest Queensland since their discovery in 1923. Mining of the major 1100 Orebody (copper) began in the 1960's and many geological studies have been conducted over the years trying to understand aspects of sedimentology, structure and geochemistry associated with this deposit. The 3000 and 3500 orebodies are northeast of the 1100 Orebody. Collectively, they are known as the Deep Copper orebodies as they are located 1.2 to 1.8 kilometres below the surface. In 1993 production began from the 3000 Orebody. This provided an excellent opportunity for the study of an orebody that is a smaller version of the 1100 Orebody. The 3500 Orebody has a geometry similar in style to the 650 orebody. The 650 Orebody was one of the first copper orebodies discovered in the 1940's. It occurs west of the 3000 Orebody and above it (between 7 level and 15 level). The following report presents the results of this work.

## **1.2 Scope**

The scope of this thesis is to describe the geological features of the 3000 and 3500 orebodies (Enterprise Mine) at Mount Isa. All previous work on the Mount Isa copper orebodies has been done on the 1100 and 1900 orebodies, which occur as, separate entities to the south. Aspects of the Deep Copper orebodies that are similar to the 1100/1900 orebodies will be briefly described where there are already detailed descriptions in the literature.

The importance of structural controls on the distribution of the copper mineralisation and associated alteration 'rock types' is the main focus of this thesis. Cobalt grade is significantly higher in the Deep Copper orebodies and its distribution and relationship to structure is also described. The emphasis throughout is on features that can be observed visually by the mine geologist without the requirement for microstructural work.

---

## 1.3 Methodology

### 1.3.1 Structural Study

Underground development mapping and diamond drilling data was available for the 3000 Orebody over a strike length of 400 metres (5900mN to 6300mN). The underground mapping data presented here are from four of the major mine sublevels, 23A (2280 mRL), 24A (2220 mRL), 25A (2160 mRL) and 26B (2100 mRL). The elevation at surface is 3500 mRL. Mapping data was collected from drive walls, faces and backs at 1:250 scale and plotted on floor plans at 1:500 scale. The major fault structures described are those that could be correlated between each of the sublevels. The diamond drilling data was used to infill gaps in the mapping data. Diamond drilling data was available for the 3500 Orebody over a strike length of 600 metres (5900mN to 6500mN). Diamond drillhole information is collected from east-west fans drilled on a 30 metre X 30 metre spacing. The sections are named according to the mine grid northing (e.g. 6330 mN). The data was collated on 30 metre sections. The sections presented in this report are on a 90 metre spacing, which is considered sufficient to define the changes in the geometry of the orebodies. All of the information is based on mesoscale to mine scale observations and no thin section work was done. Where stereonet data are presented they have been prepared using the GEORIENT program developed by Dr R.J.Holcombe of the Department of Earth Sciences, University of Queensland.

### 1.3.2 Grade Distribution Study

The figures produced in chapter 5 were compiled using the Enterprise Mine geostatistical model. The model was derived using the point kriging method with variograms derived by G.F. Raymond (1993). Prior to kriging the diamond drillhole and development sampling data was composited to 5m intervals (downhole). At the time the kriging programs were written, the volume of data at Mount Isa and processing constraints necessitated the use of 5m composites. At the time this thesis was originally submitted (April 1988) this was the only model available. In August 1998, a re-evaluation of the kriging process (Schofield, 1998), enabled a model for the 3500 Orebody using 3m composites to be established. The relevant figures throughout the thesis have been modified using this model. The database available

for cobalt is approximately one third the size of the copper database. The geological logging detail used in the copper mines at Mount Isa results in the assay sample lengths ranging between 1.5m and 3m.

## 1.4 History

The following is a short history of the exploration and development of the Deep Copper orebodies.

By 1962 the significance of the greenstone contact with respect to copper exploration had been recognised and exploration targets had been identified in the area between 6150 mN and 7400 mN above this contact zone. The sinking of K57 Shaft (now R62 Shaft) was in progress and there was a need for a drillhole to test for water and ground conditions in the vicinity of the proposed ore handling facilities. This provided the first opportunity to test one of the exploration targets. Drillhole L57 SE Decline intersected 34.3m @ 4% Cu in the silica-dolomite alteration around 24 level. This was the discovery hole of the 3000 Orebody. The drillhole was discontinued as it was at the limits of the drill rig in use. If the rig had been capable of drilling a further 34m it would have intersected the 3500 Orebody (100m @ 5% Cu). This orebody was not discovered until 1967. In 1979 the orebodies were referred to as the footwall lens and hangingwall lens of 3000 Orebody. In the 1980's the footwall lens became known as the 3500 Orebody. Between 1981 and 1984 a project team was set up to develop a method for access to the 3000 Orebody. In May 1984, due to a shortage of capital funds and an expected increase in 1100 Orebody reserves, the project team was disbanded. A further eighteen months of exploratory drilling in the southern 1100 Orebody did not substantially increase the reserves. By mid 1986 it was realised that access to the 3000 Orebody was urgently required and a decline from 20 level was commenced. In 1987 work began on the mining of the T62 Decline which was designed to haul ore utilising electric powered Kiruna trucks. Construction of this decline provided access for confirmatory diamond drilling which when completed allowed an "informed decision to mine" to be made for the Initial Mining Block in the 3000 Orebody in 1991. Production from the first stope started in March 1993.

In February 1995 a review of the Deep Copper Mine was completed and a feasibility study started. By late 1996 this study was complete and a project team had been put together to oversee the expansion of the Deep Copper Mine from a 1.5 mtpa operation to a 3.5 mtpa operation. Production from the first 3500 Orebody stope started in December 1996. In August 1998 the Deep Copper Mine was renamed the Enterprise Mine. The 3000 and 3500 orebodies are still referred to as the Deep Copper orebodies.

## 1.5 Regional Geology

The Mount Isa Group is a sequence of Middle Proterozoic sedimentary rocks that occur in the Leichhardt River Fault Trough within the Western Fold Belt of the Mount Isa Inlier located in Northwest Queensland (Fig 1.1 & Fig 1.2). (Plumb *et al.* 1980; Blake, 1987). The eastern boundary of the Leichhardt River Fault Zone is defined in part by the Gorge Creek-Quilalar Fault Zone, which consists of narrow north trending downfaulted blocks of sandstone, argillite and carbonates of the Surprise Creek Beds, alternating with upfaulted blocks of Kalkadoon-Leichhardt basement rocks. Parallel to the major boundary faults the metasediments are tightly folded along north plunging fold axes. The western boundary of the fault trough, the Mount Isa Fault Zone consists of a set of north trending reverse faults of which the Mount Isa Fault is the principal one. The faults are subparallel to bedding and cleavage of the near vertical to slightly overturned Judenan Beds west of Mount Isa and to the eastern contact of the Sybella Granite (Glickson *et al.* 1976).

The major deformation and metamorphism within the Leichhardt River Fault Trough can be related to an east-west compression, which resulted in the formation of north trending folds and probably the Mount Isa Fault Zone. The peak of this phase probably postdates both the emplacement of the Sybella Granite (ca.1650my) and the deposition of the Mount Isa Group. It was accompanied by regional metamorphism which was followed by dyke intrusion and younger faulting (Glickson *et al.* 1976).

The Mount Isa Group outcrops in the Mount Isa District as a narrow belt one to ten kilometres wide and approximately eighty kilometres long, trending north-south. The sequence unconformably and disconformably overlies the Myally Subgroup and

the Eastern Creek Volcanics. In most areas the strata dip at 60° to 80° to the west. The Mount Isa Group contains eight formations. From top to bottom they are:

Magazine Shale Kennedy Siltstone Spear Siltstone Urquhart Shale Native Bee Siltstone	upper Mount Isa Group
Breakaway Shale Moondarra Siltstone Warrina Park Quartzite	lower Mount Isa Group

Most of the sequence consists of shales and siltstones. Coarse grained sediments are generally absent except in the Warrina Park Quartzite and the Moondarra Siltstone. The sequence is subdivided into upper and lower Mount Isa Groups on the basis of local unconformities occurring at the contact of the Breakaway Shale with the Native Bee Siltstone. This boundary also marks a lithological change from predominantly siliceous to predominantly dolomitic rocktypes (Neudert, 1983). The depositional age of the Mount Isa Group is  $1670^{+20}_{-17}$  my based on U-Pb zircon dating of tuff beds from the Urquhart Shale (Page, 1981).

Fig 1.1 Locality Map (Adapted from Blake, 1986)

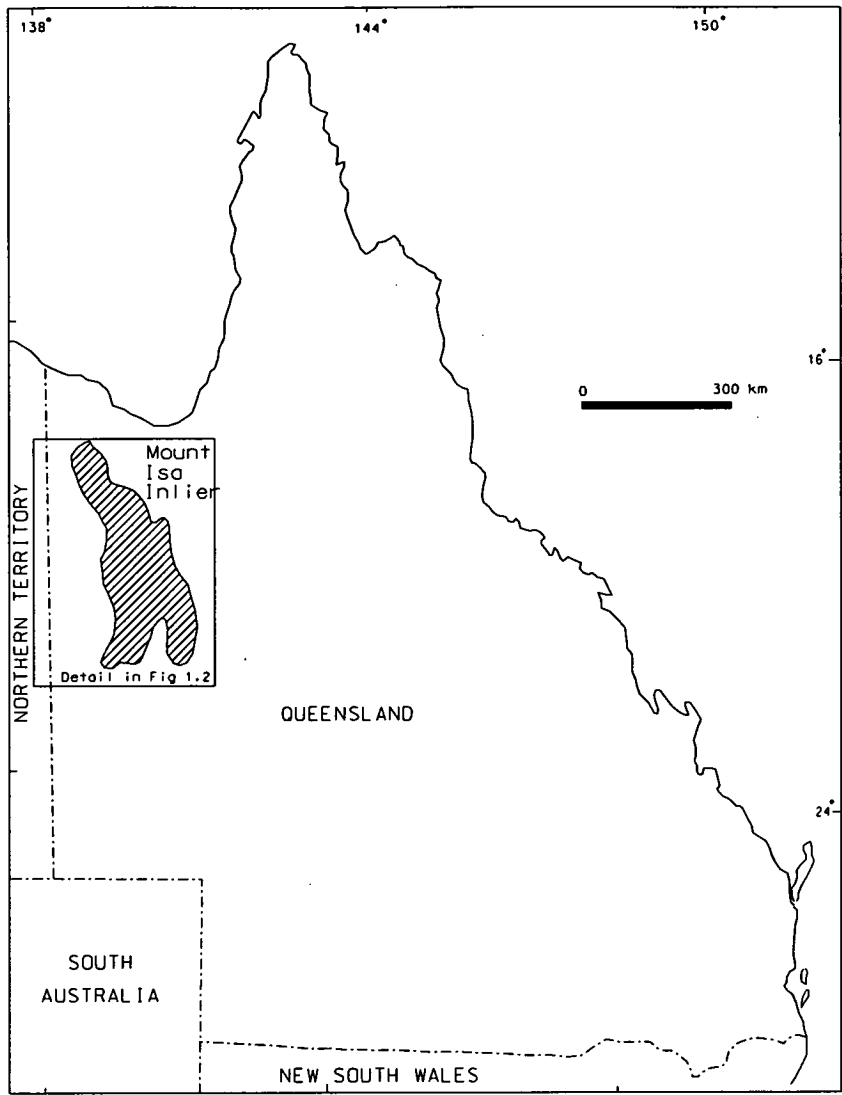
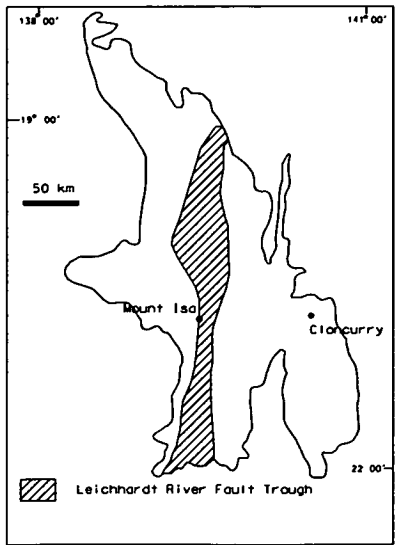


Fig 1.2: Leichhardt River Fault Trough. (Adapted from Blake, 1987)





## 1.7 Mine Sedimentology

The two stratigraphic units occurring in the immediate vicinity of the Deep Copper orebodies are the Urquhart Shale and the Native Bee Siltstone. The following sedimentological descriptions are from Neudert (1983, 1996).

### 1.7.1 Urquhart Shale

The Urquhart Shale occupies the stratigraphic interval between the Native Bee Siltstone and the Spear Siltstone. The formation contains a cyclic succession of carbonate rich and carbonate poor facies. Four facies types are distinguished:

1. Dark grey, carbonate-poor and carbonaceous rhythmite (centimetre thick couplets of parallel-laminated siltstone and non-laminated mudstone).
2. A carbonate-rich variant of (1) which contains a significant proportion (~50%) of carbonate cemented siltstone and/or mudstone layers.
3. A dark grey rhythmite facies similar to (1) but containing numerous carbonate crusts and nodules (mainly calcite).
4. A carbonate-rich siltstone facies which often contains current-laminated deposits, erosional contacts and flutes.

Pyritic siltstones occur throughout the formation. The distribution of fine grained pyrite is facies controlled. Pyrite is most abundant in the rhythmite facies with crusts and nodules (3) and is least abundant in the carbonate-rich siltstone facies (4).

The Urquhart Shale formation has been subdivided into an informal upper and lower unit. The presence of carbonate nodules, flat-pebble conglomerates, medium-scale ripples and pseudomorphs after sulphate crystals in the lower Urquhart Shale and their general absence in the upper Urquhart Shale is the basis of the subdivision. The contact between the upper and lower unit is gradational (Neudert, 1983).

### 1.7.2 Native Bee Siltstone

The Native Bee Siltstone forms the base of the upper Mount Isa Group, resting partly unconformably on the Breakaway Shale. The sequence displays a characteristic interbedding of thin rock units of mainly (1) homogeneous shale, (2) laminated siliceous shale and (3) carbonate rich siltstone, with both dolomite and calcite. In drill core, light coloured units are carbonate rich while shale beds and siliceous siltstones are darker shades of grey. At several stratigraphic locations distinct

feldspathic chert markers interrupt the sequence. Seven zones containing large scale cross-beds are intercalated within the sequence.

The contact between the Native Bee Siltstone and the overlying Urquhart Shale is not clearly defined and usually cannot be determined in the field because of close lithological similarities. In the mine area, the formation boundary is arbitrarily defined at the change from non-pyritic rocks to rocks containing fine-grained pyrite. The Native Bee Siltstone also tends to exhibit a “striped” appearance with alternating light and dark layers.

### 1.7.3 Depositional Model

The entire upper Mount Isa Group was deposited in a shallow water depositional system in which semi-emergent environments recurred even during deposition of the now-mineralised sedimentary strata. The model put forward by Neudert (1983) is of a playa lake system in which sediments were deposited in flood plain, saline mud flat and perennial lake subenvironments. The composition of the intrabasinal sediment source evolved in time from carbonate (Native Bee Siltstone), to carbonate-sulphate (Urquhart Shale), to Na-evaporites (Kennedy Siltstone). The ore-hosting sediments formed during the main sulphate precipitating stage of the basin brine.

## 1.8 Regional Structure

Work by several authors (Wilson, 1973; Winsor, 1986; Bell *et al.* 1988) has determined that three phases of deformation have affected the Mount Isa Group on a regional scale.

The first folding event ( $D_1$ ) resulted in east-west folds ( $F_1$ ) with wavelengths of tens to hundreds of metres. A penetrative slaty cleavage ( $S_1$ ), usually making a low angle to bedding, is developed locally. A number of east-west faults developed. Some of these faults have fault fill with a fracture cleavage fabric having a geometry consistent with  $S_2$  in the surrounding rocks. This suggests that they originated pre or early syn- $S_2$ . The first movement on these faults was probably dip slip. Subsequent strike slip on some of these faults late during  $D_2$  resulted in local development of drag folds. A common feature of the pre- $S_2$  faults is quartz filling. These quartz zones

are interpreted to have formed via solution transfer accompanying cleavage formation during  $D_2$  (and/or  $D_3$ ).

The second folding event ( $D_2$ ) produced open N-S folds and a regional slaty cleavage  $S_2$ . An episode of faulting occurred post- $S_2$  to pre- $S_3$  probably towards the end of the second deformation. Such faults appear to be geometrically related to  $F_2$  folds. Abundant N-S trending dykes are located within the Eastern Creek Volcanics. They are interpreted to have developed as a relaxation effect along the axial plane of  $F_2$  folds, late or post- $D_2$ .

The third folding event ( $D_3$ ) produced locally developed NNW-SSE trending folds at a low angle to  $F_2$  folds and a NNW-SSE slaty cleavage ( $S_3$ ). The folds are commonly flexures, not persisting for any great length and are often north plunging. Some plunge reversals are evident and these are generally associated with E -W trending faults. NNW -SSE trending faults developed parallel to  $S_3$ . They are steeply dipping, straight to slightly curved and are interpreted to have formed post- $S_3$ . Clean white quartz and fragments of the adjacent country rocks locally occur as fault fill. There is no evidence that this fault fill predates any of the cleavages found in the area. Originating as normal dip slip faults they have later undergone a period of sinistral strike slip movement.

The two deformation mechanisms (folding and faulting) probably overlap considerably. This is because  $F_2$  and  $F_3$  folds have clearly influenced the geometry of faults and some folds may have their geometry controlled/influenced by faults developed early in the structural history (Winsor, 1986). In Winsor's 1986 paper all of the cleavages are described as slaty and there is no mention of crenulation cleavages. In the mine area  $S_3$  has been observed as a pervasive slaty cleavage in dolomitic shale and as a crenulation cleavage in black carbonaceous shale (Swager, 1985).

## 1.9 Mine Structure

### 1.9.1 Early Structural Ideas

#### 1.9.1.1 1942

The significance of faulting and folding of the Mount Isa Group sediments with respect to the development of the copper orebodies has been postulated for many years. In 1942 Roland Blanchard and Graham Hall published the paper “Rock Deformation and Mineralisation at Mount Isa”. In it they describe three events to explain the rock deformation and associated mineralisation observed at Mount Isa.

1. “Major overthrust movement, followed by brecciation, and by invasion of silica.”
2. “Crushing and fracturing movement, followed by invasion of coarsely crystalline “dolomite””.
3. “Main shearing movement, which is divided into three periods, known as the first, second, and third generations of sulphide deposition.”

During all three generations shearing via movement along bedding planes was an important component of the deformation history. “The final phase of the shearing movement manifested itself in part by reopening and slight displacement along various strike faults, together with further restricted shearing which “sprang out” along bedding planes from such faults, and constituted the feeble dying phase of shearing for the district. To a far greater extent the movement (third generation) expressed itself in pronounced fracturing that cut across both country rock and sulphide bands, particularly in the vicinity of the orebodies”(Blanchard and Hall, 1942).

At the time this paper was written, 7 level (300 m) was the lowest producing level. Development on 8 and 9 levels consisted only of exploratory drives. The tops of the 650 and 750 copper orebodies were being explored by drilling and occasional openings. The major 1100 Orebody (12 level and below) had not yet been discovered. Though there has been a lot of modification to the structural model since that time many of the concepts raised are still valid.

### 1.9.1.2 1961

A structural model put forward by Murray (1961) proposed three periods of faulting:

- **Stage 1:** Early development of major strike faults (Mark I) (*The term strike fault is not specifically defined in either, Blanchard and Hall (1942) or in Murray (1961). My interpretation of their usage is that it implies that the fault generally followed the strike of local stratigraphy*). The Mark I faults are a series of dip slip strike faults, some of which can be traced for distances of several kilometres. They appear on the surface as knife edge contacts between different rock types and where the thickness of units within the stratigraphic sequence is known, displacements of over 300 metres have been demonstrated.
- **Stage 2:** Regional thrust from the south produced a series of events:
  1. Initial development of bedding plane slip.
  2. Development of major folds (e.g. Mount Isa Fold).
  3. Development of minor folding (bedding plane slip continues throughout folding episodes).
  4. Ruptures of fold axes giving overthrust structures along shear planes and Mark II (west block up) strike faults (e.g. Urquhart Shear). Mark II faults are narrow shear zones subparallel to bedding. Shear zones of this type exhibit a strong development of polished graphitic foliation surfaces, and quartz occurs as fault fill or augen-shaped bodies in the shear foliation (Mathias & Clark, 1976). Faults such as the Urquhart Shear form parallel to the axial plane of the major folds. The Mark I faults are folded with the bedding.
  5. This movement described in point 4 was believed to be responsible for the formation of broad zones of shearing, fracturing and brecciation, which now form the silica-dolomite orebodies.
  6. Movement on the Mount Isa Fault Zone renews movement on earlier shear planes and caused development of Mark III strike faults. These break cleanly along and across bedding, displacing ore horizons and are not related to any folding.

- **Stage 3:** Relaxation of compressive deformation led to the development of a transverse fault system and cross fracture pattern in the mine block as well as down dip (normal) movement along planes of the Mark III faults.

#### 1.9.1.3 1972

In 1972 the Deep Copper orebodies were referred to as the hangingwall lens and footwall lens of the 3000 Orebody. The footwall lens (now 3500 Orebody) was thought to be a stratigraphically controlled deposit folded by the Mount Isa Fold between 6090 mN and 6270 mN. Where the ore horizon intersected the axial planes of the fold zone it was thickened and enriched. The hangingwall lens was described as a set of en echelon lenses, which had an overall trend of 330°. They appeared to be stratigraphically controlled with brecciated zones developed along the axial plane direction of the fold (Stoker, 1972). Fig 1.3 presents the 1972 sectional interpretation of the Deep Copper orebodies showing the postulated influence of the Mount Isa Fold on the orebodies and the enveloping silica-dolomite alteration front.

#### 1.9.2 Contemporary Ideas

The stage 2 events of Murray (1961) represent a composite of structures that are now interpreted to have formed during  $D_3$ . Detailed structural studies on the 1100 copper orebody by Perkins (1979, 1984) and Bell *et al.* (1988) resulted in the structural model that is applied to the Mount Isa deposits today. Within the mine there is no direct evidence of the first deformation episode which is postulated to have involved north to south movement on large scale thrusts (Bell, 1991). The mine sequence lies on the western limb of a large scale  $D_2$  anticline. This limb rests against a complex postlithification, pre- $D_2$  fault contact (Basement Contact Fault / Paroo Fault) and the chlorite schists (Eastern Creek Volcanics) beneath it. During  $D_3$  a series of fold zones, with subvertical, north-northwest to south-southeast striking axial planes ( $S_3$ ) and steeply south plunging stretching lineations, developed on the  $D_2$  fold limb. The largest  $D_3$  fold in the mine is the Mount Isa fold (Fig 1.4) which has a wavelength of 200 to 400 metres and a near vertical short limb. Other fold zones are usually not wider than 10 to 20 metres. Fig 1.5 is a cross section through the southern end of the Enterprise Mine. This shows the major structural elements that are discussed in the

following sections of this report. Specifically the Basement Contact Fault, faults such as the Urquhart Shear and associated structures and the Mount Isa Fold Zone.

Fig 1.3: 1972 Interpretation of the Deep Copper orebodies (After Stoker, 1972).

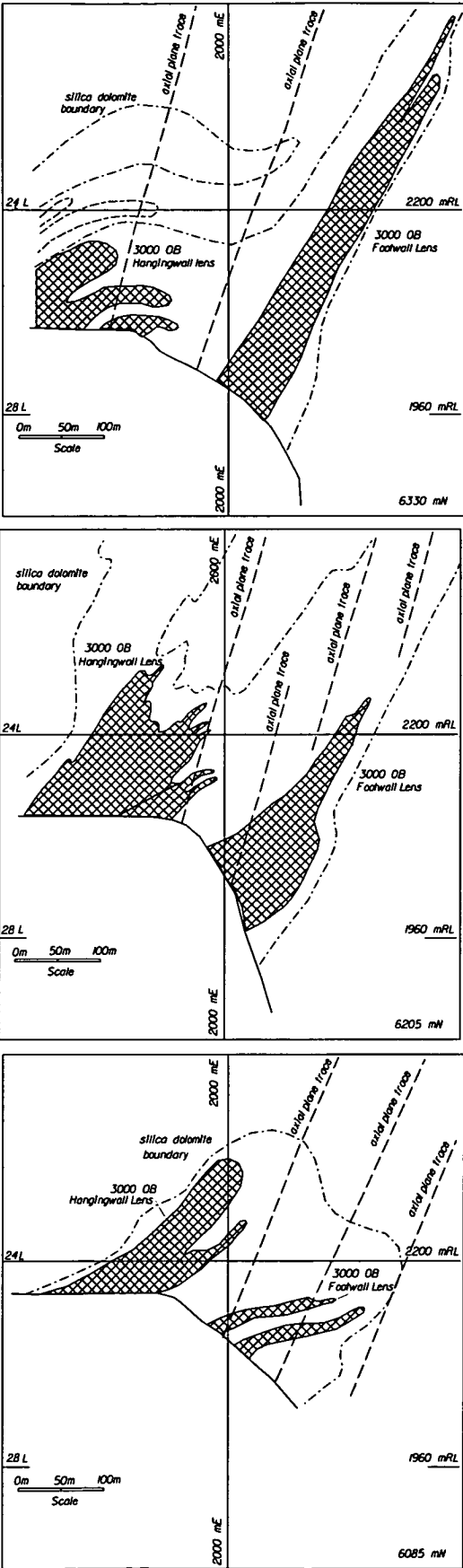
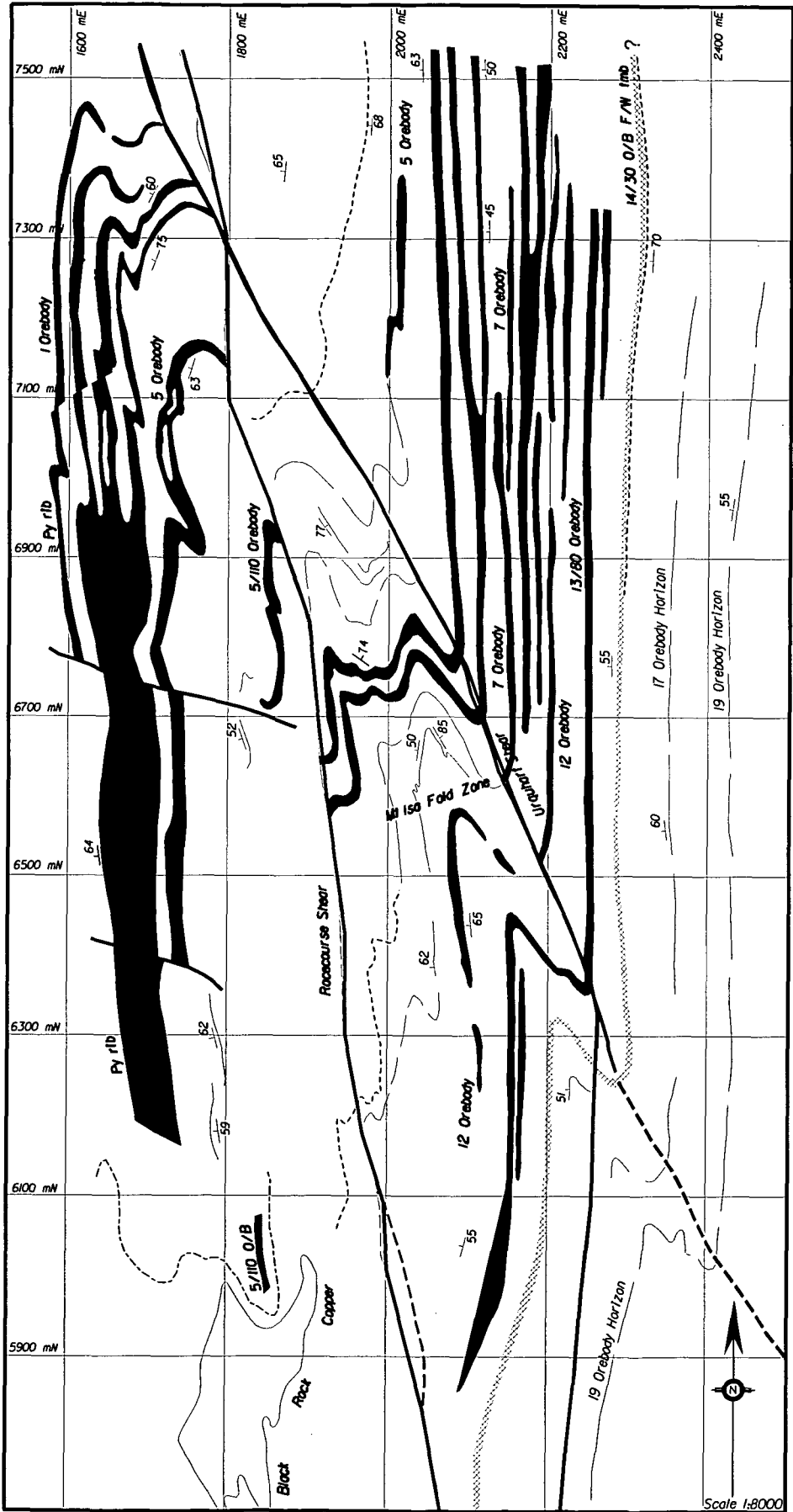




Fig 1.4: Surface plan of the Mount Isa Fold Zone (From MIM internal exploration review, 1992).





# Alteration

## 2.1 Introduction

Historically the alteration associated with the Mount Isa copper orebodies has been referred to as the “silica-dolomite”. Over the years there has been a blurring of terminology, such that the names given to different lithological units within the copper mines at Mount Isa, actually reflect the original host rock, the dominant style of alteration and the texture. This chapter provides a description of these alteration ‘rock types’ and their distribution, as observed in the Enterprise Mine.

Details of talc alteration, phyllosilicate alteration and associated Pb-Zn mineralisation which occur on the footwall of the 3500 Orebody are described, as is the relationship between copper grade and silicification. The descriptive section is based on data collected for this study. The discussion section provides an interpretation of the observations, and where possible, comparisons with relevant previous studies on the 1100 Orebody are made.

## 2.2 ‘Rock Type’ Descriptions

The original dolomitic shale host has been altered to any of four ‘rock types’:

1. Fractured siliceous shale.
2. Siliceous shale.
3. Irregularly brecciated dolomitic shale.
4. Recrystallised shale.

These subdivisions are the same as those defined by Mathias and Clark (1975) with the addition of siliceous shale as a separate entity. Detailed mineralogical descriptions of these ‘rock types’ can be found in Knights (1975). He describes samples from the 1100 Orebody, which have very similar characteristics to rocks from the Deep Copper orebodies. The following descriptions are based on a combination of descriptions by Mathias and Clark (1975) and Knights (1975).

### 2.2.1 Shale and Pyritic shale

Interbedded dark grey, carbonate-poor and carbonaceous rhythmite (centimetre thick couplets of parallel-laminated siltstone and non-laminated mudstone) and carbonate (dolomite)-cemented siltstone (Neudert, 1996). Pyritic shale is classified depending on its fine grained pyrite content, either 5% - 20% (P) or >20% (Y). Fine grained pyrite is interpreted to have formed during diagenesis of the sediments (Neudert, 1983). It forms dull bronze coloured laminae and millimetre scale bands. Later dissolution and recrystallisation processes can lead to centimetre scale bands of pyrite with thin laminae of carbonaceous material.

### 2.2.2 Fractured siliceous shale

Equivalent to the brecciated siliceous shale described by Mathias and Clark (1975). A black to dark grey variably brecciated carbonaceous chert. Fragments of silicified shale are set in a grey quartz-sulphide matrix. There is a wide range of textural types ranging between two end members:

1. Fractured chert with fractures infilled with chalcopyrite; clasts are angular and show little displacement relative to each other.
2. Angular to subrounded clasts occur in a matrix of massive sulphide (chalcopyrite and pyrite, lesser pyrrhotite).

### 2.2.3 Siliceous shale

Very dark grey to black carbonaceous chert with well preserved bedding textures. The bedding can be outlined by fine grained pyrite laminae or by millimetre scale white chert laminae. Associated copper mineralisation tends to be low grade with the chalcopyrite infilling fractures that both crosscut and are parallel to bedding. Originally included by Mathias and Clark (1975) with brecciated siliceous shale - this 'rock type' occurs with sufficient regularity to place it as a separate unit. Boundaries with fractured siliceous shale are often gradational but they can generally be mapped out. A variant of siliceous shale is pyritic siliceous shale in which fine grained pyrite laminae make up greater than 5% of the rock.

### 2.2.4 Irregularly brecciated dolomitic shale

A pale grey breccia of dolomitic and/or siliceous fragments set in a crystalline dolomite-quartz matrix. The percentage of matrix material can vary between 5% and 95%. The less matrix-rich forms are more like a shale cut by anastomosing dolomite veins. The defining characteristic is that bedding textures are not preserved in situ. Individual clasts may exhibit bedded textures. These clasts can be markedly rotated with respect to adjacent “normal” bedding orientations.

### 2.2.5 Recrystallised shale

A well bedded rock with alternating bands of black/grey shale and light grey crystalline dolomite and recrystallised quartz. Porphyroblastic textures can develop in the coarse dolomite layers distorting original layering and in some cases producing a boudinage texture. Bedded fine grained pyrite and recrystallised coarse grained pyrite are common. Chalcopyrite and pyrrhotite are associated with dolomite-quartz veins with sporadic coarse grained pyrite. Pyrrhotite can occur as layers concordant to bedding. The dolomite layers display varying degrees of recrystallisation. An increase in the dolomite to quartz ratio is accompanied by an increase in the dolomite grain size. The end product is an accumulation of coarsely equigranular dolomite, which retains in part some relict bedding. Relict bedding is defined by primary layering of carbonaceous material and fine grained pyrite.

### 2.2.6 Summary

The ‘rock type’ names reflect the dominant style of alteration and the major textural characteristics of the lithological unit being described. The original dolomitic shale/siltstone may have been either silicified or dolomitised, and it may or may not be brecciated. The textural character is based on the degree of brecciation and the extent to which bedding features have been preserved.

Alteration	Texture	‘Rock Type’
Silicification	Brecciated	Fractured siliceous shale
Silicification	Bedding preserved; little or no brecciation	Siliceous shale
Dolomitisation	Brecciated	Irregularly brecciated dolomitic shale
Dolomitisation	Bedding preserved; little or no brecciation	Recrystallised shale

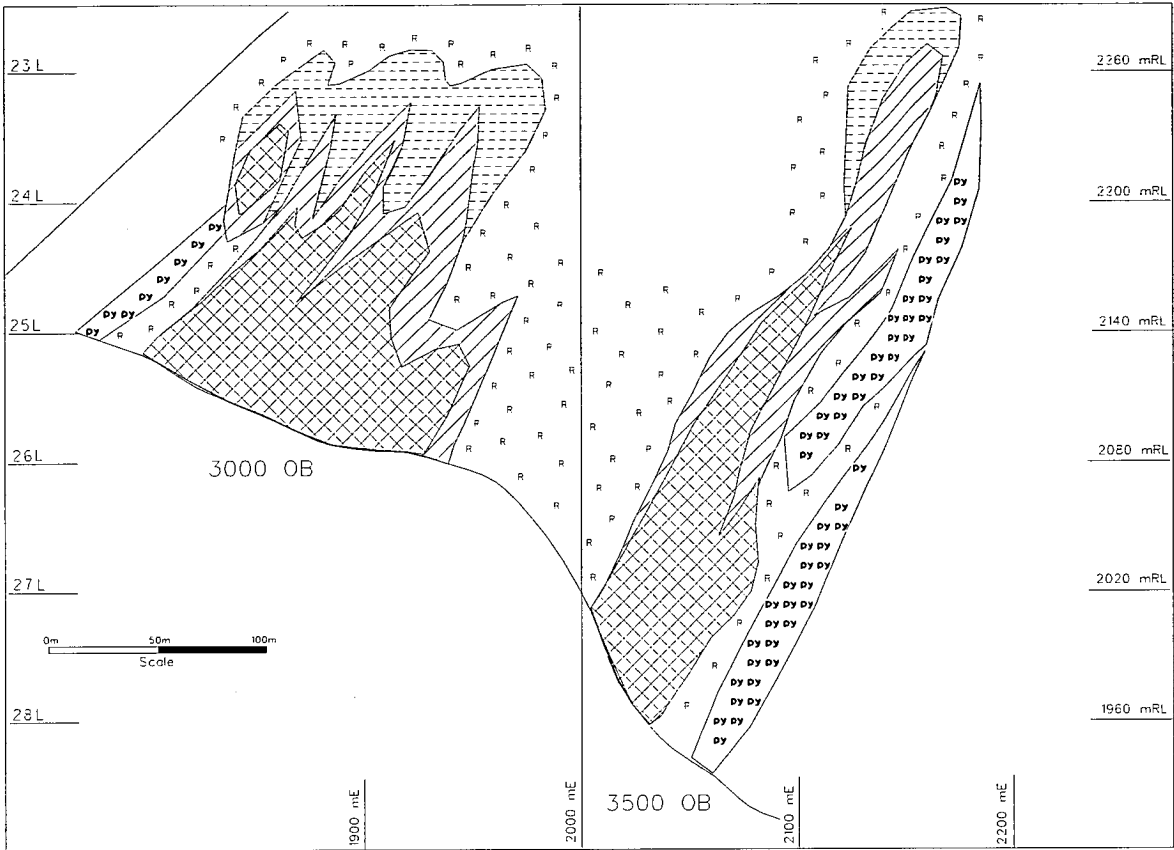
## **2.3 Rock type Distribution and Formation**

### **2.3.1 Distribution**


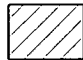
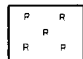

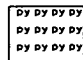
#### *2.3.1.1 Deep Copper orebodies*

The distribution pattern of the four main 'rock types' remains broadly consistent from section to section for both the 3000 Orebody and the 3500 Orebody. For this reason I have presented in Fig 2.1 an idealised section of the two orebodies with the characteristic distribution of the different 'rock types'.

Fig 2.1: Generalised distribution of alteration ‘rock types’ around the Deep Copper orebodies.



LEGEND

-  Fractured siliceous shale
-  Siliceous shale
-  Recrystallised shale
-  Irregularly brecciated dolomitic shale
-  Pyritic shale (> 10% fine grained pyrite)

Fractured siliceous shale forms the core of the orebody adjacent to the basement contact fault. Moving up-dip and away from the core the degree of brecciation diminishes and the fractured siliceous shale grades into siliceous shales. In the 3000 Orebody fractured siliceous shale is dominant over siliceous shale. The 3500 Orebody has a more 'layered' appearance with bands or lenses of fractured siliceous shale intercalated with siliceous shale. Both orebodies have up-dip lobes, which though separate from the main orebody have a central zone of silicification. Recrystallised shale occurs around the edges of the siliceous zones. It is the dominant rock type between the two orebodies. The contact with siliceous shales can be gradational or sharp. Sections of the recrystallised shale can be pyritic. Very strongly pyritic shale layers (>20% fine grained pyrite) occur in the hangingwall of the 3000 Orebody and in the footwall of the 3500 Orebody. There is a slight increase in fine grained pyrite content at the southern footwall edge of the 3000 Orebody and the southern area of the 3500 Orebody (5800 mN - 6150 mN). The main body of shale/recrystallised shale between the two orebodies is low in pyrite content and isolated very thin lenses of lead and zinc mineralisation do occur. Irregularly brecciated and dolomitic shale and crystalline dolomite are restricted to the up-dip limits of the orebodies. This zonal distribution of the siliceous and dolomitic 'rock types' is equivalent to that described around the 1100 Orebody by Perkins (1984) and Waring (1990). Fig 2.2 shows the distribution of the 'rock types' in the 1100 Orebody on section 4200 mN (from Waring, 1990). This is approximately two kilometres south of the "type" section shown in Fig 2.1. In Waring's section, siliceous shale and fractured siliceous shale have been grouped together, as have the dolomitic rock types, recrystallised shale and irregularly brecciated dolomitic shale.

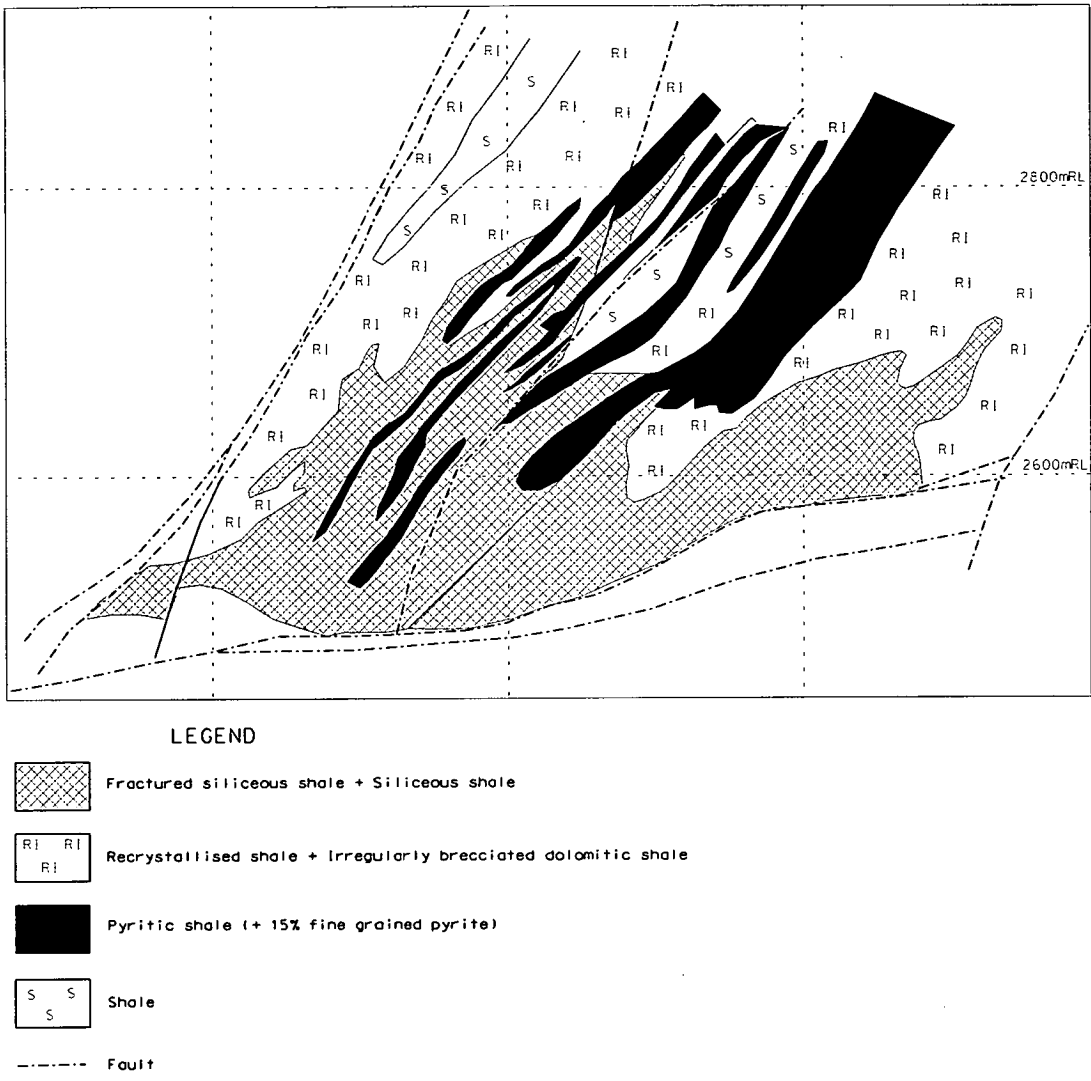
### *2.3.1.2 Comparison with 1100 orebody*

Waring (1990) described a zonal distribution of siliceous and dolomitic rock types in the 1100 Orebody. An inner siliceous zone occurs adjacent to the Buck Quartz Fault/Paroo Fault (this fault system is in the same relative position to the orebody as the basement contact fault is to the Deep Copper orebodies). An outer zone of dolomitic alteration surrounds the siliceous core. The margin of the two zones is irregular and individual contacts may be "knife-edged" or gradational. Features such as stylolitic seams, carbonaceous fault planes or stratiform pyrite define abrupt



contacts. Gradational contacts result from partial dolomitisation, such as incipient development of recrystallised shale or through partial silicification. Patches of silicification do occur away from the inner core in up-dip extensions of the orebody. Bands of >15% fine grained pyrite interfinger with siliceous and dolomitic rock types.

Fig 2.2: Alteration 'rock type' distribution in the 1100 Orebody at 4200 mN  
(Adapted from Waring, 1990).



### 2.3.2 'Rock Type' Formation

#### 2.3.2.1 *Silicification and Dolomitisation Alteration Processes*

Studies by Swager (1983, 1985) and Perkins (1984) concentrated on determining the mechanics of formation of the 'silica-dolomite' rock types. Episodes of alteration were linked to different stages of the three deformation events. A summary of their work follows.

The N-S  $D_2$  event produced a weak  $S_2$  cleavage and widespread  $D_2$  veins and the NNW-SSE  $D_3$  phase was responsible for development of the macroscopic fold zones in the mine area and  $S_3$  cleavage.  $D_3$  folds developed initially by some flexural slip on  $S_2$  and/or bedding, followed by the main flattening stage during which  $S_3$  was formed. Pressure solution is interpreted to be the main  $D_3$  deformation mechanism on the basis of microstructural evidence involving both new  $D_3$  and old  $D_2$  elements. Dissolution and solution transfer of dolomite +/- quartz out of the shales was partly controlled by the pre-existent  $S_2$  seams, which consequently played an important role in the development of  $S_3$  seams. Before  $D_3$ , the  $D_2$  seams formed a continuous layering in the carbonaceous shales but only isolated planar anisotropies in the dolomitic shales. In the carbonaceous shales, shortening in fold hinges could only take place by microfolding of the  $S_2$  layering and subsequent  $S_3$  crenulation cleavage development. In the dolomitic shales  $S_3$  cleavage probably formed in thin zones of intensive shear and solution transfer. Dolomitic siltstone and pyrite beds responded to deformation by a component of brittle deformation in siltstone (microveining and boudinage) and irregular extension fracturing in pyrite beds. Dolomite replacement veins and pseudobreccia complexes (breccia veins) developed with varying intensity when fluid pressures exceeded  $\sigma_3$  during the  $D_3$  stress regime. They formed during the same time as large scale three stage carbonate and silica replacement processes.

The recrystallised shales are interpreted as the first stage products of the total replacement process in which solution migration of dolomite and quartz resulted in layer controlled porphyroblastic dolomite replacement and discontinuous pseudomorphic silicification. They are the recrystallised (dolomite growth in situ) and silicified (dolomite replacement by quartz) equivalents of the normal dolomitic

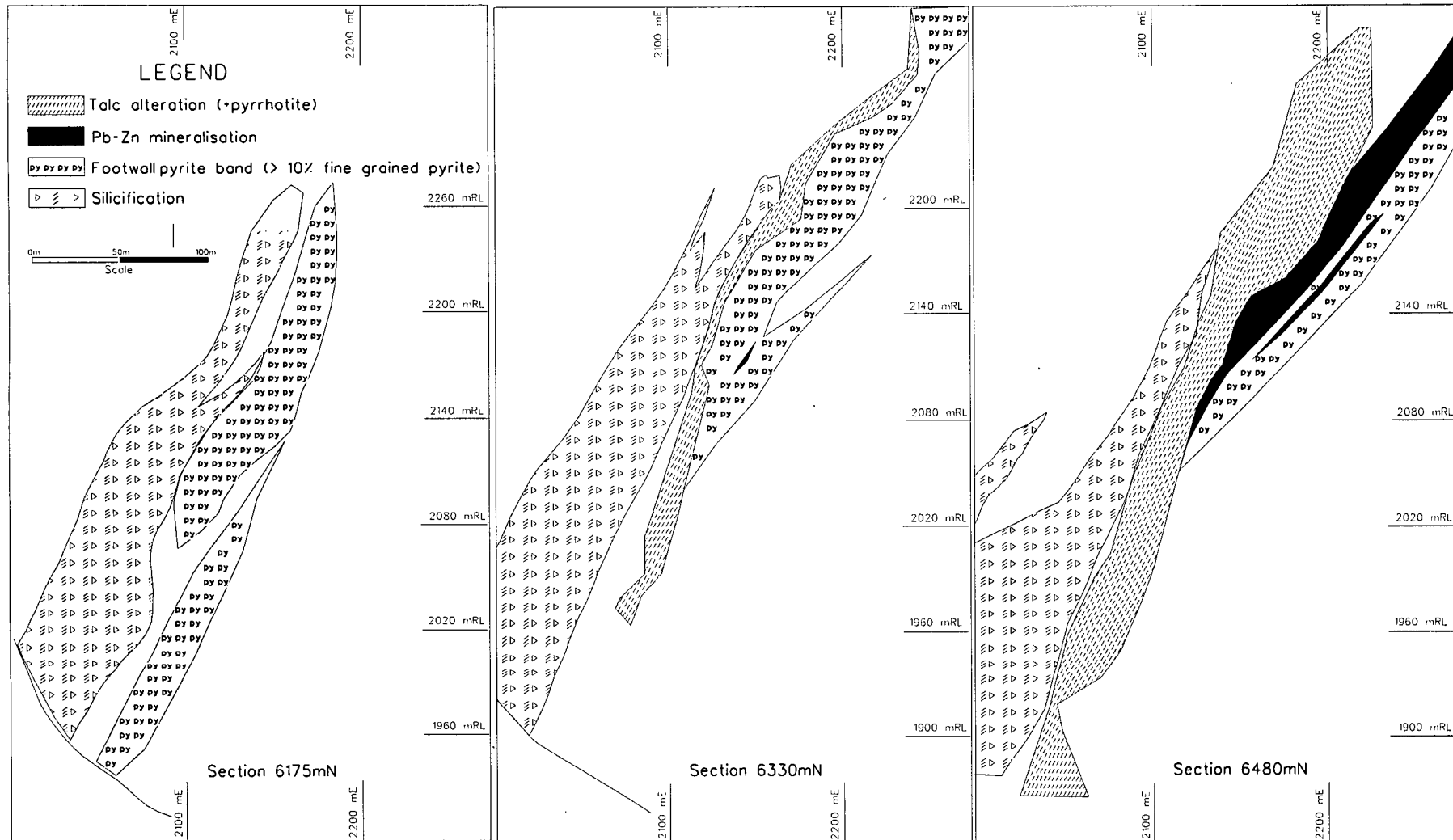
Urquhart Shale. The more shaly layers were preferentially silicified, whereas the dolomitic siltstones underwent recrystallisation. The processes of recrystallisation and silicification are considered as one event even though silicification probably continued in the dolomite rich layers after carbonate growth ceased. These processes postdated the  $D_2$  deformation and had stopped before the  $D_3$  deformation was complete (early syn- $D_3$ ). This timing constraint is from the interpretation (by Swager, 1985) that  $D_2$  veins in the recrystallised shales lost their original fibrous textures during recrystallisation. During this first stage dolomite did not replace quartz.

The second stage development of irregularly brecciated dolomitic shale is ascribed to an early syn- $D_3$  period of dolomitisation involving exaggerated carbonate growth and replacement of siliceous shale. In favourable zones, combinations of bedding and fracture-controlled replacement continued until total dolomitisation of the former shales occurred. Rotated fragments within irregularly brecciated dolomitic shale and associated breccia veins show different orientations of less intensely developed  $S_3$  cleavage. Quartz-filled (late)  $D_3$  fractures also occur within irregularly brecciated dolomitic shale/crystalline dolomite. Bedding parallel stylolites often occur along the contact between siliceous layers and dolomitic layers.

The third stage involved further silicification with associated chalcopyrite mineralisation. There is a preferential replacement of dolomitic matrix and veins by chalcopyrite +/- pyrrhotite. Chalcopyrite was associated with extension both subparallel and subperpendicular to bedding. Deposition occurred before the end of  $D_3$ . The extension structures suggest the mineralisation occurred under high fluid pressures. The fractured siliceous shale breccias represent the end product of total silicification and chalcopyrite replacement. All forms and stages of dolomitic pseudobreccias are preserved by pseudomorphic quartz replacement in silicification zones, which form the cores of the copper orebody systems, and also occur in smaller patches throughout the silica dolomite alteration.

The zonal arrangement of dolomitisation halos around silicification cores results from progressive silica introduction and consequent continuous mobilisation of dolomite. As silicification continued and the fluids interacted with an increasing volume of shale, their composition changed. The capacity of the fluids to replace dolomite by quartz decreased with increasing distance from their point of entry into the shales. The transition from siliceous to recrystallised shales represents this decrease in silicification intensity. Extensive dissolution of dolomite by the silicifying fluids changed the fluid composition until it became (over)saturated with carbonate and started to redeposit dolomite, resulting in the development of crystalline dolomite/irregularly brecciated dolomitic shale. The final stage involving the deposition of chalcopyrite and quartz completed the development of the virtually carbonate-free and copper-rich fractured siliceous shales.

Fig 2.3: Cross sections at 6175 mN, 6330 mN and 6480 mN showing the distribution of the footwall pyrite band, talc+pyrrhotite zone and Pb-Zn mineralised zone. This figure is explained in the following section.



## 2.4 3500 Orebody Footwall Alteration

The immediate footwall of the 3500 Orebody consists of a band of fine grained pyrite (+10% pyrite) and two adjacent zones of distinctive alteration. A talc rich zone with pyrrhotite and a phyllosilicate zone associated with a band of lead and zinc mineralisation. Neither of these alteration zones occurs on the footwall of the 3000 Orebody. Fig 2.3 shows the spatial distribution of these features in a series of cross-sections progressing from south to north.

### 2.4.1 Footwall Pyrite Band

From the southernmost extent of the main lens of the 3500 Orebody up to approximately 6330 mN, there is a well defined band of fine grained pyrite in the footwall of the orebody. This band contains greater than 10% pyrite and is concordant with bedding.

### 2.4.2 Talc Alteration

North of 6330 mN a zone of talc and pyrrhotite begins to develop in the same position relative to the orebody as the pyrite band to the south. This talc zone intensifies towards the north and begins to encroach on the up-dip portions of the orebody from 6480 mN. Recent drilling at 6750 mN shows that the talc (+ chlorite) envelops the orebody, occurring on the hangingwall and the footwall. The talc occurs in a recrystallised shale horizon. It constitutes up to 30 wt% of the rock and is closely associated with increased chlorite and pyrrhotite concentrations. The talc zone is not strictly stratabound and its distribution changes from south to north. It is often localised in bedding plane shears or fault margins, but within the matrix of the recrystallised shale it appears to be pseudomorphic after dolomite.

### 2.4.3 Pb - Zn Mineralised Zone and Phyllosilicate Alteration

Immediately to the footwall of the talc-pyrrhotite zone there occurs a zone of patchy lead and zinc mineralisation with an associated alteration assemblage of phyllosilicate minerals. The Pb-Zn bands are concordant with bedding and are truncated by the footwall contact of the 3500 Orebody. As the talc-pyrrhotite zone intensifies to the north so does the increase in abundance of lead and zinc. The

boundary between the talc-pyrrhotite zone and the Pb-Zn horizon is quite sharp with the first occurrence of galena and sphalerite coinciding with a marked decrease in pyrrhotite and an increase in pyrite. Radiating needles of stilpnomelane are ubiquitous. The alteration assemblage associated with this Pb-Zn mineralisation is characterised by alternating beds of distinctive mineralogies. Microscopic examination of several samples by Knights (1996, 1997) identified the following mineral associations:

- Iron rich carbonate - siderite and magnesian siderite.
- Iron rich phyllosilicates - biotite, ferrostilpnomelane.
- Barium mineralogy - barite, barium feldspars {celsian -  $\text{BaAl}_2\text{Si}_2\text{O}_8$ , hyalophane -  $(\text{K},\text{Ba})\text{Al}_2\text{Si}_2\text{O}_8$ } and barium carbonates {norsethite -  $\text{BaMg}(\text{CO}_3)_2$ }.
- Iron-poor sphalerite (honey-coloured) + magnetite.

#### 2.4.4 Interpretation

##### 2.4.4.1 Talc Alteration

Talc formation can be ascribed to a reaction between dolomite and silica:



dolomite                  quartz                                  talc                                  calcite

( from Deer, Howie and Zussman, 1992)

Waring (1990) described two forms of talc from the 1100 Orebody.

1. A low-Fe talc which occurs as a discontinuous rim around the highly siliceous core of the 1100 Orebody south of 4500 mN.
2. A high-Fe talc which occurs in broadly stratabound zones where the silica-dolomite alteration has interacted with fringe Pb-Zn mineralisation.

In terms of its observed spatial relationship to the 3500 orebody the talc zone on the footwall of the 3500 Orebody has the same characteristics as the high-Fe talc described by Waring (1990). There has been no mineralogical analysis done to determine the iron content of the talc in the footwall zone.



#### 2.4.4.2 Phyllosilicate Alteration and Pb-Zn Mineralisation

Swager *et al.* (1987) described three distinctive phyllosilicate zones at the margins of the silica-dolomite bodies. The phyllosilicate zones were defined by the presence of minerals such as talc, stilpnomelane and biotite, which are absent from the bulk of the shales and silica-dolomite 'rock types'. The zones have different mineralogies at different structural-stratigraphic positions relative to the adjacent silica-dolomite lobe geometry:

1. Talc-stilpnomelane zone - within recrystallised shales at the footwall of lobes.
2. Biotite zone (+ stilpnomelane) - in Pb-Zn orebodies and lateral equivalents adjacent to silica-dolomite.
3. Chlorite zone - hangingwall contacts of Pb-Zn orebodies with silica-dolomite lobes (usually at a higher structural/stratigraphic levels than the biotite zone).

This exact zonation was not observed on the footwall of the 3500 Orebody. The talc zone included a high percentage of chlorite and, at least on the mesoscale, did not contain visible stilpnomelane. Stilpnomelane was always associated with the Pb-Zn mineralisation. Swager *et al.* (1987) stated "all zones have pyrrhotite, rather than pyrite as the dominant or only Fe-sulphide". This is only partly true on the 3500 Orebody footwall. Pyrrhotite is the characteristic Fe-sulphide in the observed talc zone, however the Pb-Zn mineralised zone boundary coincided with a marked decrease in pyrrhotite with an associated increase in pyrite. Carbonates associated with the Pb-Zn mineralisation are more Fe-rich and include siderite, magnesian siderite, ankeritic dolomite and ferroan dolomite (Swager, 1983). The origin of the Fe-carbonates is not known, and may be either sedimentary or diagenetic, possibly related to the late diagenetic Pb-Zn mineralisation (Neudert, 1983).

The pyrrhotite may be partly introduced and/or locally derived, for example by breakdown of pyrite (Swager *et al.* 1987). The observation that the talc-pyrrhotite zone occupied the same position relative to the 3500 Orebody as the pyrite band suggests this may be the case. It would seem more than coincidental that the only apparent difference between there being pyrite or pyrrhotite-talc immediately adjacent to the copper orebody is the absence or presence of Pb-Zn mineralisation. The lack of preferred orientation (particularly of stilpnomelane) and the absence of S<sub>2</sub>

fabrics suggests post-D<sub>2</sub> growth of the phyllosilicates. Stilpnomelane and talc distribution suggest that they have overprinted the recrystallised shales formed during the first silica-dolomite alteration stage, which occurred early during D<sub>3</sub> (Swager *et al.* 1987).

## 2.5 Copper Grade Relationship with Silicification

### 2.5.1 Observations

For both orebodies there is a very close association between silicification and copper mineralisation. The term silicification is used here to correspond with the occurrence of the 'rock types' fractured siliceous shale and siliceous shale. Copper mineralisation is always associated with silicification. The degree of silicification however is not directly proportional to the copper grade. Zones of siliceous shales, fractured siliceous shales and silicified slaty shale occur with very low copper grades. The presence of pyritic stratigraphy is generally associated with low (<2.0%) copper grades. Bands of pyritic shale are a cause of grade variation across the orebodies. Figures 2.4 and 2.5 show the silicification boundary and the 2.5% copper grade contour on section 6205 mN and 2150 mRL (25A sublevel) respectively. The 2.5% copper grade contour is the cutoff used for economic mineralisation in the Enterprise Mine.

Fig 2.4: Section 6205 mN - silicification and economic mineralisation.

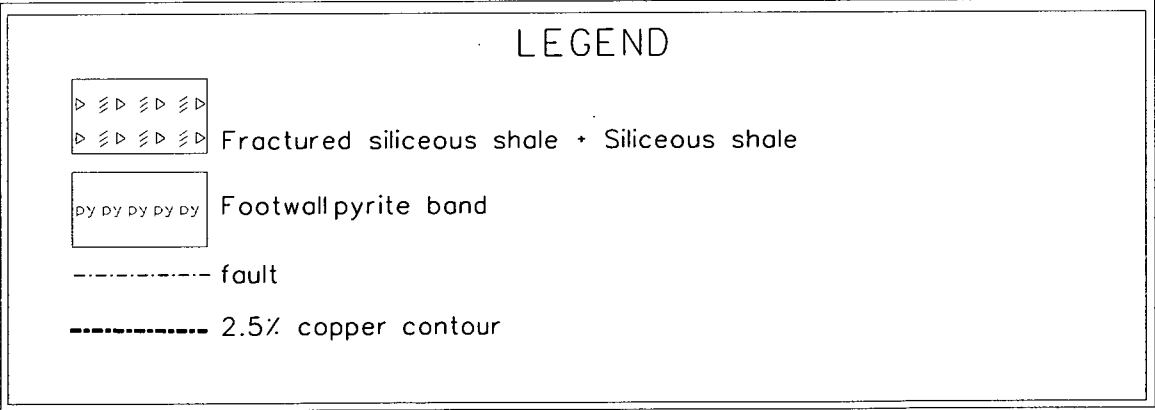
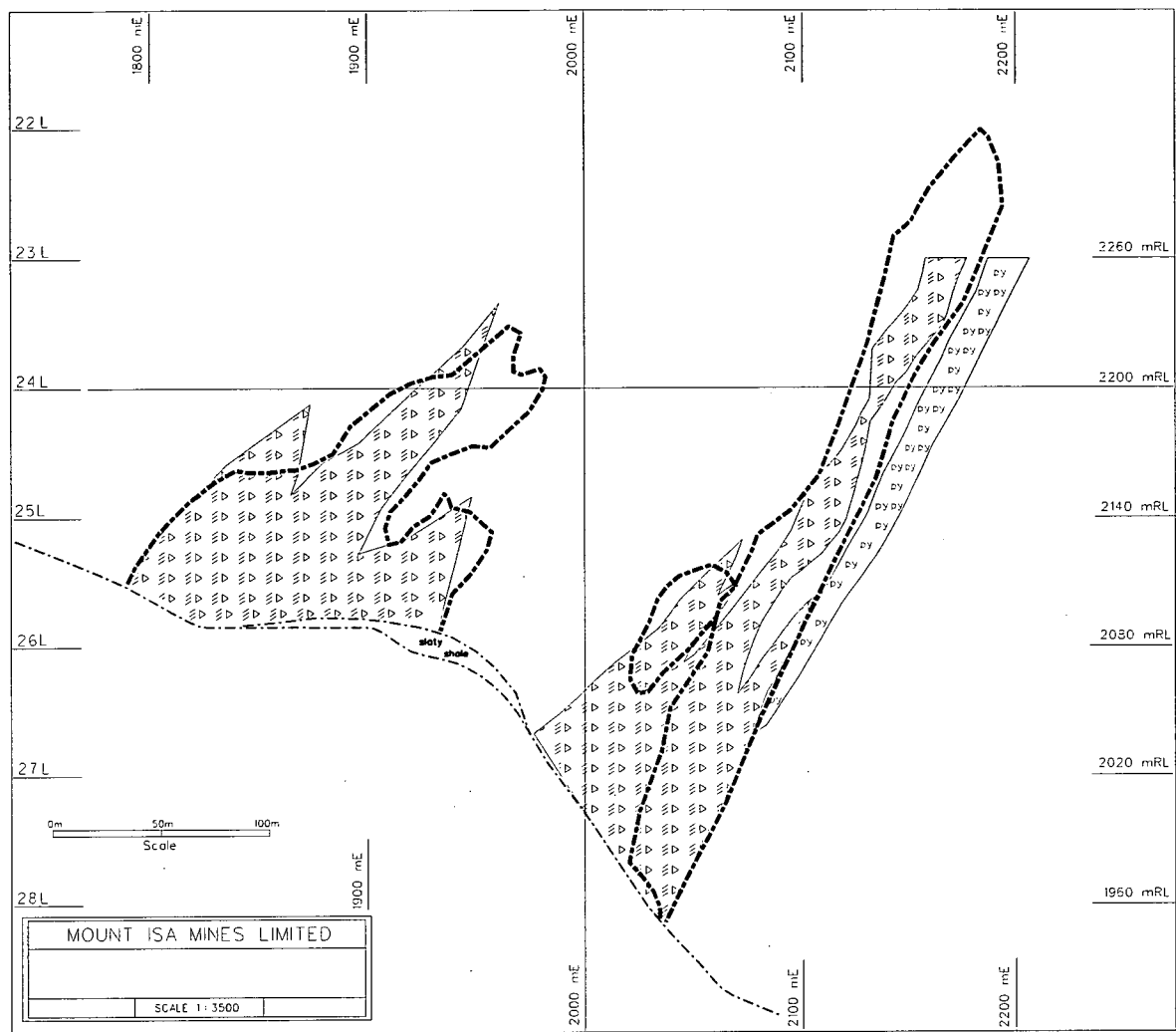
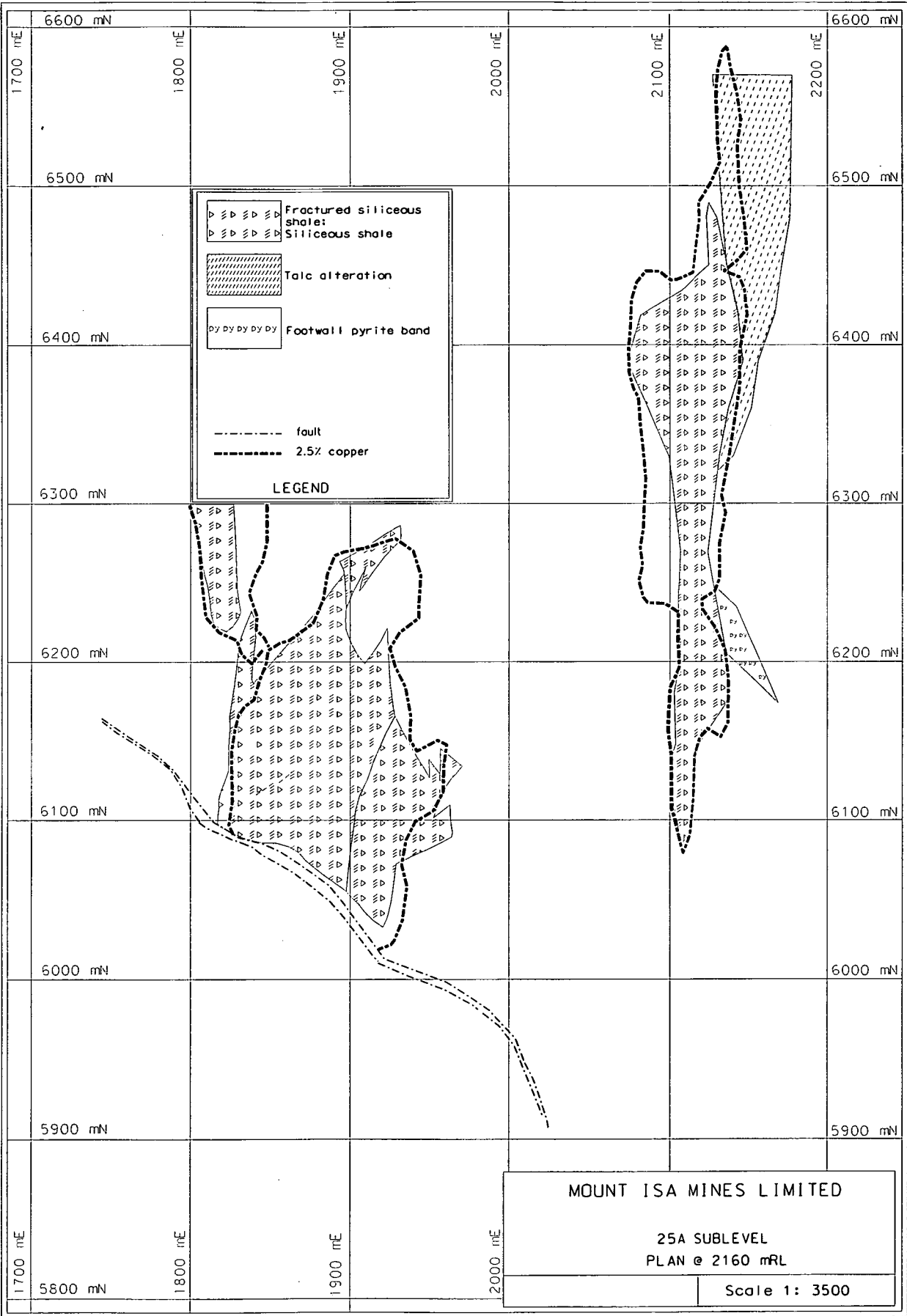


Fig 2.5: Plan 25A (2150 mRL) - silicification and economic mineralisation.



### 2.5.2 Interpretation

Waring (1990) described the following relationship between copper grade and silicification in the 1100 Orebody. Copper grade contours show a zonal distribution pattern of decreasing copper grade away from the Buck Quartz Fault, modified by a secondary dependence on lithology. The spatial association between highly siliceous rocks and chalcopyrite, and the increase in copper grade with silicification suggests a close link between silicification and chalcopyrite deposition. However there is no direct correlation between the degree of silicification and chalcopyrite concentration, particularly for fractured siliceous shale (i.e. the highest degree of silicification does not imply high copper grades). Two possible reasons for this were proposed:

- 1/ silicification is paragenetically separate (earlier) than the bulk of chalcopyrite deposition.
- 2/ silicification is not directly responsible for chalcopyrite deposition; although synchronous, chemically separate processes are involved.

The 3000 and 3500 orebodies show the same relationship. Unfortunately there is only a limited database of silica assays available. A statistical comparison between silica and copper assays is not possible at this time. However, silica is now routinely assayed and as drilling of the orebody extensions continues, a suitable amount of data will be available in the future.

## 2.6 Conclusions

- The “silica-dolomite” alteration ‘rock types’ and their broad distribution patterns are the same for both the 1100 Orebody and the Deep Copper orebodies. Perkins (1984) concluded that the zonal distribution of silica dolomite could be explained as a continuous alteration profile caused by progressive development of an inner silicification front and a concomitant outer dolomite replacement front. He proposed that the disposition of the copper orebodies suggested that the alteration began in a series of focuses. Waring (1990) inferred that there was a single input zone to the entire copper orebody system, south of the orebodies. His observed south to north variation of the silica-dolomite system (i.e. increasing dolomite and decreasing silicification) was described by a model in which several batches

of ore fluid, flow from south to north through a linear array of compositionally variable host rock segments, with assumed sequential equilibration at each segment. The fluid composition evolved in response to chemical reaction with the host rock.

- The 3000-3500 orebody system supports Perkins view of multiple focuses. I conclude that each orebody represents a separate focus. Though they are smaller versions of the 1100 Orebody the percentage of silicified rock types to dolomitic rock types is similar to that of the main body of the 1100 Orebody.
- The stilpnomelane dominant alteration is restricted to the Pb-Zn mineralised zone. Neither talc-pyrrhotite or stilpnomelane alteration occurs on the footwall of the 3000 Orebody where there is no significant occurrence of Pb-Zn mineralisation. The talc- pyrrhotite zone does not occur south of 6330 mN where there is no footwall band of Pb-Zn mineralisation. The intensity of talc-pyrrhotite increases northwards and up-dip, corresponding to an increase in the thickness of the Pb-Zn mineralised zone. The spatial correlation between the footwall fine-grained pyrite band and the talc- pyrrhotie zone suggests that much of the pyrrhotite has been derived at the expense of the fine grained pyrite.

## Basement Contact Fault

The significance of the basement contact fault and the basement rocks themselves has been proposed since the early days of the copper mine (1100 OB). An extract from Cordwell *et al.* (1963) states ... “ The greenstone basement is a major ore control. It is believed that upward extension of subsurface faults originating in fault blocks in the ‘greenstone’ basement was the major control for deposition of the silica-dolomite orebodies. It is considered that hydrothermal solutions entered these faults from channels along the almost flat lying ‘greenstone’ basement.”

This statement serves as an introduction to this chapter in which the physical character and geometry of the basement contact fault beneath the Deep Copper orebodies is described. In chapter four a system of faults, which affects the orebodies, is described. The faults have not originated from within the basement rocks below the contact but they are associated with the geometry of the basement contact fault itself.

The basement contact fault is a complex structure within the Enterprise Mine, which forms the base beneath the copper orebodies. It juxtaposes upper Mount Isa Group against the older Eastern Creek Volcanics. It is analogous to the Paroo Fault, which is mapped at the surface. The Paroo fault crops out east of the Mount Isa Fault and dips steeply west, approximately parallel to bedding. At depth it curves sharply to form an almost flat-dipping structure beneath the Mount Isa copper mines (Fig 3.11).

### 3.1 Contact Zone and Basement Rock Types

The contact zone refers to the volume of rock immediately adjacent to (above and below) the basement contact fault. It can vary in width between five metres and fifty metres. Basement refers to the Eastern Creek Volcanics. The Eastern Creek Volcanics are comprised of both metabasalts and quartzites.

Historically a set of descriptive terms has been applied to the rocks within the basement part of the mine (Mathias & Clark, 1976). These include carbonaceous

mylonite, buck quartz, slaty shale, quartzite, greenstone and siliceous greenstone. They do not necessarily imply the genetic origin of the rock. The same names are used here to allow for ease of correlation if any future work is done on comparing the geological similarities between all the Mount Isa copper orebodies.

### 3.1.1 Carbonaceous Mylonite

This term refers to a black strongly foliated rock containing augen shaped fragments of composite recrystallised quartz, shale rock fragments and occasional porphyroblastic carbonate. The well foliated matrix consists of graphite and fine grained quartz. It is derived from dissolution processes associated with shearing of the original dolomitic siltstones and shales (Mathias & Clark, 1976; Knights, 1975). Its occurrence defines the position of the basement contact fault. It may or may not be associated with buck quartz.

### 3.1.2 Buck Quartz

Buck quartz is massive white vein quartz, which does not show any overprinting foliation or cleavage. It occurs either as massive quartz with minor carbonaceous mylonite (e.g. 25A 330XC) or as a zone of irregularly layered quartz and carbonaceous mylonite which on a gross scale is layered parallel to the confining fault surfaces.

### 3.1.3 Character of the basement contact fault

The basement contact fault has undergone a complex history of movement. It is a shear zone, which generally has well defined boundary faults. The lower contact with the Eastern Creek Volcanics is always sharp and planar. Within the limits of individual exposures the upper surface of the contact is most commonly a strongly planar surface but locally is less well defined particularly where it is adjacent to slaty shale. Another characteristic used to define the limits of the basement contact fault is that it does not contain any copper mineralisation. This feature is used in determining boundaries between the fault and slaty shale zones as the slaty shale zones can be weakly mineralised.



---

Carbonaceous mylonite and buck quartz occur only within the boundary faults of the basement contact fault and display structural features such as multiple foliations, folds, kink bands and crenulations. Fig 3.1a & b show an example of this from 29E below the 3500 Orebody.

**Fig 3. 1a : 740 Xcut 29E. Basement Contact Fault. Layered buck quartz and carbonaceous mylonite. Clay gouge on sharp lower contact with greenstone.**

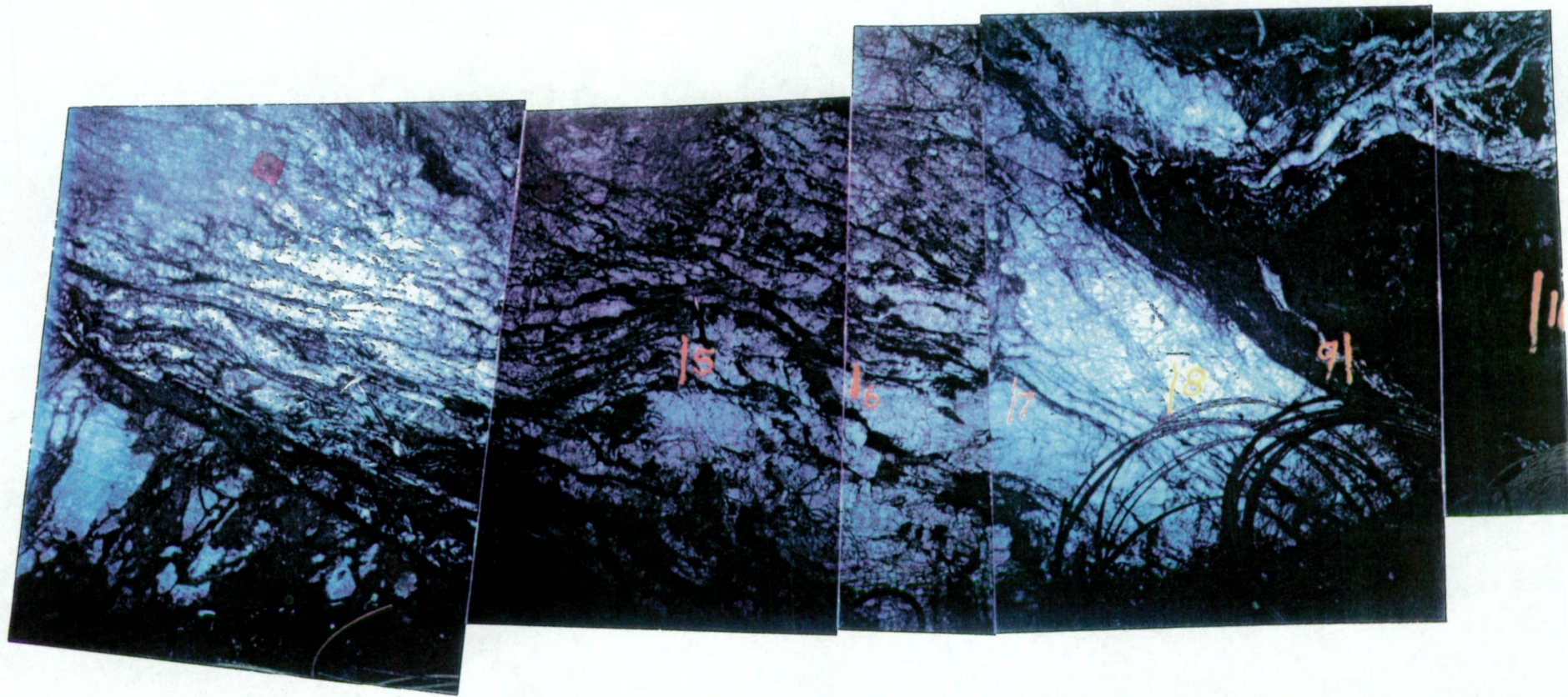
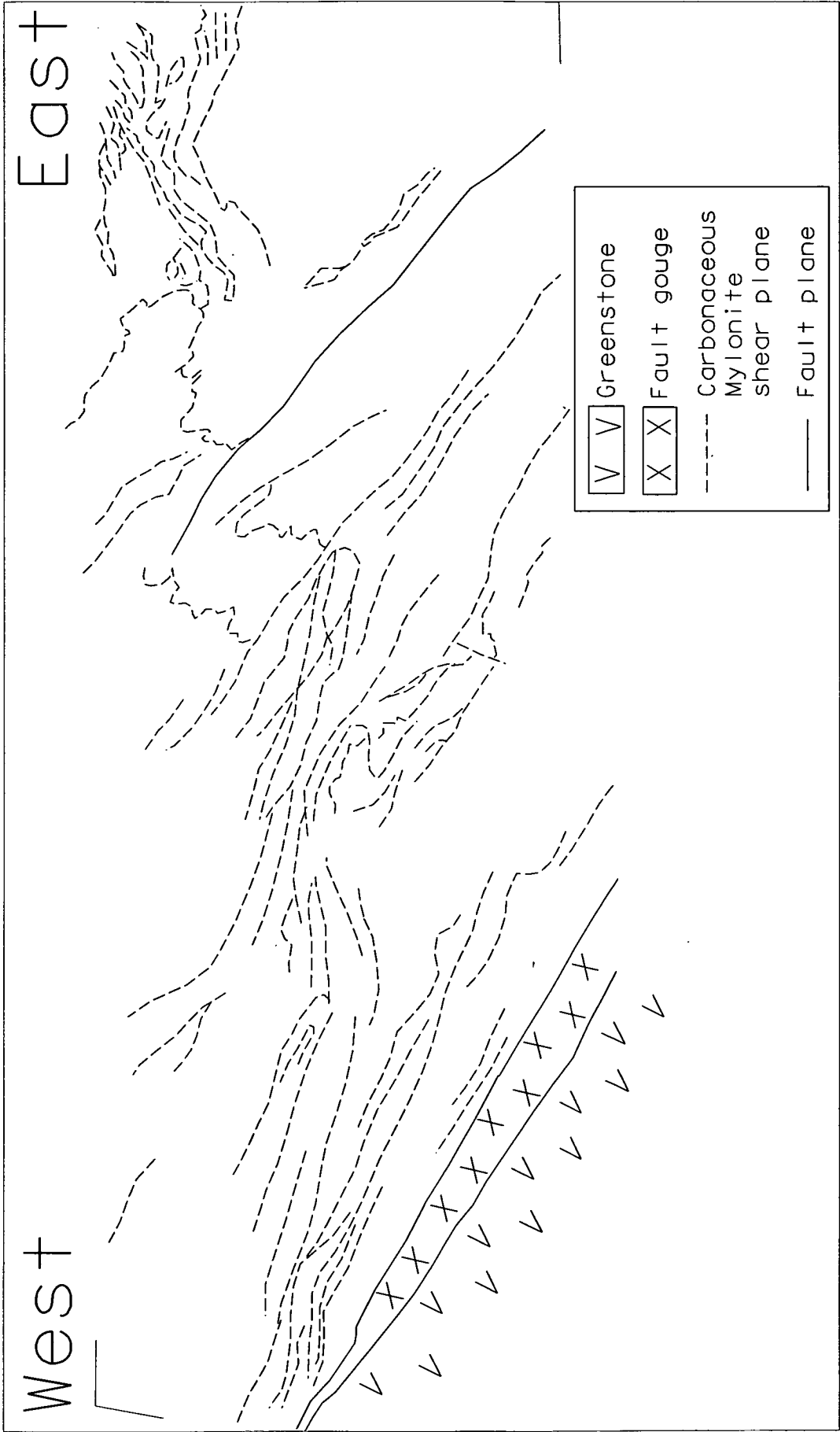


Fig 3.1b: 740 Xcut 29E. Interpretation of figure 3.1a.



### 3.1.4 Slaty Shale

This is a dark grey to black slate with a well developed penetrative cleavage. Slaty shale is a similar rock to carbonaceous mylonite, which has undergone less dissolution and has a greater dolomite component. It contains >5% pyrite cubes in trails parallel to the dominant local foliation. The foliation largely obliterates bedding textures. Slaty shale can contain weak copper mineralisation. Slaty shale does not form within the boundary shears of the basement contact fault but occurs immediately above it.

### 3.1.5 Quartzite

Light grey to buff, fine grained feldspathic quartz arenites. A vague banding is imparted to the rock by concentrated layers of fine grained mica and chlorite. The layering is interpreted as bedding. Adjacent to the basement contact fault this layering is less apparent and the rock is massive with abundant chlorite filled joints/fractures. In localised areas the rock has a shattered texture (more easily observed in diamond drillcore).

### 3.1.6 Greenstone

A dark green to grey, fine grained mass of foliated chlorite enclosing variable sized patches of quartz. The schistosity is marked by alignment of quartz-chlorite lenses together with trains of leucoxene, rutile and sphene. In one of the deeper diamond drill holes greenstone was intersected which had retained its original porphyritic texture. The greenstones are interpreted as basalt flows, sills and dykes, which have undergone greenschist metamorphism to chlorite schists (Mathias & Clark, 1976).

### 3.1.7 Siliceous Greenstone

This term embraces metamorphosed and silicified rocks, which may be of either volcanic or sedimentary origin. It is typically a pale green to dark green-grey quartzose rock with variable chlorite and sericite and/or rutile components. Coarse grained pyrite cubes are always present immediately adjacent to the basement contact fault (i.e. within 5 to 10 metres). Diamond drilling of the area beneath the contact fault on 26B delineated healed shear zones parallel to the contact several metres into

the greenstone/siliceous greenstone. The shears were characterised by, foliated breccias with augens of strained quartz, in a matrix of quartz-chlorite.

The siliceous greenstone is interpreted to be derived from the extensive alteration by hydrothermal fluids of greenstone and/or quartzite. All of the exposures beneath the Deep Copper orebodies have greenstone/siliceous greenstone in contact with the basement contact fault.

### 3.2 Geometry of Basement Rocks

Bedding in the quartzites is the same as in the overlying shales, dipping variably between 40° and 75° to the west (Fig 3.3a). Rare small scale folds have been mapped. Facing directions have not been determined. 'Ripplemark-like' features occur on bedding plane surfaces in some localities. However it is not conclusive whether they are of true sedimentary origin.

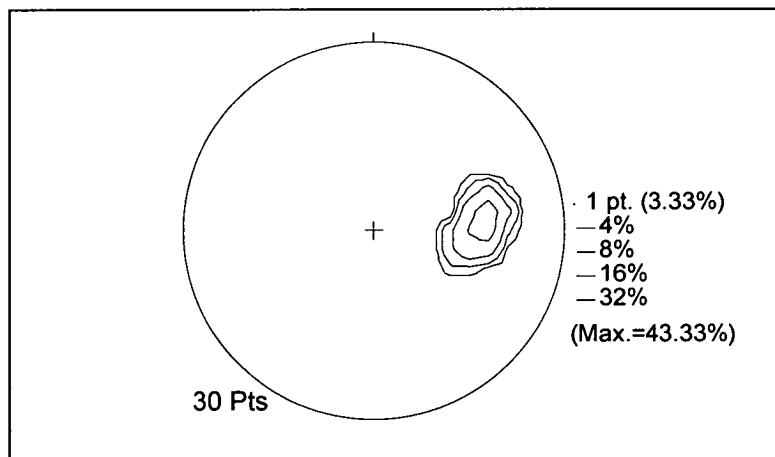


Fig 3.2: Equal area Stereogram of poles to bedding in quartzites.

In the zone immediately adjacent to the basement contact fault, bedding is rarely discernible and complex fault bounded blocks of greenstone, siliceous greenstone and quartzite occur. This zone usually extends up to 50 metres from the base of the contact fault. On sublevels 26B and 26L bedding is rarely identifiable in the quartzites up to 100 metres from the fault. Fig 3.3 shows interpretation of the quartzite and greenstone of the Eastern Creek Volcanics from mapping on 28D, directly beneath the southern 3000 Orebody. The greenstone occurs as a series of

---

NNW trending belts with very high angle dips of 70° to 90° both east and west (Fig 3.3). The greenstone/quartzite boundaries are faults, which are sharp and clearly cut across the bedding in the quartzites (Fig 3.4a & b).

Fig 3.3: Detailed mapping of the Eastern Creek Volcanics beneath the basement contact fault, on 28D.

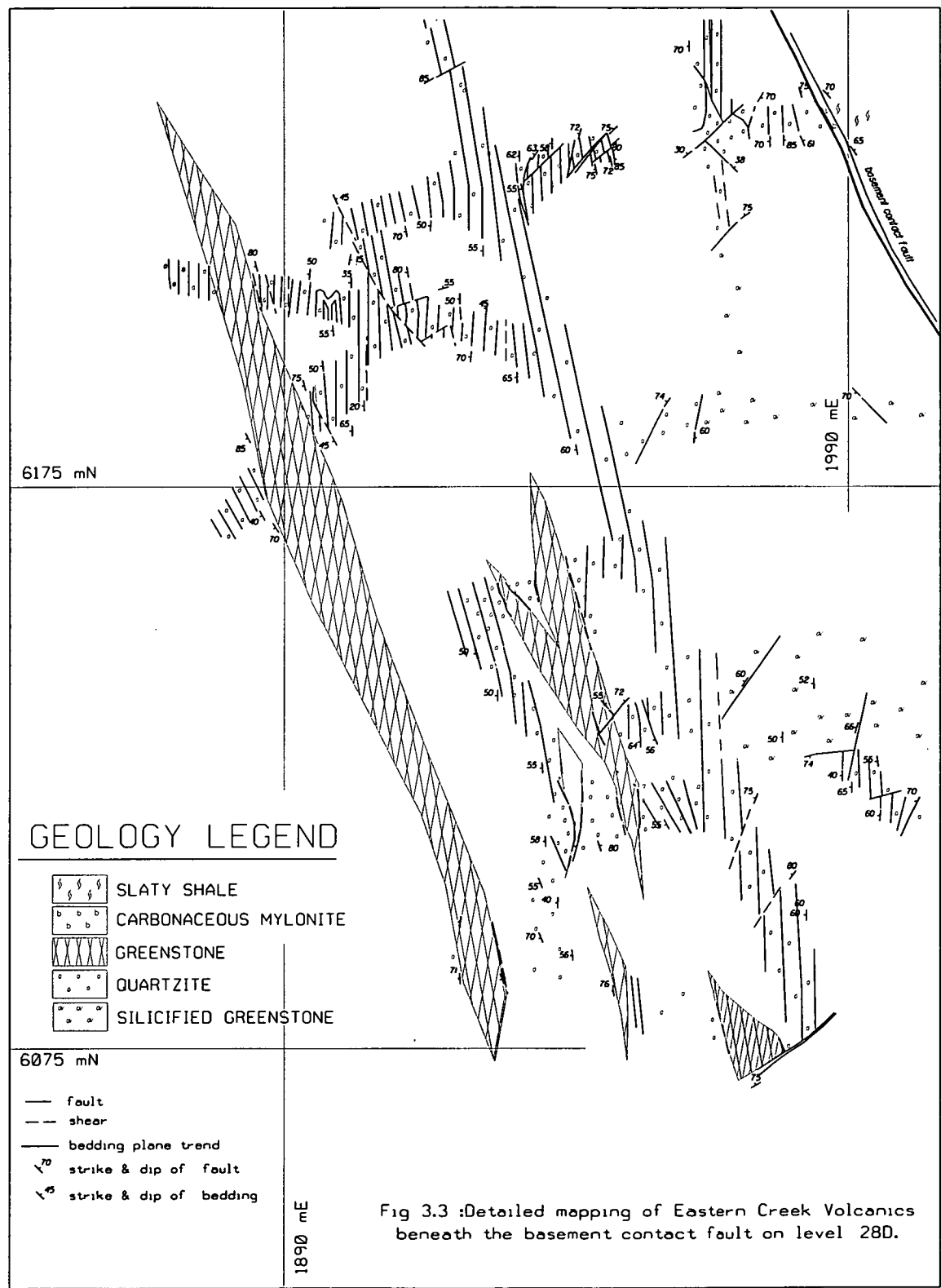
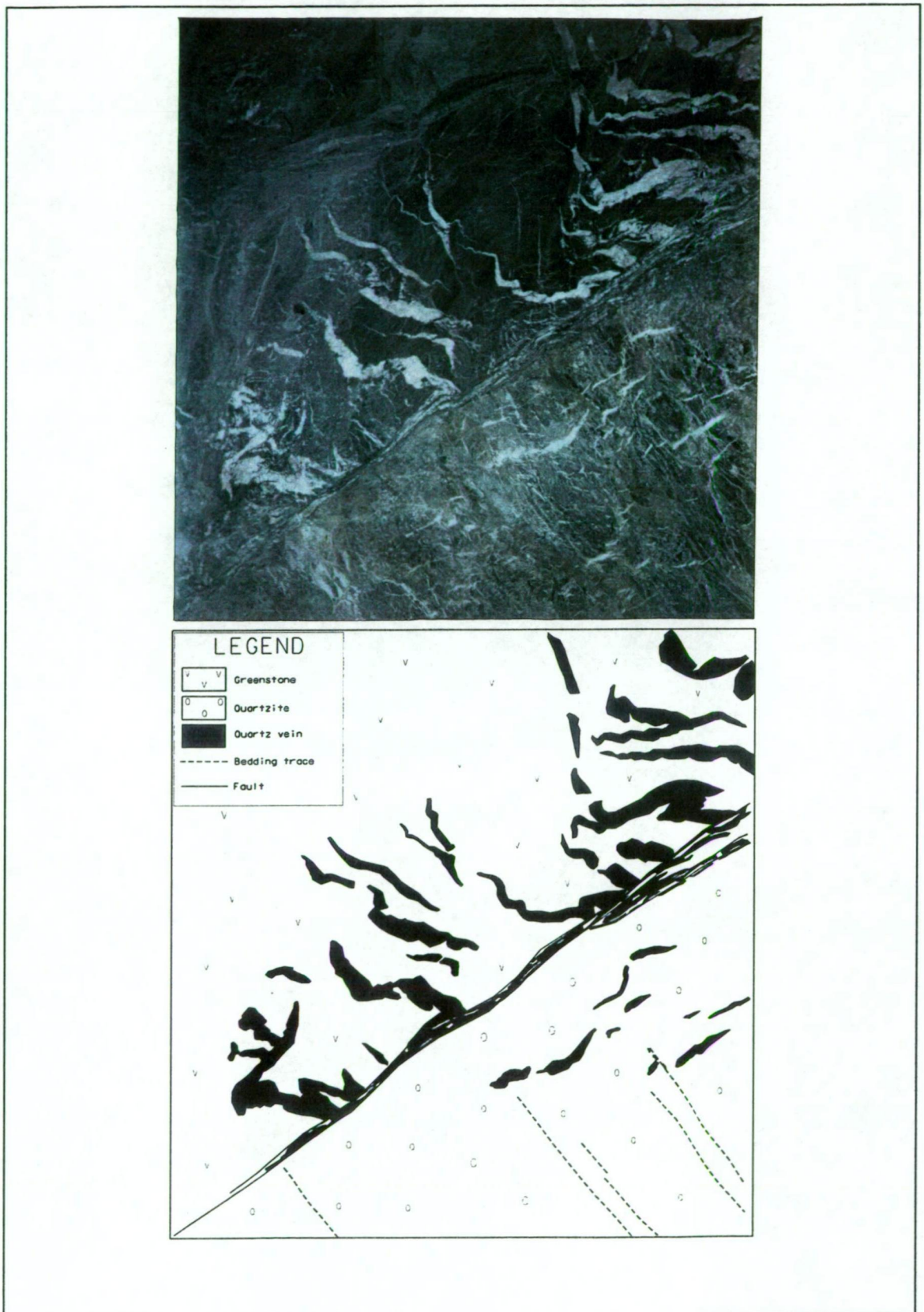




Fig 3.4a & b: Photograph and interpretative sketch of a quartzite/greenstone contact. T62 Decline 30A sublevel. Fault is dipping east and bedding in quartzite is dipping west. (Width of view 1.5m, looking south)





### 3.3 Significance of geometry of Eastern Creek Volcanics

The greenstones underlying the orebodies have no development of primary layering to define folding. Small folds have been observed in the quartzites. Feldspathic quartzites belonging to a separate structural block in the Copper Mine (1100 Orebody; 5000 mN-6000 mN) have a shallow to intermediate northeast dip (Perkins, 1984). Observations by Bell *et al.* (1988) at the southern end of the mine determined that bedding in the greenstones/quartzites below the basement contact fault is parallel or at a small angle to the contact. This is not the case beneath the Deep Copper orebodies.

Bell's (1991) "folded  $D_1$  thrust duplex" model predicted that bedding in the quartzites should overall tend to young downward in spite of subsequent effects of  $D_2$  and  $D_3$ . West dipping bedding that youngs east is predicted from this interpretation of north to south movement of the duplex. His Fig 17A (Bell, 1991 p1616) shows a quite complex fold geometry beneath the 1100 Orebody. This has not been observed in the Enterprise Mine. More study would need to be made to try and verify the facing of the quartzites below the 3000 Orebody to determine if their geometry supported or disproved Bell's model.

### 3.4 Basement Contact Fault Geometry

Beneath the Deep Copper orebodies the basement contact fault has a general northwesterly strike and dips at  $50^\circ$  to  $60^\circ$  towards the northeast.

Fig 3.5a shows a contour map of the upper surface of the basement contact fault. Fig 3.5b presents stereonet data from the six localities shown on Fig 3.5a. The data plotted on the stereonets is the orientation of the upper and lower boundary shear planes of the fault zone at each location. Local geometries are quite complex and rapid changes in dip and strike occur. From early exposures in the mine it seemed that steeper sections of the fault had a lesser thickness of carbonaceous mylonite/buck quartz developed in them than shallow dipping sections. Subsequent

development however has shown there is no consistency to this observation. In one exposure on 26D the fault zone dips at 20° and is 0.5 m thick.

The following section gives details on some of the complexities in the basement contact fault geometry.

#### 3.4.1 3000 Orebody

Figures 3.6, 3.7 and 3.8 show detailed mapping of a flexure in the basement contact fault on three adjacent sublevels (each separated by 20 vertical metres, position marked on Fig 3.5a). The 'normal' dip-dip azimuth of the fault zone on each of these sublevels is 45°- 65° to the northeast. On 26L and 26B there is an abrupt, almost 90° change in strike of the fault zone with a corresponding shallowing of the dip to less than 30°. The flat section is approximately 50 metres wide and dips approximately 17° to the NNW. Complex shearing effects associated with pockets of slaty shale (and lack of exposure) obscure the nature of the inflexion points. On both 26L and 26B very high grade copper ore lies directly on the upper contact surface of the basement contact zone coincident with the flexure in the fold surface. Moving up to 26D the same marked change in strike and dip occurs but a band of weakly mineralised slaty shale occurs between the basement contact fault and the base of the high grade ore. The slaty shale-ore boundary is parallel to the strike of the basement contact fault but is steeper in dip (56° to 85°). The NNW trend of the axial plane of the flexure suggests it is related to movement during D<sub>3</sub>.

#### 3.4.2 3500 Orebody

Very little is known about the detail of the basement contact fault zone below 3500 Orebody. Early indications were that the 3500 Orebody was above a steeper section of the basement contact fault, which was unusual when compared with the 1100 and 3000 orebodies. Recent development on 29E at 6510 mN and 6600 mN exposed a 7 metre thick zone of carbonaceous mylonite and buck quartz, which dips at 25° (Fig 3.1a & b). Mapping showed that it represented a small scale (~10 metre) flexure in the basement contact fault. Weak to moderate mineralisation occurs above this position. Fig 3.9 shows detailed mapping of this exposure. The evidence though is

---

not conclusive that the structural control on the 3500 orebody is the same as that for the 3000 Orebody.

In the upper levels of the Lead Mine at Mount Isa there occur two copper orebodies (500 and 650) which also do not have any direct contact with the basement contact fault. The 3500 Orebody has a geometry that correlates more with these orebodies than with the 1100 or 3000 orebodies.

Fig 3.5a: Contour map of the upper surface of the basement contact fault (contours at 10m intervals). The marked locations are those where the fault zone orientation was measured and where the detailed information for Figs 3.6, 3.7,3.8 and 3.9 was collected.

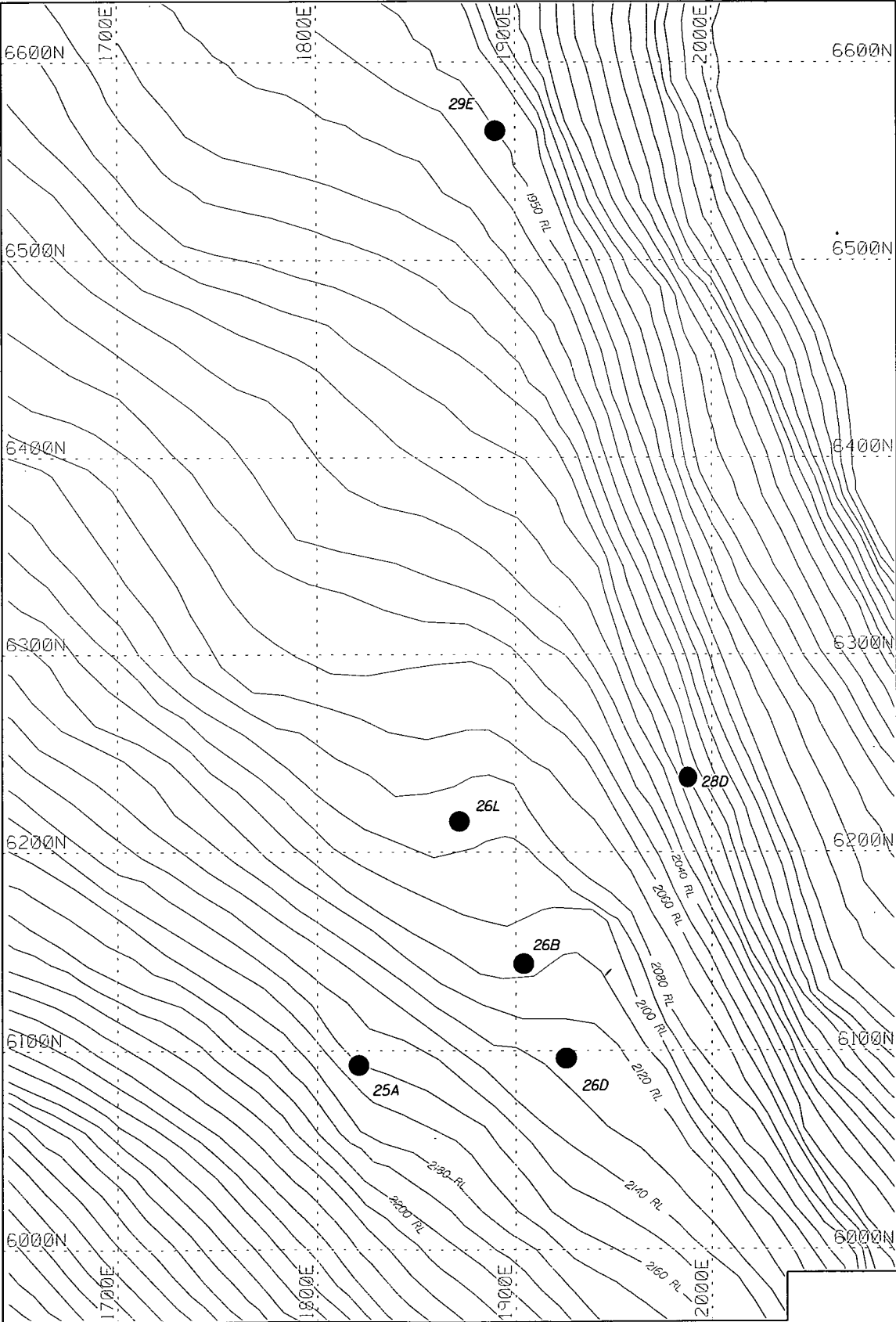


Fig 3.5b: Equalarea stereograms of poles to fault planes, from the six localities shown in Fig 3.5a.

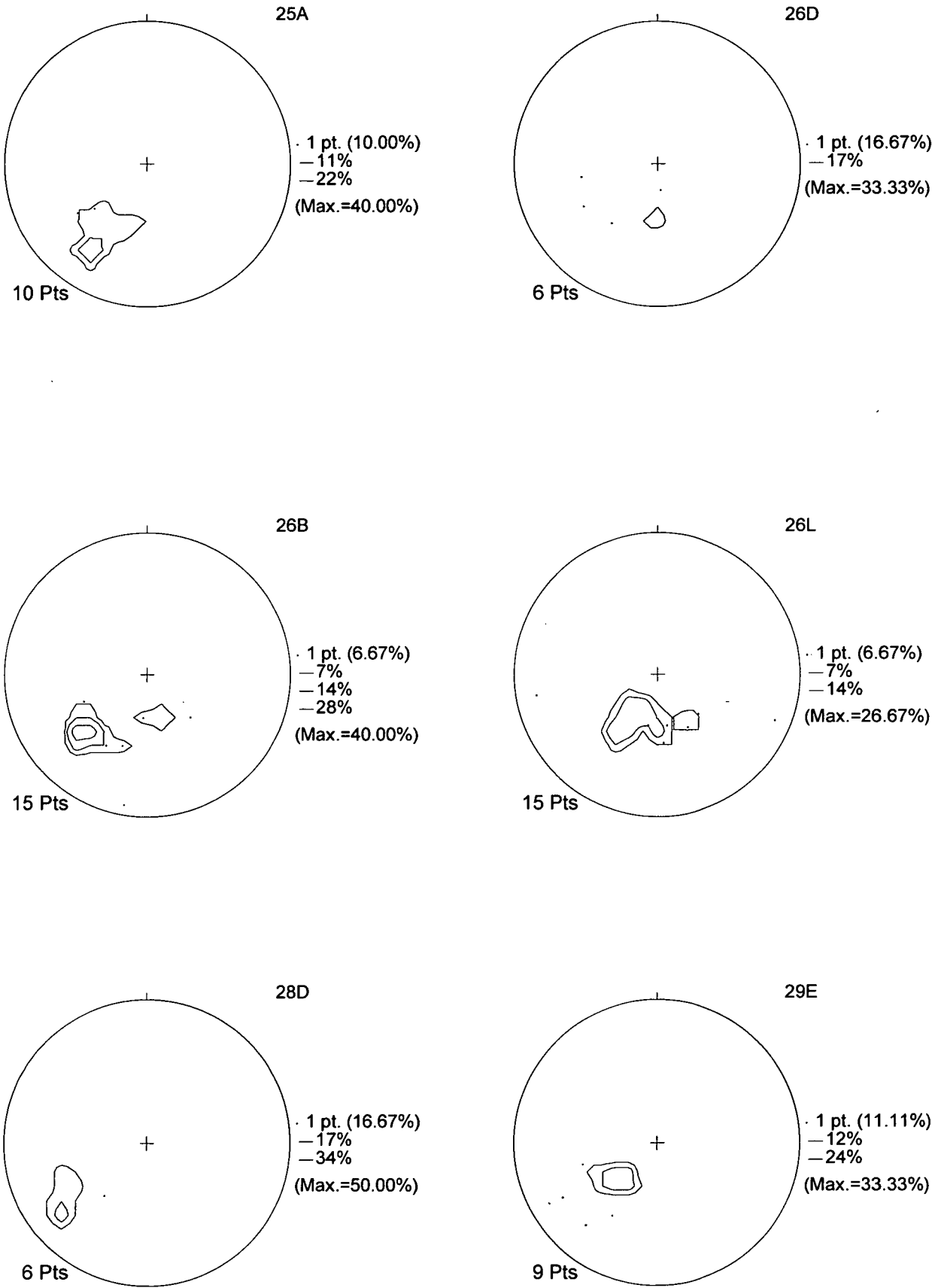


Fig 3.6: Detailed mapping of the basement contact fault on 26L below the 3000 Orebody.

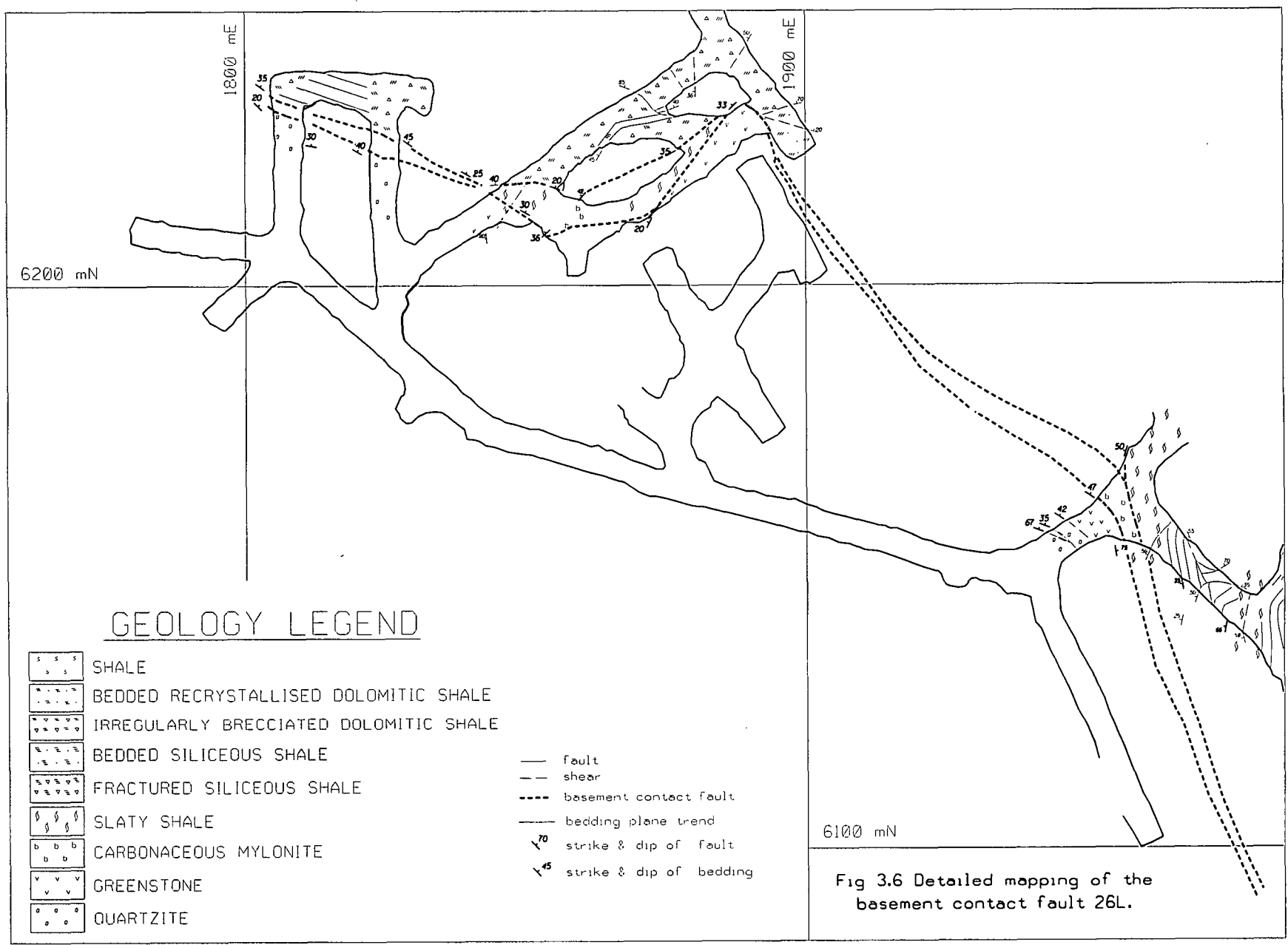


Fig 3.7: Detailed mapping of the basement contact fault on 26B below the 3000 Orebody.

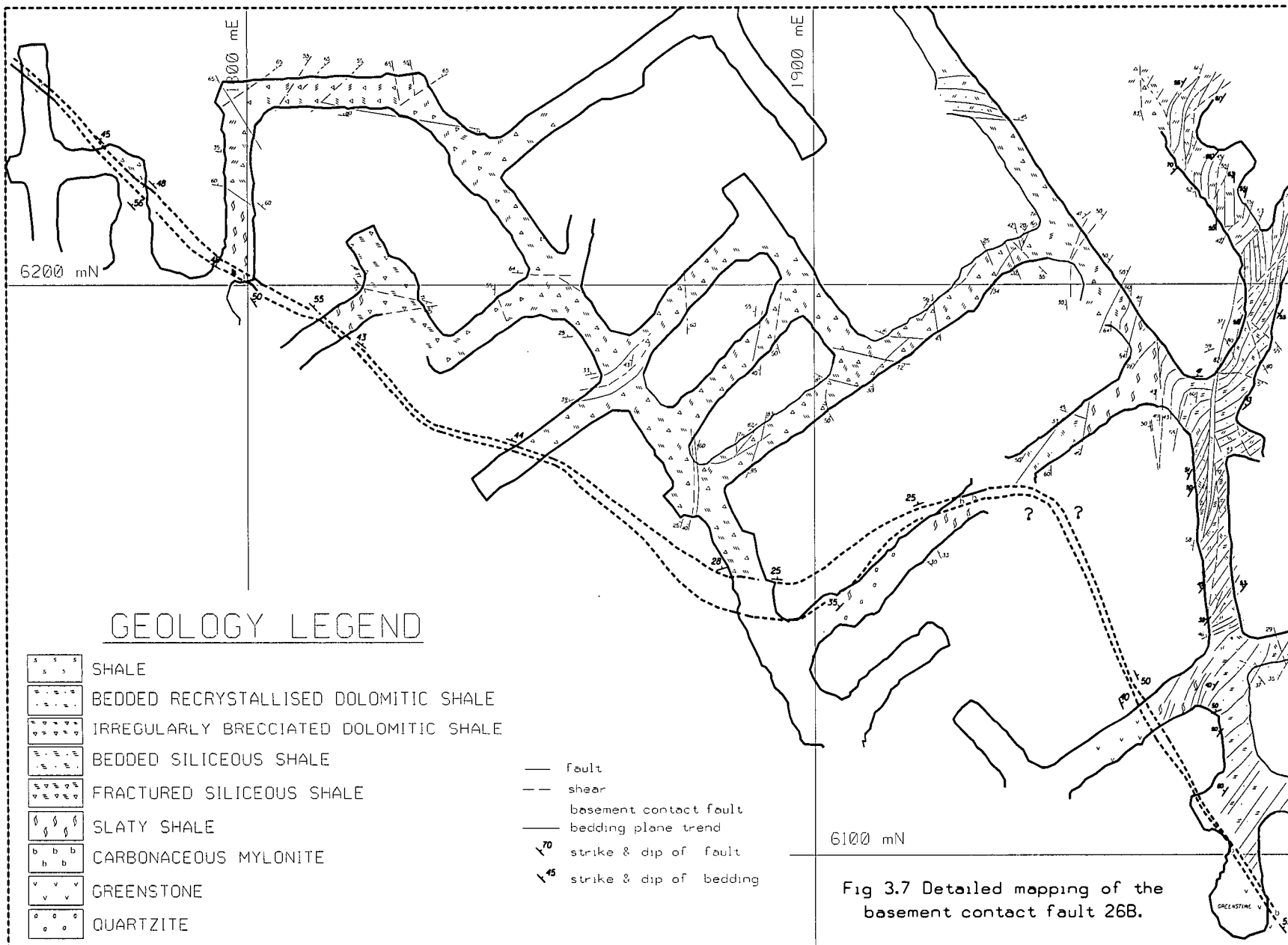
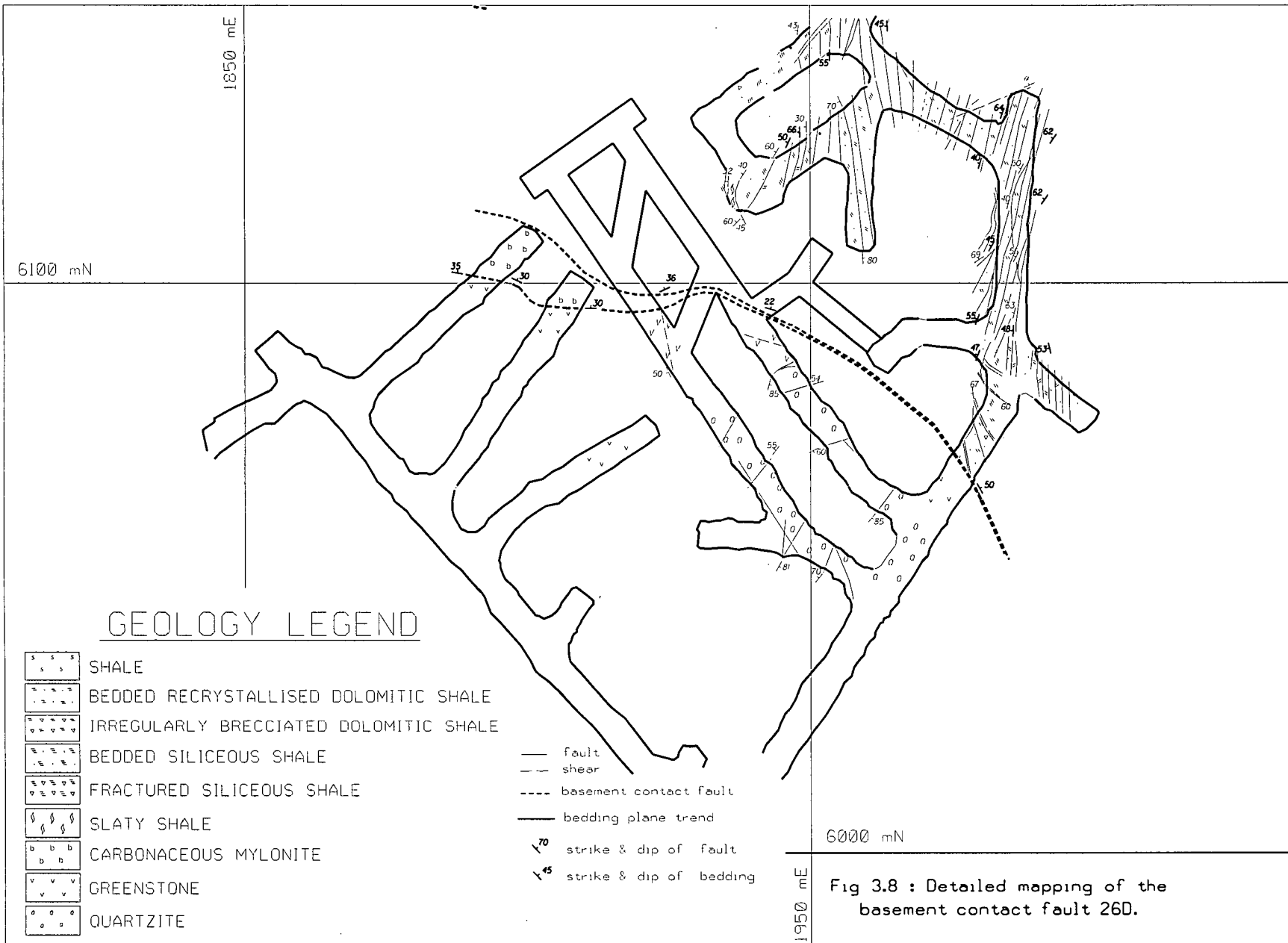
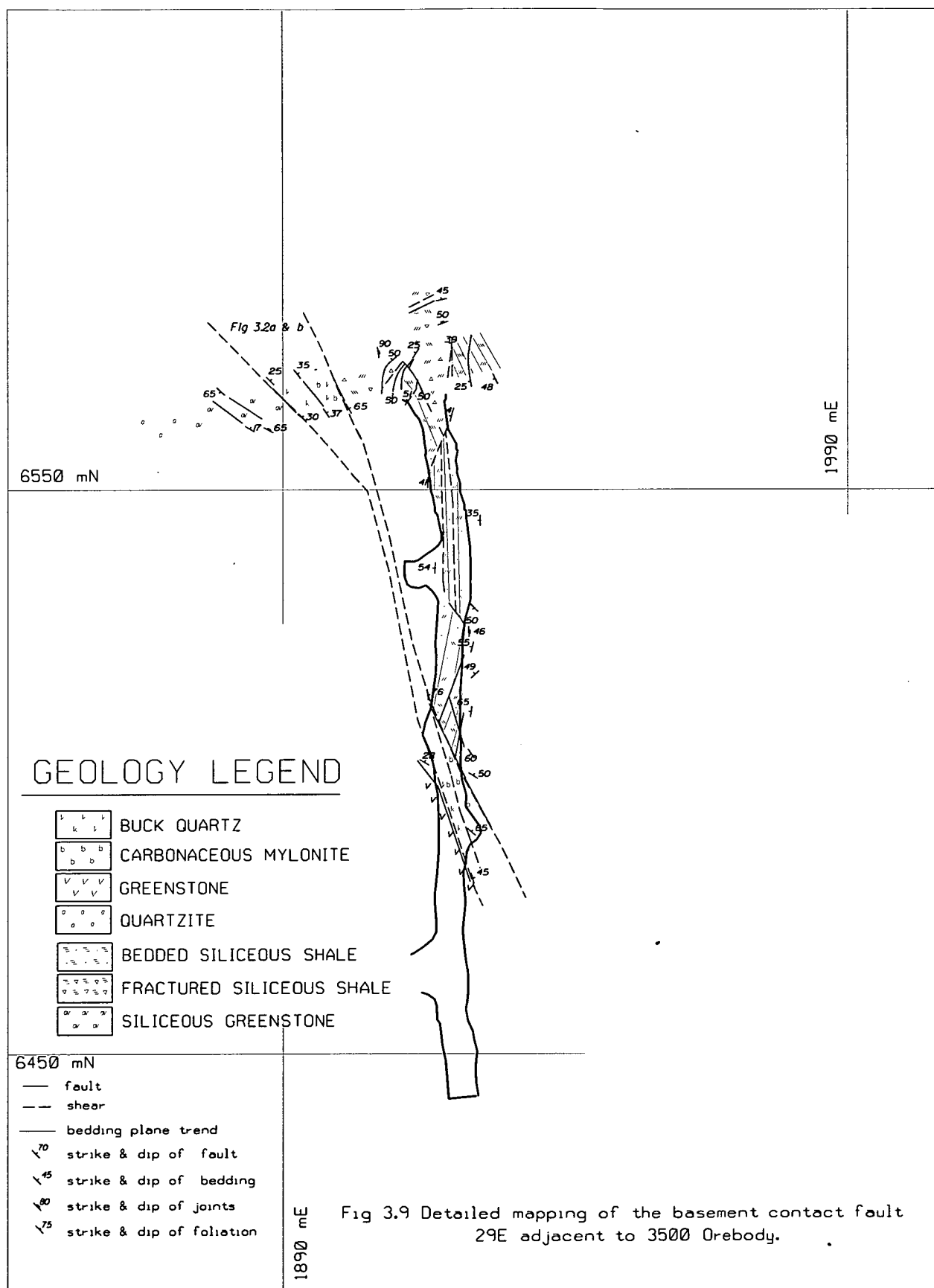


Fig 3.8: Detailed mapping of the basement contact fault on 26D below the 3000 Orebody.





**Fig 3.9: Detailed mapping of the basement contact fault on 29E adjacent to the 3500 Orebody.**



### 3.5 Slaty Shale Distribution

Weakly mineralised slaty shales of variable thickness sometimes occur between the basement contact fault and the copper ore. The slaty shale-ore contact tends to be sharp and defined by a shear plane. The thickness of the slaty shale lenses is highly variable. There are insufficient exposures of slaty shale to be able to confidently map out its distribution beneath the 3000 Orebody. It generally occurs in areas where the basement contact fault shows marked changes in local geometry. Slaty shale also develops along the fault where the orebody has lifted off the fault, as observed on 26D sublevel. Its sporadic occurrence does not exclude the possibility that slaty shale was initially developed along the whole area influenced by the flexure and has since been obliterated by development of the orebody breccia. For example at the basement fault-orebody contact on 25D there is no slaty shale developed, however there is a breccia with slaty shale like clasts in a chalcopyrite matrix. This breccia has a well developed shear texture and in localised positions the boundary between the fault and the orebody is difficult to define.

From drilling of a pilot hole for M62 shaft, 200 metres west of the central core of the 3000 Orebody, it was observed that there was no slaty shale developed at all. Only a thin (0.5m) band of sheared greenstone/siliceous greenstone marked the basement fault itself. This position occurs outside the zone that exhibits potential effects of  $D_3$ .

Insufficient data is available to define the distribution of slaty shale below 3500 Orebody.

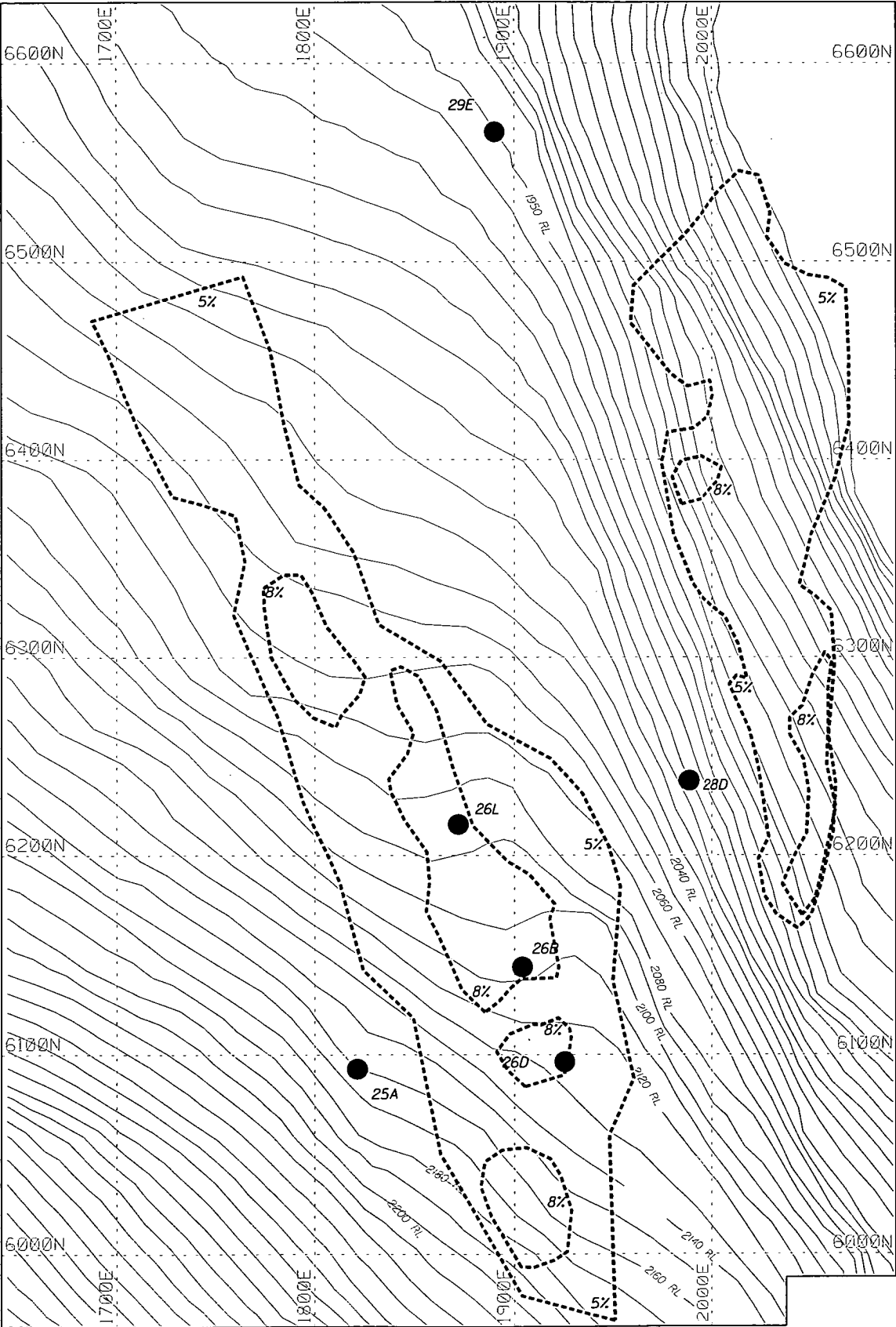
### 3.6 Copper Distribution

The flexure in the basement contact fault coincides exactly with the highest grade core of the 3000 Orebody. This relationship is shown in Fig 3.10 where the 5% and 8% copper contours are plotted over a contour map of the upper basement surface. There is a clear NNW trend to the orebody. This direction equates to the orientation of structures formed during  $D_3$ . The flexure in the basement contact fault dies out to the SSE at 6000mN. This is approximately the southern limit of the 3000 Orebody.

---

The relationship between the 3500 Orebody and the basement contact fault is less clear. Where the 3500 Orebody directly abuts the basement contact fault it does show the influence of the NNW direction but overall it has a north-south trend. The > 8.0% copper lenses of the 3500 Orebody generally do not occur directly adjacent to the fault but are up dip of it. A possible control on these is discussed in chapter 4.

Fig 3.10: 5% and 8% copper contours of the 3000 and 3500 orebodies overlain on the contour map of the upper surface of the basement contact fault. The copper contours are representative of copper grade distribution immediately adjacent to the fault surface.



### 3.7 Discussion

The basement contact fault can be defined as a major zone of shearing of variable width and complex history, incorporating both Mount Isa Group rocks and Eastern Creek Volcanics. The 'greenstone contact' of Perkins (1979) is defined as a sharp contact between chlorite schist and carbonaceous schist (mylonite). This contact equates to the lower boundary of the basement contact fault as described in this chapter. Perkins (1979) noted that late carbonaceous shear zones often complicate observation of the contact, but frequently it can be seen as a completely healed structure.

The basement contact fault is described as a curved surface with flat lying sections cross-cutting the shales at a high angle, which change to steep sections which curve towards parallelism with bedding. This geometry is postulated to have developed via folding, the flat sections being fold hinge zones. There is a broad parallelism between the hingelines in the basement contact fault and the axial plane to folding in the mine. Perkins (1979) proposed a model of an anastomosing fault, which was folded by the  $D_2/D_3$  deformations. The folds would tend to die out on the steeply dipping parts of the zone where the dip was subparallel to their axial plane. In Bell *et al.* (1988) the contact is described as having formed as a lateral thrust ramp during  $D_1$  and to have essentially reached its present day configuration after  $D_2$ . The flatter sections of the basement contact fault are at a moderate to high angle to the  $S_3$  cleavage orientation, and particularly the extension direction  $L_3$  of that deformation. This configuration is interpreted to have caused a lower pressure regime in the upper Mount Isa Group dolomitic rocks above the contact (Perkins, 1984). Structures formed as a result of a ductility contrast with the underlying greenschist during these events, with preferred fracturing in the dolomitic sediments and cleavage development in the basalts.

Bell *et al.* (1988) further describe a process whereby the combined effects of  $D_1$  and  $D_2$  resulted in a pre- $D_3$  geometry at the base of the mine where steeply west dipping bedding in the dolomitic shales abutted shallowly west dipping bedding across a shallow west dipping fault. The totally different bedding orientations on either side of the contact and the ductility contrast between the greenschists and the shales

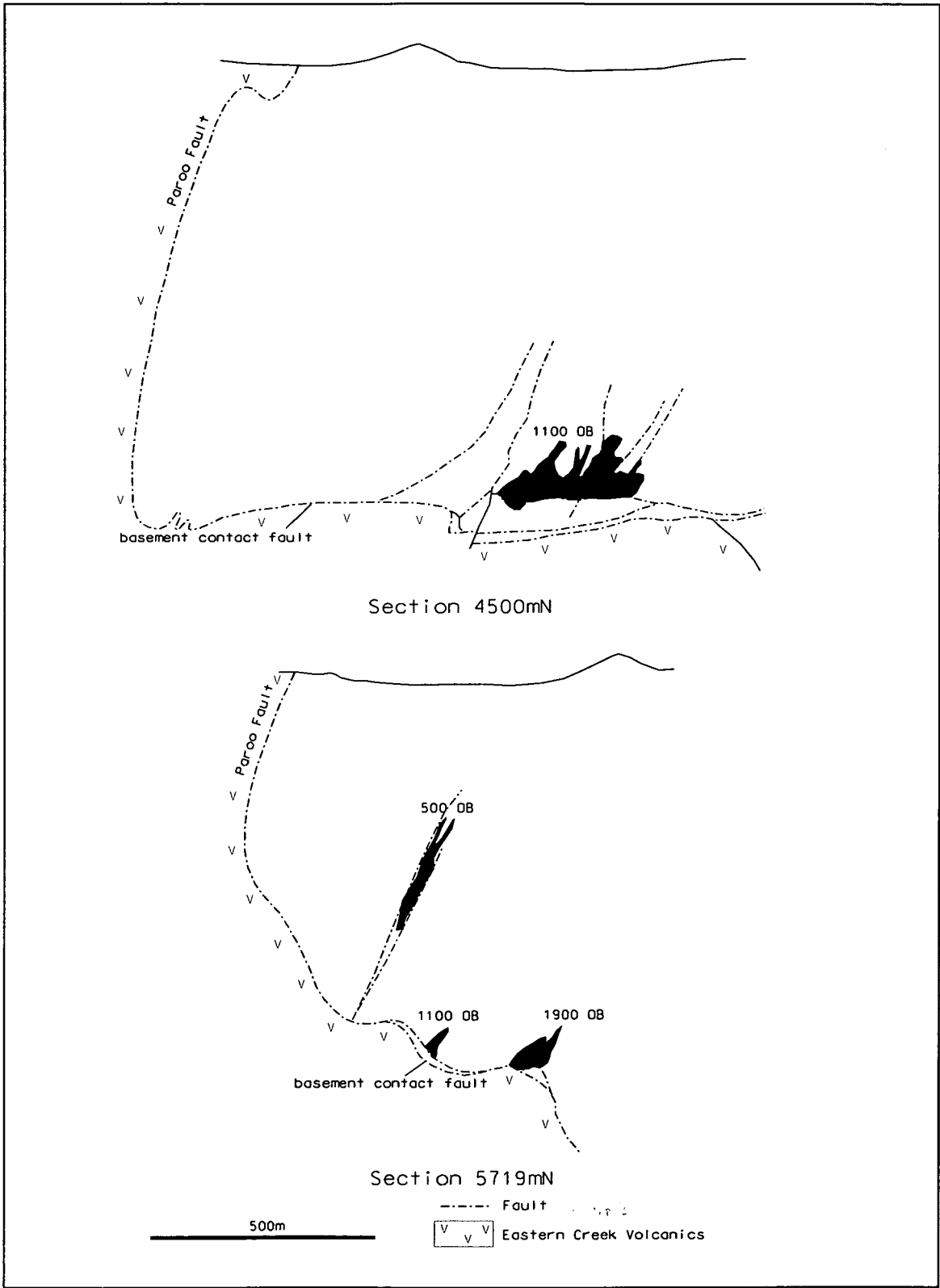
---

meant the basement contact fault formed a major structural discordance, and thus, a plane of weakness along which fracturing and fluid access could occur during  $D_3$ .

On a large scale the basement contact fault forms an almost flat to very shallowly dipping structure beneath the 1100 and 1900 orebodies (Fig 3.11). The relationship to folding is not particularly clear beneath the main body of the 1100 Orebody (section 4500mN). However moving northwards to where the 1100 Orebody narrows and the adjacent 1900 Orebody has developed, the basement contact fault has a geometry similar to that described beneath the Deep Copper orebodies. The 1100 Orebody seems to sit in a synformal hinge whereas the 1900 orebody is positioned more towards the inflexion point where the fault is interpreted to dip steeply away to the east.

An interesting feature is that the separation distance of approximately 200m to 250m between the 1100 Orebody and 1900 Orebody is the same as the distance between the 3000 Orebody and the 3500 Orebody. Recent work suggests the 1900/1100 orebody system is associated with a separate  $D_3$  fold zone (personal communication. P.Jones, November 1998). The similarity in distance between the orebodies may be related to the wavelength of the folds.

Fig 3.11: Section 4500 mN and section 5719 mN showing flat sections of basement contact fault below the 1100 Orebody and the 1900 Orebody (Adapted from Bell *et al.* 1988).



---

### 3.8 Conclusions

The data presented here for the 3000 Orebody suggests that flexures in the basement contact fault, which act as very strong controls on the localisation of mineralisation, are related to  $D_3$  fold zones. The preliminary data from 29E also suggests that the position of the 3500 orebody may be linked to a small flexure in the contact.

The importance of a contrast between bedding orientation between the shales and quartzites/greenstone on either side of the contact, as discussed by Bell *et al.* (1988) is questionable as the bedding angles observed in the basement quartzites below the Enterprise Mine are not substantially different from the shales. Also a ductility contrast between greenstone and shale causing preferential fracturing in the shales is not necessarily an important factor as there is volumetrically a minor amount of greenstone below the Enterprise Mine. Where it does occur immediately adjacent to the contact it is also extensively silicified and brecciated.

The basement contact fault does form a major structural discordance beneath the mine and it enabled large scale fluid access to occur during the  $D_3$  deformation period.

Accepting that the basement contact fault is a major control there is still the question of the control on the up dip extensions of the orebodies. As well there is the problem of orebodies such as the 500 Orebody and 650 Orebody which do not lie adjacent to the basement contact fault. The 3500 Orebody has a closer alliance to this style of orebody as its highest grade core (+8% copper) has only tenuous links to the contact.

The following chapter describes a series of faults, which are closely associated to the basement contact fault and the orebodies. It is suggested that these structures also form a strong control on the distribution of the copper mineralisation.



## Orebody Structure

### 4.1 Introduction

Data from underground mapping and diamond drillholes has defined a substantial network of interconnected faults/shear zones throughout the two orebodies. The main copper mineralisation occurs directly above the basement contact fault with smaller orebodies present at higher levels detached from the contact. The detached orebodies show that copper bearing fluids have been transported upwards but no authors to date have really discussed how this occurs. From observations made during this study I suggest that the system of mainly bedding parallel faults associated with the orebodies acted as conduits for the hydrothermal fluids.

The following sections describe the physical character of the faults and their geometry and distribution patterns in each of the Deep Copper orebodies.

#### 4.1.1 Terminology

Shear zones can be divided into brittle, brittle-ductile and ductile types on the basis of the shear zone or fault rocks, and the nature of the offset across the zone. Brittle shears are characterised by gouge and fault breccia, and displacement markers show abrupt offset across the zone. Brittle-ductile shears are zones of schist/mylonite series rocks across which there is both continuous and discontinuous offset of markers. The discontinuous offset is along discrete slip surfaces. Ductile shears are characterised by mylonite series rocks and continuous offset of external markers (Ramsey, 1980).

Most shear zones comprise an array of differently-oriented segments such that as a whole, they have a complex anastomosing geometry with many associated shears and fractures. If a structure passes from an incompetent lithology into a competent lithology along its length, then brittle deformation features commonly will occur in the competent unit and ductile features in the incompetent unit (Hodgson, 1989).

In the following sections of this thesis the term fault is applied to discrete planar surfaces which may or may not have associated fault gouge material. The majority of

the structures described are fault bounded shear zones, which have a highly variable width and have a strongly foliated internal structure. Discrete faults occur within the shear zones and splay faults link the boundary faults. The term bedding plane shearing is used in a strictly descriptive manner to describe shear zones where the internal foliation is parallel to the bedding orientation in the adjacent rocks.

## 4.2 Physical Character

The major physical features of the faults within and immediately adjacent to the orebodies are:

- Zones of variable thickness (< 10 cm to 6 metres) displaying brittle-ductile shear fabrics. Well defined discrete fault planes form within these zones. The discrete faults are planar to slightly curved and splay structures are common. At flexures in the fault plane's dilatant zones occur which are filled with quartz and sometimes pink (Mn-rich) calcite and/or chalcopryrite. Open space vugs are rare but do occur with well developed quartz and calcite crystals and/or sepiolite (a fibrous clay mineral).
- A well developed anastomosing geometry with the main structures being parallel to the local bedding orientation. The shear zones shallow in dip as they approach the basement contact fault.
- The shear zones often occur on the boundaries of different rocktypes.
- The shear zones are less mineralised than the adjacent wallrock and often there is a marked enhancement of grade immediately outside the fault boundary of the shear zone.

### 4.2.1 3000 Orebody

The following table lists the physical features of the shear zones at a number of localities on 24A sublevel. Fig 4.1 shows the position of these locations relative to the interpreted geology.

abbreviations used in table: bps = bedding plane shearing

C = siliceous shale

F = fractured siliceous shale

R = recrystallised shale

S = shale

Location		mE	mN	Dip	Width	Description
1	255XC	1864	6034	40 - 45	1.0m	strong bps shale + quartz veins; bedding disrupted to east of fault.
2	R607DDR	1866	6074	55	0.75m	bps shale
3	330XC	1912	6160	55 - 70	2.5m	strong bps shale + quartz + calcite veins
4	360XC	1920	6203	40 - 60	2.0m	sharp low angle transverse fault; bps shale and quartz veins (yellow)
5	210XC	1893	6000	55	1.0m	strong bps; R - C contact
6	255XC	1902	6063	55 - 60	0.5 - 1.0m	sheared R - F contact; grade hangingwall
7	270XC	1902	6080	45 - 60	0.5 - 1.0m	sheared FC - R contact; grade hangingwall
8	330XC	1934	6177	45 - 70	0.5 - 1.0m	sheared FC - R contact; grade hangingwall
9	240XC	1912	6043	35 - 45	0.5m	sheared C; C - FC contact; grade hangingwall
10	S611CO	1940	6120	65	0.5 - 1.0m	sheared C
11	300XC	1950	6152	45 - 75	1.0m	strong bps; R - F contact
12	330Xc	1962	6195	55 - 60	0.5 - 1.0m	sheared F - SC contact; sharp grade footwall
13	180XC	1955	6004	70	0.1m	sharp healed planar surface; apparent reverse movement (~ 1m)
14	210XC	1964	6050	34 - 45	3.0m	strong sheared S and quartz veins; C - F contact; grade footwall
15	225XC	1965	6073	45 - 50	0.5 - 1.0m	zone of discrete bps bands; approximate grade footwall
16	300XC	1988	6167	65 - 75	0.5 - 1.0m	approximate grade footwall; convoluted bedding east of structure

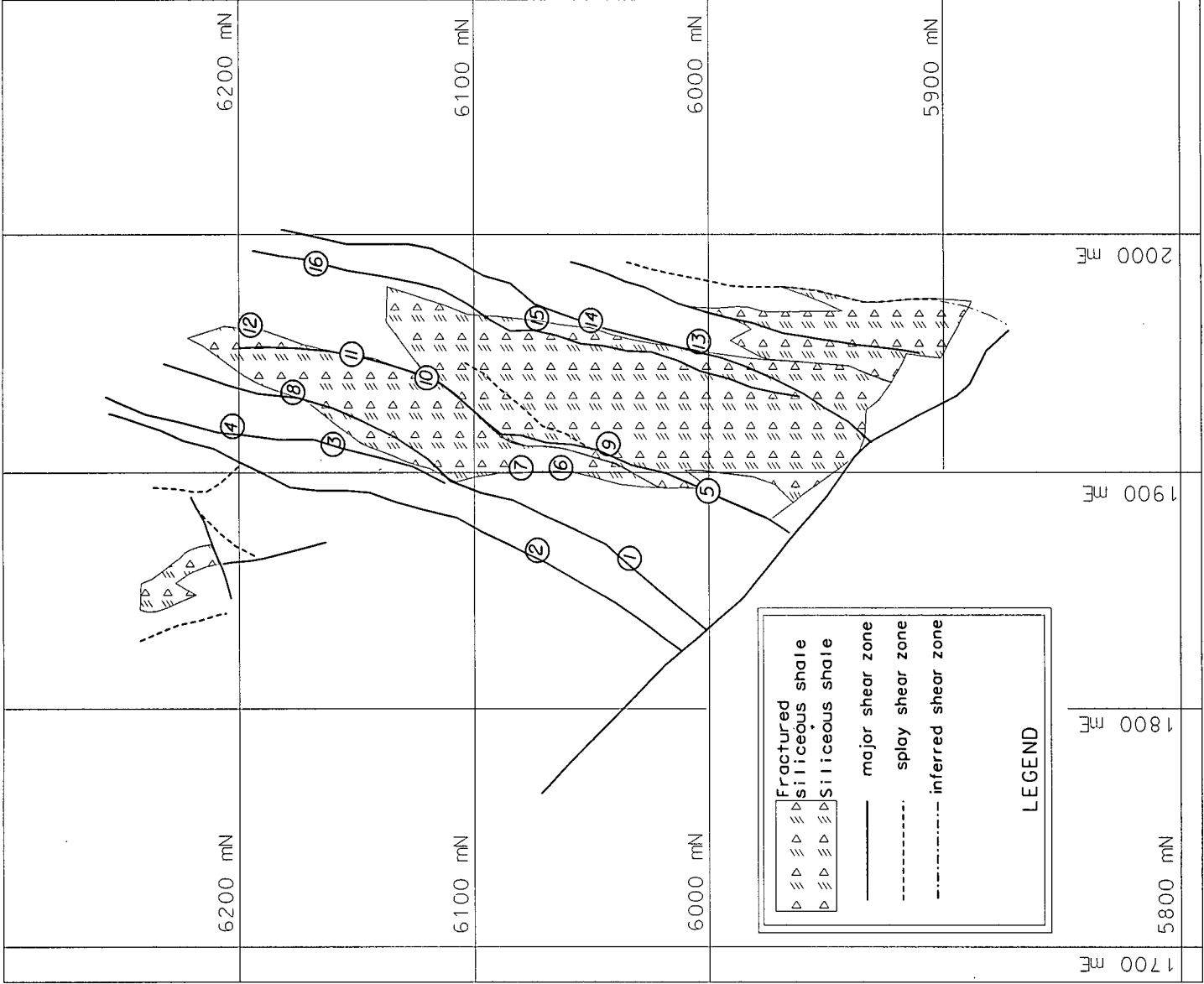
Table 4.1 - Physical characteristics of faults and shear zones on 24A sublevel.

The dips of the shear zones are variable but are generally subparallel to adjacent bedding. The thickness of a shear zone can change abruptly from > 2m to 10cm over a strike length of 5m. The shear zones vary in physical character depending on the alteration 'rock type' they are passing through. Immediately above the basement contact in the high grade massive brecciated fractured siliceous shale the shear zones tend to be narrow (<10cm - 1.5m) with relatively sharp boundaries. Though bedding orientation can be difficult to observe in the breccias, the faults are subparallel to remnant bedding features preserved within them. The siliceous clasts in the breccias generally have a random orientation. The majority of the shear zones are weakly mineralised and siliceous. The shear zone boundary can be very sharp and marked by an increase in the copper grade (Fig 4.2).

Where bedded 'rock types' are present the shear zones are wider with discrete fault planes separated by highly fissile bedded shales with a marked increase in the amount of graphite on the bedding plane surfaces (Fig 4.3). The shear zones can be traced up dip to 23A but they become increasingly difficult to correlate as they become very narrow and merge into bedding. Quartz filled tension veins sometimes develop adjacent to the shear zones.

Not all 'rock type' or grade boundaries coincide with faults/shear zones. The sharp footwall contact of the 3000 Orebody at the southern end of 24A sublevel is defined by a shale-fractured siliceous shale boundary. There is no evidence of shearing. At some localities the distribution of the copper mineralisation correlates with specific stratigraphic horizons without any noticeable faults.

Fig 4.1: Locations of faults and shear zones described in table 4.1.



---

Fig 4.2: 3000 Orebody R618 CO 26B. Close up of a shear zone with a sharp boundary fault showing a marked transition to very high grade copper mineralisation. Well developed internal foliation within the black carbonaceous body of the shear zone. The shear zone is weakly mineralised. Dipping  $35^\circ$  to the NW, this shear zone would intersect the basement contact fault  $\sim 20$  metres down dip in the plane of the shear zone (looking east) (length of hammer 32 cm).

Fig 4.3: 3000 Orebody 85 Xcut 23A. One metre wide fault zone adjacent to a small lens of fractured siliceous shale (looking south) (distance between the two rockbolts is 0.9 m).



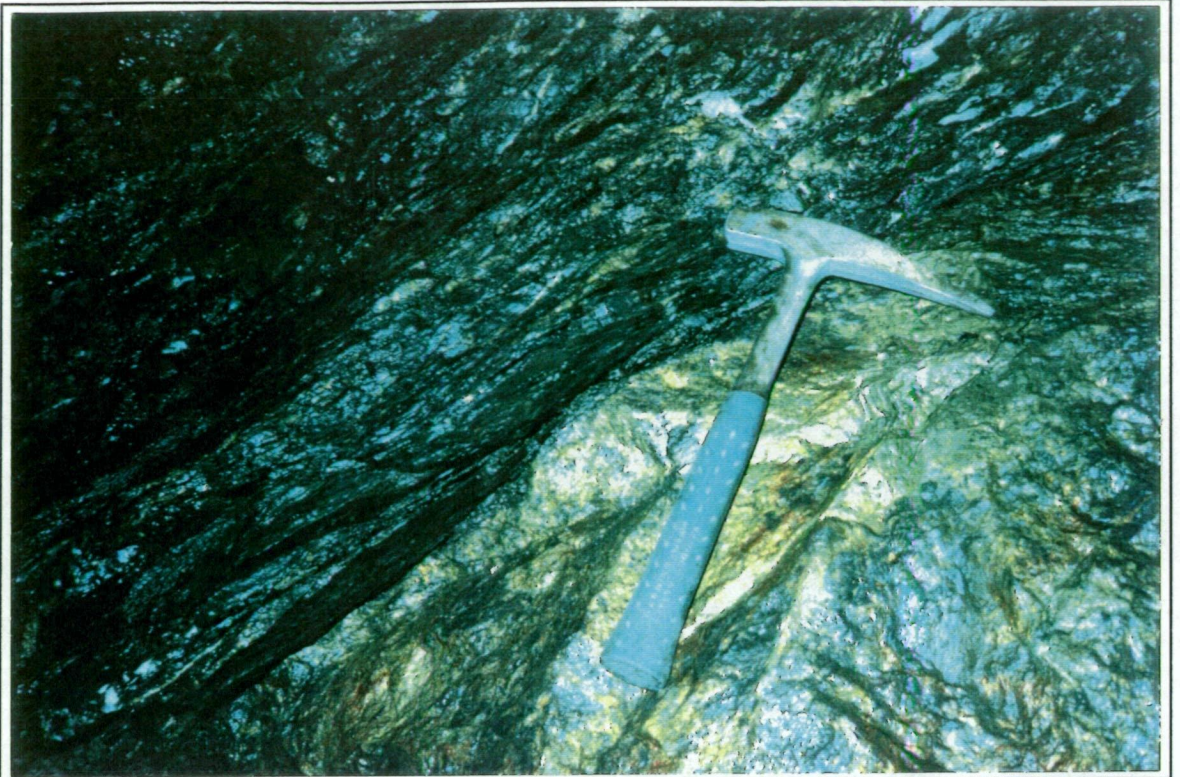


Fig 4.2



Fig 4.3

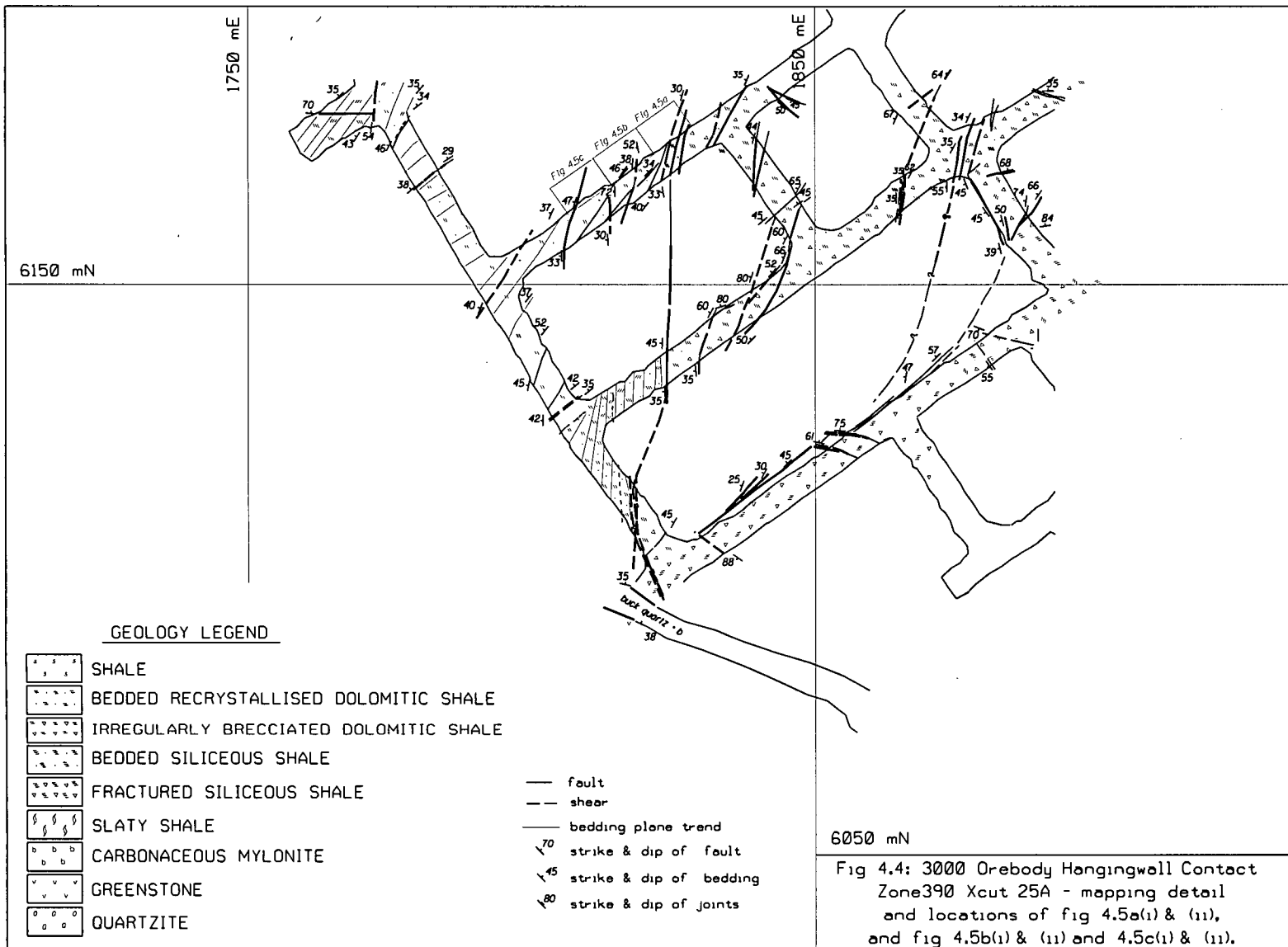
### 4.2.2 3000 Orebody Hangingwall Contact

Fig 4.4 shows detail of mapping of the 3000 Orebody hangingwall contact on 25A sublevel and the location of the underground exposure shown in Figs 4.5a(i) to 4.5c(ii). The photos show a 16 metre wall exposure of the hangingwall boundary and the relationship of faults/shear zones to bedding and copper mineralisation.

The general bedding orientation at this location is between  $30^{\circ}$  and  $40^{\circ}$  towards the northwest. This atypical orientation is a result of rotation of the bedding due to movement against the basement contact fault. Discrete fault planes (+/- quartz fill) at a similar angle to the bedding are associated with zones of sheared shale. The hangingwall boundary of the orebody is sharp (~ paint mark 2, Fig 4.5a) and marked by a fault. Small patches of copper mineralisation west of this boundary are associated with faults/shear zones (@ paint marks 5, Fig 4.5b and 7, Fig 4.5c). The intervening bedded shales between the shear zones are unmineralised except for minor chalcopyrite veins. At paint mark 7 (Fig 4.5c) there is an example of the splay geometry of the faults with a steeper than bedding fault branching from a bedding parallel fault.

An interesting feature from the mapping is that the set of NNE trending shear zones converges towards a point on the basement contact fault (A on Fig 4.4). At this point the basement fault flattens in dip from  $50^{\circ}$  to  $\sim 30^{\circ}$  and is filled with 3m of white buck quartz and minor carbonaceous mylonite. None of the shear zones cut through the basement contact fault.





**Fig 4.5 a(i): 3000 Orebody Hangingwall Contact Zone 390 Xcut 25A looking northwest. (white paint lines are two metres apart)**

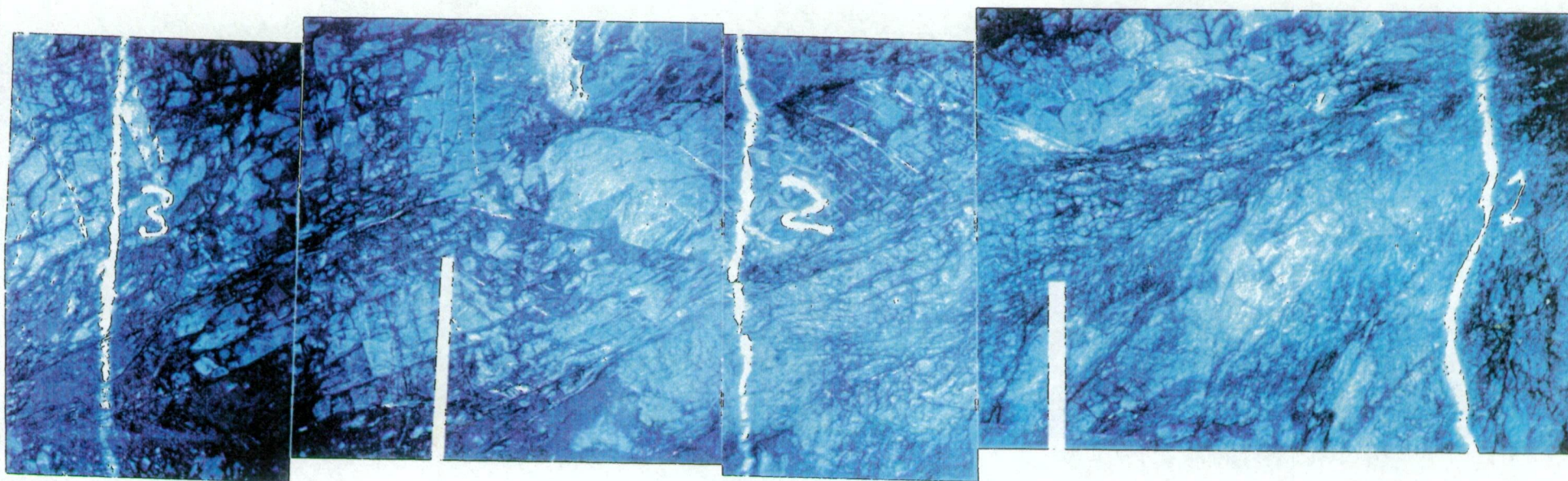
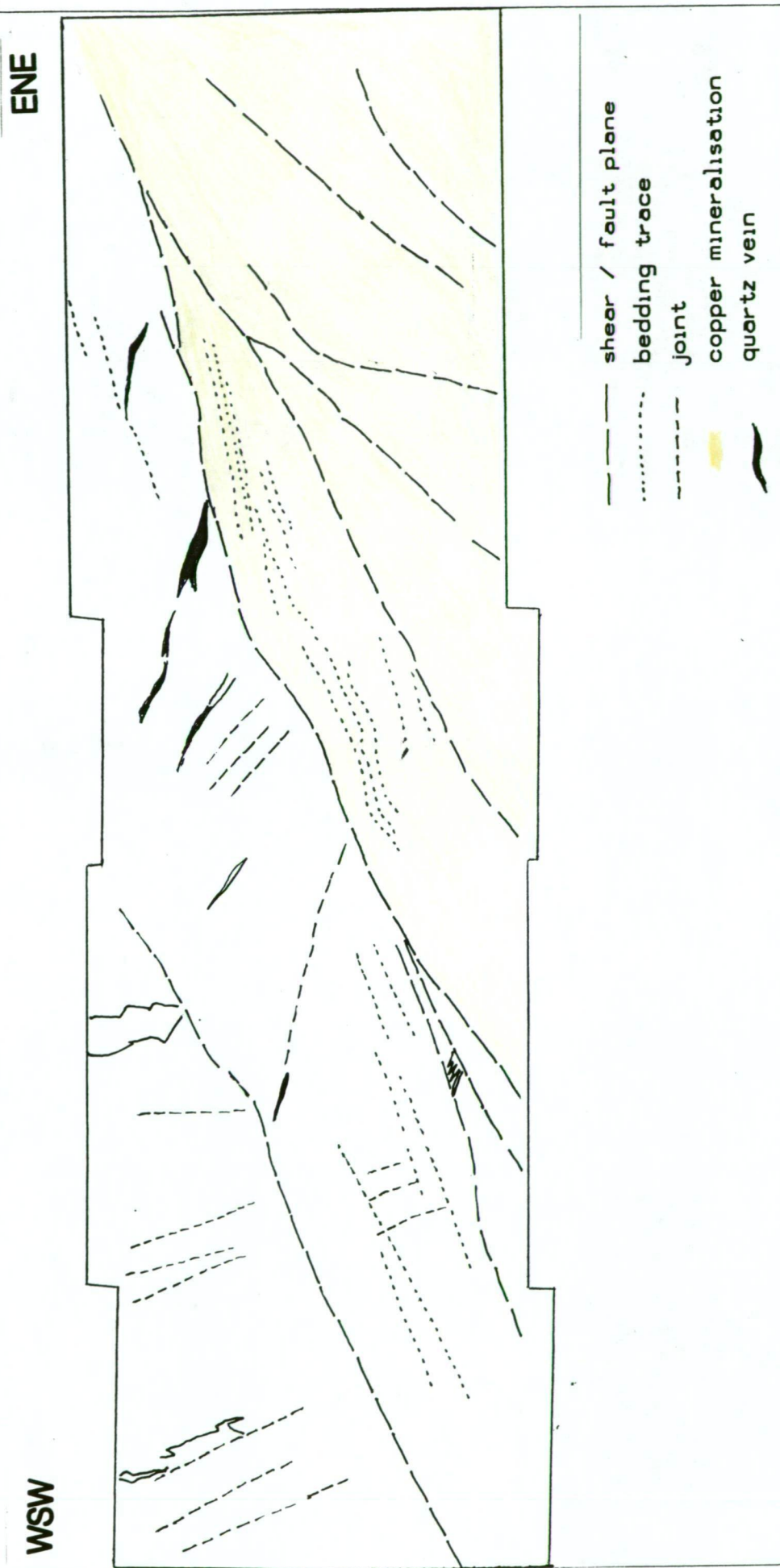


Fig 4.5a(ii): 3000 Orebody Hangingwall Contact Zone 390 Xcut 25A looking northwest. Drawing of main structural features and copper mineralisation.





**Fig 4.5 b(i): 3000 Orebody Hangingwall Contact Zone 390 Xcut 25A looking northwest. (white paint lines are two metres apart)**

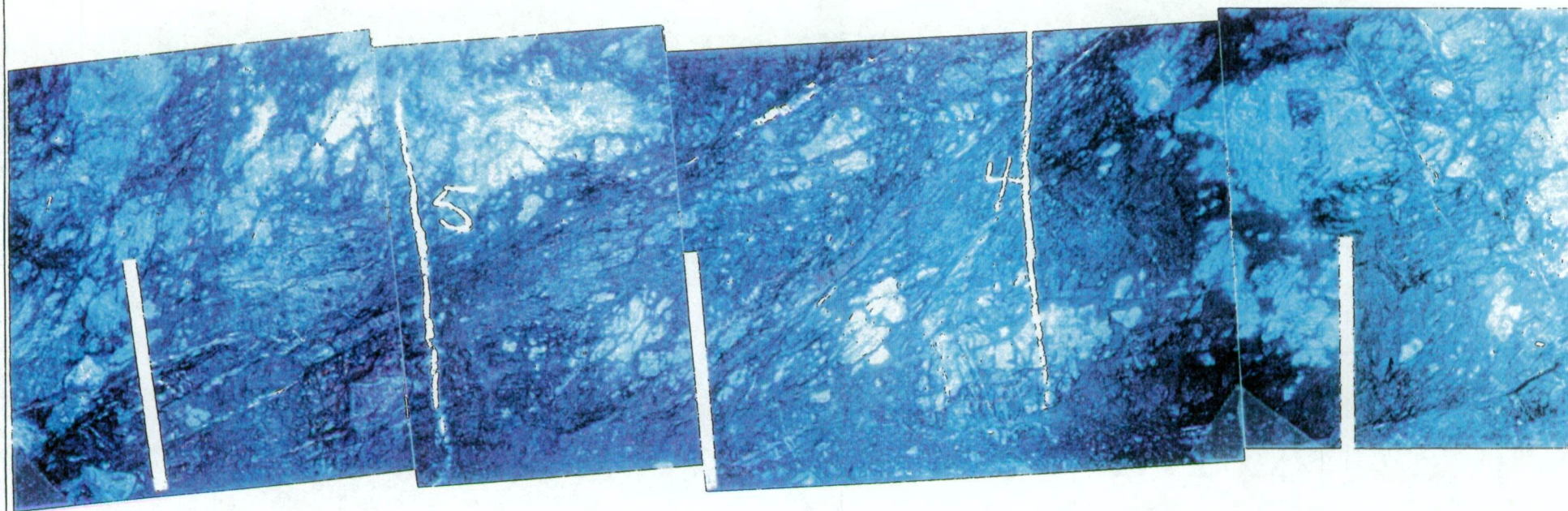


Fig 4.5b(ii): 3000 Orebody Hangingwall Contact Zone 390 Xcut 25A looking northwest. Drawing of main structural features and copper mineralisation.





**Fig 4.5 c(i): 3000 Orebody Hangingwall Contact Zone 390 Xcut 25A looking northwest. (white paint lines are two metres apart)**

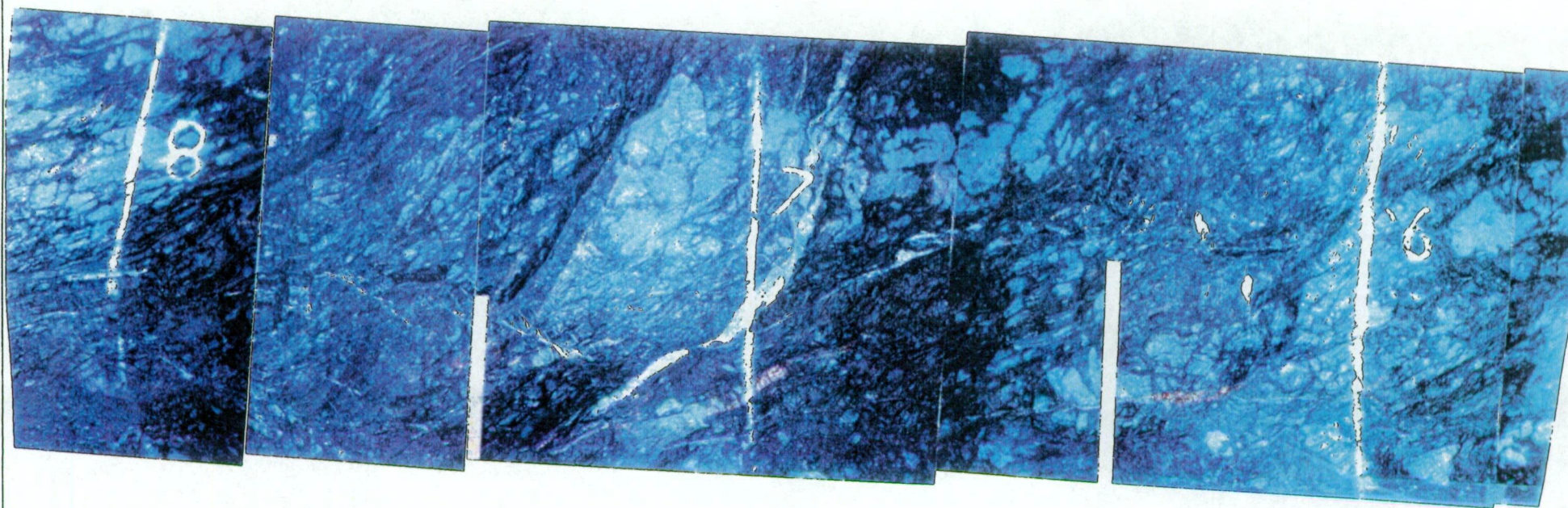
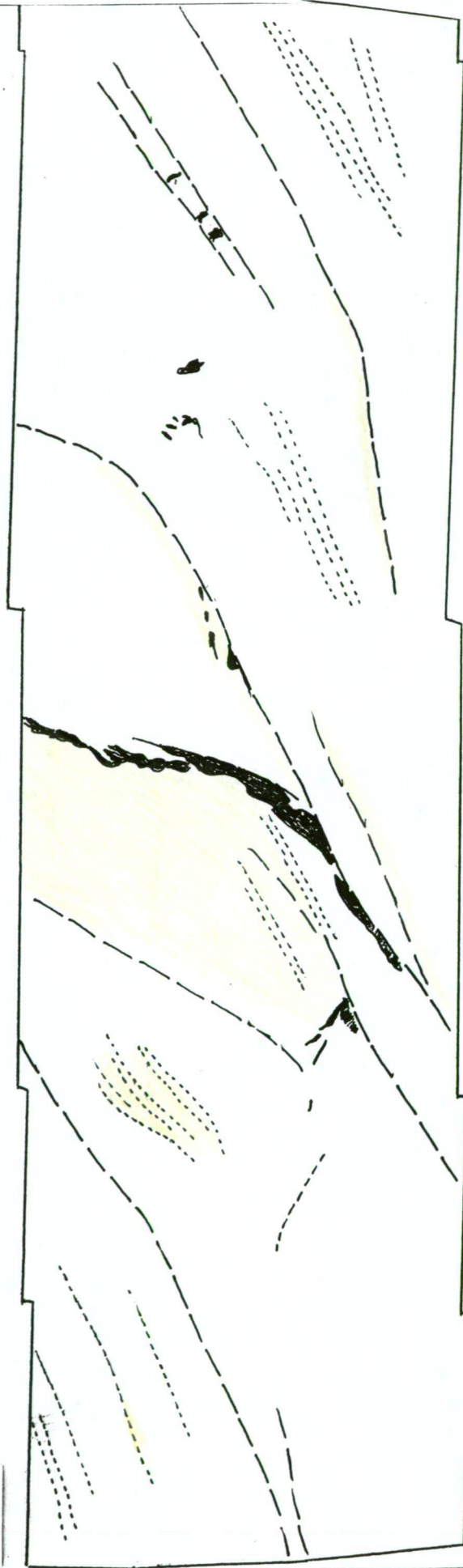


Fig 4.5c(ii): 3000 Orebody Hangingwall Contact Zone 390 Xcut 25A looking northwest. Drawing of main structural features and copper mineralisation.

WSW

ENE



- shear / fault plane
- ..... bedding trace
- - - joint
- yellow copper mineralisation
- thick black line quartz vein

### 4.2.3 3500 Orebody

Shear zones in the 3500 Orebody have the same character as the 3000 Orebody shear zones. The anastomosing nature of the shear zones is very evident and there is a corresponding high variability in thickness with individual structures decreasing from 3 m to < 0.5 m over a strike length of <10 m. Correlation of individual shear zones is more difficult from one sublevel to the next. Five major shear zones have been identified. Dips range between 50° to 80° reflecting the generally steeper bedding orientation of the 3500 Orebody. The hangingwall boundary of the orebody is not everywhere related to a fault. The footwall boundary is very sharp and is always marked by a shear zone. The frequency of structures across strike is higher in the 3500 Orebody than in the 3000 Orebody. This is probably a direct function of the much stronger bedding in the 3500 Orebody. Breccia bands/lenses are present but are thinner and intercalated with bedded and sheared siliceous shales. On some sublevels the 3500 Orebody gives the appearance of being a single complex shear zone.

Recent mapping in the 3500 Orebody has identified a set of east dipping faults within the orebody. They form as narrow (<0.5m) well defined faults with a rubble, clay gouge infill. Some contain open vughs and are water bearing. Where they are observed adjacent to the west dipping shear zones there is no clear evidence to show that they displace the west dipping structures (or vice versa). They may represent a set of linking splays between the west dipping structures. Due to limited exposures they have not been shown on the accompanying plans and sections.

A feature observed in the 3000 Orebody but which became more obvious in the 3500 Orebody was the occurrence of intensely mineralised bands of siliceous breccia immediately adjacent to the fault, zones. An example of this is shown in Fig 4.6 where a 0.5m wide zone of shearing is adjacent to a 1 m wide band of chalcopyrite, pyrite and pyrrhotite ore. The pyrite and pyrrhotite form well developed layers parallel to the shear zone. Fig 4.7 shows an exposure of massive breccia against a sheared siliceous shale band.



---

Fig 4.6: 3500 Orebody U61 NDR 26B. The 1 metre thick layered chalcopyrite, pyrrhotite and pyrite ore is bounded by graphitic shear zones 0.3 to 0.5 metres thick. Note that the shear zones are also mineralised. The layering of the pyrrhotite is parallel to the shear zone foliation which in turn is parallel to the local bedding orientation (looking up - 1m paint lines).

Fig 4.7: 3500 Orebody 515 Xcut 26B. Boundary between massive fractured siliceous shale breccia and sheared siliceous shale zone. The sheared siliceous shale shows the characteristic appearance of the shear zones within the 3500 Orebody. The contact with the breccia is a sharp fault plane (looking south - 10cm markers on pole).



Fig 4.6

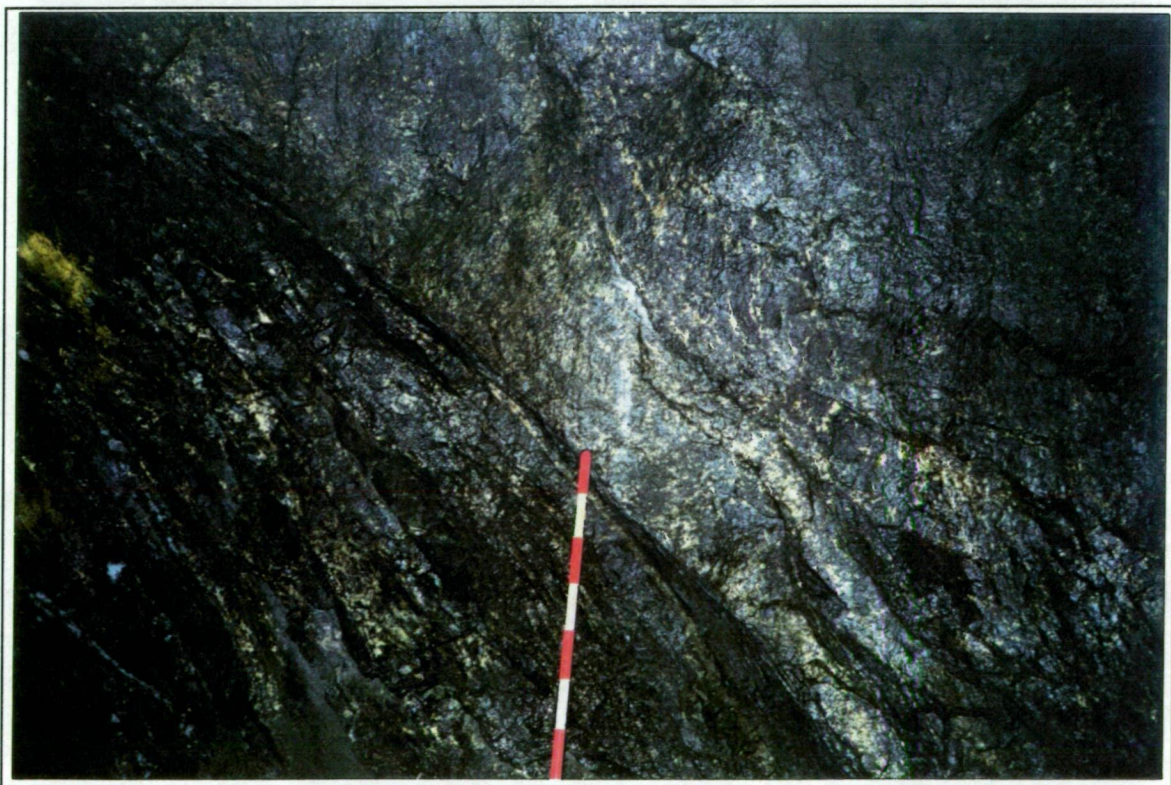


Fig 4.7

### 4.3 Local Copper Grade Variations

The shear zones are markedly less mineralised than the adjacent breccias (Fig 4.6 and Fig 4.7). There is often a distinct enhancement of copper grade immediately adjacent to the boundary faults of a shear zone (on both the footwall and the hangingwall).

This feature was used as a tool for interpretation of the faults in diamond drillcore.

#### 4.3.1 Detail of 3500 Orebody - 6390 mN section

Core from four drillholes from section 6390 mN was examined to determine if there was any direct relationship between the faults and the distribution of the copper mineralisation. Fig 4.8 shows the assay data and interpreted faults from this section in the 3500 Orebody. Five complex shear zones were identified. Lithologically they coincided with transitions from siliceous breccia 'rock types' to more bedded zones. The bedded zones contained clearly visible brittle-ductile shearing textures. As mentioned previously there is often a drop in grade in the shear zones with a corresponding enhancement in grade immediately adjacent to the shear zone boundaries. This feature was readily visible in each of the holes.

Samples were collected for bulk mineralogical analysis from a shear zone and its adjacent wall rock. The purpose of this was to test a hypothesis that the shear zones may have formed preferentially in stratigraphic intervals that were originally more pyritic, and thus more susceptible to respond to shearing processes in a ductile manner rather than by brittle fracture. Two samples from drillhole 891131 at 142.9m and 144.7m (sample No's 891131A and 891131B) and two samples from drillhole 891138 at 138.7m and 139.2m (sample No's 891138A and 891138B). The drillholes are adjacent to one another but the samples represent two different shear zones. The A samples are from mineralised breccia within 0.5m of the shear zone boundary and the B samples are from within the shear zone. The samples were examined by quantitative X-ray diffraction (XRD) analysis.

The XRD analysis was done in the MIM laboratory by A.Mandile the industrial mineralogist.

The values are in weight percent.

Absolute errors, on average, range from 0.5 to 4wt%.

The detection limit is 1wt%.

Sample No	Chalcopyrite wt%	Pyrite wt%	Dolomite wt%	Quartz wt%	Chlorite wt%	Talc wt%	Feldspar wt%
891131A	59.3	<1.0	<1.0	36.3	3.4	<1.0	<1.0
891138A	59.9	1.3	<1.0	37.7	1.1	<1.0	<1.0
891131B	4.2	9.7	<1.0	73.5	11.6	<1.0	<1.0
891138B	5.2	4.8	<1.0	81.9	6.3	<1.0	1.4

Table 4.2 – Results of quantitative bulk mineral XRD analysis of 3500 Orebody samples.

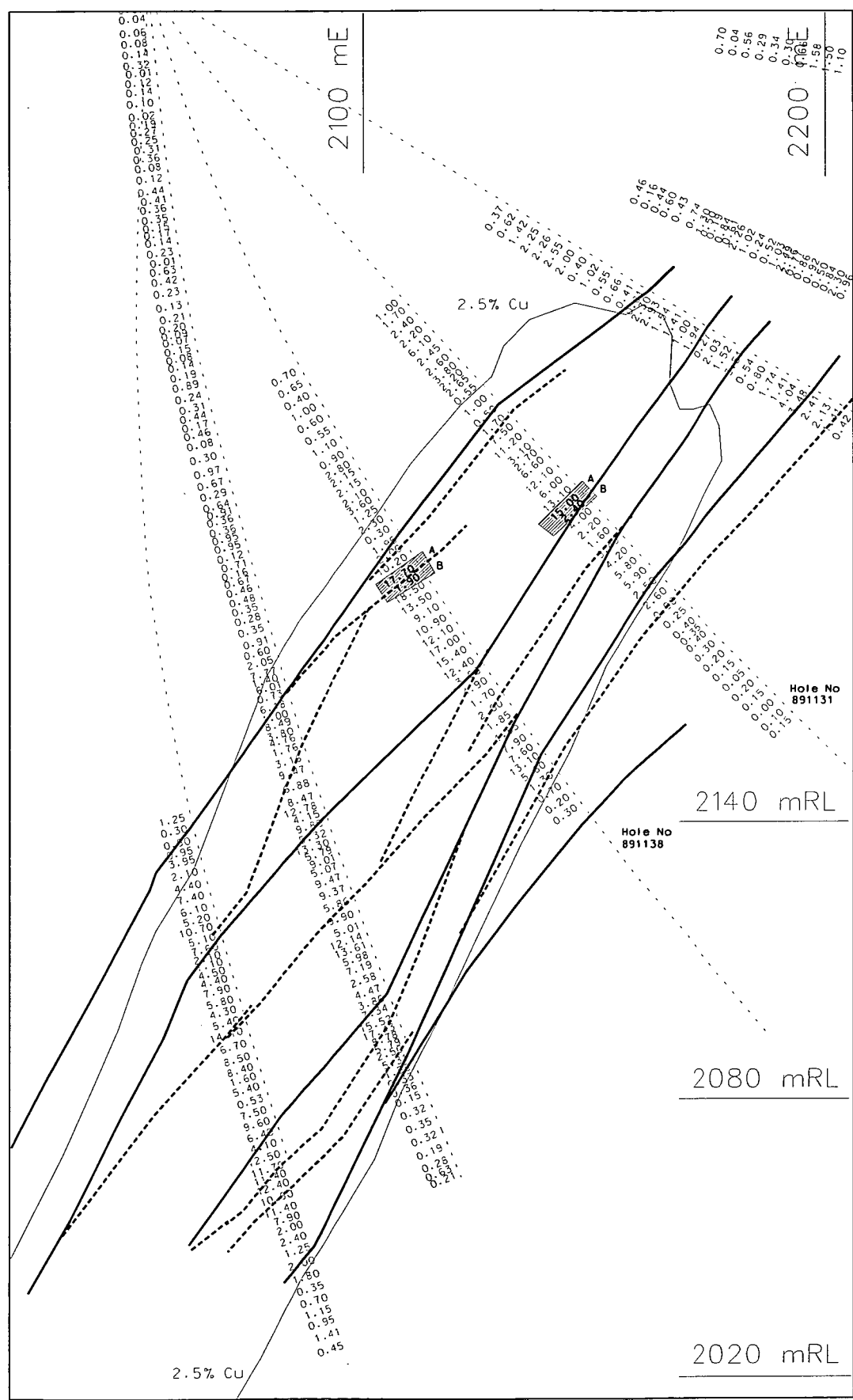
The shear zones contain visible graphite but the XRD analysis method used is not able to measure organic compounds. The results show that there is more chlorite and pyrite in the shear zone. The majority of the pyrite is very fine grained (<20 microns) and associated with carbonaceous material (observation via optical microscopy by A.Mandile). The results also show that the shear zones are siliceous.

These results could represent either a concentration of less soluble minerals within the shear zone or a possible difference in the precursor stratigraphy between what are now a shear zone and a breccia band. The original stratigraphy consisted of alternating laminated (pyritic?) graded siltstones separating massive bedded siltstones (Neudert, 1983). The finely laminated sections of the stratigraphy may have been more susceptible to shearing processes during deformation. In some cases bands of pyritic shale occur which are poorly mineralised. These pyritic layers often show more ductile deformation including small centimetre-scale folds.

Similarly in diamond drill core from the 3000 Orebody the same localised grade variations associated with shear zones can be observed. Not all grade variations of this type can be directly related to faults.



Fig 4.8: Cross section 6390 mN - assay data from diamond drillholes with interpreted shear zones. Highlighted assays show position of samples for mineralogical analysis.



## 4.4 Shear Zone Geometry and Distribution Patterns

The shear zone distribution patterns within the 3000 and 3500 orebodies differ slightly and are described separately. For the purpose of this study the shear zones have been correlated over a vertical distance of 240 metres. Figures 4.9 a-d are a set of plans at 60 metre vertical intervals showing shear zone geometry with respect to silicification (distribution of fractured siliceous shale and siliceous shale 'rock types') and the 2.5% copper grade boundary. As described in chapter 2, silicification and copper grade are closely linked and the silicification outline corresponds very closely to the orebody limits. Figures 4.10 a-f are a corresponding set of east-west cross sections (looking north) at ~ 90 metre intervals (6025mN, 6115mN, 6205mN, 6300mN, 6390mN and 6480mN). Information on the 3000 Orebody is sparse north of 6250mN and it has not been included on the three northernmost sections.

### 4.4.1 3000 Orebody shear zones

The major sets of structures trend SSW-NNE and uniformly dip westwards. There seems to be two groups of these NNE trending fault systems. The first on the footwall edge of the orebody, and the second on the hangingwall of the orebody. A 25 to 50 metre zone of fractured siliceous shale, which has a much lower component of remnant bedding, separates the two groups. The shear zones in the footwall group tend to be narrower and more discrete. The hangingwall group is a whole series of splay structures that are linked to each other by less well developed anastomosing fractures. Towards the northern edge of the currently exposed 3000 Orebody some NE trending structures are prominent and some of the NNE structures terminate against them. The shear zones flatten in dip towards the basement contact fault but their strike generally does not change as they approach the basement.

### 4.4.2 3500 Orebody shear zones

The nature of the shear zones in the 3500 Orebody is the same as in the 3000 Orebody but they strike more N-S. North of 6030mN five main shear zones have been delineated. There is a high frequency of small faults in between them. Recent detailed underground mapping shows that the shear zones are corridors of N-S striking fractures with NNW-SSE and NNE-SSW linking splays.

Fig 4.9a: Alteration and Shear zones - 23A sublevel.

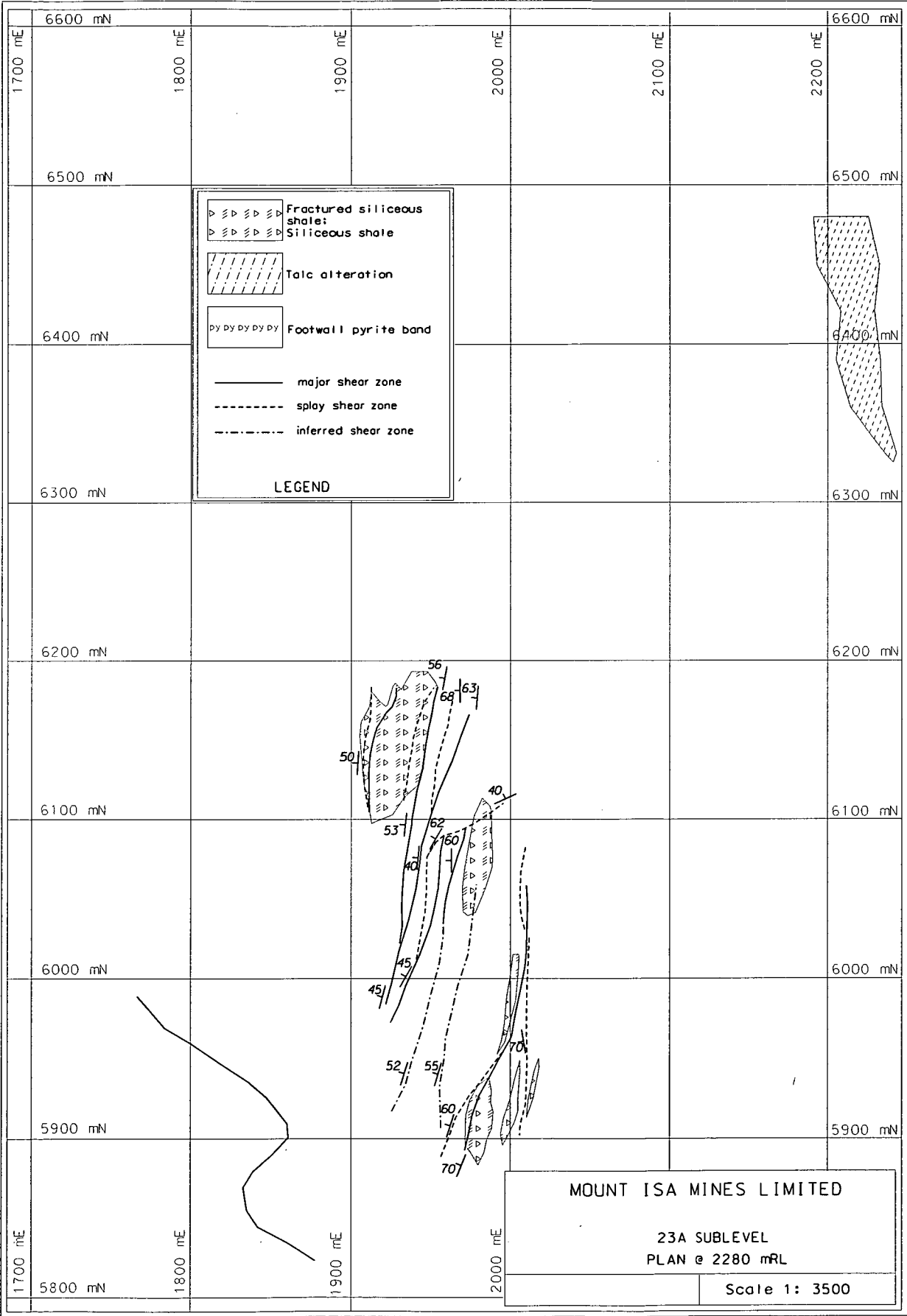


Fig 4.9b: Alteration and Shear zones - 24A sublevel.

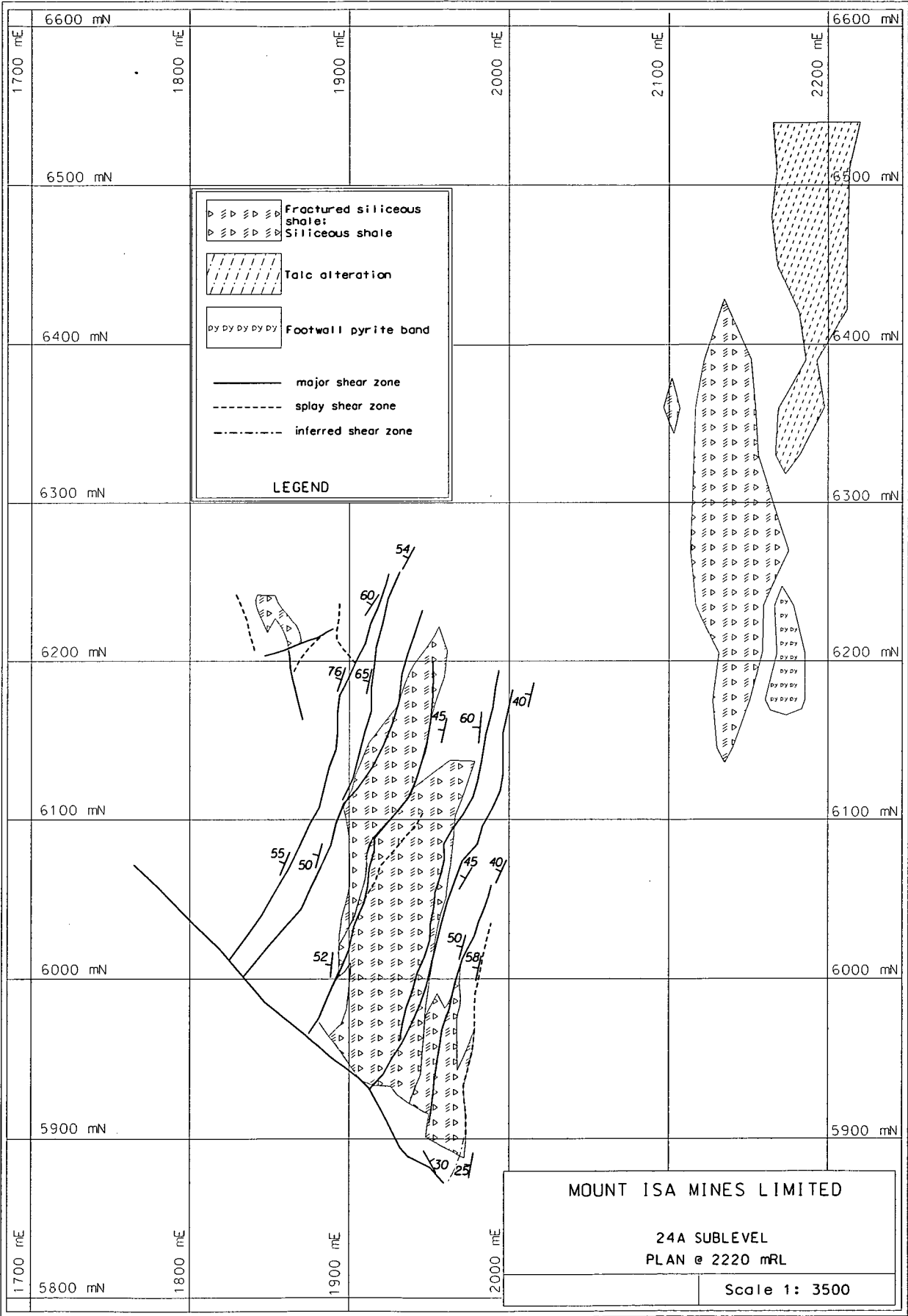




Fig 4.9c: Alteration and Shear zones- 25A sublevel.

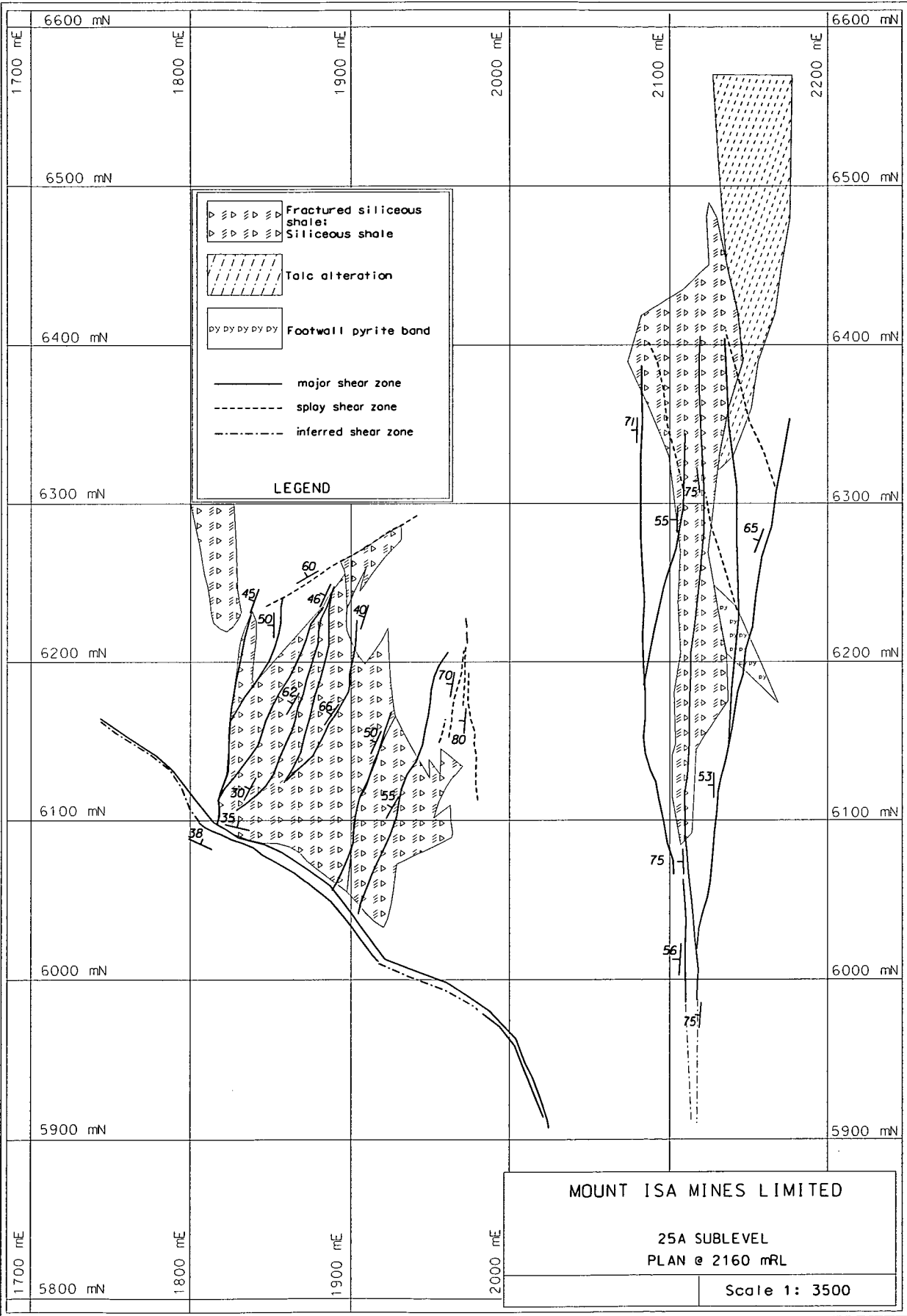


Fig 4.9d: Alteration and Shear zones - 26B sublevel.

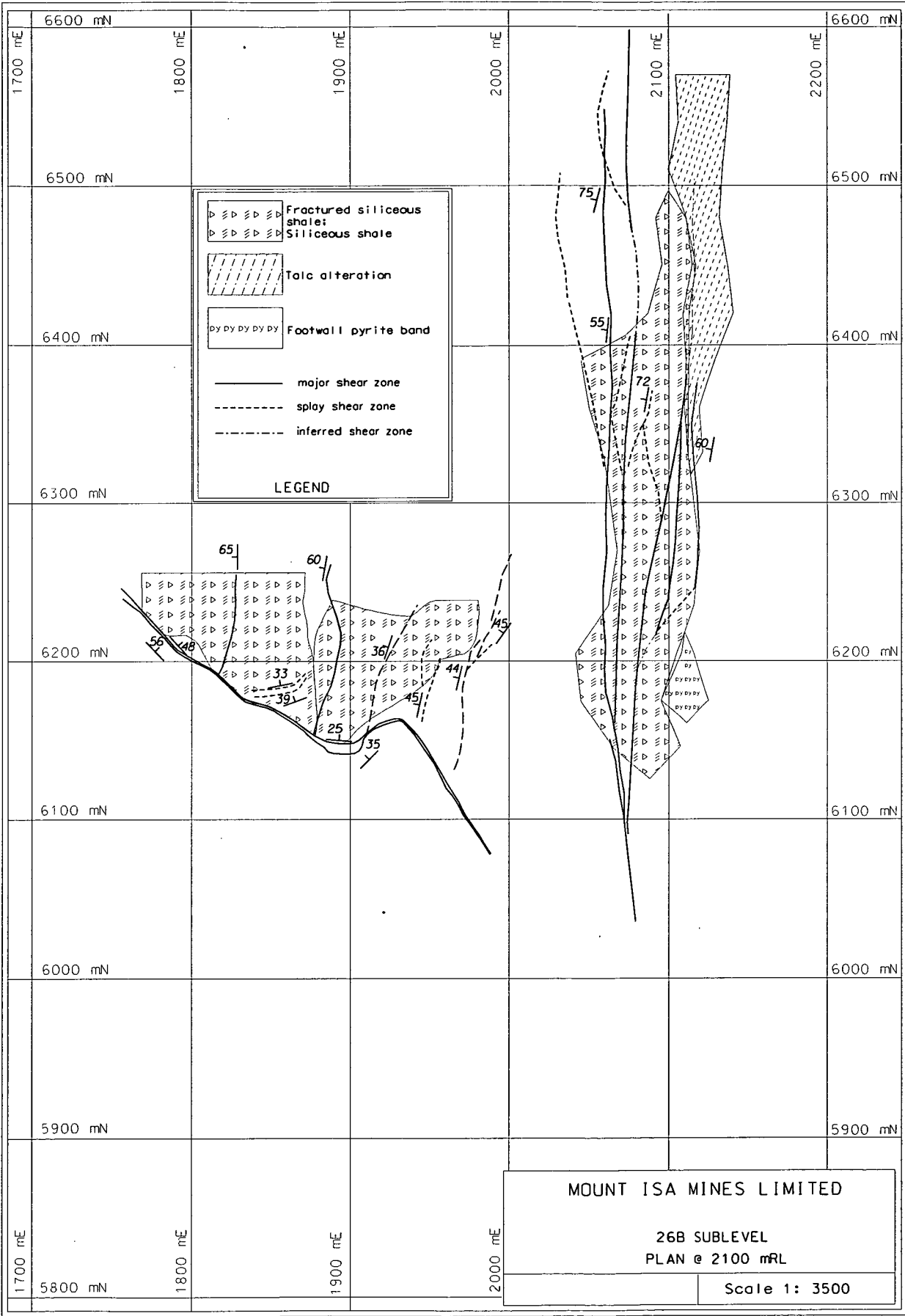


Fig 4.10a: Alteration and Shear zones - 6025 mN cross section.

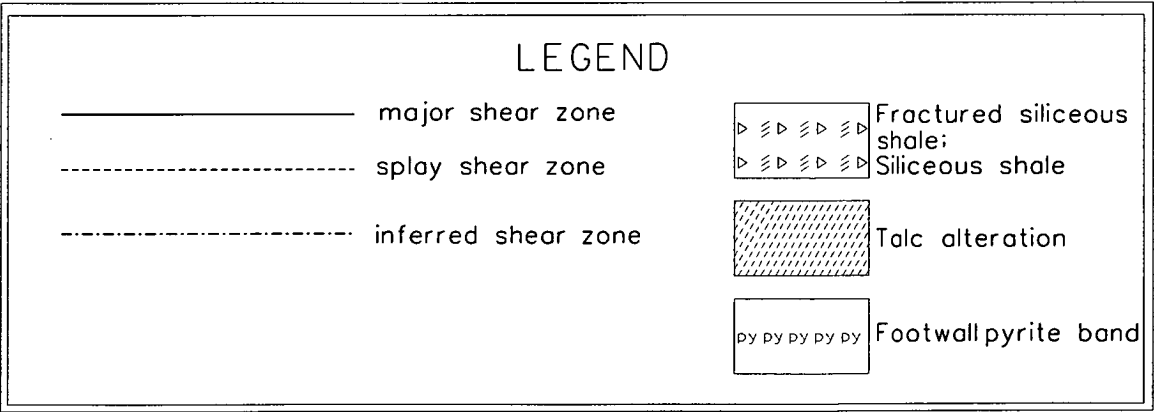
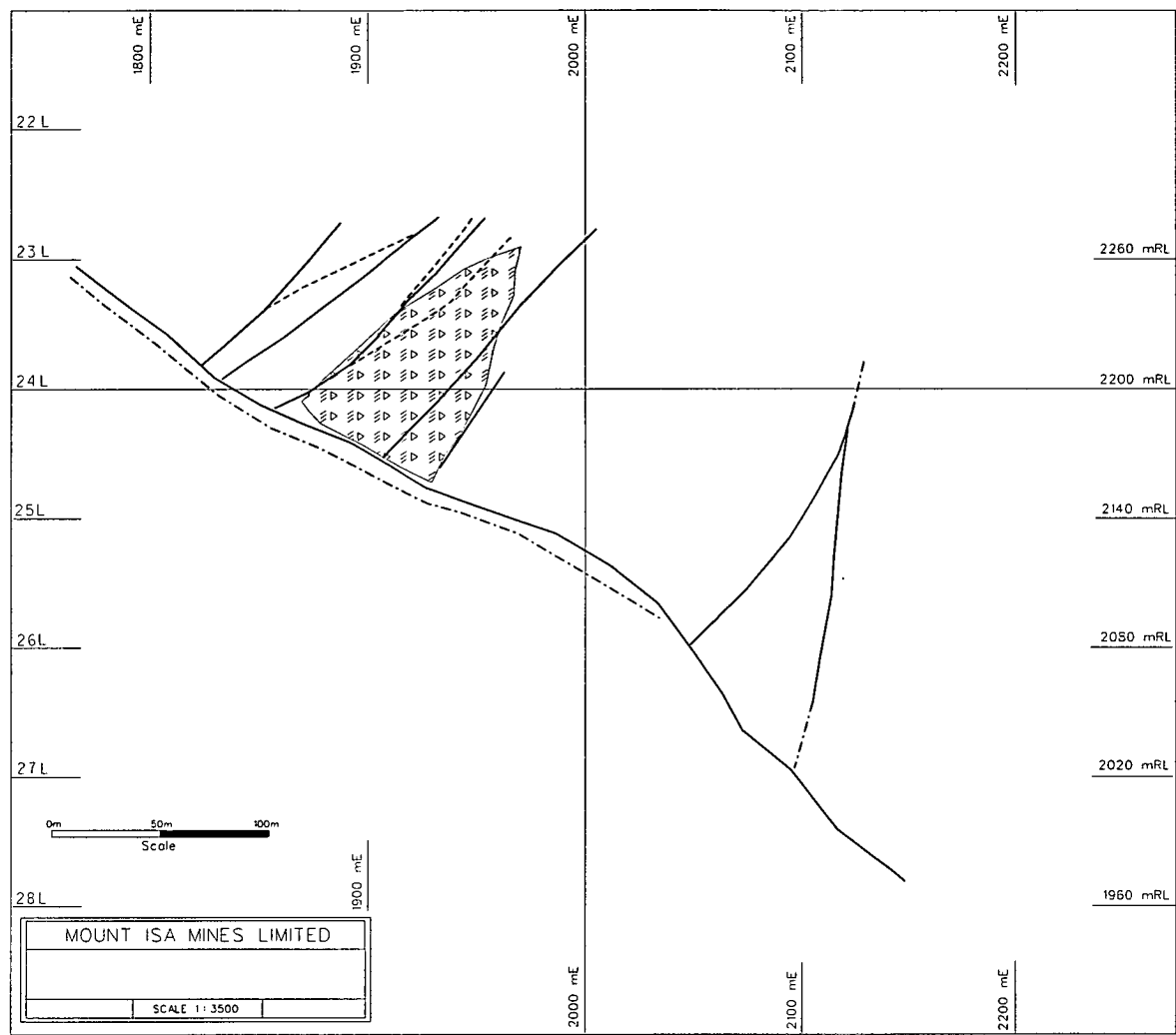


Fig 4.10b: Alteration and Shear zones - 6115 mN cross section.

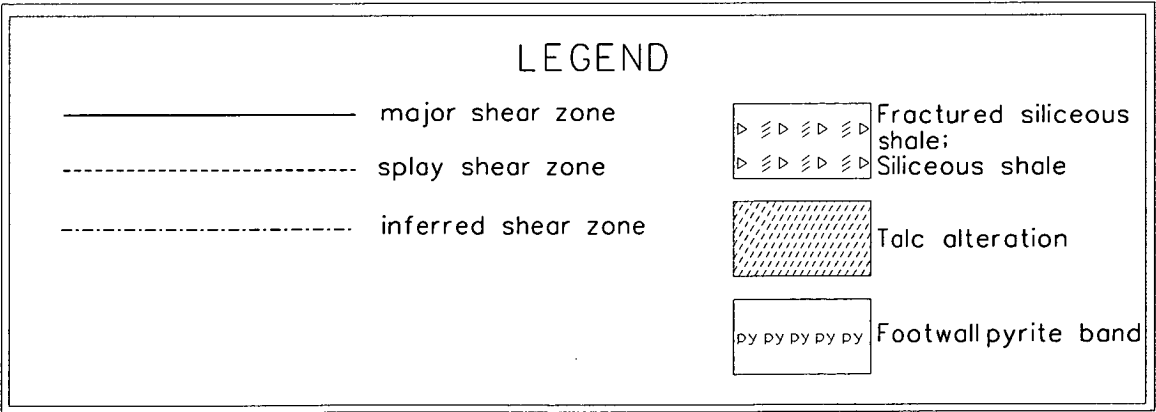
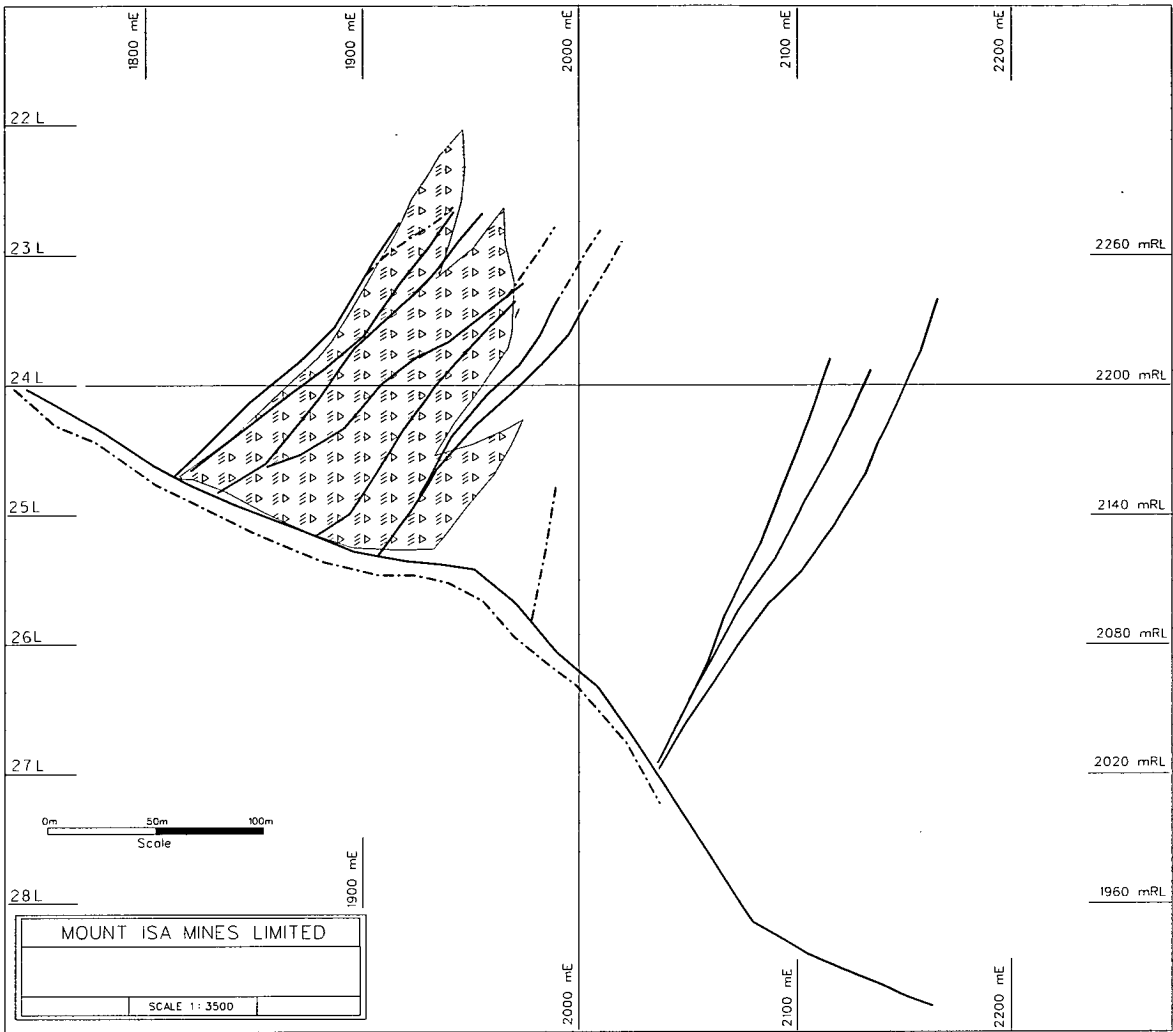


Fig 4.10c: Alteration and Shear zones - 6205 mN cross section.

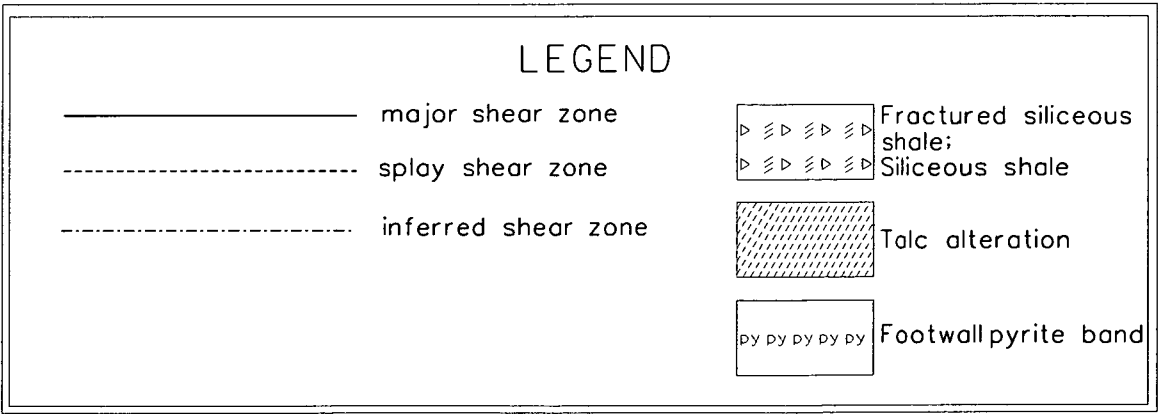
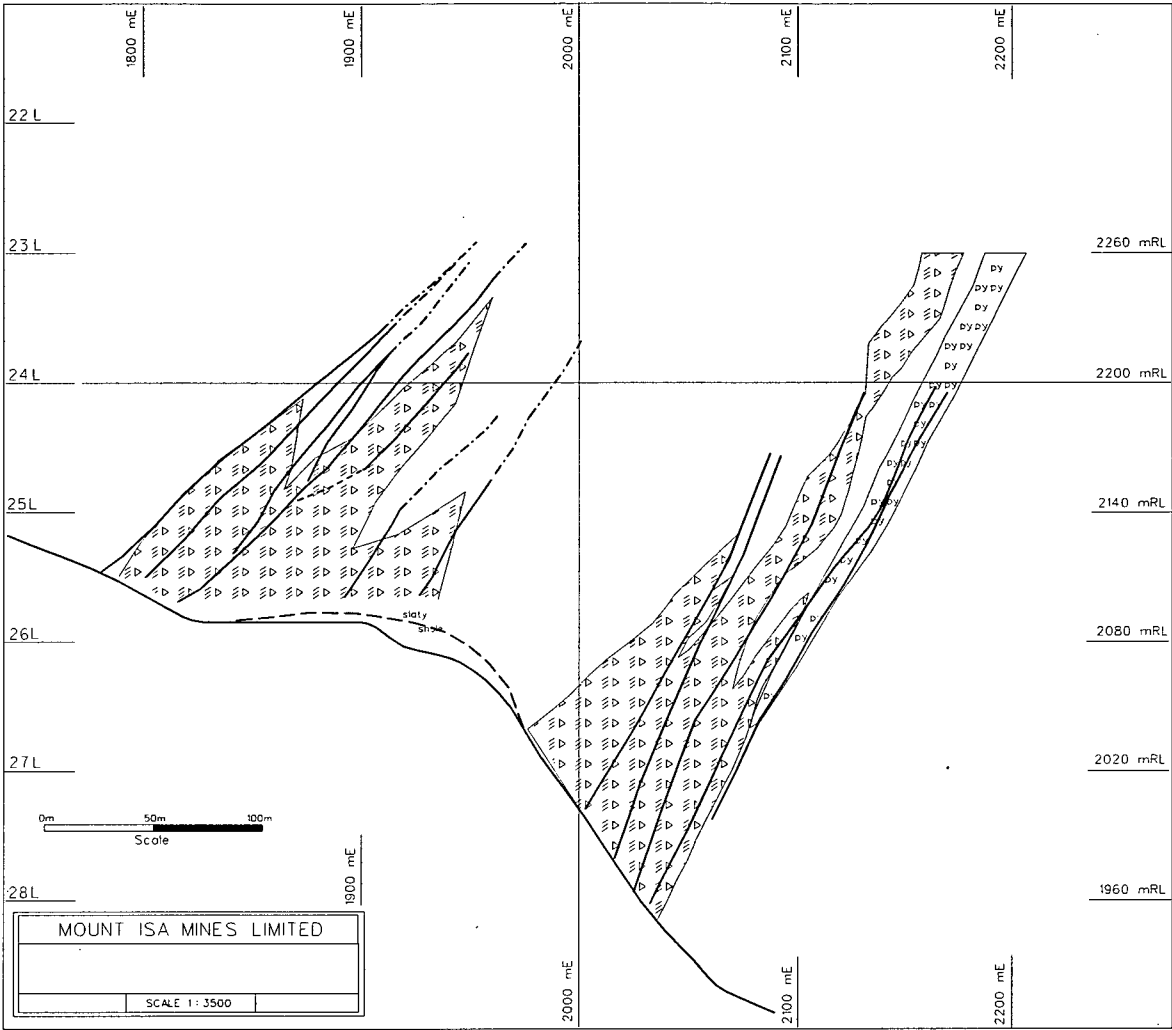


Fig 4.10d: Alteration and Shear zones - 6300 mN cross section.

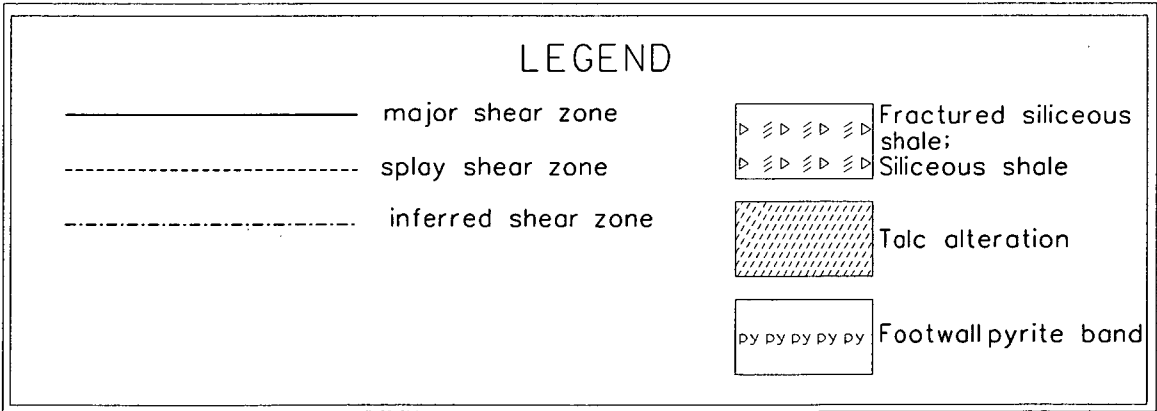
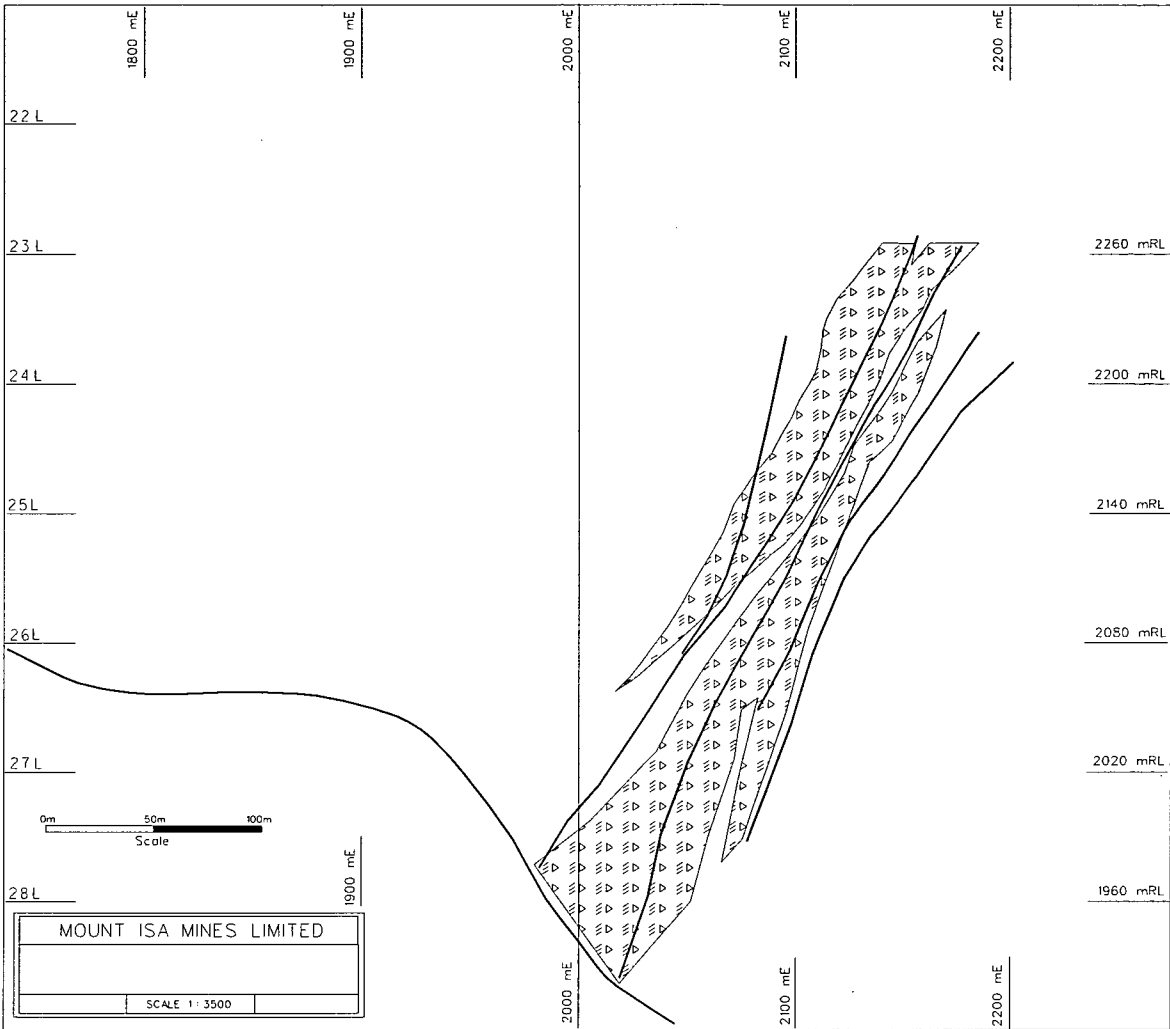


Fig 4.10e: Alteration and Shear zones - 6390 mN cross section.

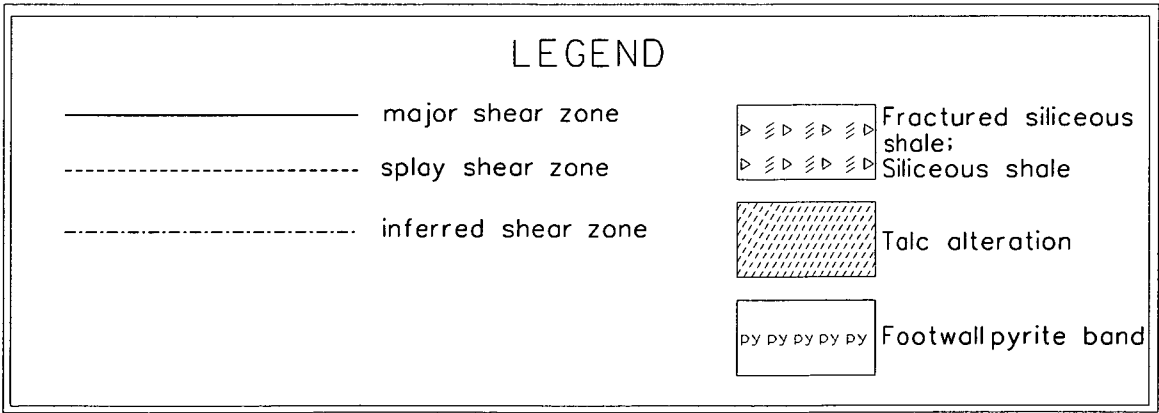
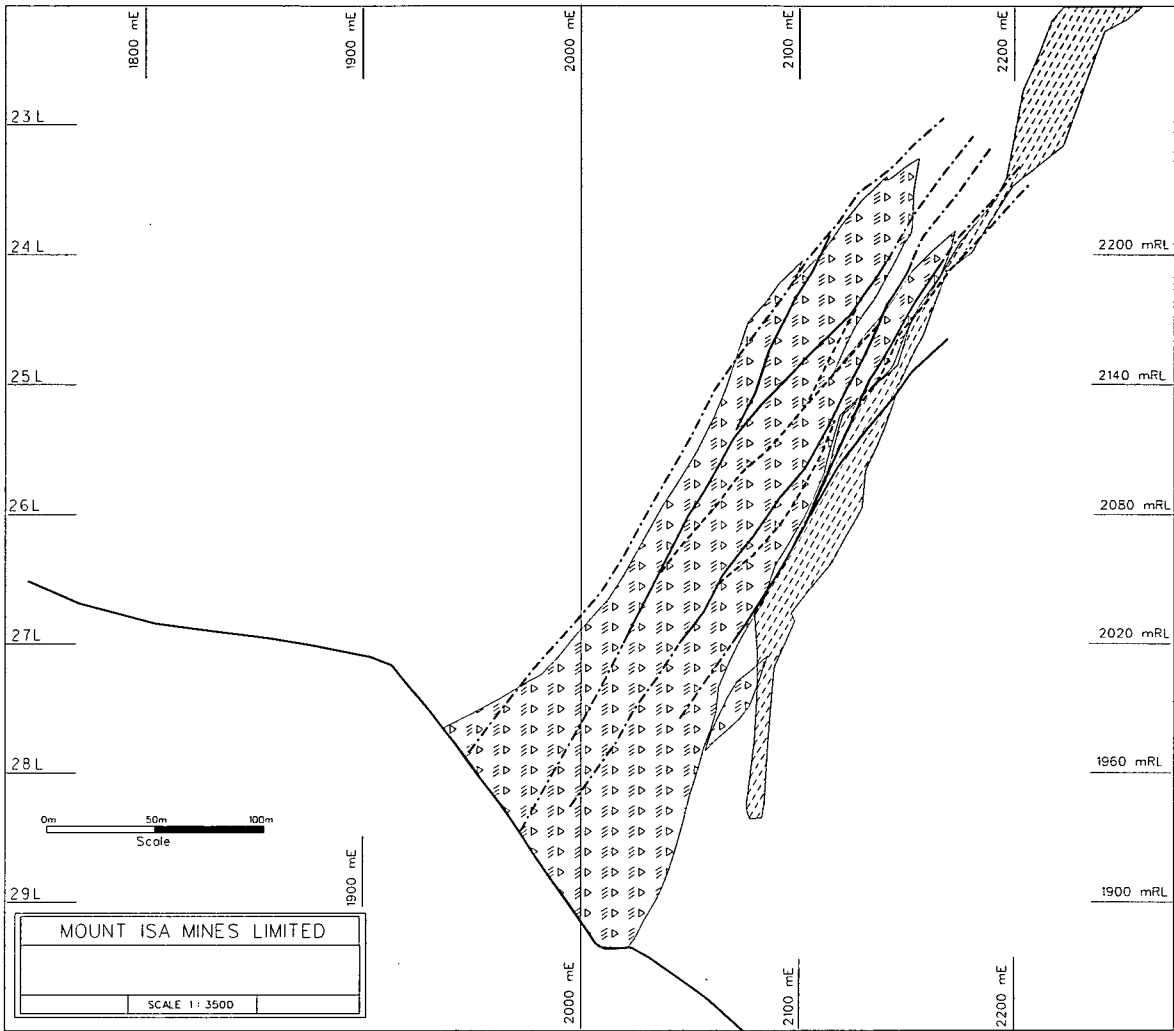
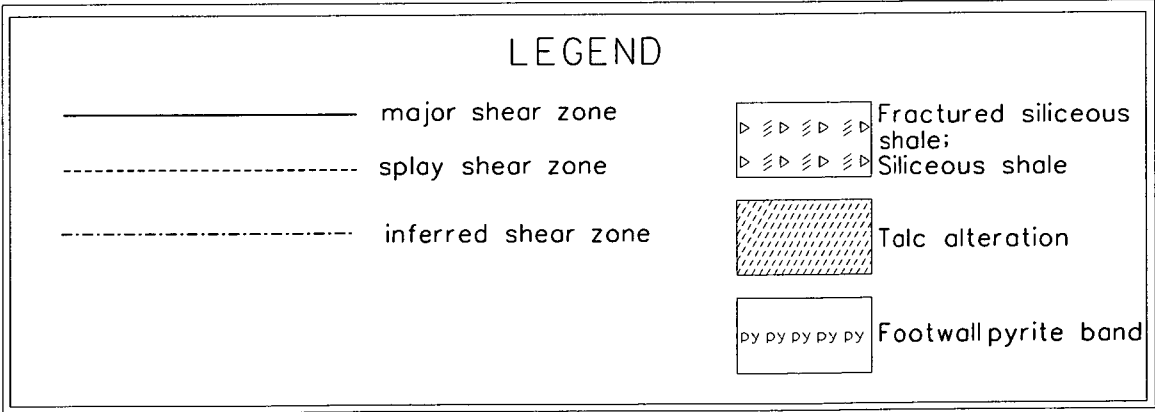
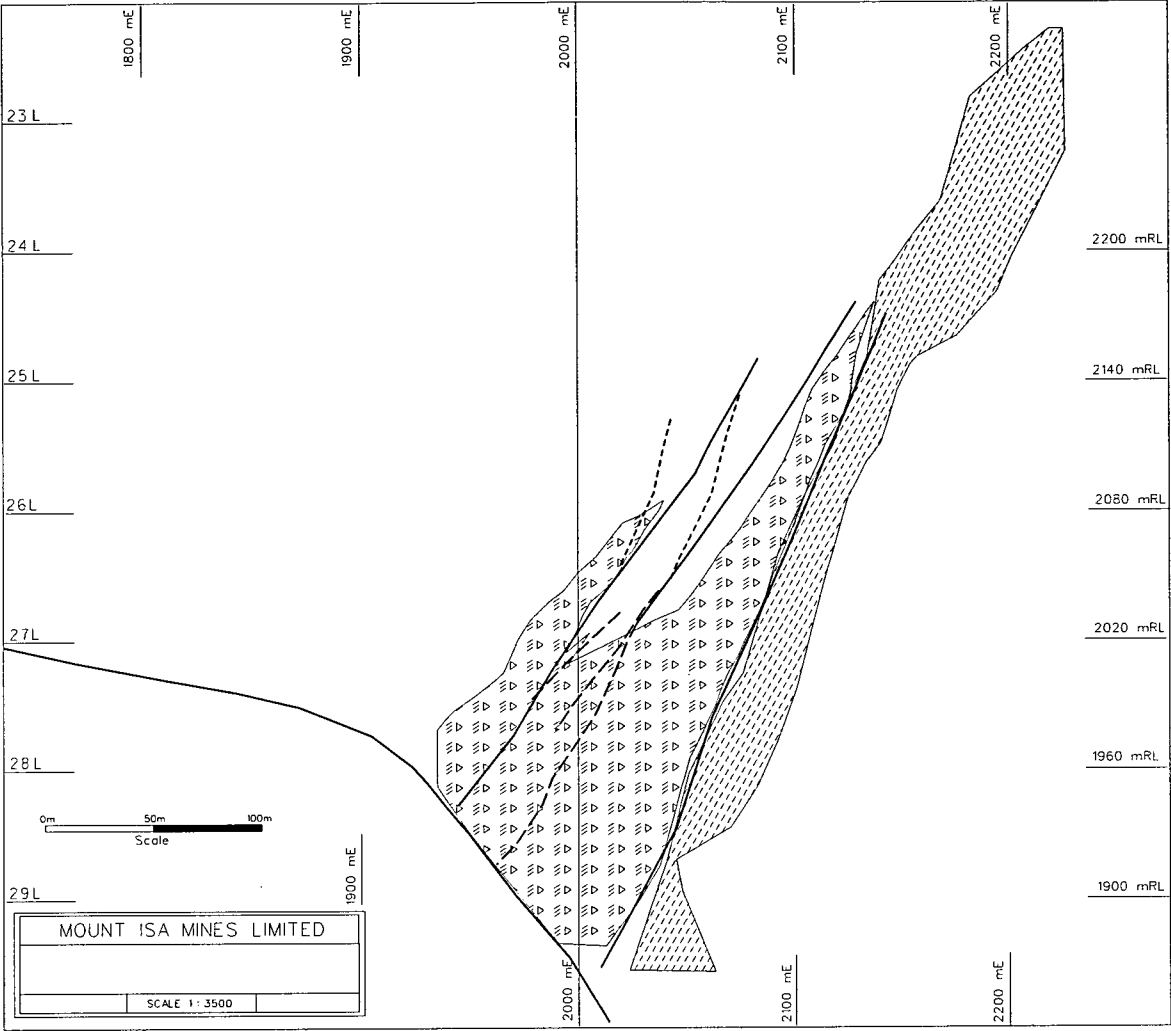


Fig 4.10f: Alteration and Shear zones - 6480 mN cross section.





#### 4.4.3 Urquhart Shear

South of 6030mN the shear zone distribution is quite different with a 10m to 20m wide zone of near vertical and bedding parallel splay structures. This zone has been interpreted as the expression of the Urquhart Shear. The Urquhart Shear is a major fault that has been mapped at surface down to 17 level. At surface the Urquhart Shear is a steeply west dipping structure (Fig 1.5). In the Enterprise Mine south of 6030mN, outside the limits of the orebody the Urquhart Shear is interpreted as a complex zone of ~ 10 metres width. The best exposure of this zone is in the 160 xcut on 25A as shown in Fig 4.12. Here it is composed of a linked splay set of near vertical to east dipping faults and west dipping bedding parallel shear zones. Movement on the faults has clearly disrupted the adjacent bedding. Quartz and dolomite veining +/- chalcopyrite is well developed.

North of 6030mN it is difficult to define the Urquhart Shear as a particular shear zone. The structure appears to widen and propagate into at least five separate orebody shear zones observed in the 3500 Orebody.

The shear zones in the 3500 Orebody (and the 3000 Orebody?) may represent splay structures that have developed linking the basement contact fault and the Urquhart Shear (Fig 4.13).

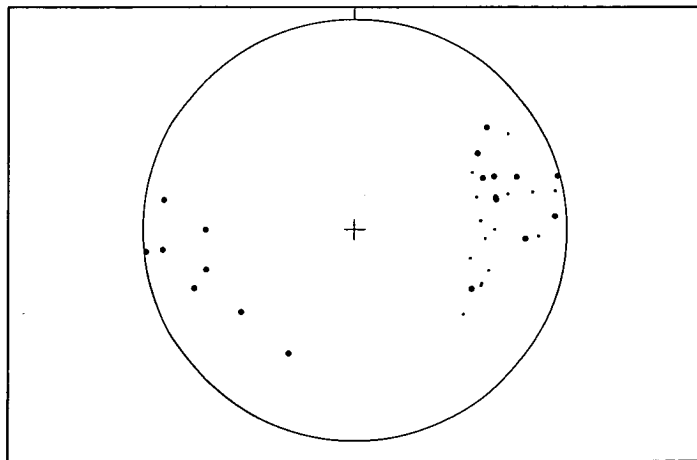
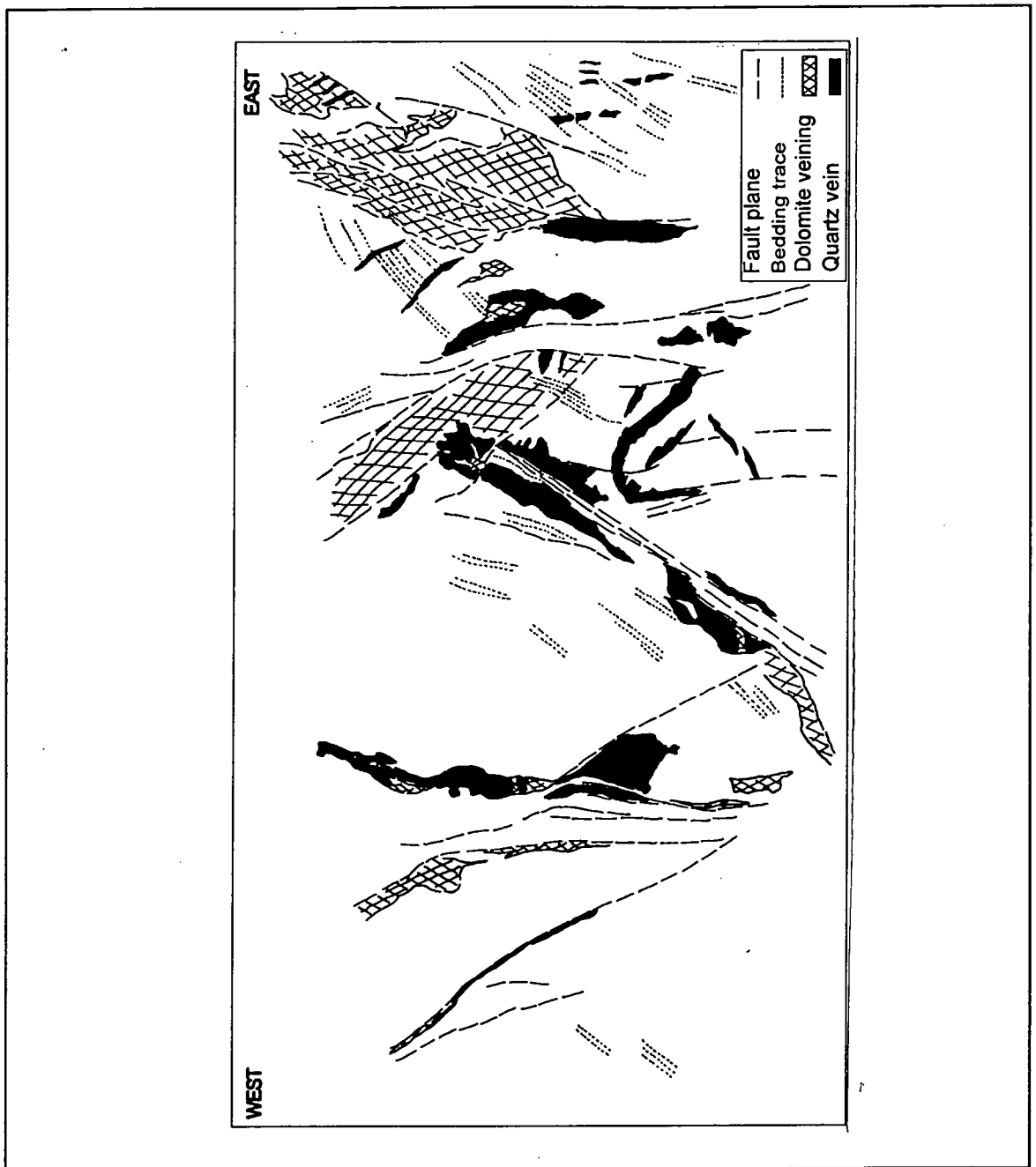


Fig 4.11: Poles to fault surfaces (large dots) and bedding (small dots) from within the Urquhart Shear zone (measurements taken from location shown in Fig 4.12).

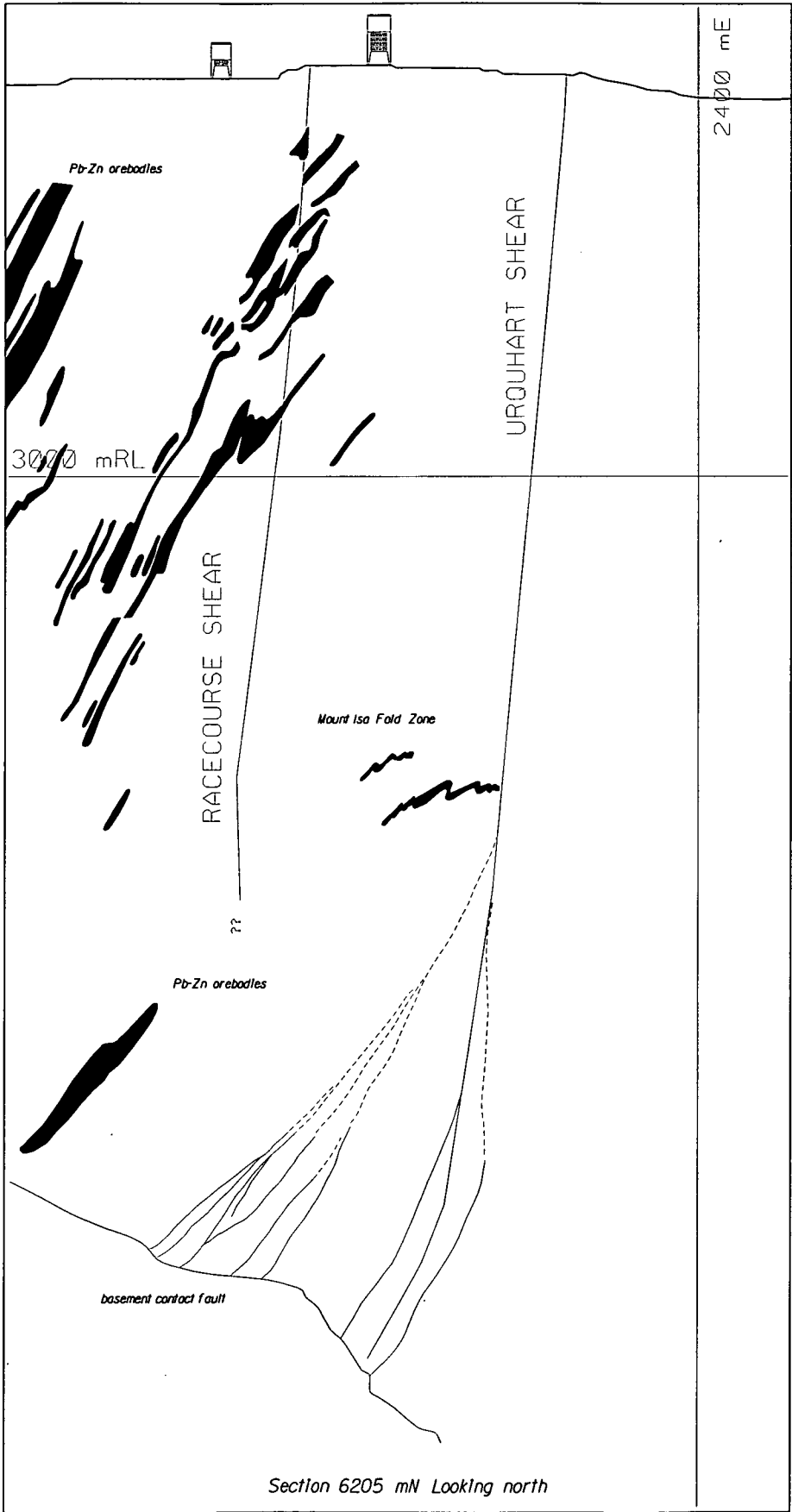
Fig 4.12: Interpretation of underground exposure of the Urquhart Shear. 160 Xcut 25A (looking north - field of view 9m).



#### 4.4.4 Mount Isa Fold Zone

The Mount Isa Fold is the largest fold in the mine (Lead Mine and Enterprise Mine). It has a wavelength of 200 to 400 metres and plunges to the north at  $45^\circ$  to  $60^\circ$  with a near vertical axial plane. Orientation and axial plane cleavage characteristics indicate it to be a  $D_3$  fold. This fold is transected by two major shear zones, the Urquhart Shear and the Racecourse Shear (Perkins, 1995).

Fig 4.13: Schematic diagram of possible relationship between the shear zones in the 3000 and 3500 orebodies and the Urquhart Shear and the Mount Isa Fold Zone.



## 4.5 Fault Movement

Slickenlines are generally developed on the graphitic surfaces of discrete faults on the boundaries of, or within the shear zones. The striations are visible but the sense of movement is difficult to determine as they have little relief and very poor development of steps as in quartz slickenfibres. The dominant direction of movement is dip slip. Rare occurrences of strike slip movement indicators have been observed.

In some locations a very weak cross hatch effect was observed, suggesting two movement directions at right angles to each other.

The nature of the orebody and host silica-dolomite 'rock types' has obliterated any potential marker beds. At one location a 10 cm pyrite bed indicated apparent reverse dip slip movement of ~ one metre.

Figure 4.14 shows plunge and trend data of slickenlines plotted on the plane of the fault surface. Figure 14.15a & b shows the typical expression of slickenlines on fault surfaces in the orebodies.

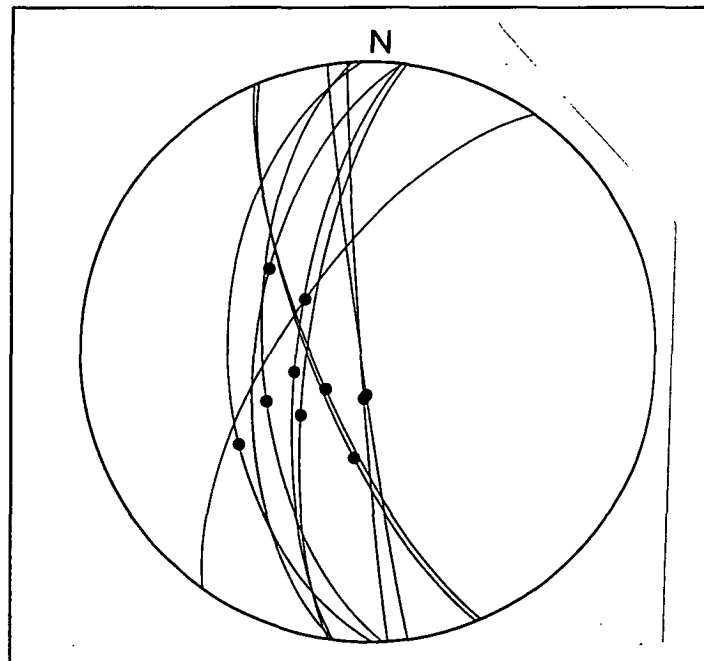


Fig 4.14: Plunge and trends of slickenlines on 3500 Orebody fault surfaces.

---

Fig 4.15a: 3500 Orebody corner 435 Xcut and V60 FWDR 25A. Slickenlines on graphitic fault surface in shales on the footwall of 3500 Orebody (Looking southwest. Pencil 14cm).

Fig 4.15b: 3500 Orebody U61 NDR off 395 Xcut 28D. Slickenlines on fault surface within the 3500 Orebody (Looking east. Pencil 17cm).

Fig 4.15b

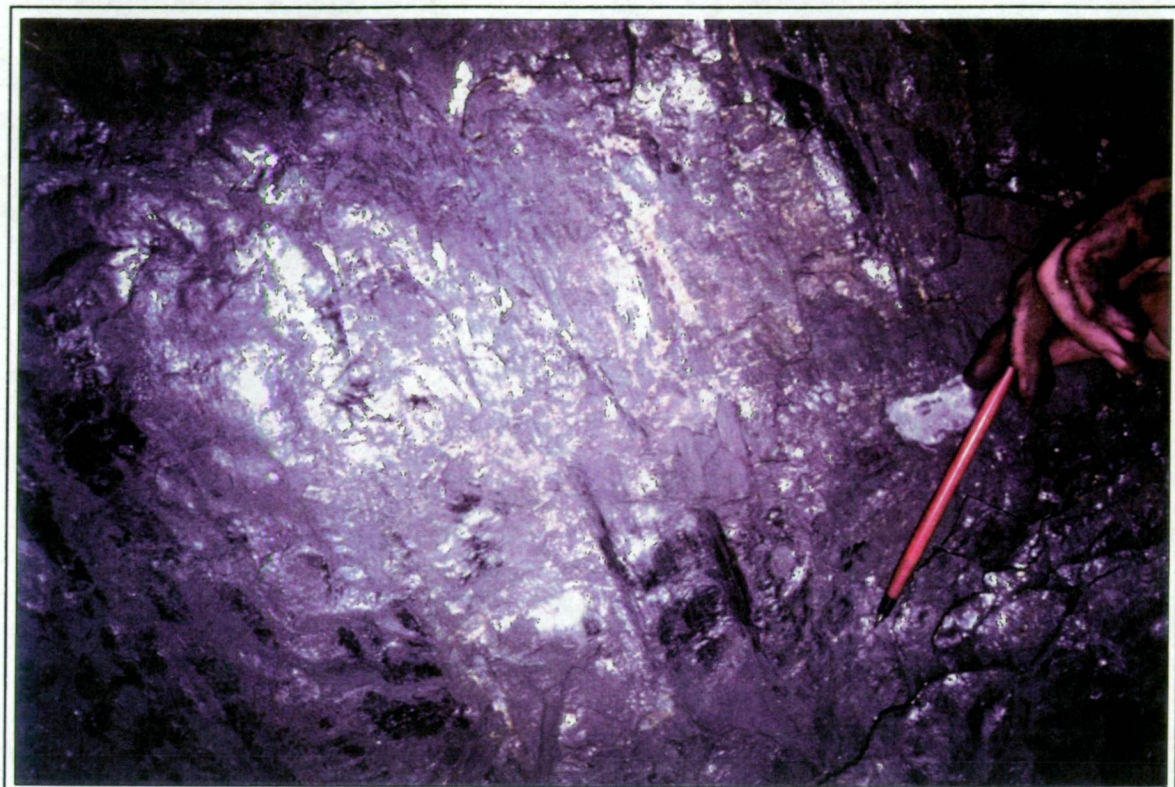


Fig 4.15a



4.6 Orientation Data

Fig 4.16 gives a summary of all the data available on bedding and fault orientations. All of the data is from the 3000 Orebody area as only very limited underground exposure was available from the 3500 Orebody. Figs 4.17a and 4.17b show how closely shear zone geometry is linked to bedding when broken down to individual levels. There is a greater component of northwesterly dipping structure as you progress down from 23A to 26B. This affects the shear zones as well as the bedding, though the effect on bedding is more pronounced. On 25A the strike of the bedding turns markedly from N-S to SW-NE and the dips flatten from 50° to 30°. The cause of this rotation is the proximity to the flatter dipping folded sections of the basement contact fault. Where bedding parallel shear zones approach the basement contact fault, they also have been observed to flatten in dip. None of the orebody shear zones have been observed to cut across or displace the basement contact fault.

Fig 4.18 shows detail of rotated bedding adjacent to the contact on 25A.

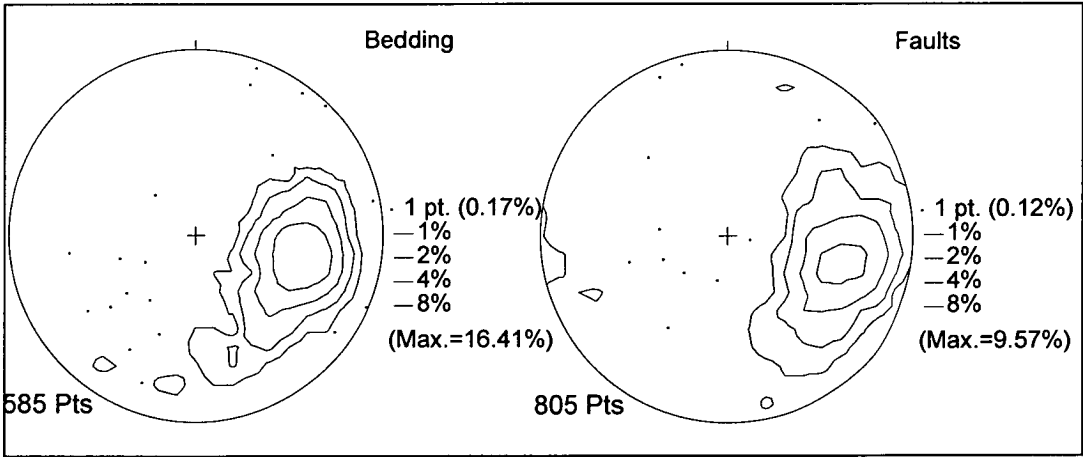


Fig 4.16: Orientation data for all bedding and faults 3000 Orebody.



Fig 4.17a: Comparison of poles to bedding data for each sublevel in the 3000 Orebody.

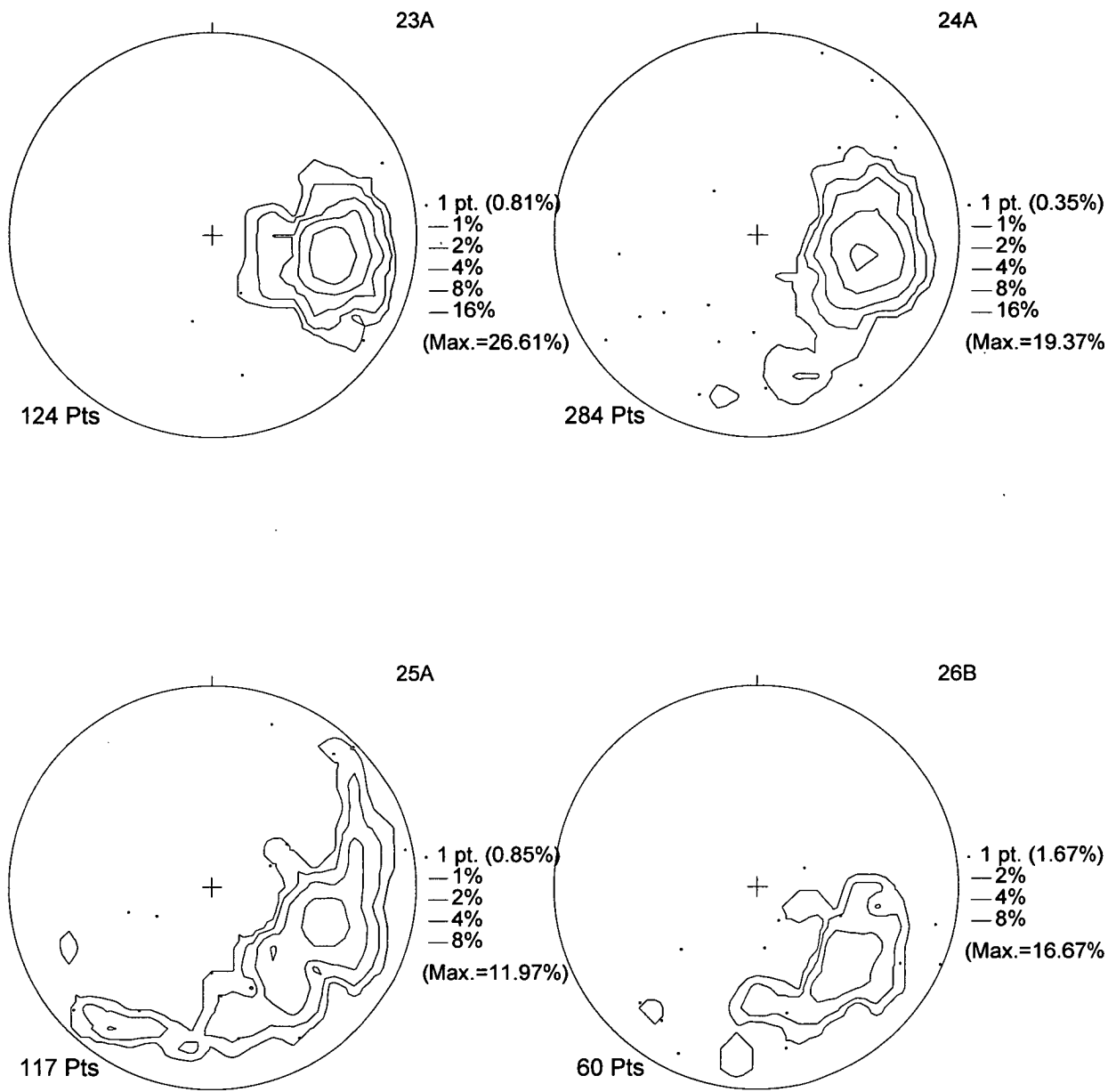




Fig 4.17b: Comparison of poles to fault plane data (within shear zones) for each sublevel in the 3000 Orebody.

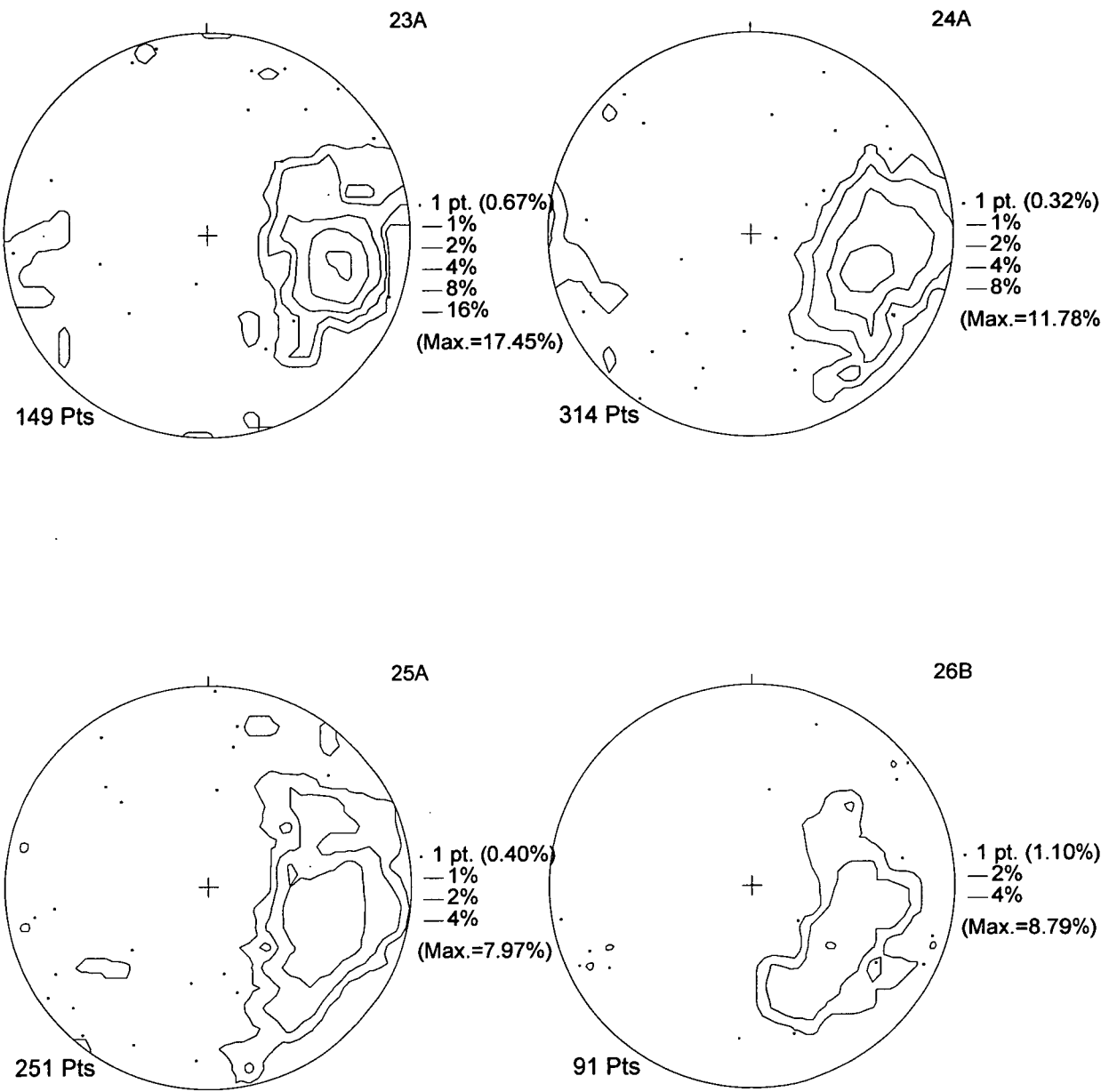
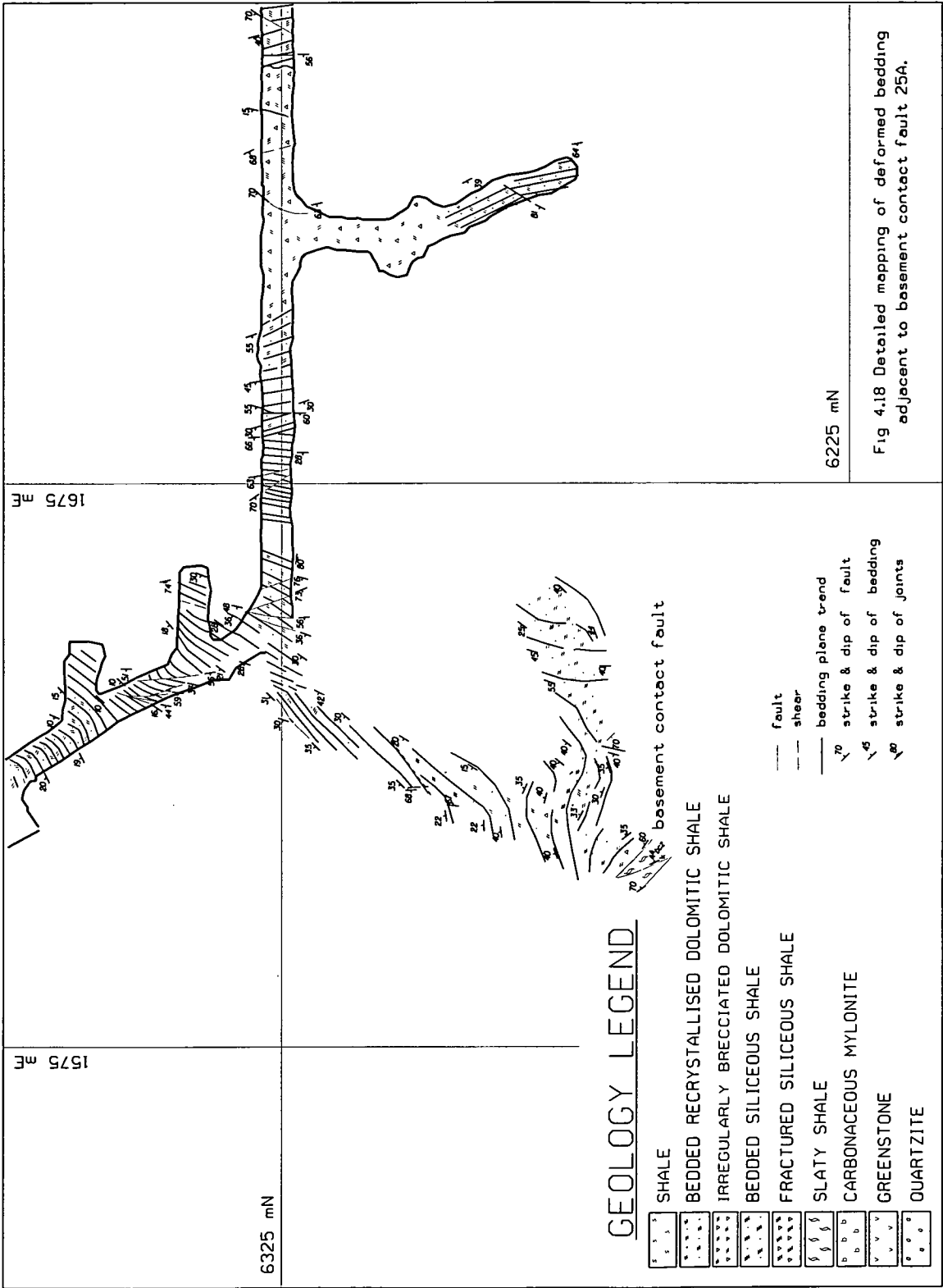


Fig 4.18: Detailed mapping of deformed bedding adjacent to the basement contact fault.



---

## 4.7 Discussion

### 4.7.1 Orebody Formation

Studies by Perkins (1984), Swager (1985) and Bell *et al.* (1988) concentrate on the replacement model for formation of the Mount Isa copper orebodies and on the structural framework which caused their formation.  $D_3$  folds in the basement contact fault are a primary structural control on the localisation of the mineralising fluids. During  $D_3$ , antithetic shearing on bedding commenced. It is inferred that reactivation of the bedding above, but not below the basement contact fault led to brittle failure and localised opening of the contact. High fluid pressure resulted in fracturing and local brecciation of the dolomitic rocks. The degree of fracturing in the greenschists below the contact was minor because bedding development in these rocks is weak and at an orientation that did not allow ready propagation of fractures away from the contact. From these conclusions there must have been large scale channeling of hydrothermal fluids through the shales. The scale of fracturing decreased rapidly away from the basement contact. This generated an upward closing zone of fractured rock. The commonly strata-bound nature of the silica dolomite lobes indicates that bedding was a structural anisotropy along which, but not across which fluid flow could easily proceed. Joints, veins and bedding parallel fractures in the shale layers provided effective pathways for the fluids (Bell *et al.* 1988).

This study attempts to describe more fully the nature of these pathways.

For both orebodies fracturing is confined to the immediate area of the copper mineralisation. In the hangingwall of 3000 Orebody, the footwall of the 3500 Orebody and in the area between the orebodies, faulting of the style described is very restricted. Any faults/shear zones that do occur tend to be discrete and < 20 cm in width. Although the major copper mineralisation occurs directly above the basement contact fault, smaller orebodies are present at higher levels detached from the contact. This suggests that the copper bearing fluids could be transferred toward higher locations without depositing their entire load in the conduits. No authors to date have really discussed how this occurs.

An antiformal hinge zone that occurs between the two orebodies defines the Mount Isa Fold Zone. The bedding becomes very contorted with the development of small scale folds with wavelengths of one to five metres. The folds plunge  $60^\circ$  to  $75^\circ$  to the northwest/north (range  $330^\circ$  to  $010^\circ$ ). The more northerly plunges occur on the eastern edge of the fold zone. Intense folding occurs in a pyritic horizon above the orebodies ( $\sim 22$  L). There is no significant copper mineralisation within the axial plane region of the fold. The hinge areas of flexures in the basement contact fault follow the trend of the Mount Isa Fold plunge (though at a much shallower angle).

As mentioned previously it is difficult to define a single structure as the Urquhart Shear. My suggestion is that it has 'feathered out' at depth as it interacts with the basement contact fault. The orebody shear zones flatten in dip and seem to terminate at the basement contact fault as none have been observed to displace the basement. The orientation of bedding and shear zones and the indicators that bedding plane slip was an important process suggests that the shear zones formed towards the latter stages of development of the Mount Isa Fold, possibly as accommodation structures as the folds progressively tightened. A lot of the work done on the region has shown that there is a strong relationship between folding and faulting and that the two processes act together. In chapter one I presented the interpretation of the orebodies as it was in 1972 when it was thought that they may have been folded by the Mount Isa Fold ( $D_3$  fold). This is not the case and the data presented suggests that the Deep Copper orebodies formed syn (but late) with the fold and that the fold geometry strongly influenced the position of the orebodies.

#### 4.7.2 Ductility contrasts

One of the major difficulties in determining the timing of the shear zones associated with the 3000 and 3500 orebodies is that they often occur on the boundaries of mapped alteration 'rock types'. This is a result of the descriptive terminology used in the mine, which is partly based on the degree of brecciation or preserved bedding in the rocks. This leads to the problem of whether the faulting causes the brecciation or whether the shear zone is using a boundary between pre-existing 'rock types' of contrasting competency. The mineralogical data from the shear zones and adjacent

breccia zones suggests there may have been an initial influence of primary sedimentology on the layers that preferentially took up strain by brittle-ductile shearing rather than hydraulic fracturing. Considering the pre-D<sub>3</sub> attitude of bedding the shear component of deformation and any flexural slip during folding may have preferentially been accommodated within the finely laminated sections of the stratigraphy. These would then behave as conduits for the invading fluids, channelling alteration preferentially up along bedding and invading the rock adjacent to and between the shears. As the rock undergoes dolomite recrystallisation and silicification the actively shearing sections of the stratigraphy would maintain the fluid access. The silicification however would conceivably cause the system to 'self-heal' away from the actively deforming zones and therefore inhibit fluid migration into the massive bedded siltstones. When the massive units between the shear zones are silicified the competency contrast between the shear zones and the silicified beds could produce a breccia in the massive units. When the degree of replacement of the rock by chalcopryite is almost complete the competency contrast between the shear zone and the rock would drop and even the shear zones may become mineralised to the extent that they are no longer recognisable.

Observations by Valenta (1994) at the Hilton Mine, Mount Isa determined that the primary large scale focus for syntectonic copper mineralising fluids was a zone of intense veining at the intersection of the Paroo Fault (basement contact fault) and the hangingwall fault. Structural focussing of the fluid flow through pre-existing orebodies was related to displacement at fault intersections and to competency contrasts in the focussing of migrating metal bearing fluids. Layers with a large proportion of sphalerite and galena deformed in a ductile manner at relatively high strain rates and low differential stresses. Dolomite and pyrite layers deformed in a brittle manner under the same conditions. Fluid flow was focussed into brittle layers resulting in the precipitation of chalcopryite and gangue minerals in microfractures.

The movement of the fluids from the shear zones into the breccia bands could be described by a process described by Cosgrove (1993) where high fluid pressures play an important role in shear failure, for example, in the initiation of bedding plane slip either during thrusting or flexural slip folding. During tectonic compression pore

fluid pressure increases until it is of sufficient magnitude to cause the formation of, or reactivation of a bedding plane thrust. Further movement on the thrust drives out the fluids from the slip zone and the resulting drop in pore fluid pressure causes the thrust to lockup temporarily. Continued action of the applied stress causes the fluid pressure to increase again until the conditions for hydraulic fracturing are reestablished and the process is repeated.

#### 4.7.3 Fracture Networks

Considering the degree of fracturing associated with the orebodies it may be possible to apply the concept of fault-fracture meshes to the development of the Deep Copper orebodies (fig 4.19). Sibson (1989; 1996) discusses the factors, which allow the development of extensive low-displacement fault fracture networks, and the flow of large volumes of fluid. The infiltration of pressurised fluids into stressed heterogeneous crust may induce a range of differently oriented brittle structures that become progressively interlinked into a structural mesh which adds to the permeability of the rock mass. The resulting bulk structural permeability within the rock mass can be regarded as 'self-generated' by the infiltrating fluids. Much of the structural permeability developed in fault-fracture meshes is likely to be transitory, as microcracks, fractures and faults may all become infilled with low permeability hydrothermal precipitates, alteration products and/or clay rich gouge. Permeability enhancement through faulting and fracturing in hydrothermal systems competes with permeability reduction as a consequence of fluid flow and precipitation, so that deformation within fault-fracture meshes, either continual or intermittent, is necessary for them to remain effective as high permeability structural conduits.

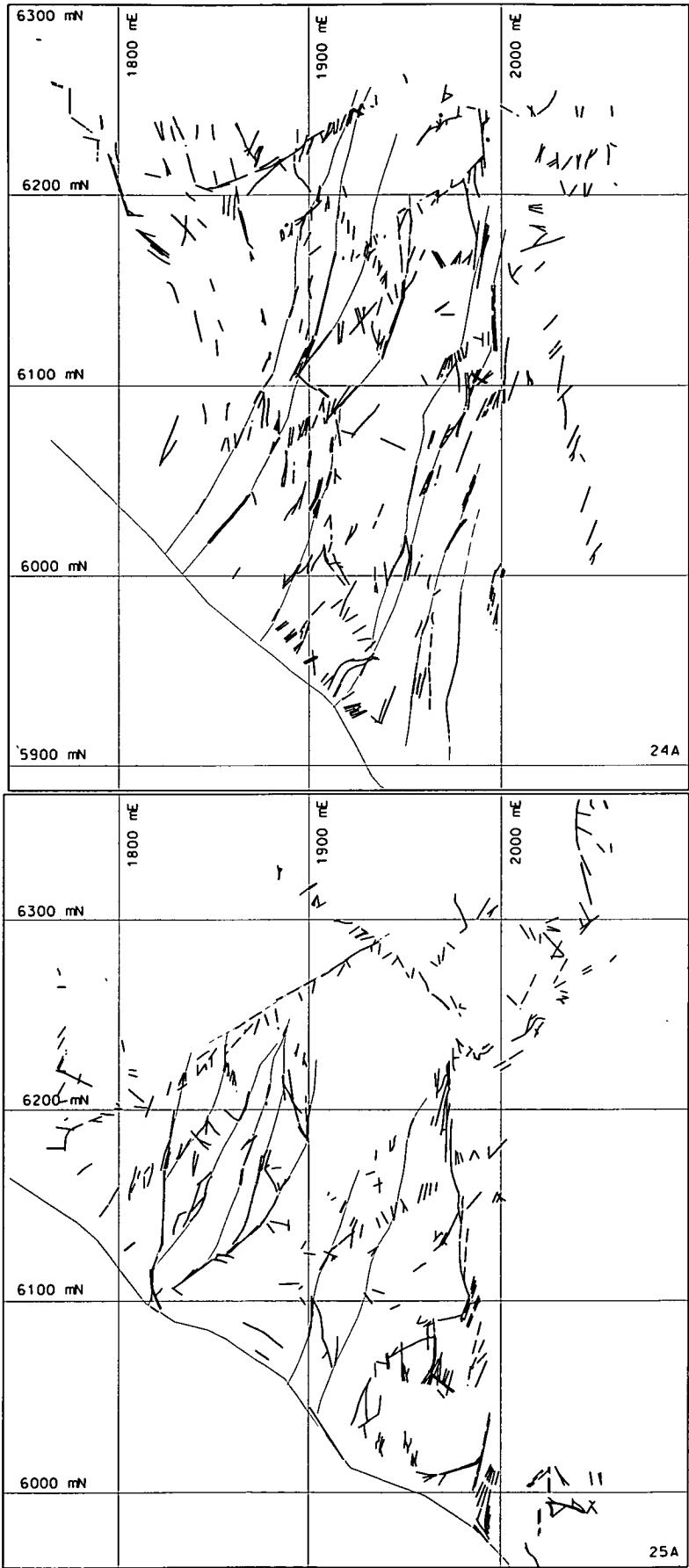
Faults that act as impermeable seals except immediately postfailure when they become highly permeable channelways for fluid discharge, may behave as fluid-pressure-activated valves wherever they transect a suprahydrostatic fluid pressure gradient. Such fault-valve behaviour is particularly likely for faults that remain active while unfavourably oriented for frictional reactivation in prevailing stress fields. The most extreme fault-valve action is likely to be associated with high angle reverse faults (Sibson, 1990). High angle reverse faults generally appear to have developed through the reactivation of earlier formed faults, or through progressive

---

misorientation of faults in the prevailing stress field (e.g. wherever formerly extended crust comes under compression). Mesh activation in a compressional thrust fault regime requires lithostatic fluid pressures. The extent and rate of mesh development and propagation is strongly affected by fluid supply, the maintenance of an appropriate hydraulic gradient and the permeability characteristics of the rock mass.

Many mesothermal gold-quartz lodes are hosted on faults that were undergoing high angle reverse or reverse-oblique motion at the time of mineralisation. Many deposits of this kind have tremendous vertical extent. Typically the hosting fault zones exhibit mixed brittle-ductile character and are comparatively small displacement structures (<100m). Two main vein sets occur: lenticular fault-veins lying subparallel to schistosity within the steeply dipping shear zones, and flats (subhorizontal extension veins). Favoured localities for mesh development include short-lived irregularities along large displacement fault zones such as dilational jogs, lateral ramps, transfer faults and other forms of link structure (Sibson, 1996).

Fig 4.19: Fault network on 24A and 25A sublevels - 3000 Orebody





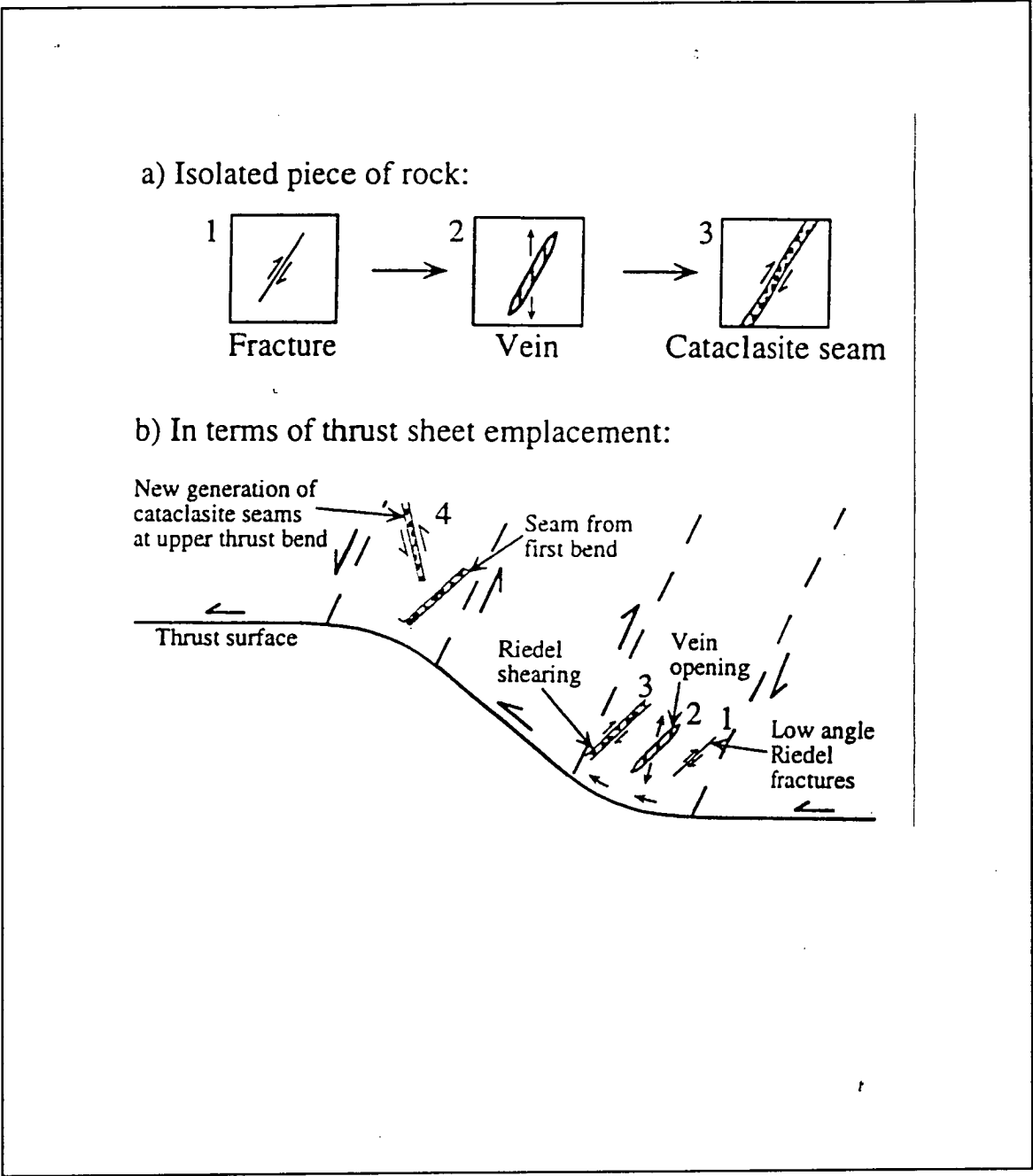
#### 4.7.4 Geometrical Considerations

Finding a structural model that may describe the geometries of the shear zones observed in the Enterprise Mine has been difficult. The majority of fault movement indicators suggest dip-slip (reverse) movement on steeply dipping faults approximately parallel to bedding. Most thrust related models assume relatively flat-lying bedding prior to movement. However  $D_1$  and  $D_2$  resulted in the bedding being in a steep orientation prior to  $D_3$  and hence prior to the formation of the orebodies and related structures.

Wibberley (1997) describes a model of thrust sheet deformation by steep shear above thrust bends. Shear strain is at a minimum when the shear plane bisects the ramp\flat angle. Strain associated with deformation during movement of the hangingwall sheet over the bend is accommodated by the generation of faults, which form via low angle Riedel shearing (Fig 4.20). From his diagram, if this mechanism applied to the shales above the basement contact fault at the beginning of the  $D_3$  deformation then the sense of shear above the flexures would be steep reverse (*i.e.* approximately parallel to bedding). This could then induce bedding parallel shearing. The splay geometry of the faults could be due to development of subsidiary shear planes (e.g. reidel shears\P shears) within the broad zone above the thrust bend.

Wibberley's model may explain why the fracture sets have developed where they are observed in the Enterprise Mine. Arboleya and Engelder (1995) describe a thrust fault within Cambrian dolomites in which boundary faults acted as concentrated slip zones bounding subsidiary shears, which developed along original bedding planes. The original bedding played the role of reidel shears as the main boundary shears were at a low angle to the bedding. Rotation of the subsidiary shears during continued shear strain led to the development of a range of differently orientated structures. This could be a process, which explains the local geometries and internal structure of some of the shear zones described in the 3000 and 3500 orebodies.

Fig 4.20: Model for the generation of fractures at thrust bends by low angle Riedel shearing in steep shear zones. **(From Wibberley, 1997)**



#### 4.7.5 Reactivation of Pre-existing Structures

The Leichhardt River Fault Trough of the Mount Isa Inlier comprises fault blocks, which exhibit different local deformational histories and structural orientations. Many structural patterns in the stratigraphically highest cover sequences do not occur in adjacent fault blocks that expose older and mechanically stronger rocks. Pre-existing fault geometry has played a large role in controlling the structural patterns during later shortening. The structures developed during the shortening of previously extended regions are expected to be much more variable than those found in classical thrust belts which deform a layer-cake stratigraphy (O'Dea and Lister, 1995).

The basement contact fault has been interpreted to have been close to its present position before  $D_2$  (Bell, 1991). The history of its development is disputed (Blake and Stewart, 1992) but its impact on processes during  $D_2$  and  $D_3$  is very important to the understanding of the development of the Mount Isa copper orebodies.

The development of  $D_3$  shear zones was essential for rapid fluid incursion into the rock and they facilitated rapid silicification of large volumes of rock. It was therefore possible to generate a block of silicified rock that behaved in a brittle fashion during continued deformation. The attitude and the internal stratigraphy of the Urquhart Shale at Mount Isa was such that it was possible to develop numerous regularly spaced bedding parallel shear zones between massive siltstones and this geometry led to the development of the ore system.

This conclusion differs from previous work by Perkins (1984) in which the majority of faults within the orebodies were considered to be late (post  $D_3$ ) and to not have a direct impact on the localisation of the ore.

## Copper and Cobalt Mineralisation

### 5.1 Introduction

This chapter outlines the distribution of copper and cobalt within the Enterprise Mine orebodies. A set of plans and sections on the same levels and northings as those previously used in this report show the 2.5%, 5.0% and 8.0% copper contours and the 0.1%, 0.15% and 0.3% cobalt contours. Each copper section has the corresponding cobalt section on the following page so that direct comparison can be made between the distribution patterns of both elements.

### 5.2 Copper - Relationship to 'Rock type'

Copper mineralisation in the form of chalcopyrite is mainly present in and along veins. There is a preferential replacement of dolomitic veins and matrix material. As described in chapter two, silicification and copper mineralisation are closely associated. Copper grades decrease outwards and upwards with the change from the core of silica-rich/dolomite-poor 'rock types' to the outer dolomite-rich/silica-poor 'rock types'. Fractured siliceous shale has a higher copper grade than siliceous shale. Recrystallised shale and irregularly brecciated dolomitic shale is generally weakly mineralised. Some of the upper lenses/pods have an irregularly brecciated dolomitic shale-like texture but are still substantially silicified where > 2% copper occurs. The up-dip closure zone of the 2.5% copper contour on the sections (figs 5.5a-5.10a) corresponds with the zone of interfingering of siliceous and dolomitic 'rock types'.

There is a decrease in copper grade where there is an increase in fine grained pyrite. Fine grained pyrite is a minor component of the 3000 Orebody and is mainly concentrated on the footwall of the 3500 Orebody, outside the limits of economic mineralisation.

On a hand specimen scale, as the copper grade increases the textural characteristics of the host rock changes. The following points summarise the major textural characteristics that I have observed in the two copper orebodies:

- 
- Essentially non-mineralised (<0.5% Cu): networks of recrystallised dolomite veins in recrystallised shale or siliceous shale.
  - Weak to moderate copper mineralisation (0.5% - 2.5% Cu): silicified shale and recrystallised shale - chalcopyrite replaces dolomite within the veins forming a network. Where the copper grade is less than 1.5% the vein networks are fine with average vein width less than 4mm. Above 1.5% the veins are generally greater than 4mm in width.
  - Strong copper mineralisation (>2.5% - 7%): complex network of veins and brecciated appearance with partial replacement of vein dolomite and matrix dolomite with chalcopyrite.
  - Massive chalcopyrite matrix with clasts of silicified shale (>7% Cu). The massive chalcopyrite may show a weakly foliated or sheared texture.
  - Where pyrrhotite occurs it has a character similar to chalcopyrite. It is not abundant in the orebodies and can occur as layers in the recrystallised shales outside the limits of economic copper mineralisation.

Swager's (1983, 1985) work on microstructures indicated that chalcopyrite and pyrrhotite deposition overprinted the recrystallised and silicified shales. The main deposition phase of copper occurred before the end of D<sub>3</sub>.

### 5.3 Copper Distribution

Figures 5.1a to 5.10a and figure 5.11 accompany this section. As mentioned in section 1.3.2, the contours in the figures are derived from geostatistical models using 5m composites (3000 Orebody) and 3m composites (3500 Orebody) of the copper assay data and 5m composites of the cobalt assays. Where information from mapping was available the model derived contours were corrected to fit the observed grade boundaries. The location of the shear zones is based on physical observations from mapping and drillcore. Shear zone interpretation is also based on the characteristics described in section 4.3.1, where the grade in shear zones tends to be markedly lower than the immediately adjacent wall rocks. Rounding effects to the shape of the orebodies due to the compositing is mainly confined to the up dip limits of the orebodies.

### 5.3.1 3000 Orebody

Copper distribution in the 3000 Orebody is characterised by a set of en-echelon lenses that give an apparent NNW trend to the orebody. The actual ore boundaries trend NNW close to the basement contact fault and swing around to the NNE and N-S moving up-dip and away from the basement.

In section view the 3000 Orebody has a very lobate geometry with the highest grade concentration adjacent to or just above the basement contact fault. High grade loci do occur up dip and distinctly separate from those near the basement fault. Grade decreases in a concentric manner away from these loci.

The first economic copper grades (+ 2.5%) of 3000 Orebody begin at 5900mN. From 5900mN to 6100mN the orebody is a single lens with a > 5.0% core developing at 5950mN. At 6100mN - 6205mN a hangingwall lens occurs with its high grade core at 6145mN. A second hangingwall lens occurs between 6210mN and + 6330mN (no data available to close off northern limit).

### 5.3.2 3500 Orebody

Copper distribution in the 3500 Orebody is also characterised by high grade lenses (+ 5.0%) enveloped by the 2.5% copper contour. The orebody has an overall N-S trend. The first economic copper grades of 3500 Orebody occur between 5900mN and 6010mN in what is known as the southern pod. It is 120 to 150 metres above the basement contact fault and to the footwall of the inferred position of the Urquhart Shear. Between 6010mN and 6055mN there is no ore (Fig 5.5a). From 6055mN to 6510mN the distribution is as follows:

- 6055mN-6160mN - Start to get a hangingwall lens adjacent to the basement contact fault and footwall lenses above the basement. These coalesce to a single orebody by 6130mN.
- 6160mN-6285mN - Two discrete >5.0% lenses, one adjacent to and one above the basement fault and enveloped by >2.5% copper (Fig 5.7a).
- 6285mN-6405mN - The highest grade section of the orebody. A very sharp footwall boundary and a higher concentration of copper on the footwall. The two >5.0% lenses have coalesced to a single lenticular

lens (Fig 5.8a). Between 6375mN and 6405mN there are hangingwall and footwall >8.0% loci within the >5.0% lens (Fig 5.9a).

- 6405mN-6495mN - The 200 metre up-dip extension of the orebody narrows rapidly and there is no more >8.0% copper.

I mentioned in the introduction to chapter one that the 3500 orebody had characteristics similar to the 650 Orebody. The 650 Orebody is one of a set of copper orebodies (400, 500 and 750) which occur in the upper levels of the Copper Mine (1100 Orebody – Fig 3.11) and the Lead Mine. The similarities are:

1. The high grade loci of the orebodies have no observable direct link with the basement contact fault. In the case of the 400 to 750 orebodies they are spatially quite separate from the basement contact fault.
2. The influence of shear zones is very strong.

Spratt (1953) gave the following description of the Black Star Copper Orebody (650 and 750 orebodies). “... The structural pattern is dominated by faults. On the western side are a series of E-W cross fractures but these are believed to have played no part in the control, structural or mineralogical, of the deposition of the orebody. The major fault or shear zone is on the footwall, and striking north-south, forms the boundary between the host rocks for the copper and the silver-lead-zinc orebodies. Springing out of this fault and striking roughly N20°W are a series of faults of undetermined displacement which sometimes form shear zones, sometimes occur as single planes. ...It is suggested that the initial shearing produced fracture systems, which were later filled with dolomite, transported along the shears. Later, renewed movement along the shears resulted in fracturing of both dolomite and silicified shale which in turn served for the deposition of chalcopyrite out of the shear channel.”

Fig 5.1a: Copper mineralisation and shear zones - 23A sublevel.

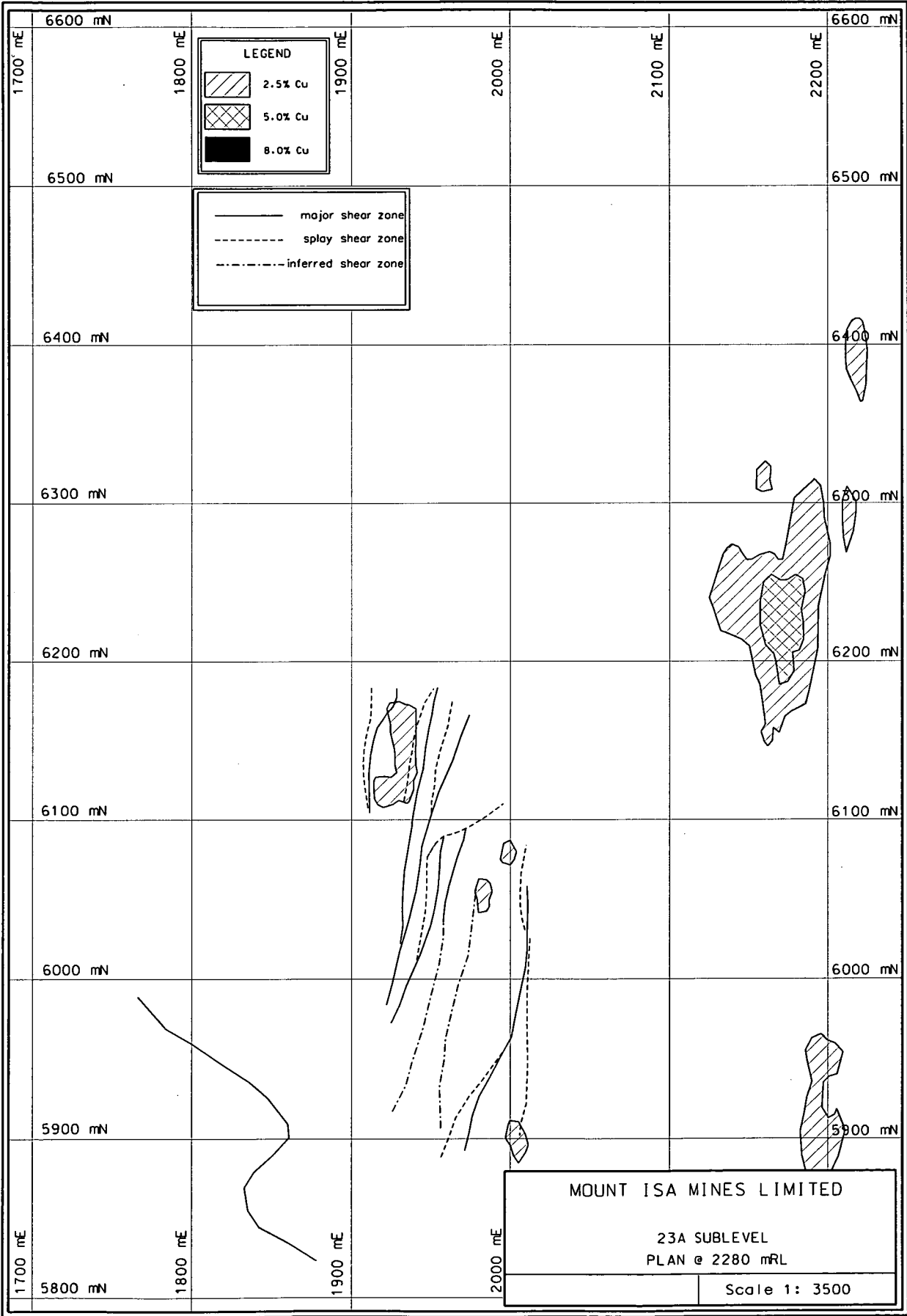




Fig 5.1b: Cobalt mineralisation and shear zones - 23A sublevel.

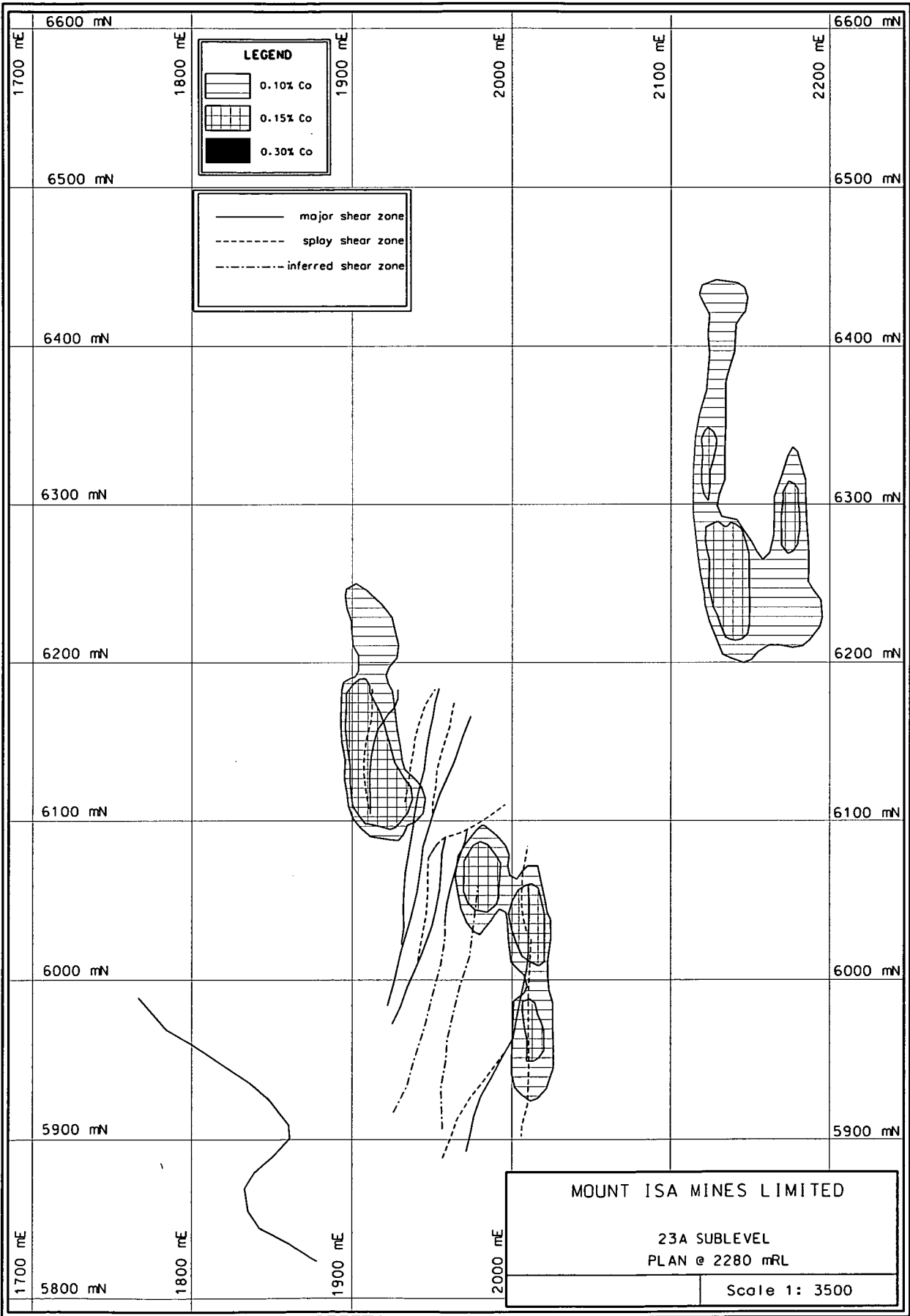


Fig 5.2a: Copper mineralisation and shear zones - 24A sublevel.

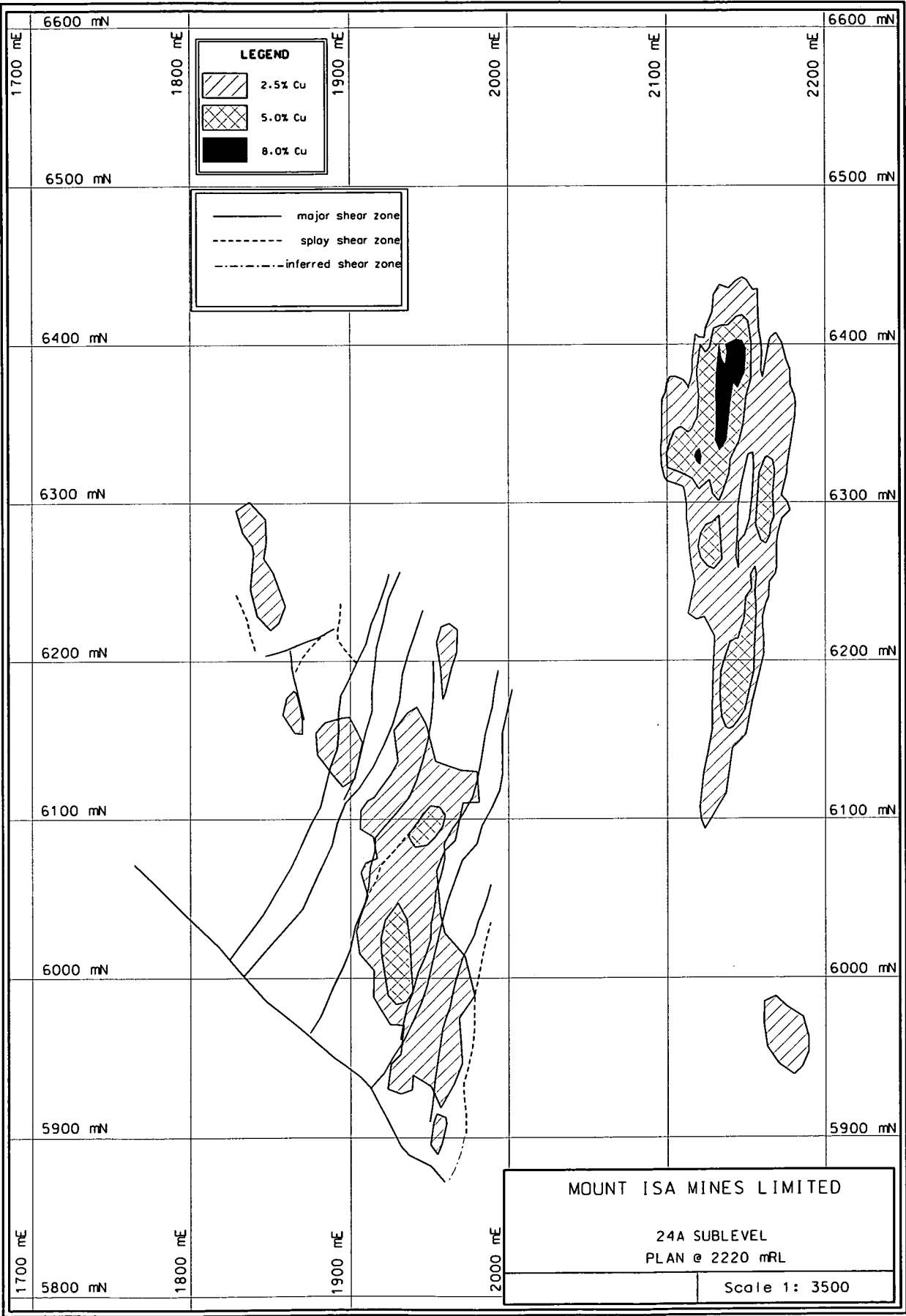


Fig 5.2b: Cobalt mineralisation and shear zones - 24A sublevel.

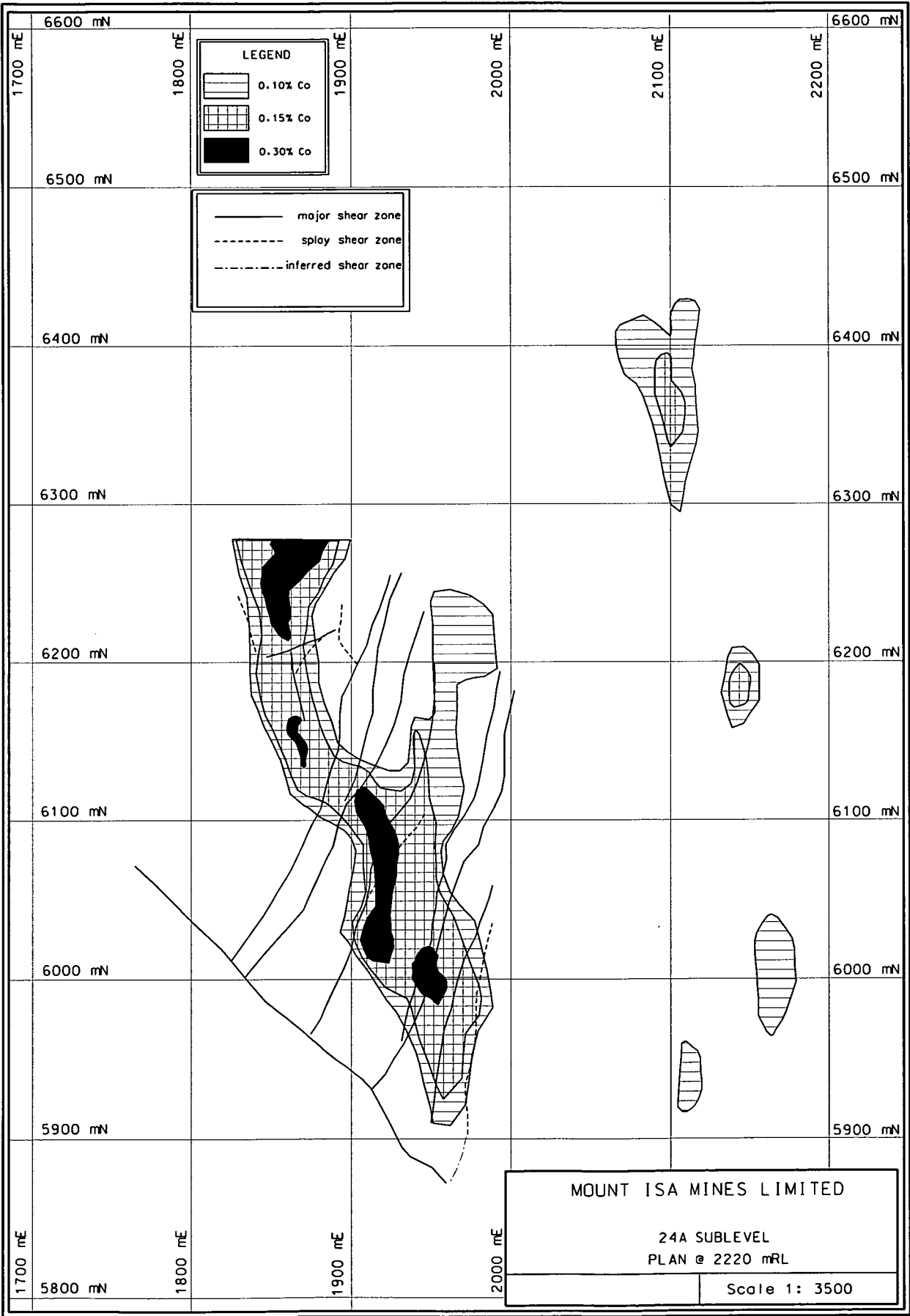


Fig 5.3a: Copper mineralisation and shear zones - 25A sublevel.

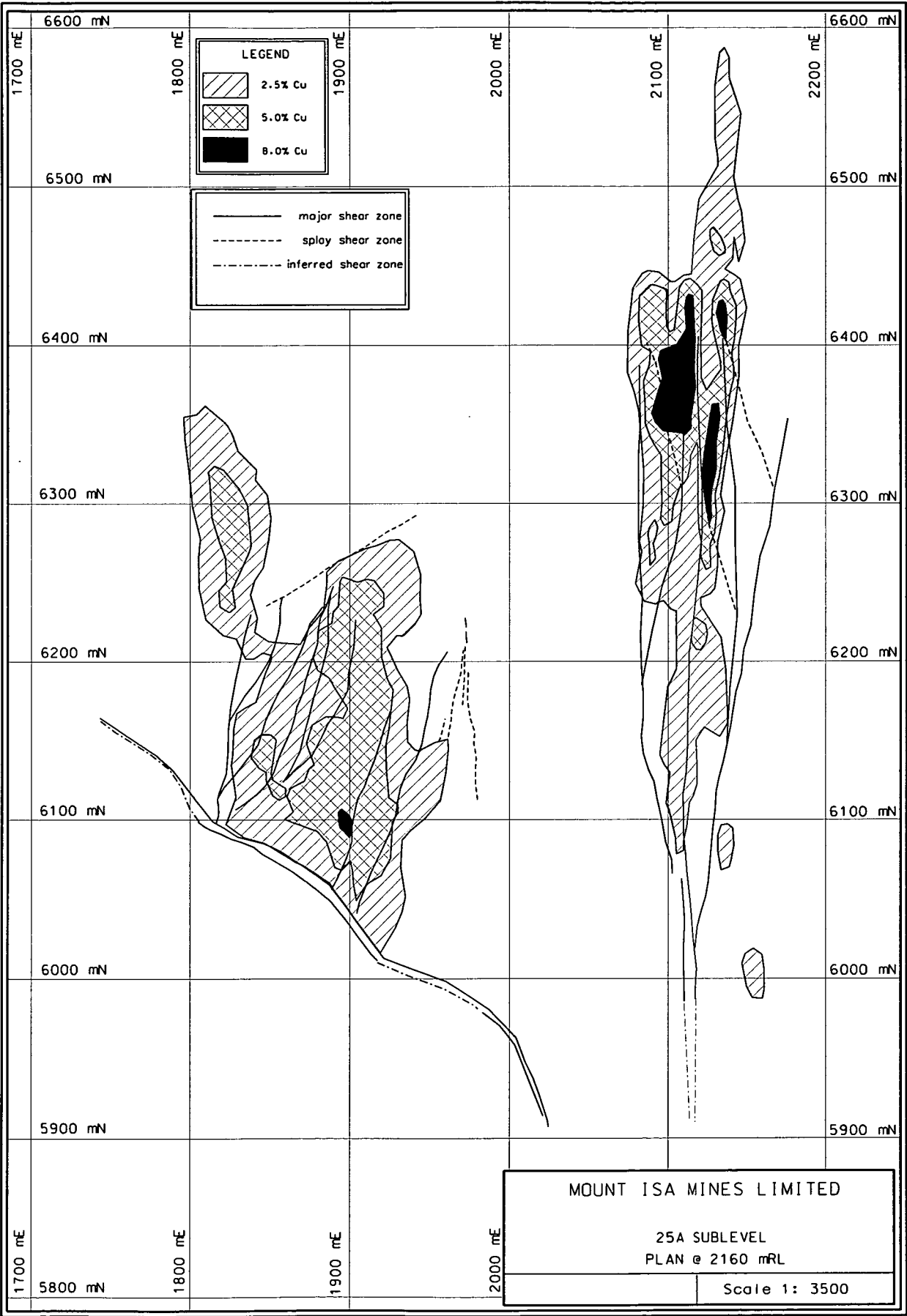


Fig 5.3b: Cobalt mineralisation and shear zones - 25A sublevel.

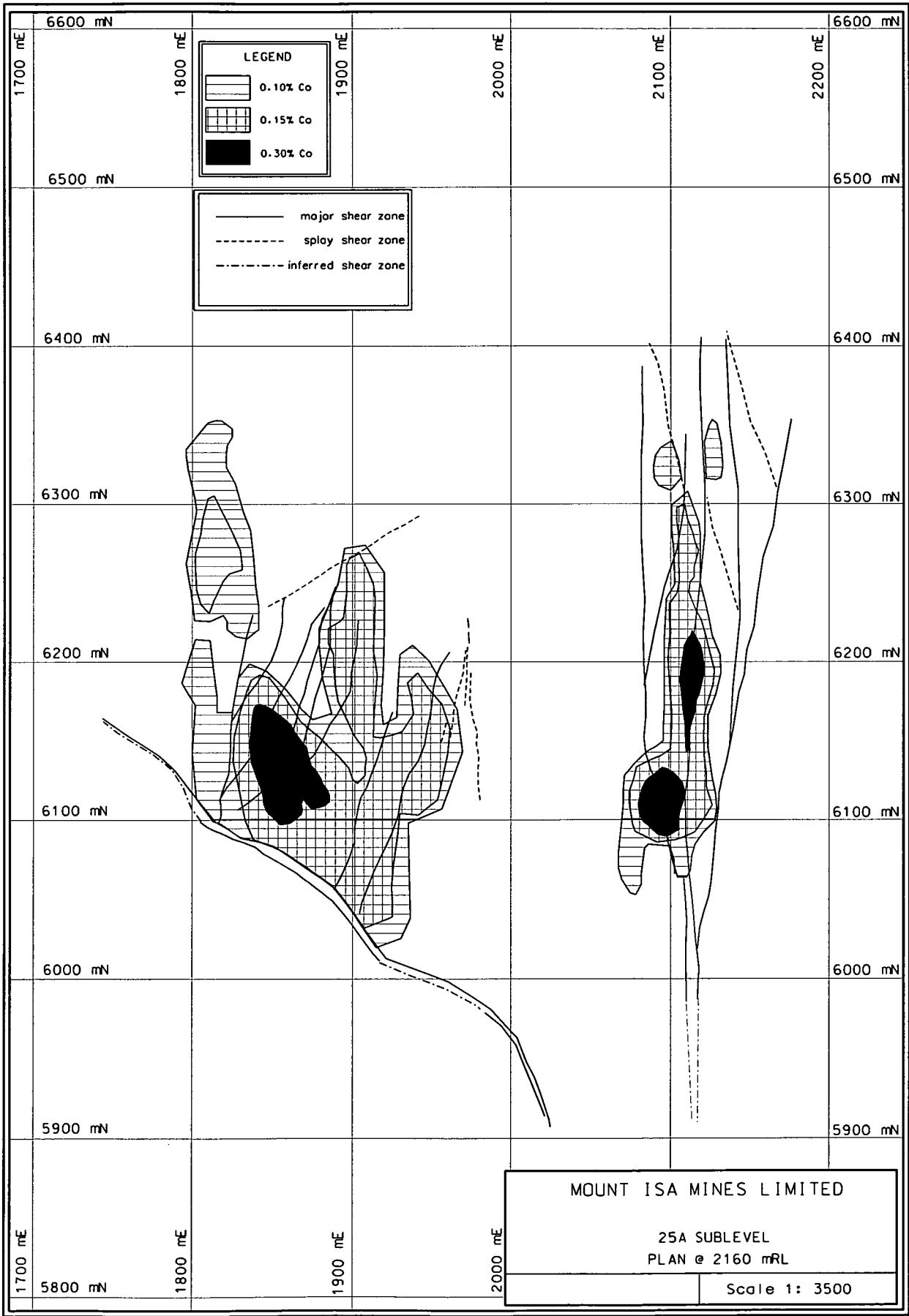


Fig 5.4a: Copper mineralisation and shear zones - 26B sublevel.

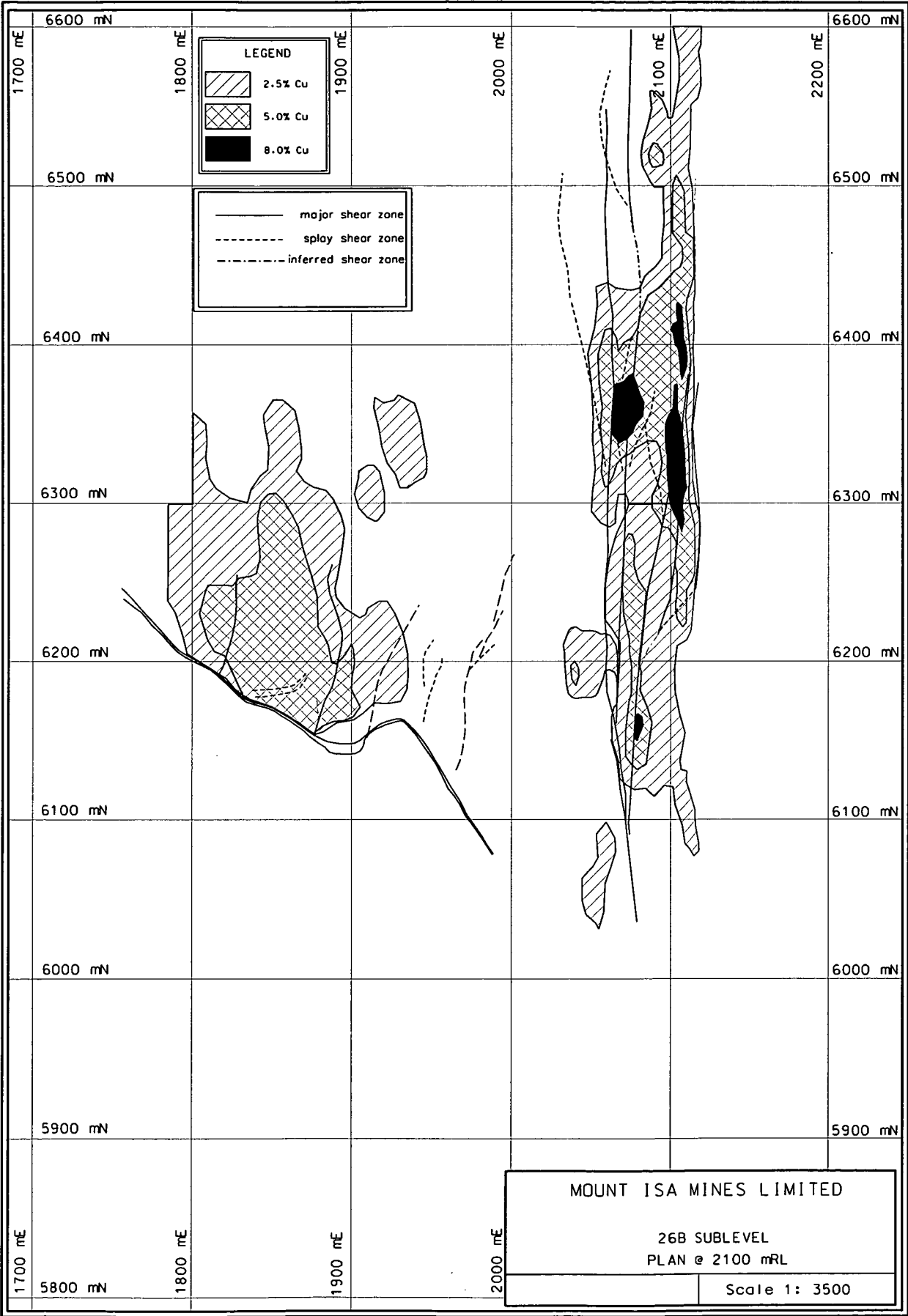


Fig 5.4b: Cobalt mineralisation and shear zones - 26B sublevel.

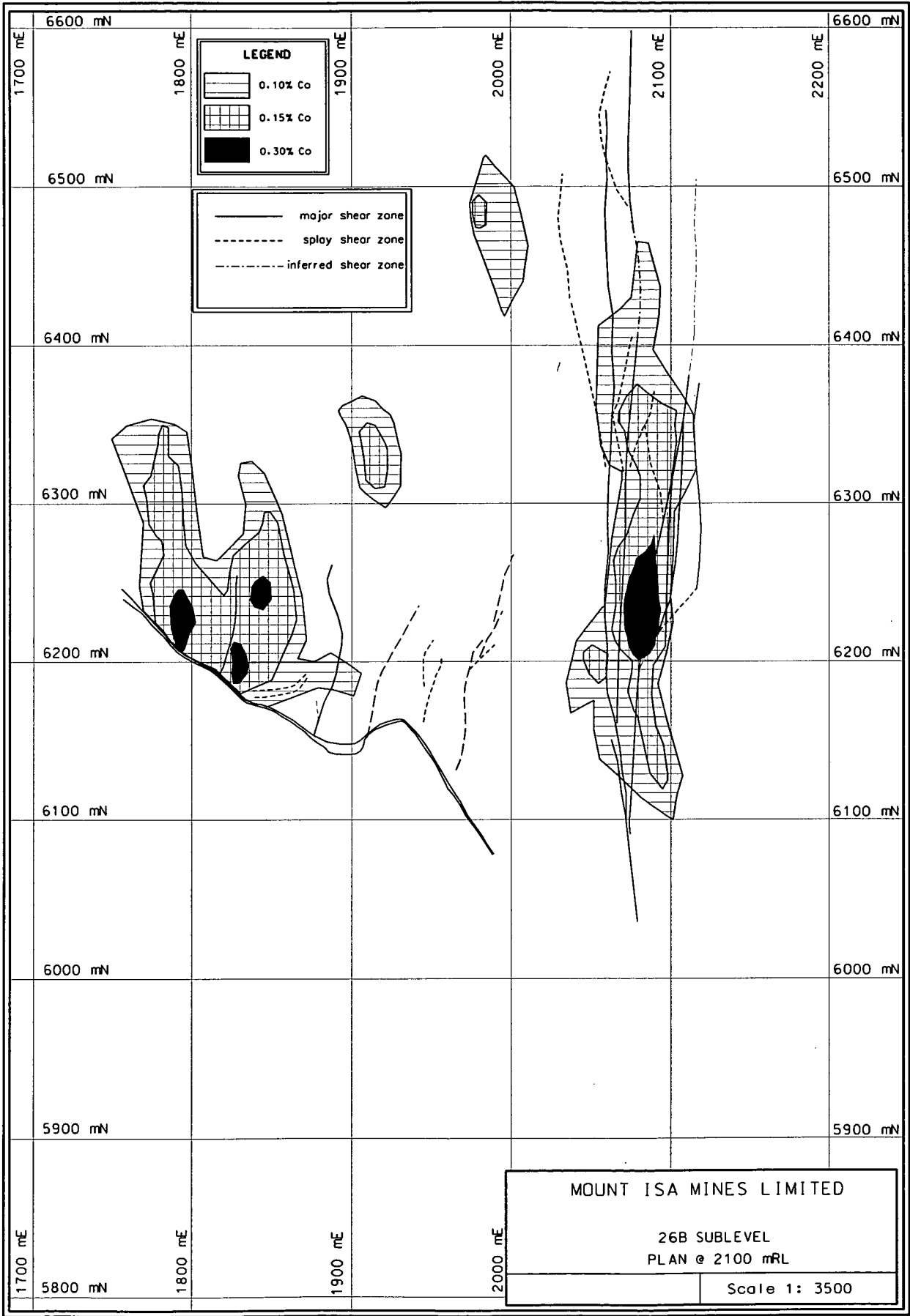


Fig 5.5a: Copper mineralisation and shear zones - 6025 mN cross section.

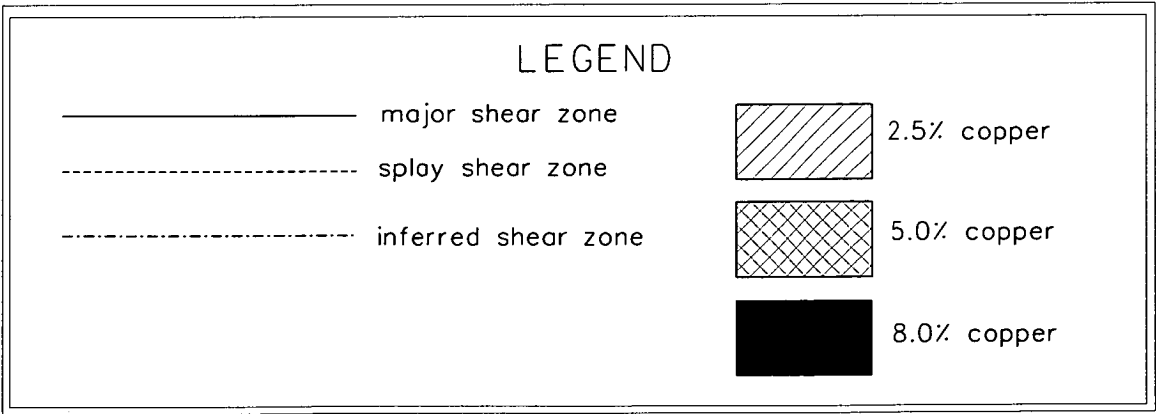
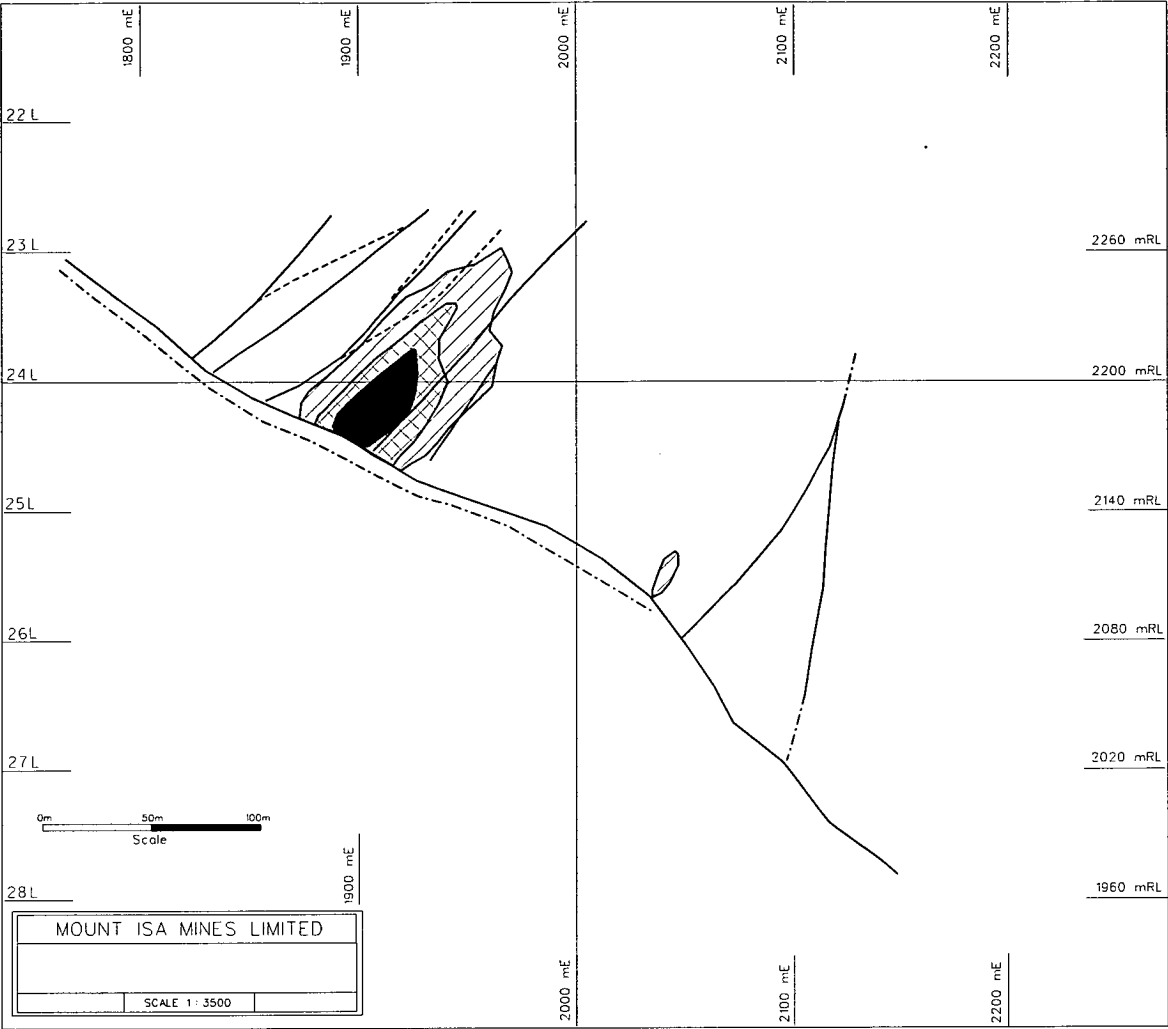




Fig 5.5b: Cobalt mineralisation and shear zones - 6025 mN cross section.

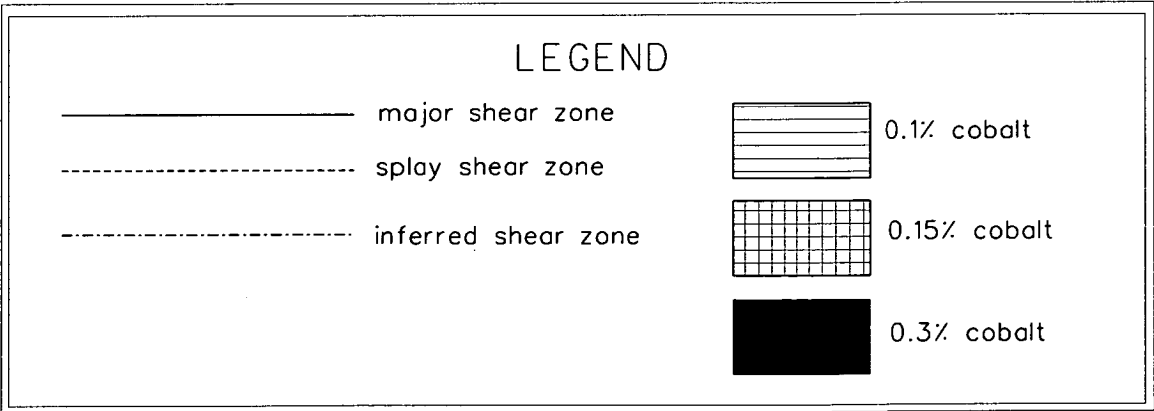
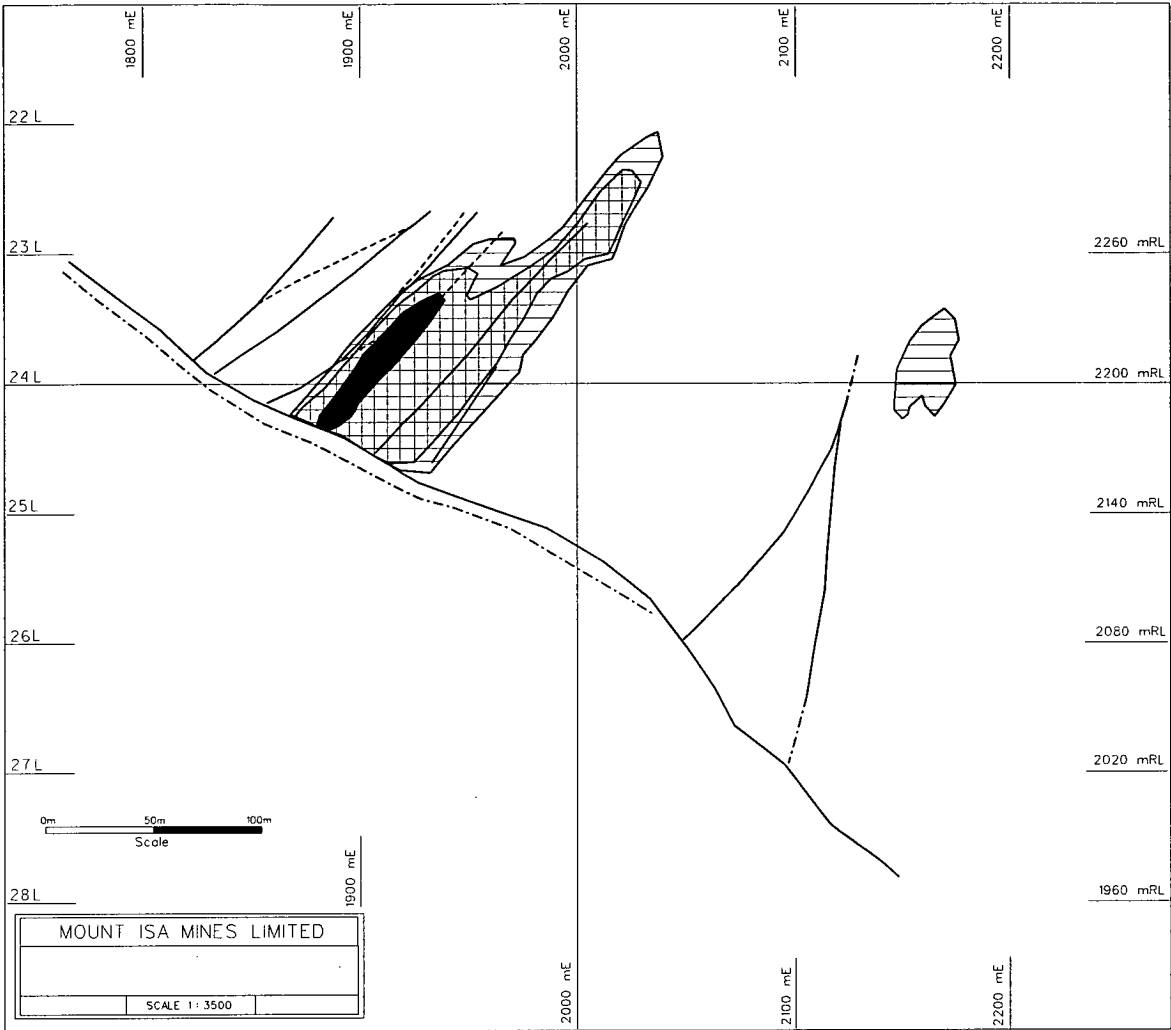


Fig 5.6a: Copper mineralisation and shear zones - 6115 mN cross section.

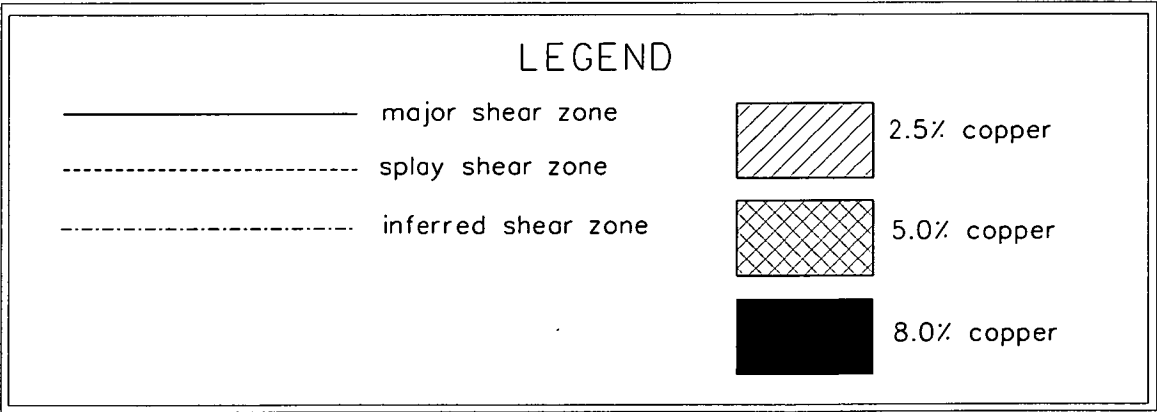
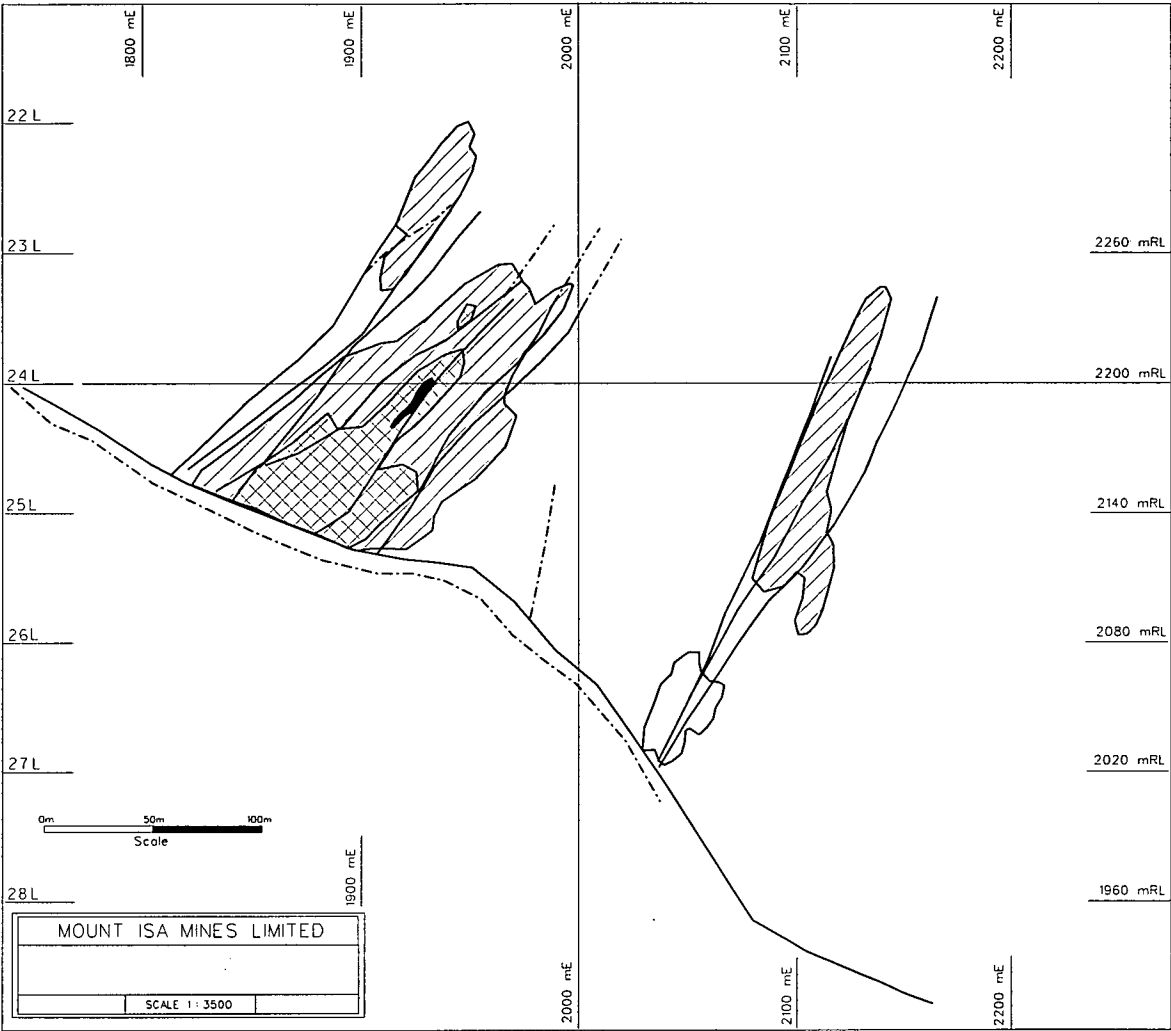


Fig 5.6b: Cobalt mineralisation and shear zones - 6115 mN cross section.

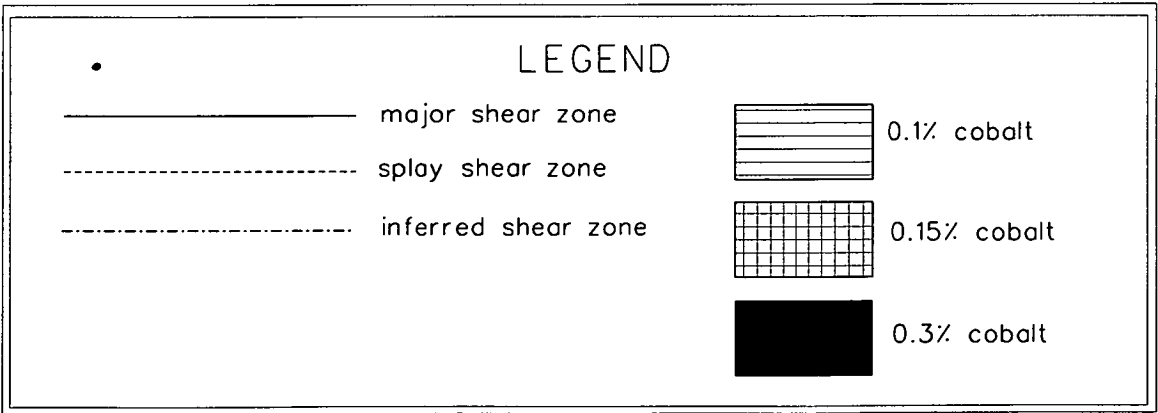
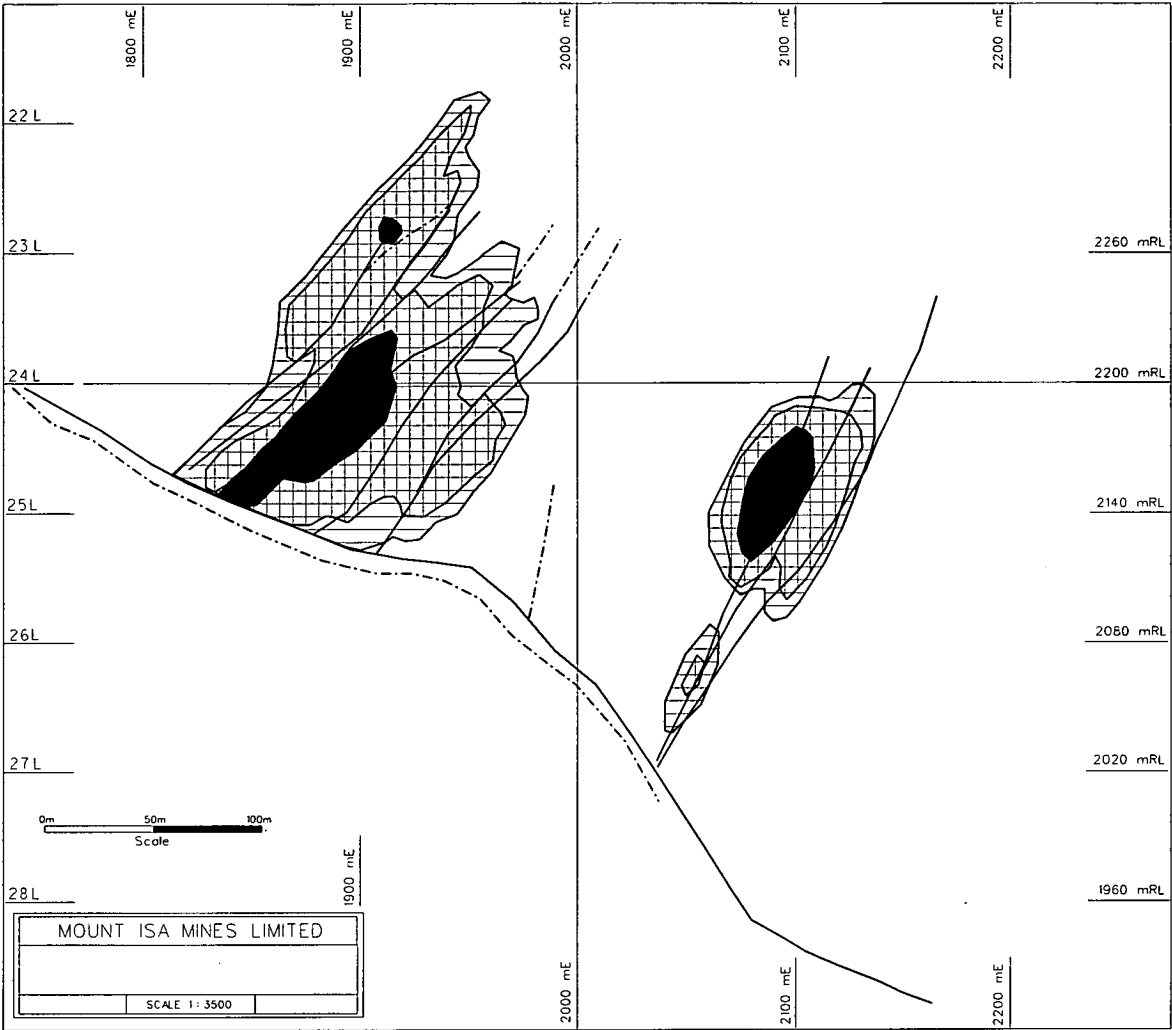


Fig 5.7a: Copper mineralisation and shear zones - 6205 mN cross section.

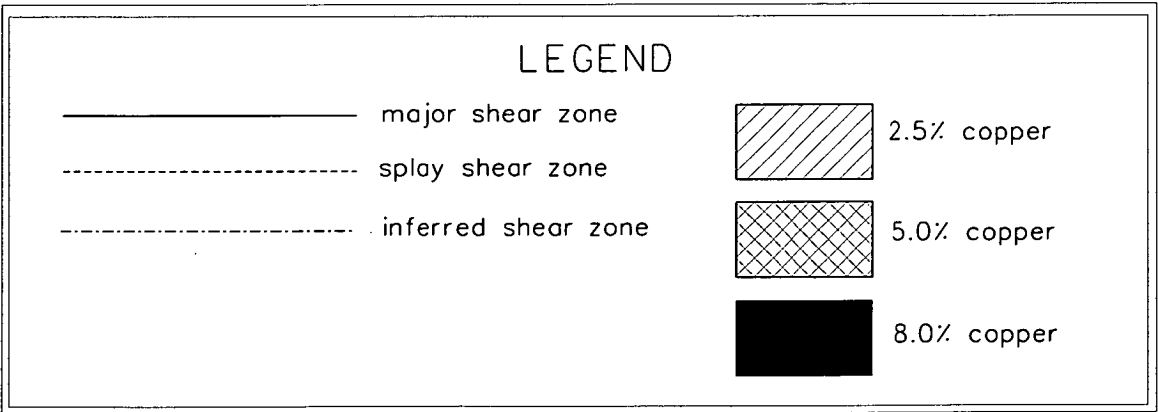
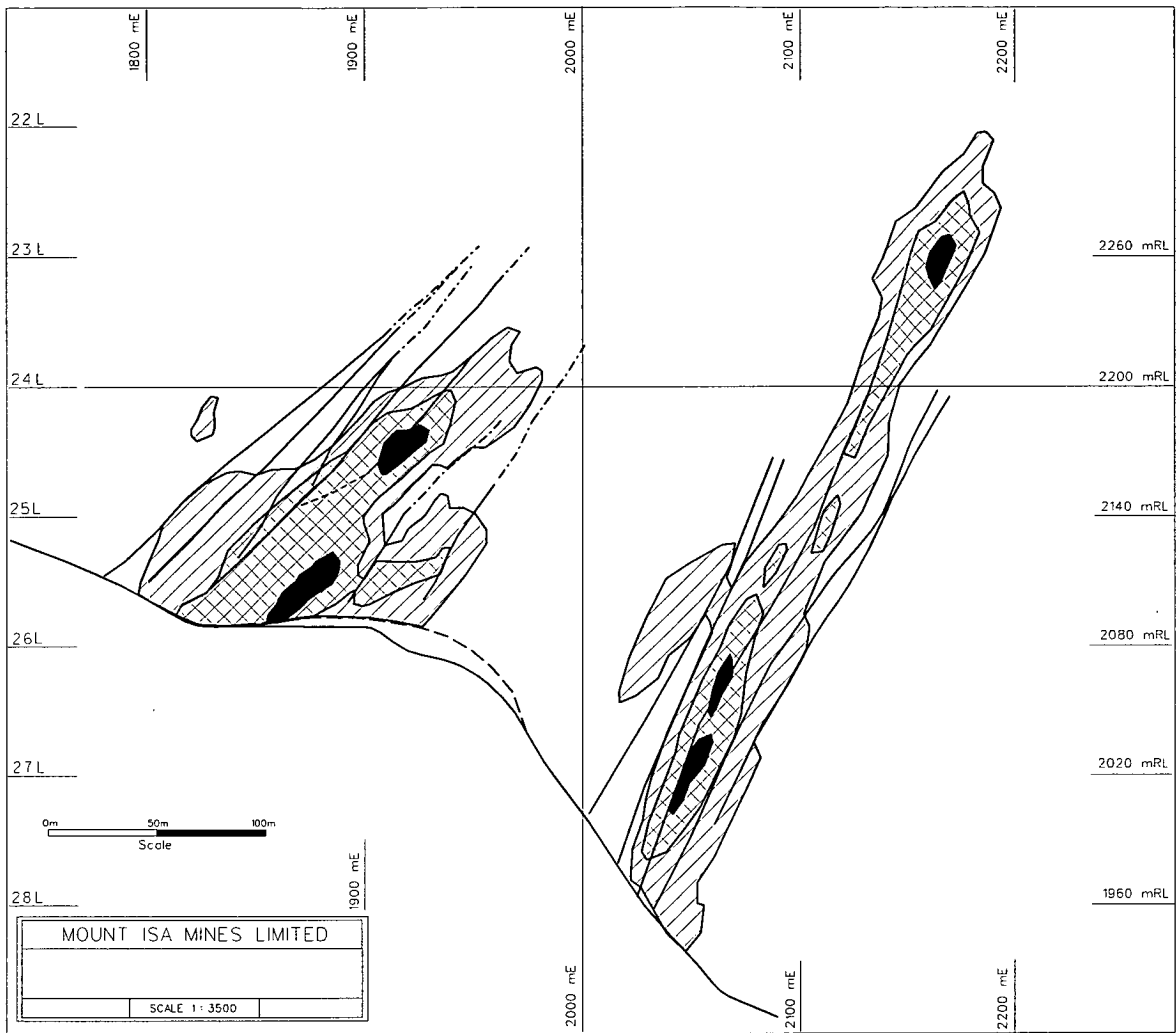


Fig 5.7b: Cobalt mineralisation and shear zones - 6205 mN cross section.

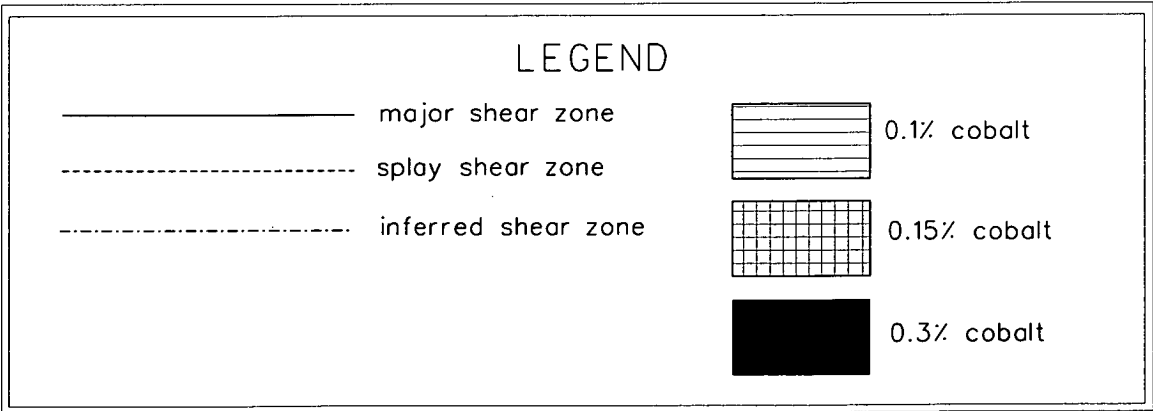
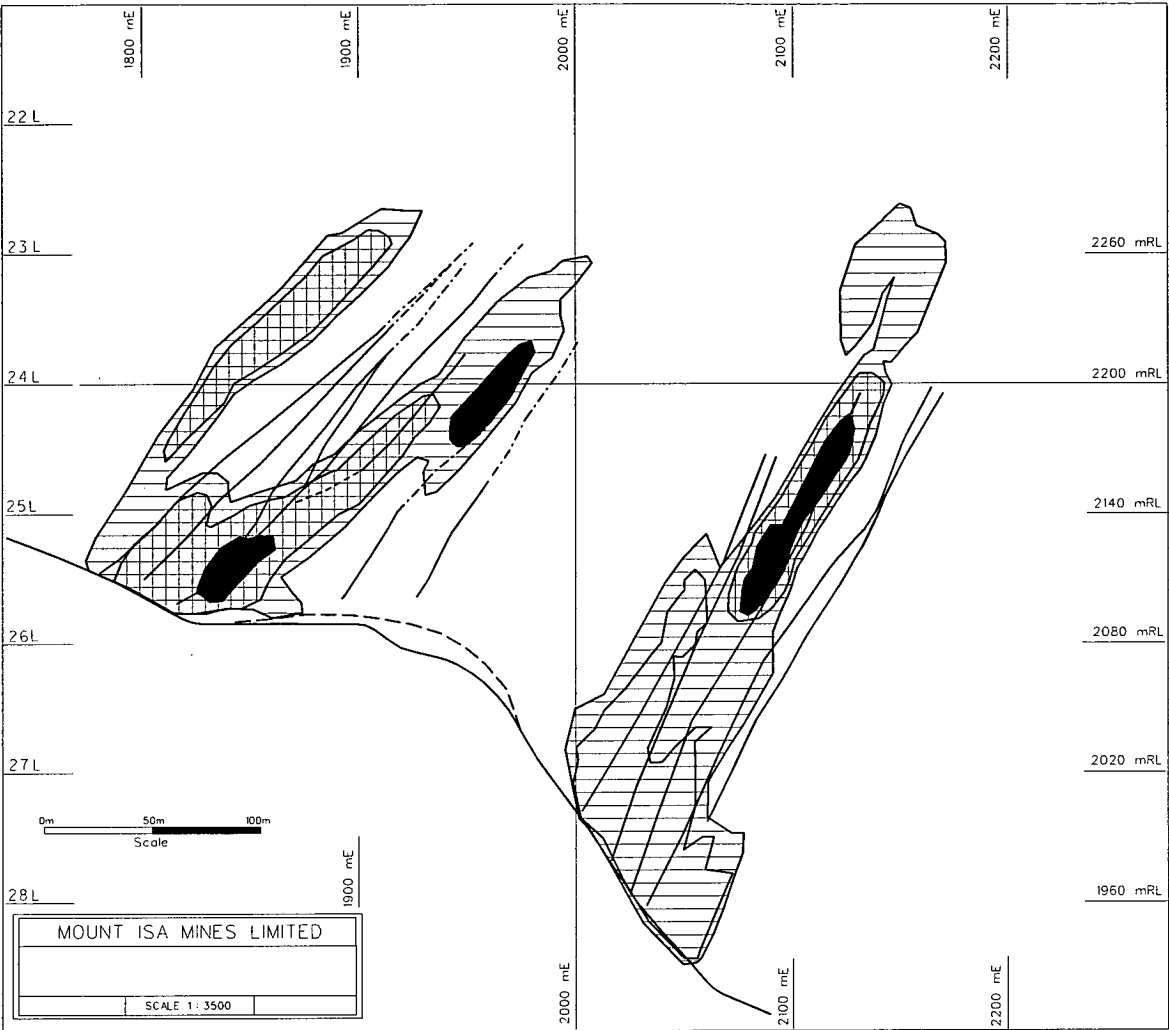


Fig 5.8a: Copper mineralisation and shear zones - 6300 mN cross section.

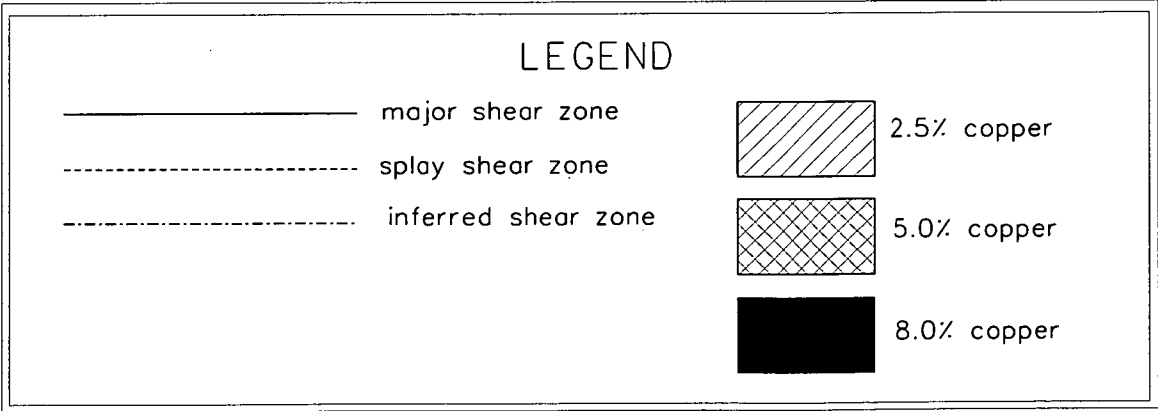
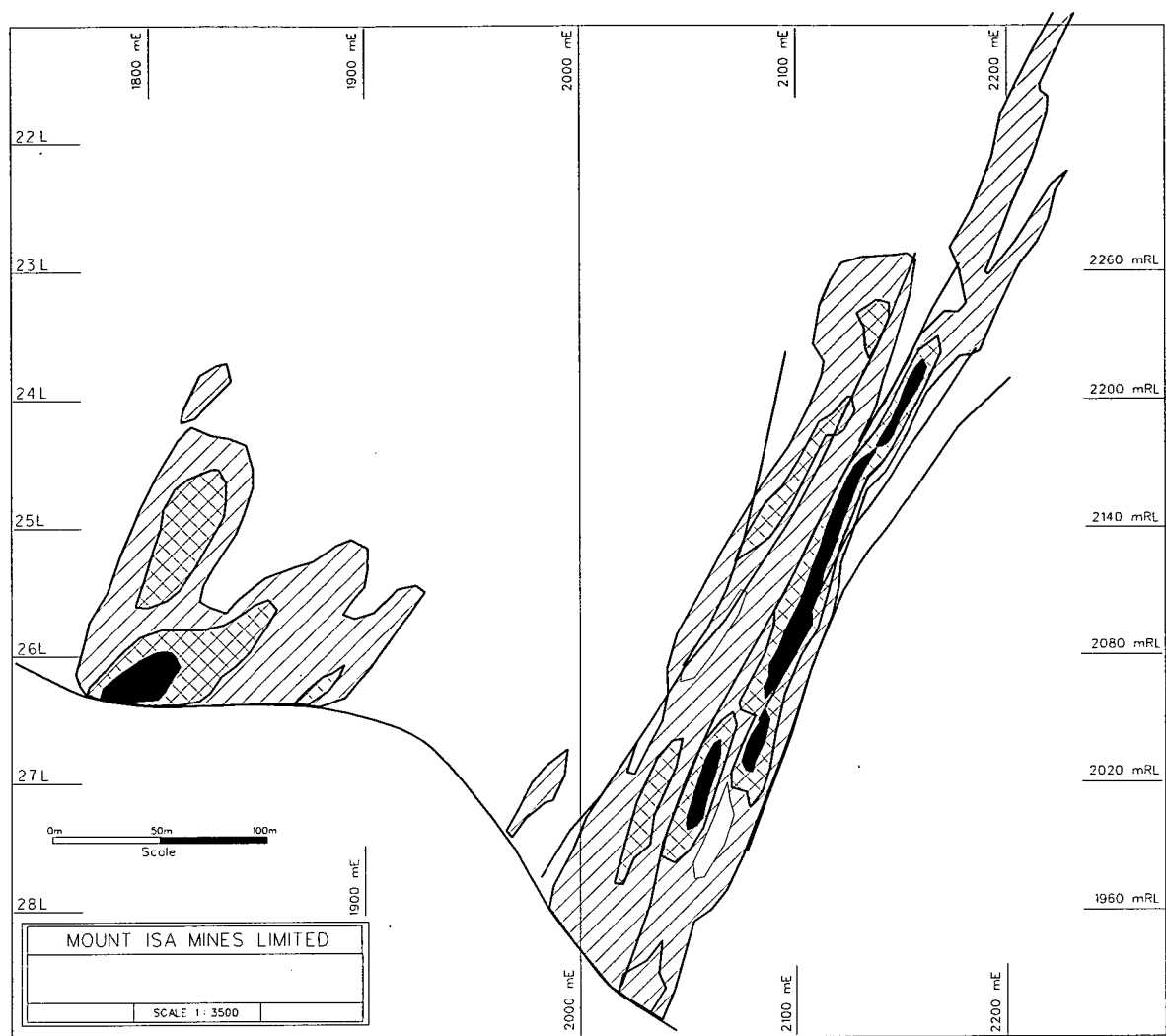


Fig 5.8b: Cobalt mineralisation and shear zones - 6300 mN cross section.

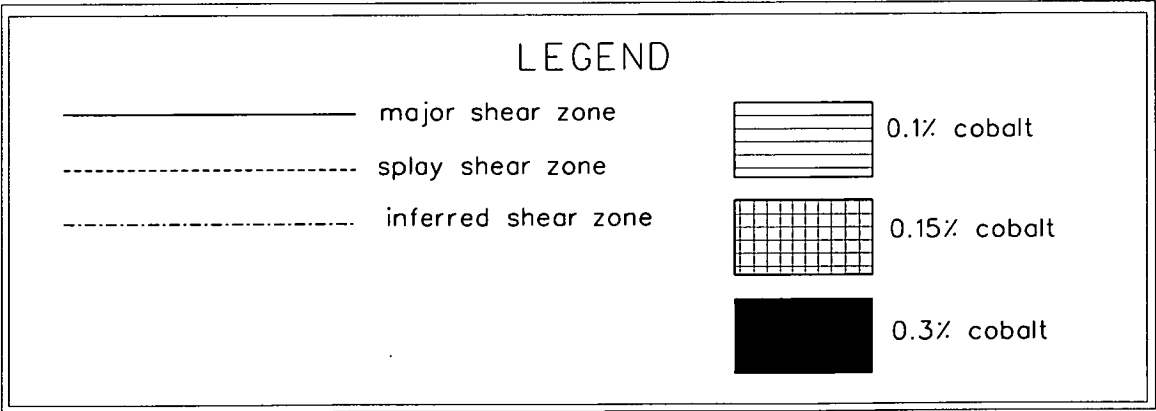
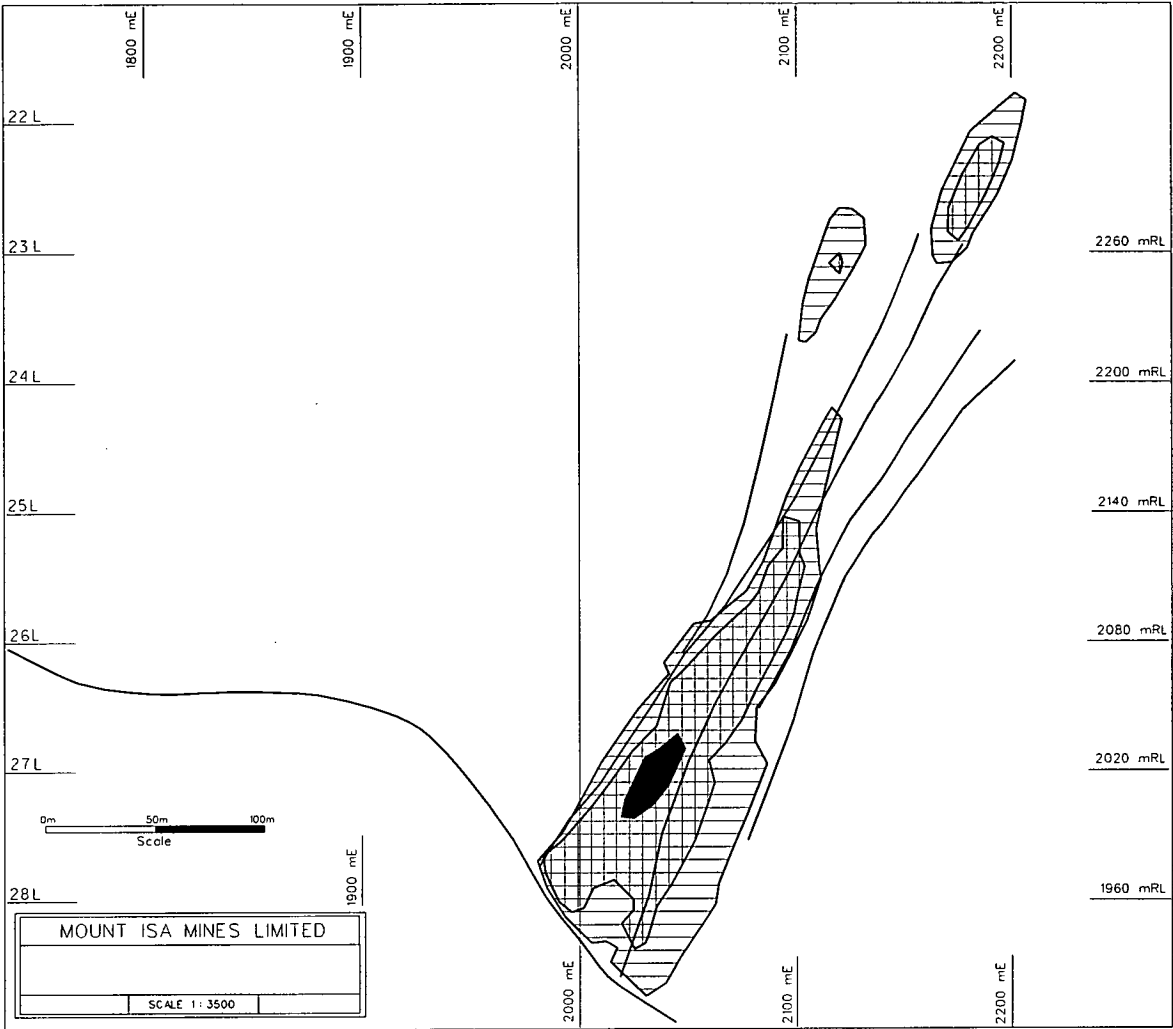


Fig 5.9a: Copper mineralisation and shear zones - 6390 mN cross section.

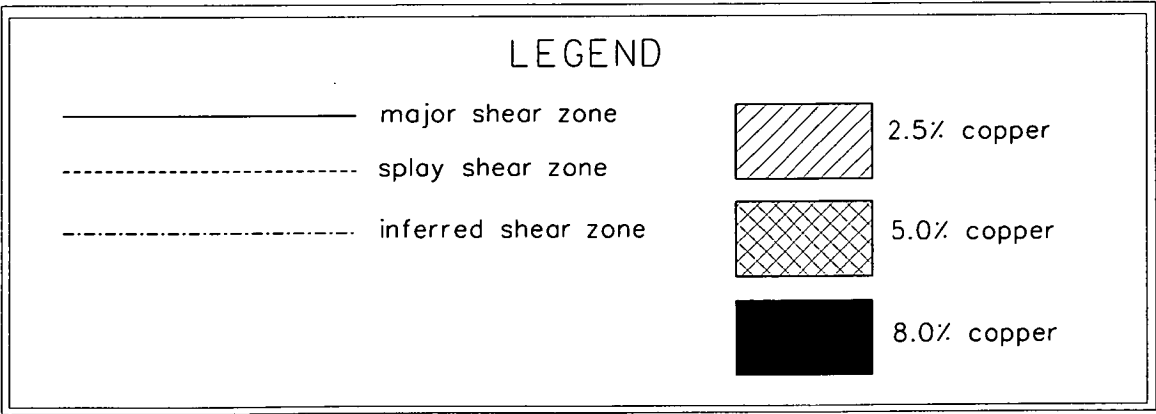
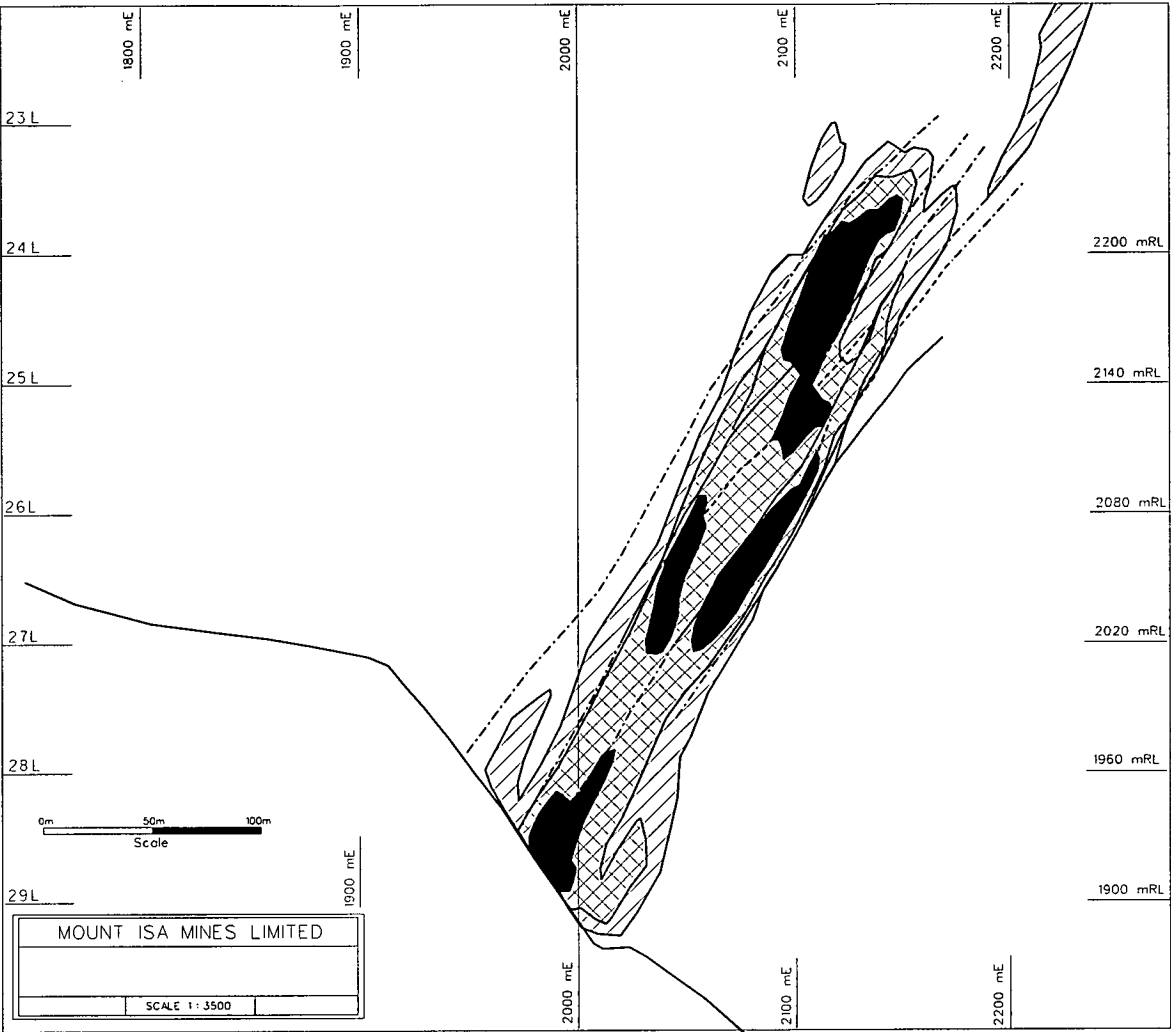




Fig 5.9b: Cobalt mineralisation and shear zones - 6390 mN cross section.

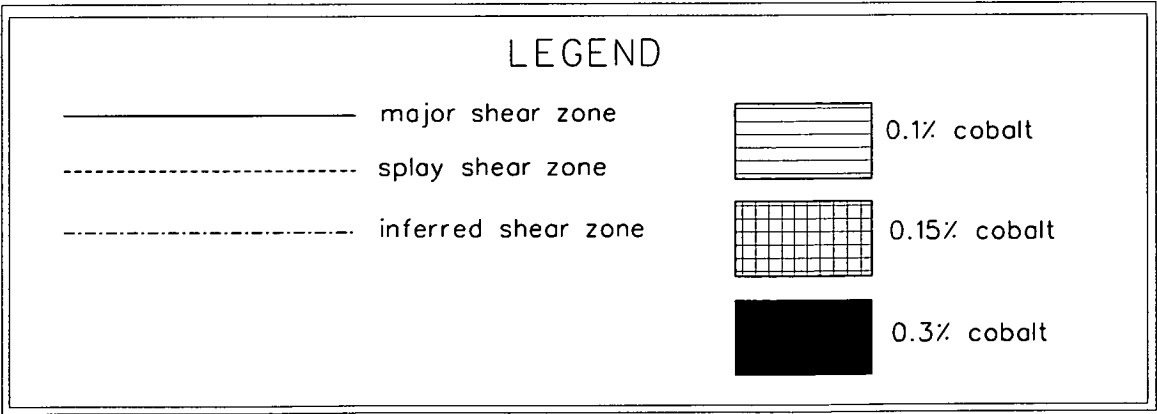
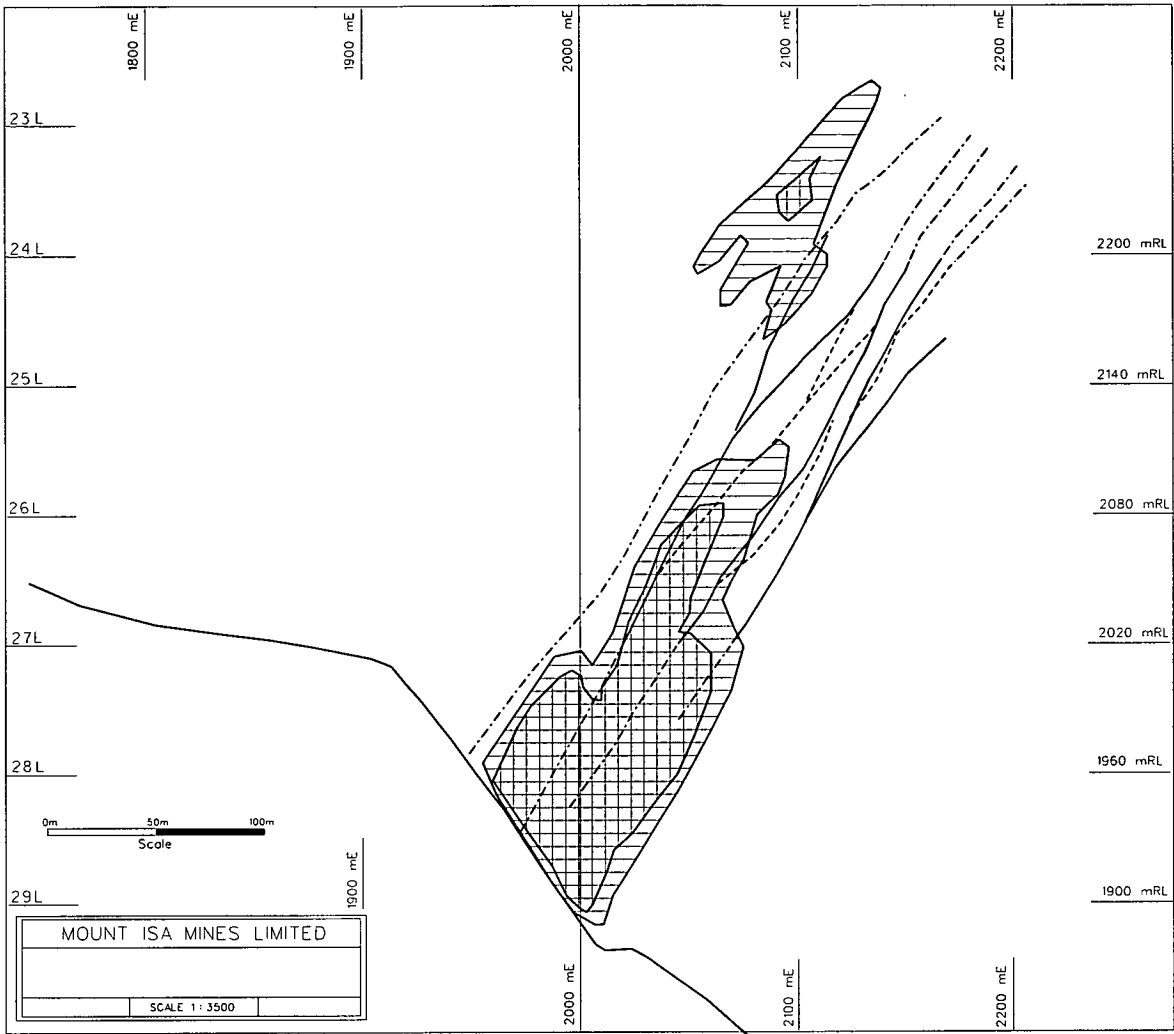


Fig 5.10a: Copper mineralisation and shear zones - 6480 mN cross section.

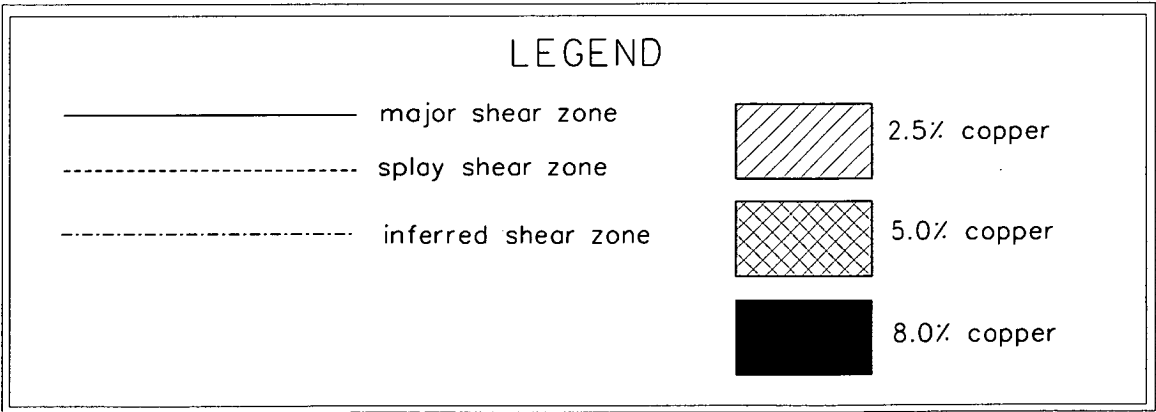
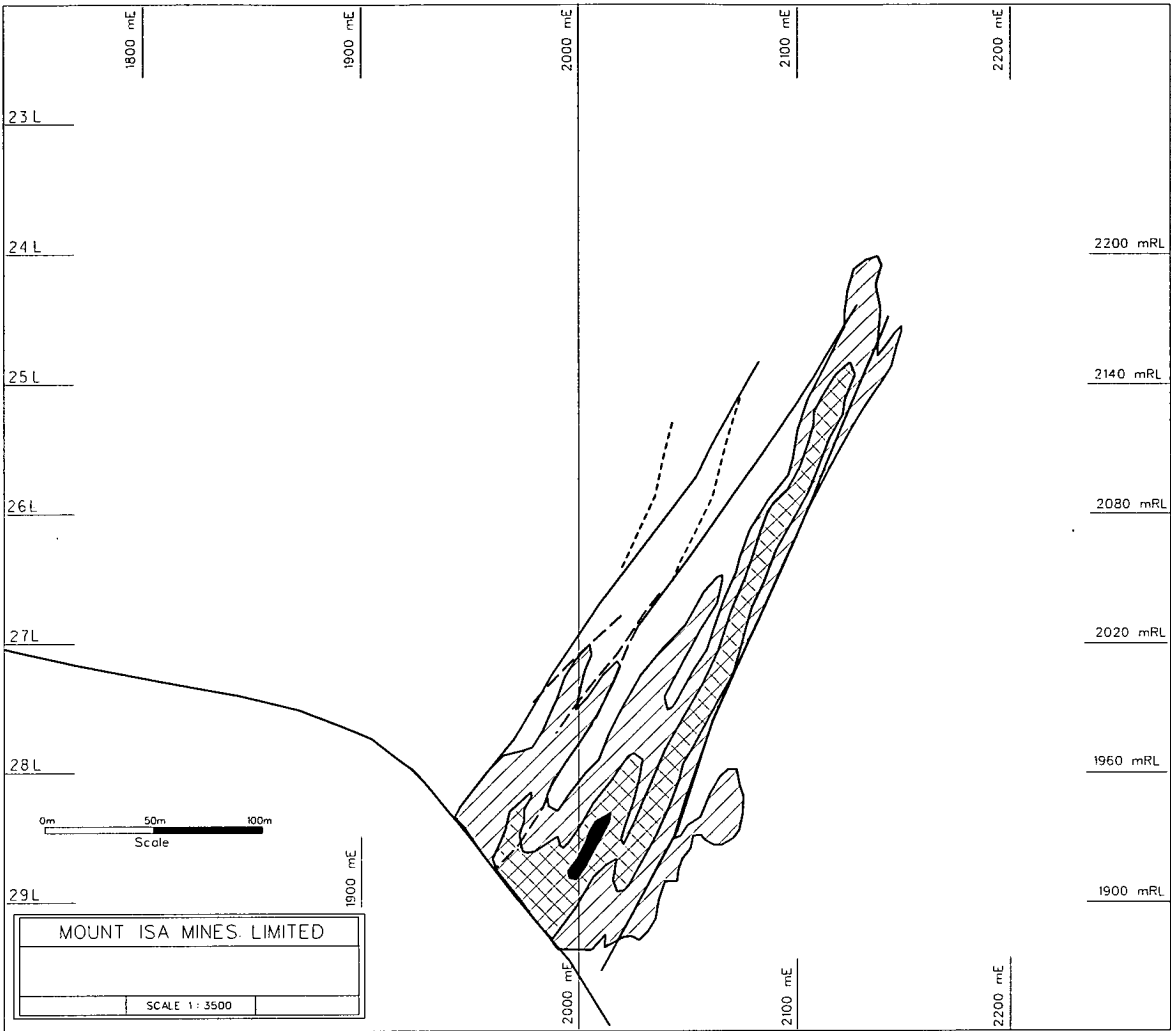
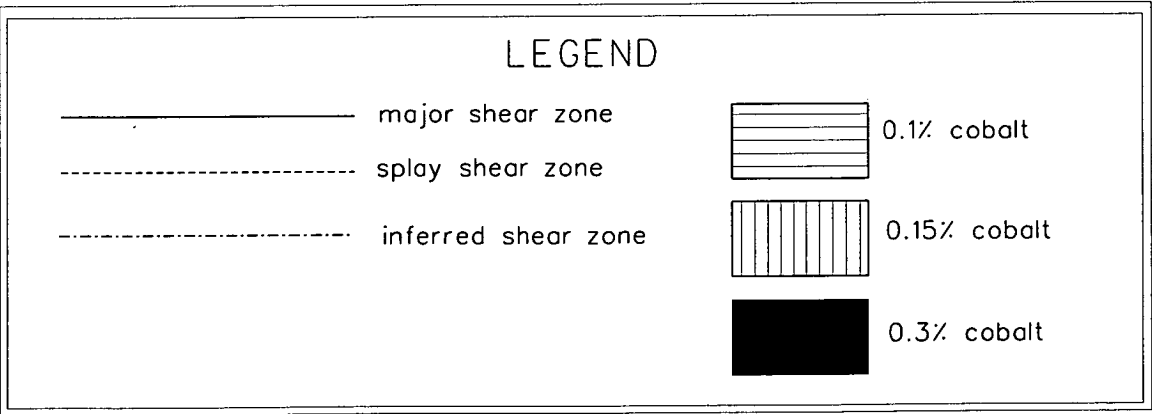
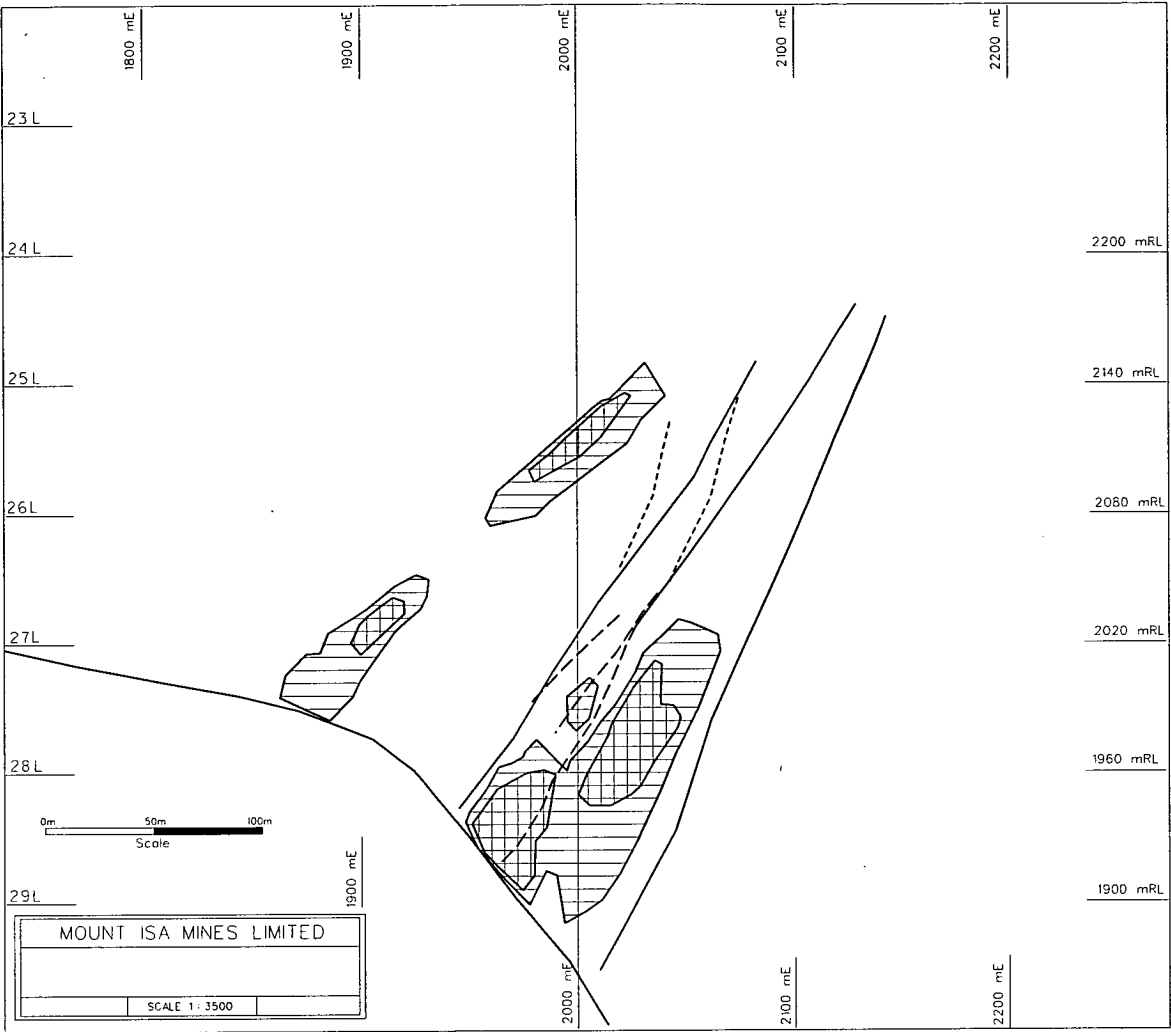


Fig 5.10b: Cobalt mineralisation and shear zones - 6480 mN cross section.



## 5.4 Copper - Relationship to Structure

Not all orebody contacts are associated with faults or shear zones. Particularly in the upper levels of the 3000 Orebody the mineralisation seems to 'leak out' along particular bedding planes. The 3000 Orebody has an irregular en echelon footwall boundary, which seems to be controlled, by the position of the antiformal axial plane region of the Mount Isa Fold. The orebody is not folded and mineralisation always stops abruptly at the first occurrence of small scale folded shale horizons on the footwall. The NNW trending en-echelon pattern of the 3000 Orebody is parallel to a flexure in the basement contact fault. The up-dip lobes follow the general trend of the bedding parallel shear zones. From south to north the footwall boundary of the 3000 Orebody steps across from one shear zone to the next. The cause of this is not clear. The nature of the southern and northern boundary of each lens is obscure. Very limited exposure of these areas underground suggests either (i) a lensing out towards converging shear zone splays or (ii) a set of almost ENE-WSW trending structures that bound the mineralised block. The hangingwall boundary of the 3000 Orebody lenses is sharp and defined by shear zones (Figs 4.5a(i) – 4.5c(ii)).

The footwall boundary of the 3500 Orebody is very sharp and marked by a major shear zone. This footwall shear zone is discordant to bedding in the footwall, particularly where the stratigraphy is defined by bedding concordant Pb-Zn mineralisation. Pyritic shales on the immediate footwall are often tightly folded. This may represent drag from movement of the fault. The hangingwall boundary of the 3500 Orebody is generally sharp. However in some locations thin bands/lenses of mineralised fractured siliceous shale\ siliceous shale occur outside the economically defined hangingwall boundary. These bands are strongly controlled by the local bedding orientation and are not related to any obvious faults\shear zones.

An interesting feature of both orebodies is the occurrence of upper and lower 'pods' of high grade copper (foci of mineralising fluids?)(e.g. >5% pods enveloped by 2.5% contour). This may be related to positions of dilation zones

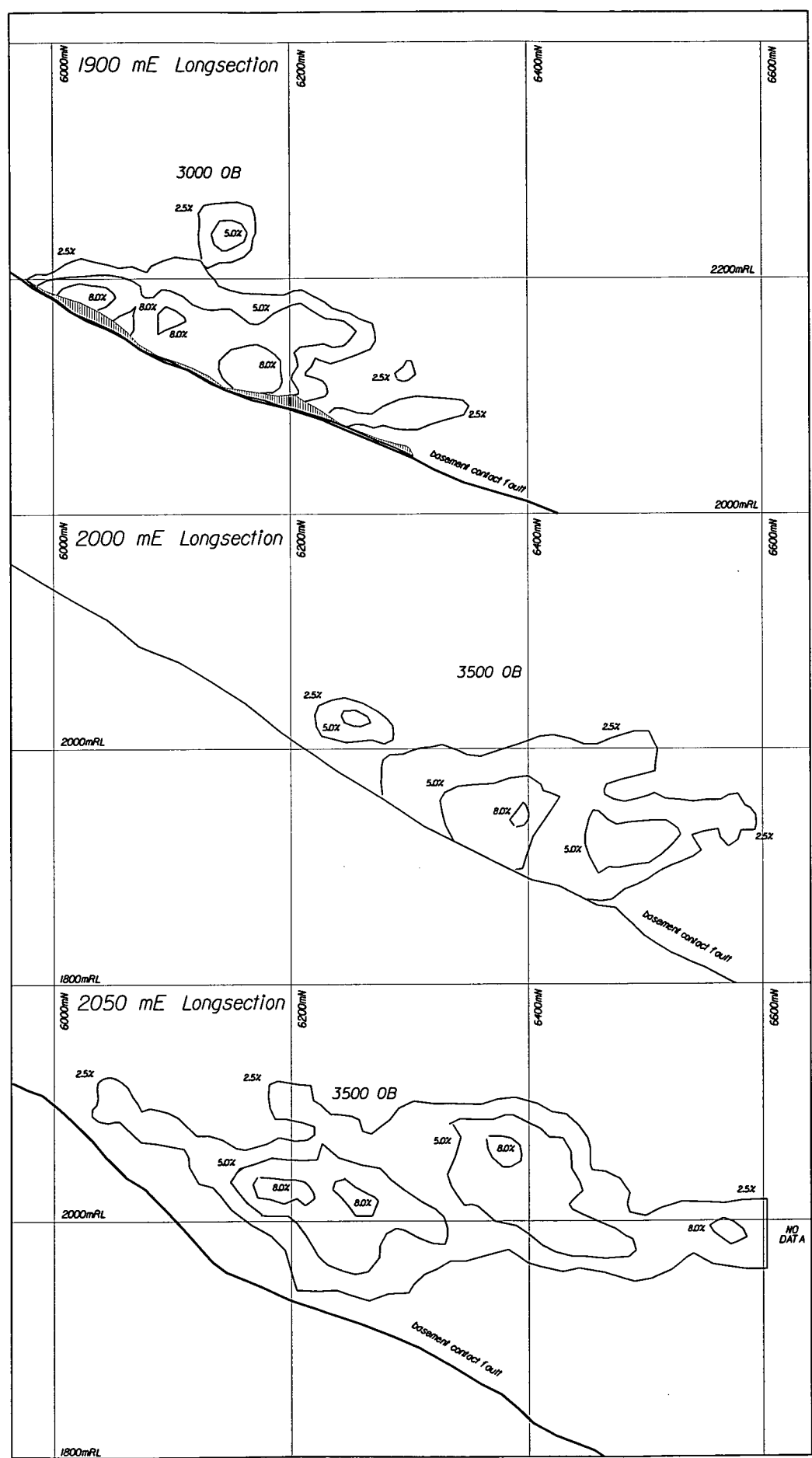
---

within a system of anastomosing shear zone structures but no clear evidence for this has been observed. Recent drilling of the 3500 Orebody to the north shows the same pattern repeating but with  $> 2.5\%$  pods enveloped by a  $1.5\%$  contour. The location of multiple foci does not suggest that there was a single high grade zone which has been displaced by later fault movement.

Fig 5.11 shows a set of longsections through both orebodies. Two features are observed:

1. High grade copper loci occur immediately adjacent to the basement contact fault. Where the loci are spatially separate from the basement contact fault they still show a trend parallel to the plunge of the fault (particularly in longsection 2050 mE).
2. The northern extremities of the orebodies have a horizontal trend. The exact control on this is unclear.

Fig 5.11: Copper mineralisation - Longsections at 1900mE, 2000mE and 2050mE.



## 5.5 Cobalt - Relationship to 'Rock type'

Cobalt associated with the copper deposits at Mount Isa occurs predominantly as either allosclase or cobaltite.

Cobaltite: (Co<sub>0.87</sub> Fe<sub>0.11</sub> Ni<sub>0.02</sub>)<sub>1.00</sub> As<sub>0.93</sub> S<sub>1.01</sub>

Allosclase: (Co<sub>0.75</sub> Fe<sub>0.25</sub> Ni<sub><0.01</sub>)<sub>1.00</sub> As<sub>0.92</sub> S<sub>1.09</sub>

The distribution of cobalt with respect to the alteration 'rock types' is more difficult to define than copper as the cobalt minerals are not visible to the naked eye unless they occur in high concentrations (>0.5%). Observations in recent drill core from the 3500 Orebody indicate that high concentrations of cobalt occur in stylolitic features in recrystallised shale where cobaltite and carbonaceous material have been concentrated. Cobaltite is common in siliceous pyritic shales occurring as mantled overgrowths on fine grained pyrite and coarse grained pyrite and as vein infilling in fractured chalcopyrite (Knights, 1975). A sample collected from adjacent to the Urquhart Shear in the 3500 Orebody is described (thin section) as follows: a dark grey banded shale consisting of alternating layers of fine and coarse grained quartz with occasional cobalt rich zones. Minor dolomite, muscovite and biotite are present with occasional small patches of chlorite. Cobaltiferous layers vary in thickness from a few centimetres to approximately 1 cm and consist of finely disseminated cobaltite and allosclase. The pyrite content of the cobalt rich layers is very low, but very fine carbon is disseminated throughout. Evidence of minor in situ replacement of allosclase by cobaltite was noted as well as allosclase crystals enclosed within cobaltite (Landmark, 1997).

Though the textural features suggest that more cobalt may occur with the less brecciated 'rock types'; the contour data on the plans and sections does not show this.

Early work by Croxford (1974) suggested that the presence of fine grained pyrite had an important association to cobalt occurrence ... "The cobaltite crystals reach 0.05 mm across and always contain rounded to euhedral cores of framboidal pyrite. Where only massive framboidal pyrite occurs, cobaltite is generally absent

but where chalcopyrite veins transverse the pyrite, cobaltite is usually found rimming the pyrite framboids situated marginally to the veins. In places abundant pyrite framboids reside in a delicate interstitial matrix of cobaltite and alloclasite and whereas cobaltite has evidently grown on pyrite, alloclasite occupies the remaining interstitial space.” Waring (1990) briefly mentions a possible fine grained pyrite-cobalt association but does not present any detailed data. Observations from the Deep Copper orebodies do not show a direct correlation between the percentage of fine grained pyrite and cobalt. In fact the areas of highest fine grained pyrite concentration, such as the 3500 Orebody footwall, contain almost no cobalt.

The average cobalt content of the Deep Copper orebodies (combined) is 0.14% which is markedly higher than the 0.06% average for the 1100 Orebody. A brief examination of cobalt distribution in the 1100 Orebody showed that high grades (+ 0.3%) occur in the main central area of the orebody and in smaller foci to the north. The southern area of the orebody (the footwall lens and hangingwall lens) has a markedly lower cobalt content (average 0.03%).

## 5.6 Cobalt Distribution

Figs 5.1a to 5.10a and Fig 5.11 accompany this section.

In plan view the cobalt orebodies trend north-south with a weaker NNW trending component to the cobalt associated with the 3000 Orebody.

### 5.6.1 3000 Orebody

The main features of cobalt distribution are as follows:

- 5900mN - 6100mN - Generally a single elongate lens that extends up dip strongly. The highest grades (>0.3%) occur adjacent to the basement contact fault.
- 6100mN - 6250mN - At 6115mN a hangingwall lens develops. From 6175mN two >0.3% foci develop adjacent to the basement contact fault. The >0.15% contours are very elongate in the up-dip direction.



- 6250mN - 6315mN - Double foci at basement maintained but the grade has decreased to >0.15% cobalt. The hangingwall lens is becoming prominent.

### 5.6.2 3500 Orebody

The main features of cobalt distribution are as follows:

- 5900mN - 6100mN - Minor low grade discrete lenses well above the basement.
- 6100mN - 6220mN - Very high grade (>0.3%) lens centred on 2140mRL (25L). From 6145mN the 0.15% contour extends upwards from the basement. At 6210mN the lower and upper 0.15% lenses coalesce.
- 6220mN - 6285mN - Very high grade lens elongates downwards towards the basement contact fault. This is the highest grade section of the cobalt orebody.
- 6285mN - 6405mN - >0.3% cobalt occurs only as small pods.
- 6405mN - 6435mN - >0.15% cobalt lens breaks up into an upper and lower lens. Overall cobalt distribution contracts towards the basement. Small elongate lenses 100 metres from the hangingwall of the copper orebody are still present.
- 6435mN - 6525mN - Still contracting towards the basement.

## 5.7 Cobalt - Relationship to Copper and Structure

For both orebodies the majority of cobalt >0.1% occurs within the 2.5% copper contour. Its overall distribution is similar to the copper but with some differences. In plan view on 25A and 26B in 3500 Orebody the highest cobalt grades are localised 150 to 200 metres south of the highest copper grades.

A feature that shows up on the sections is that there is a small spatial separation of very high grade cobalt (+ 0.3%) from very high grade copper (+ 8.0%) with the cobalt occurring on the hangingwall side of the copper. Cobalt vs copper assays from diamond drillhole logs were plotted against each other to determine if this

was an artefact of the kriging process or if it was a real relationship. Figures 5.12a & b show the results for the 3000 Orebody and the 3500 Orebody respectively. The same pattern showed for both orebodies (*i.e.* no cobalt values higher than 0.6% occurred where the copper was >10.0%). However extreme grades such as this make up only a small proportion of the population. For the 'normal' range of values, examination of the raw data on sections shows that this spatial relationship to copper is not consistent. This suggests that there may be a bias in the data due to some smoothing affects of kriging and also with respect to the smaller quantity of cobalt assay data available. Further study would be required to determine if there is a significant relationship between cobalt and copper (e.g. geochemical constraints on the precipitation of copper versus cobalt).

The distribution of cobalt, particularly of the very high grade lenses in the 3000 Orebody, shows some influence of the basement contact fault geometry but it is not as directly linked as the copper. No obvious structural control of the cobalt has been discerned. An examination of cobalt distribution in the 1100 Orebody showed that the highest grade foci of cobalt coincide with the high grade copper occurrences. The data was not detailed enough to determine any subtle spatial differences.

Fig 5.12a: Cobalt vs copper values 3000 Orebody.

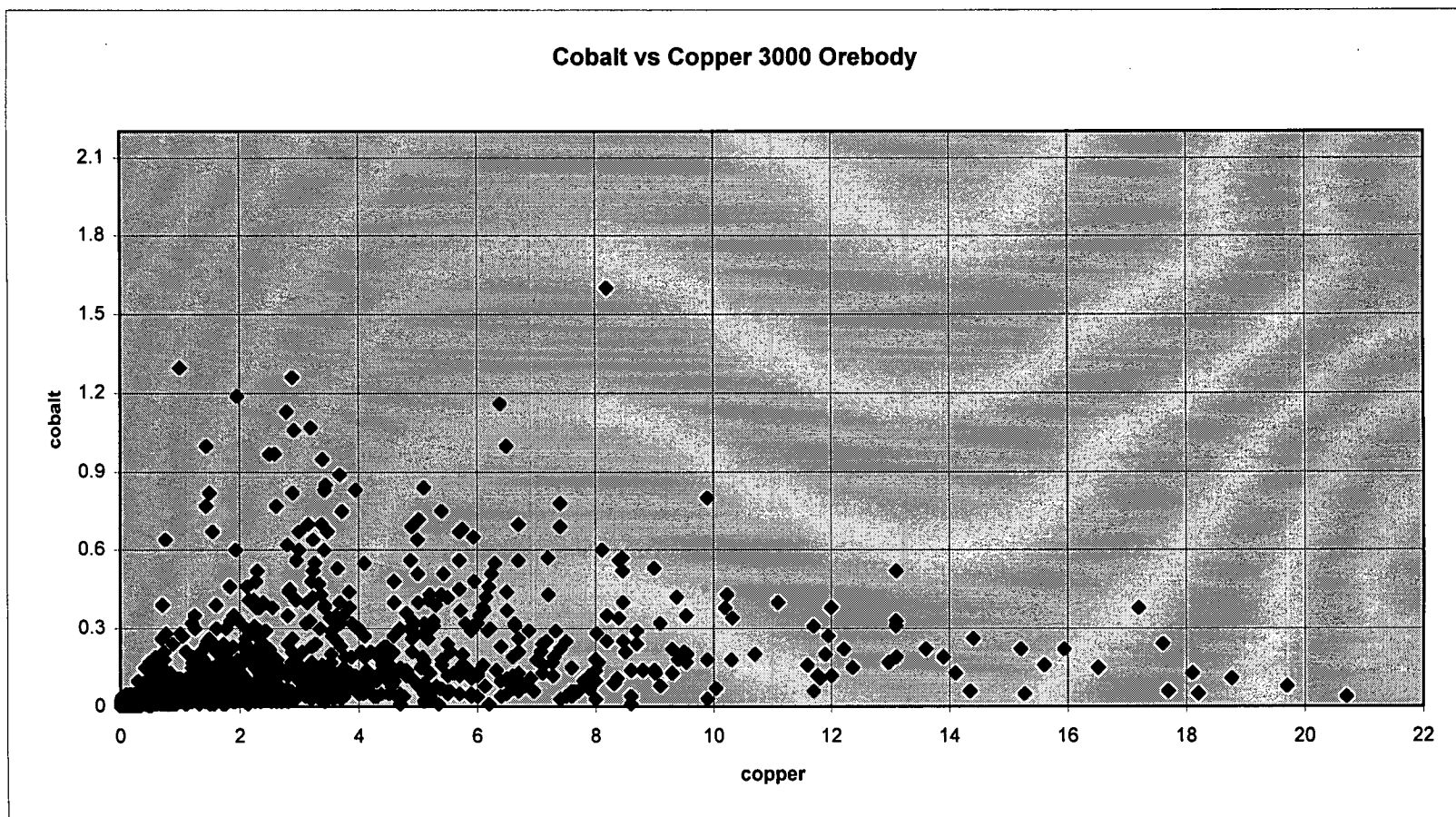


Fig 5.12a : Cobalt vs copper values from diamond drillhole data (1344 data points).

Fig 5.12b: Cobalt vs copper values 3500 Orebody.

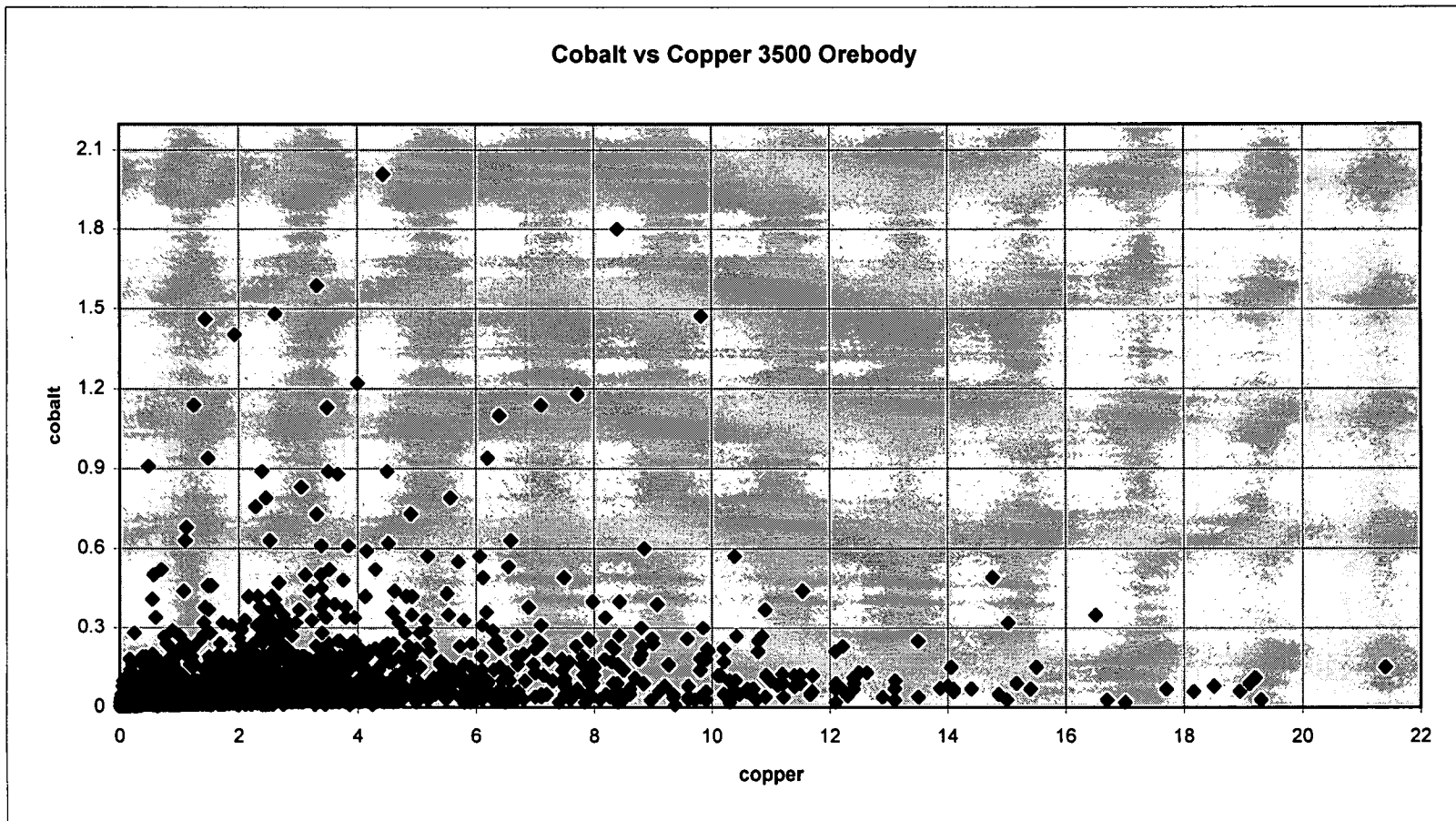


Fig 5.12b : Cobalt vs copper values from diamond drillhole data (2891 data points)

## 5.8 Discussion

Early work by Croxford (1974) on the timing of cobalt mineralisation suggested that alloclasite represented an early (diagenetic) form of cobalt that was associated with the framboidal fine grained pyrite. The alloclasite was then modified by later metamorphic or hydrothermal events to cobaltite. Perkins (1984) concluded that all of the cobalt was introduced with the copper. McGoldrick (1986) suggested that the cobalt was present in the precursor stratigraphy and that the silica-dolomite forming hydrothermal fluids added copper but did not contribute cobalt. This conclusion was partly based on the observation that cobalt together with bismuth and arsenic display remarkable 'stratiform' distributions in the 1100 Orebody. These distributions extended beyond the limits of extensive silicification and were independent of the distribution of the different silica-dolomite 'rock types'.

From my observations I tend to agree more with Perkins that the cobalt has been introduced with the copper. The presence or absence of fine grained pyrite is not an obvious constraint on the location of higher grade cobalt occurrences. In fact the areas of highest fine grained pyrite content, such as the immediate footwall of the 3500 Orebody are noticeably low in both copper and cobalt. The apparent association with carbonaceous material may be more significant. At least some of the high grade occurrences of cobalt may be a result of pressure solution processes that have redistributed and concentrated it along with carbonaceous material.

Fig 5.7b shows a 'stratiform' occurrence of cobalt in the hangingwall of the 3000 Orebody (*i.e.* outside the economic copper mineralisation), such as is described by McGoldrick (1986) in the 1100 Orebody. A detailed examination of this section showed that though the copper mineralisation is subeconomic there is still a 'layer' of copper mineralisation (1.0% to 3.5%) coinciding with this cobalt occurrence.

## Synopsis

The purpose of this study was to describe the characteristics of the 3000 and 3500 orebodies, which are part of the copper mineralised system in Mount Isa. An emphasis was placed on the structural controls on mineralisation.

**Silica-dolomite alteration** – (Sections 2.2 and 2.3) The silica-dolomite alteration associated with the Mount Isa copper orebodies has the same general distribution patterns around the Deep Copper orebodies as it does for the large 1100 Orebody from where it was originally described (Perkins, 1984; Swager, 1985; Waring, 1990). The system involved three stages of silicification and dolomitisation, which took place during the third period of regional deformation ( $D_3$ ).

*Stage (1)*- Early syn- $D_3$  recrystallisation and silicification.

*Stage (2)*- Extensive dissolution of dolomite by the silicifying fluids changed the fluid composition until it became over-saturated with carbonate components and started to redeposit and promote growth of dolomite (irregularly brecciated dolomitic shale).

*Stage (3)*- Chalcopyrite and quartz precipitated, replacing dolomite.

Dissolution of dolomite and precipitation of chalcopyrite are presumed to have occurred simultaneously. In the Deep Copper orebodies the association of economic concentrations of chalcopyrite with silicification is ubiquitous.

On the mesoscale to mine scale it is very difficult to identify separate distinct stages for the development of the silica-dolomite alteration. It seems fairly clear that the chalcopyrite replaced dolomite. However it is virtually impossible to distinguish between early and late stage silicification. The broad distribution of the bedded siliceous shales around the fringes of the siliceous breccias suggests a system where intense brecciation processes and silicification become less intense moving outwards from the input source of the hydrothermal fluids. As pore fluid pressures decrease the silicification processes become passive and preserve original textures such as bedding. The occurrence of irregularly brecciated dolomitic shale at the up dip limits

of the orebodies may simply be a function of the carbonate which has been removed from the core of the orebody being deposited once fluid flows (+ silica) decrease. The nature of the bedding controlled structures drives the fluids up dip rather than across the dip. This may explain why there is no irregularly brecciated dolomitic shale in the immediate hangingwall or footwall of the orebodies.

**Talc alteration and phyllosilicates** – (Section 2.4) Talc (+pyrrhotite) alteration and phyllosilicate alteration associated with Pb-Zn mineralisation occurs on the footwall of the 3500 Orebody. Neither talc-pyrrhotite or stilpnomelane alteration occurs on the footwall of the 3000 Orebody or south of 6330 mN where there is no significant occurrence of Pb-Zn mineralisation. The intensity of talc- pyrrhotite increases northwards and up-dip, corresponding to an increase in the thickness of the Pb-Zn mineralised zone. The spatial correlation between the footwall fine-grained pyrite band and the talc- pyrrhotite zone suggests that much of the pyrrhotite has been derived at the expense of the fine grained pyrite.

**Basement contact fault** – On a large scale the basement contact fault forms an almost flat to very shallowly dipping structure beneath the Mount Isa copper system. The basement contact fault is described as a curved surface, with steep sections which curve towards parallelism with bedding linked by flat lying sections or ramps. This geometry is postulated to have developed via folding, the flat sections being fold hinge zones. A flexure in the basement contact fault beneath the 3000 Orebody coincides exactly with the highest grade core of this orebody. There is a clear north-northwest trend to the orebody. This direction equates to the orientation of structures formed during D<sub>3</sub>. The data presented in sections 3.4 and 3.6 verifies that the position of D<sub>3</sub> related folds in the basement contact fault are a very strong control on the localisation of mineralisation in the 3000 orebody.

The 3500 Orebody has an overall north-south trend and does not have such an obvious link to the basement contact fault.

**Orebody structure and copper mineralisation** - There is a strong relationship between folding and faulting and the two processes act together. In chapter one I presented the interpretation of the orebodies as it was in 1972 when it was thought that they may have been folded by the Mount Isa Fold ( $D_3$  fold). The Mount Isa Fold does not fold the orebodies. They formed syn (but late) with the fold and their location was influenced by the position of the antiformal hinge zone of the fold. As well as the major control of the basement contact fault on the localisation of the mineralising fluids this study suggests that a system of mainly bedding parallel shear zones provided a secondary control, acting as the conduits to transport the hydrothermal fluids away from the basement contact. Local flexures in the contact control the location of these shear zones and they formed during  $D_3$ .

The shear zones form a structural mesh network (section 4.7.3) in the immediate vicinity of the orebodies. Diamond drilling between the two orebodies and in the footwall of 3500 Orebody shows well bedded shales with a marked absence of faults/shear zones. In a few localities the shear zones are extremely difficult to trace suggesting they have been completely healed by the minerals precipitated from the mineralising fluids. The shear zones have a strong influence on local variations in copper grade (section 4.3). There is a possibility that more laminated pyritic layers in the original stratigraphy were initially more susceptible to shearing. Continual modification by alteration (silicification and dolomitisation) may have caused changes to ductility contrasts throughout the deformation period and had an effect on the overall development and geometry of the sets of anastomosing splay structures.

**Orebody structure and cobalt mineralisation** - The distribution of cobalt, particularly of the very high grade lenses in the 3000 Orebody, shows some influence of the basement contact fault geometry but it is not as directly linked as the copper. No obvious structural control of the cobalt has been discerned and the nature of the relationship of cobalt to copper is very problematical. Its overall distribution still suggests to me that it was introduced with the copper and was not remobilised out of original stratigraphic layers.



---

## References

- Arboleya, M.L, and Engelder, T., 1995, Concentrated slip zones with subsidiary shears: their development on three scales in the Cerro Brass fault zone, Appalachian valley and ridge: *Journal of Structural Geology*, v. 17, No4, p. 519-532.
- Bell, T.H., Perkins, W.G., and Swager, C.P., 1988, Structural controls on development and localisation of syntectonic copper mineralisation at Mount Isa, Queensland: *Economic Geology*, v. 83, p. 69-85.
- Bell, T.H., 1991, The role of thrusting in the structural development of the Mount Isa mine and its relevance to the exploration in the surrounding region: *Economic Geology*, v. 86, p. 1602 - 1625.
- Blake, D.H., 1986, Middle Proterozoic evolution of the Mount Isa Inlier, north-western Queensland, Australia: A synthesis: *Transactions of the Geological Society of South Africa*, v. 89, p. 253-262.
- Blake, D.H., 1987, Geology of the Mount Isa Inlier and environs, Queensland and Northern Territory: Bureau of Mineral Resources (BMR) Bulletin, v. 225, 83p.
- Blake, D.H., and Stewart, A.J., 1992 (eds), Detailed Studies of the Mount Isa Inlier: Australian Geological Survey Organisation (AGSO) Bulletin, v. 243, 374p.
- Blanchard, R., and Hall, G., 1942, Rock deformation and mineralisation at Mount Isa: *Proceedings Australasian Institute of Mining Metallurgy*, No.125.
- Buchanan, D.T., Kaesehagan, F.E., and Kelsey, R.D., (date unknown), The history and economics of Mount Isa Copper: Unpublished Mount Isa Mines report.
- Cordwell, K.S., Wilson, G.L., and Lord, J.H., 1963, Geology of the area south of Mt. Isa and its application to the structural control of the Mt. Isa orebodies: *Proceedings Australasian Institute Mining Metallurgy*, No 206, p. 29-62.

- 
- Cosgrove, J.W., 1993, The interplay between fluids, folds and thrusts during the deformation of a sedimentary succession: *Journal of Structural Geology*, v. 15, Nos 3-5, p. 491-500.
- Croxford, N.J.W., 1974, Cobalt mineralisation at Mount Isa, Queensland, Australia, with reference to Mount Cobalt: *Mineral. Deposita*. Springer-Verlag (Berlin), v. 9, p. 105-115.
- Deer, W.A., Howie, R.A., and Zussman, J., 1992, An introduction to the rock forming minerals – 2<sup>nd</sup> Edition. Publ Longman Group UK Limited. 696p.
- Derrick, G.M., Wilson, I.H., and Sweet, I.P., 1980, The Quilalar and Surprise Creek Formations - new Proterozoic units from the Mount Isa Inlier: Their regional sedimentology and application to regional correlation: Bureau of Mineral Resources. *Journal of Australian Geology and Geophysics*, v. 5, p. 215-223.
- Glikson, A.Y., Derrick, G.M., Wilson, I.H., and Hill, R.M., 1976, Tectonic evolution and crustal setting of the Middle Proterozoic Leichhardt River Fault Trough, Mount Isa Region, northwestern Queensland: Bureau of Mineral Resources. *Journal of Australian Geology and Geophysics*, v.1, p. 115-129.
- Hodgson, C.J., 1989, The structure of shear-related, vein-type gold deposits: a review: *Ore Geology Reviews*, v. 4, p. 231-273.
- Knights, J.G., 1975, 1100 Orebody mineralogical examination zero N - 1000N: Unpublished Mount Isa Mines technical report, RES-GEO 9, 39p.
- Knights, J.G., 1996, The PB/ZN Mineralised Fe/Ba-Rich F/W alteration zone to 3500 O/B: Unpublished Mount Isa Mines Mineral Services Report, No 6561.
- Knights, J.G., 1997, Identification of phyllosilicate-rich alteration mineral assemblages F/W 3500 O/B Deep Copper. Unpublished Mount Isa Mines Mineral Services Report, No 6717.
- Landmark, V., 1996, Cobalt mineralisation in the 3500 Orebody. Unpublished Mount Isa Mines Mineral Services Report, No 6327.

- 
- Mathias, B.V., and Clark, G.J., 1975, Mount Isa copper and silver, lead, zinc orebodies, Isa and Hilton Mines, in :C.L. Knight, C.L., ed., *Economic Geology of Australia and Papua New Guinea*, I Metals: Australasian Institute of Mining Metallurgy Monograph 5, p. 351-372.
- McGoldrick, P.J., 1986, Volatile and precious metal geochemistry of the Mount Isa ores and their host rocks: Unpublished Ph.D. thesis, University of Melbourne.
- Murray, W.J., 1961, Notes on Mount Isa Geology: Proceedings Australasian Institute Mining Metallurgy, p105-136.
- Neudert, M., 1983, A depositional model for the Upper Mount Isa Group and implications for ore formation: Unpublished Ph.D. thesis, Research School of Earth Sciences, Australian National University Canberra.
- Neudert, M., 1996, Workshop on sedimentology of the Mount Isa Group: Unpublished report to Mount Isa Mines.
- O'Dea, M.G., and Lister, G.S., 1995, The role of ductility contrast and basement architecture in the structural evolution of the Crystal Creek block, Mount Isa Inlier, NW Queensland, Australia: *Journal of Structural Geology*, v. 17, No 7, p. 949-960.
- Page, R.W., 1981, Depositional ages of the stratiform base metal deposits at Mount Isa and McArthur River, Australia, based on U-Pb zircon dating: *Economic Geology*, v. 76, p. 648-658.
- Perkins, W.G., 1979, Isa Mine greenschist contact project - structural analysis: Unpublished Mount Isa Mines technical report, GEO 120, v. 1 & 2.
- Perkins, W.G., 1984, Mount Isa silica dolomite and copper orebodies: The result of a syntectonic hydrothermal alteration system: *Economic Geology*, v. 79, No 4, p. 601-637.
- Perkins, W.G., 1995, A study of the nature, timing, and processes in the Mount Isa Lead-Zinc orebodies, and their relationship to copper orebodies and the lead-zinc systems at McArthur River, Hilton and Mount Novit: Unpublished MIMEX Report No. 2690 (Draft).

- 
- Plumb, K.A., Derrick, G.M., and Wilson, I.H., 1980, Precambrian geology of the McArthur River - Mount Isa Region, northern Australia. *in* Henderson, R.A., and Stephenson, P.J., eds., *The Geology of Northeastern Australia*: Geological Society of Australia QLD Division, Brisbane, p. 71-88.
- Ramsey, J.G., 1980, Shear zone geometry: a review: *Journal of structural geology*, v. 2, No. 1/2, p. 83-99.
- Raymond, G.F., 1993, Revised variogram parameters for the 3000 and 3500 orebodies: Unpublished Mount Isa Mines memorandum.
- Schofield, N., 1998, Spatial continuity and estimation parameters in the copper and deep lodes at Mount Isa, QLD. Unpublished report prepared for Mount Isa Mines by Hellman & Schofield Pty Ltd.
- Sibson, R.H., 1989, High-angle reverse faulting in northern New Brunswick, Canada, and its implications for fluid pressure levels: *Journal of Structural Geology*, v. 11, No 7, p. 873-877.
- Sibson, R.H., 1990, Conditions for fault-valve behaviour. *in* Knipe, R.J., and Rutter, E.H., eds., *Deformation Mechanisms, Rheology and Tectonics*: Geological Society Special Publication, No. 54, p. 15-28.
- Sibson, R.H., 1996, Structural permeability of fluid-driven fault-fracture meshes: *Journal of Structural Geology*, v. 18, No. 8, p. 1031-1042.
- Spratt, R.N., 1953, Notes on the Black Star Copper Orebody: Australasian Institute of Mining Metallurgy Proceedings, No. 171.
- Stoker, P.T., 1972, A review of 3000 Orebody exploration: Unpublished Mount Isa Mines Technical Report, GEO 114.
- Swager, C.P., 1983, Microstructural development of the silica dolomite and copper mineralisation at Mount Isa, Northwest Queensland, with special emphasis on the timing and mechanism of mineralisation: Unpublished Ph.D. thesis, James Cook University of North Queensland.

- 
- Swager, C.P., 1985, Syndeformational carbonate replacement model for the copper mineralisation at Mount Isa, Northwest Queensland: A microstructural study: *Economic Geology*, v. 80, p. 107-125.
- Swager, C.P., Perkins, W.G., and Knights, J.G., 1987, Stratabound phyllosilicate zones associated with syntectonic copper orebodies at Mount Isa, Queensland: *Australian Journal of Earth Sciences*, v. 34, p. 463-476.
- Valenta, R., 1994, Syntectonic copper mineralisation in the Hilton Mine Mount Isa: *Economic Geology*, v. 89, p. 1032-1052.
- Waring, C.L., 1990, Genesis of the Mt Isa Cu Ore System: Unpublished Ph.D. thesis, Monash University.
- Wilson, C.J.L., 1973, Faulting west of Mount Isa Mine: *Proceedings Australasian Institute Mining Metallurgy*, No 245.
- White, N.J., Jackson, J.A., and McKenzie, D.P., 1986, The relationship between the geometry of normal faults and that of sedimentary layers in their hanging walls: *Journal of Structural Geology*, v. 8, No.8, p. 897-909.
- Wibberley, C.A., 1997, Three-dimensional geometry, strain rates and basement deformation mechanisms of thrust-bend folding: *Journal of Structural geology*, v. 19, Nos.3-4, p. 535-550.
- Winsor, C.N., 1986, Intermittent folding and faulting in the Lake Moondarra area, Mount Isa, Queensland: *Australian Journal of Earth Sciences*, v. 33, p. 27-42.